DEFINING FUNCTIONAL DRIVERS OF OESOPHAGEAL TUMOURIGENESIS

BY
JOVANA (RANKO) GOTOVAC

Submitted in total fulfilment of the requirements for the degree of Doctor of Philosophy

Division of Cancer Research
The Peter MacCallum Cancer Centre

and

The Sir Peter MacCallum Department of Oncology
The University of Melbourne

September 2019

ABSTRACT

The incidence of oesophageal adenocarcinoma (OAC) has risen rapidly over the last four decades and has a high overall mortality rate that has shown only incremental improvements over the same duration. OAC develops from the precursor intestinal metaplasia of the oesophageal mucosa known as Barrett's oesophagus. However, limited knowledge of the molecular mechanisms driving disease progression makes effective clinical management of OAC challenging. One of the common genetic events associated with the progression from Barrett's oesophagus to OAC is loss of the tumour suppressor, SMAD4 (mutated in 13% or loss of function in 34% of OAC cases). Herein, this thesis firstly investigated the effect of SMAD4 inactivation in Barrett's carcinogenesis.

Genetic knockdown or knockout of SMAD4 was sufficient to initiate tumourigenesis of dysplastic Barrett's oesophagus cell line, CP-B, *in vivo*, establishing SMAD4 loss as a crucial event driving progression to OAC. Further, low coverage whole genome sequencing (LC-WGS) analysis revealed that tumourigenic SMAD4 knockdown/knockout CP-B cell lines exhibited distinctive and consistent copy number alterations (CNAs) compared to non-tumourigenic SMAD4 wild-type parental cells. Amongst the alterations we observed were loss of chromosome arm 14q, while amplified regions include chromosome arms 6q and 12p, consistent with common CNAs found in patient tumours. This high genomic instability, characterized by structural chromosomal rearrangements within the tumours following SMAD4 loss, implicates SMAD4 as a protector of genome integrity in OAC development and progression.

Moreover, initial *in vitro* data shows that SMAD4 knockout in CP-B cell line, results in differential expression of transforming growth factor-beta (TGF-β) pathway target genes (such as *ACTA2*, *CRYAB*, *PTK2B*, *ATF3* and *CDC6*) and loss of cell cycle arrest in response to TGF-β1 cytokine compared to SMAD4 wild-type parental cells. Furthermore, SMAD4 knockout negatively regulated transcript expression of the multifunctional tumour suppressor INK4/ARF locus, demonstrating the novel and complex network of SMAD4 tumour suppressive activity.

This thesis also focused on deciphering the functional role of growth factor receptor bound protein 7 (GRB7) amplification and overexpression in OAC and its potential targeting. *GRB7* gene is positioned within known 17q12 amplicon, together with *HER2* gene encoding for human epidermal growth factor receptor 2 (HER2). GRB7 is an adaptor molecule that mediates networking of multiple cell surface receptors with downstream signalling pathways.

GRB7 high expression was found to be associated with worse survival in OAC patient cohort. Further, genetic GRB7 knockdown (siRNA) inhibited cell proliferation and clonogenic survival and induced apoptosis in GRB7 amplified and overexpressing OAC cell lines (OE19 and Eso26), without altering proliferation of the cells with normal GRB7 expression. Furthermore, whilst HER2 amplification and overexpression was also observed in OE19 and Eso26 cells, they were not uniquely sensitive to trastuzumab (HER2 inhibitor), with Eso26 cells exhibiting resistance *in vitro*. Taken together, initial findings raise the possibility that GRB7 may be a better molecular therapeutic target than HER2 in OAC with the 17q12 amplicon.

To address this possibility, OE19 and Eso26 cell line xenograft models with inducible expression of shRNA targeting GRB7 were used. Consistent with *in vitro* findings, HER2 expression did not predict sensitivity to trastuzumab, with Eso26 xenografts remaining refractory to trastuzumab treatment. Of high importance, mimicking GRB7 inhibition with inducible-shRNA significantly inhibited tumour growth in both OE19 and Eso26 xenografts. Thus, this part of the thesis demonstrates the functional role of GRB7 overexpression as an oncogenic driver independent of HER2.

In summary, the identification of functional genetic drivers and a deeper understanding of the mechanisms that underlie tumour progression in Barrett's carcinogenesis will lead to improved strategies for the clinical management of OAC patients. To this end, SMAD4 loss was sufficient for progression from dysplasia to OAC. Tumours driven by SMAD4 loss exhibit distinctive CNAs consistent with OAC and metastatic potential. In addition, GRB7 high expression predicts poor outcome in patients with OAC and as such, GRB7 represents an oncogenic driver that could be used as a therapeutic target. Crucially, this thesis provides *in vitro* and *in vivo* preclinical and molecular biology evidence for the potential therapeutic benefit of targeting GRB7 in cancer.

DECLARATION

This is to certify that

1. The thesis comprises only my original work towards the Ph.D. except where indicated in the Preface section.
2. Due acknowledgement has been made in the text to all other material used.
3. The thesis is less than 100,000 words in length, exclusive of tables, maps, bibliography and appendices.

Jovana Gotovac

September 2019

PREFACE

The majority of the work described in this thesis was performed by the candidate under the supervision of Dr. Nicholas Clemons, Prof. Wayne Phillips and Dr. Cuong Duong. Ms. Jovana Gotovac conceived and carried out all experiments (unless otherwise specified) and analysed data (unless otherwise specified).

Some of the work in this thesis has been published (Abstract (Poster Presentation #164, 30th Lorne Cancer Conference 2018) and Chapter 1. section 1.8).

Chapter 3

Dr. Clemons generated SMAD4 knockdown and knockout in CP-B cells and injected the cells in mice. Mr. Elhadi Ilch, Mr. Kenji Fujihara and Ms. Karen Montgomery (Peter MacCallum Cancer Centre, Australia) provided initial protocols and material. Dr. Tanjina Kader conducted bioinformatics analyses of Low Coverage-Whole Genome Sequencing. Dr. Sangeetha Kalimuthu (Univerisity of Toronto, Canada) performed pathological review of SMAD4 knockdown and knockout xenografts.

Chapter 4

Mr. Ilch, Ms. Mariana Corrales (Peter MacCallum Cancer Centre, Australia), provided initial protocols and material. Mr. Luis Lara performed Principal Component Analyses in R studio.

Chapter 5: Written as a manuscript for publication purposes including declaration below.

Ms. Gotovac, Dr. David Liu, Prof. Phillips and Dr. Clemons designed the study. Ms. Gotovac conceived and carried out experiments, analysed data and wrote the paper. Dr. Liu conceived and carried out shGRB7 design experiments, Ms. Michael Yates conceived and carried out IHC staining experiments, Ms. Arthi Macpherson carried out RPPA experiments, Prof. Guy Eslick provided TMAs, clinical data and survival analysis. Ms. Jovana Gotovac, Dr. Nicholas Clemons and Dr. Catherine Mitchell analysed and scored GRB7 staining on TMAs. Dr. Duong, Dr. Liu, Prof. Phillips, Dr. Clemons and Ms. Gotovac revised and edited the paper and all authors had final approval of the submitted and published versions.

ACKNOWLEDGEMENTS

There are many people that I would like to acknowledge for their support during my PhD studies.

As my supervisors, Dr. Nicholas Clemons, Prof. Wayne Phillips and Dr. Cuong Duong have my sincerest gratitude. I would like to greatly thank you for your research guidance, unconditional support and mentorship on my journey of becoming an academic molecular biologist. I deeply appreciated your patience, welcoming attitude and scientific advice. I believe that Ph.D. studies under your guidance helped me to grow and develop as an independent scientist. I will always cherish the great opportunity to be a part of remarkable, intellectual and supportive environment that you provided.

I would like to acknowledge all members of the Cancer Biology and Surgical Oncology Research Laboratory, both past and present (Dr. David Liu, Mr. Elhadi Ilch, Ms. Karen Montgomery, Mr. Michael Yates, Ms. Mariana Corrales, Mr. Kenji Fujihara, Dr. Swati Dawar, Dr. Camilla Mitchell, Ms. Sabrina Caiazzo, Mr. Francesc De las Heras, Ms. Julia Milne, Ms. Bonnie Zhang, Dr. Helen Pearson, Ms. Sophie Clare, Dr. Glen Guerra and Dr. Carlos Cabalag). A special mention to Dr. David Liu for easing me into the lab and intellectual contribution to this project. Special thank you to Mr. Elhadi Ilch for unconditional support, sharing research ideas and intellectual knowledge. Ms. Karen Montgomery and Ms. Mariana Corrales, thank you for your patience, assistance and willingness to help within the lab and with technical details. Thank you to Mr. Kenji Fujihara for collaboration in writing papers, intellectual inspiration and greatest collegiality. Indeed, thank you to all mentioned members of the Cancer Biology and Surgical Oncology Research Laboratory. Your cooperation and assistance over the last three years and a half have been immense and invaluable.

To all my friends outside of the Clemons Lab and Phillips Lab (Dr. Tanjina Kader, Ms. Aesha Ali, Dr. Sathana Dushyanthen, Dr. Shatha Abuhammad, Dr. Maria Joao Silva, Ms. Sarah Ftouni, Ms. Valeria Arcucci, Ms. Ruofei Liu, Ms. QuezadaUrban Rosalia, Mr. Athanasios Koulis, Mr. Balaji Virassamy, Ms. Natalie Brajanovski and Ms. Laura

Kirby), a big thank you for all the laughs and great companionship in and out of the workplace. You have made my Ph.D. journey such a memorable and enjoyable one.

Dr. Jessica Beach, thank you for guidance and mentorship during my Ph.D. studies, it has been invaluable hearing your advice and experience.

In addition, I owe big thank you to A/Prof. Caroline Owen, graduate research coordinator and our biggest student support, together with Niranga Nawagamuwa, for all unconditional support and advice.

Within Cancer Research, I would like to thank members from the animal facility (Ms. Stephanie Lewis Lee, Mr. Michael Durrant, Ms. Katherine Papastratos and Ms. Jacinta Carter), FACS (Mr. Ralph Rossi, Ms. Viki Milovac and Ms. Sophie Curcio), VCFG (Ms. Arthi Macpherson, Ms. Twishi Gulati, Ms. Jennii Luu and A/Prof. Kaylene Simpson), media kitchen (Mr. Graham Heffernan and Ms. Lara Sekhon), as well as microscopy and histology (A/Prof. Sarah Ellis, Dr. Jill Danne and Dr. Metta Jana). Also, I would like to thank you Dr. Kylie Gorringe and Dr. Gisela Mir Arnau (Peter MacCallum Cancer Centre, Australia) for support and advice.

Finally and most importantly, I would like to express my deepest thank you and dedication of this thesis to my wonderful family and my partner.
Thank you for standing by me before and over the years of my Ph.D. studies. Your patience, unconditional support and love will forever be sincerely cherished.

AWARDS

I am very privileged and honoured to have received the following awards during the course of my candidature.

- 2019 Postgraduate Harold Mitchell Travel Scholarship
- 2018 Best Poster Presentation Award between PhD students, 30th International Lorne Cancer Conference.
- 2015-2019 International Postgraduate Research Scholarship, University of Melbourne

SCIENTIFIC PRESENTATIONS

Some of the work in this thesis has been presented at scientific conferences.

- Seminar hosted by Prof. Tim Underwood; Somers Cancer Research, University Hospital Southampton, Southampton, UK (2019)
- CRUK International Symposium on Oesophageal Cancer 2019, London, UK. Oral presentation in the Future Leaders Session with the Title: 'Loss of SMAD4 is sufficient to promote tumourigenesis in a model of dysplastic Barrett's oesophagus' (2019)
- Seminar hosted by Dr. Med. Michael Quante; Department of Gastroenterology, Technical University, Munich, Germany (2019)
- 30th Lorne International Cancer Conference, Lorne, Victoria, Australia. Poster presentation (2018)
- Biomed Link St Vincent's Student Conference, Melbourne, Australia. Poster Presentation (2017)
- 29th Lorne International Cancer Conference, Lorne, Victoria, Australia. Poster presentation (2017)
- Student Cancer Symposium, Peter MacCallum Cancer Centre, Poster Presentation (2017)

PUBLICATIONS

Some of the work in this thesis is in preparation for submission or has been published.

Gotovac JR, Fujihara KM, Phillips WA, Clemons NJ: **TGF-beta signaling and its targeted therapy in gastrointestinal cancers.** *Discovery Medicine*, 2018, Sep;26(142):103-112.

To be submitted (September 2019)
Gotovac JR, Liu DSH, Yates MJ, Macpherson AA, Eslick GD, Mitchell C, Duong CP, Phillips WA, Clemons NJ. **GRB7 amplification is an oncogenic driver independently of HER2 amplification in OAC.**

In preparation to be submitted (November 2019)
Gotovac JR, Kader T, Lara L, Gorringe KL, Mitchell C, Duong CP, Phillips WA, Clemons NJ. **SMAD4 loss is a key driver of progression from high grade dysplasia towards OAC.**

LIST OF FIGURES

Chapter 1

Chapter 3

Chapter 4

Chapter 5

LIST OF TABLES

Chapter 2

Chapter 3

Chapter 4

Chapter 5

ABBREVIATIONS

ATCC…….American Type Culture Collection
BMP4…….Bone morphogenetic protein 4
BSA……Bovine serum albumin
CDK……Cyclin dependent kinase
cDNA…….Complementary DNA
CDX……...Caudal-regulated homeobox
CK7……Cytokeratin 7
CNAs…….Copy number alterations
DDR……...DNA damage repair
DFS…….....Disease free survival
DM…….....Double minutes
Dox…….Doxycycline
DSB……Double strand breaks
E2F1…….....E2F transcription factor 1
EGFRs……Epidermal growth factor receptors
FBS…….Fetal bovine serum
GERD……Gastro-oesophageal reflux disease
GISTIC…….....Genomic identification of significant target genes in cancer
GNI……....Gross National Index
GRB7……Growth factor receptor bound protein 7
H&E……...Hematoxylin and eosin
HDI……....Human developmental index (HDI)
HER2……..Human epidermal growth factor receptor 2
HGD……...High grade dysplasia
HKG……...Housekeeping genes
HR…….....Homologous recombination
IHC…….Immunohistochemistry
Indel……Insertion/deletion
LC-WGS…….Low Coverage-Whole Genome Sequencing
LGD……...Low grade dysplasia
LVD……Lymphatic vascular density
MAPK…….Mitogen-activated protein kinase

MGMT……O-6-Methylguanine-DNA Methyltransferase

MUTYH……..Adenine DNA glycosylase

NSG……...NOD-SCID IL-2Rγ knockout

OAC……...Oesophageal adenocarcinoma

OGG1…….N-glycosylase/DNA lyase

OSCC……Oesophageal squamous cell carcinoma

$p16^{INK4A}$……..Cyclin dependent kinase inhibitor 2A

PARP…….Poly(adenosine diphosphate ribose) polymerase

PBS…….Phosphate buffered saline

PCR…….Polymerase chain reaction

PFS…….Progression free survival

PH…….....Pleckstrin homology

PI…….....Propidium-iodine

PI3K……Phosphatidylinositol 3-kinase

qRT-PCR…….Quantitative Real-Time PCR

RA…….....Ras-associating

RTKs……..Receptor tyrosine kinases

SEER……....Surveillance, Epidemiology, and End Results Program

sgRNA……...Single guide RNA

SH2……Src-homology 2

SH3……Src-homology 3

SNVs……....Single-nucleotide variants

STR……Short tandem repeats

TBS……Tris-buffered saline

TetO……...Tet-operating

TetR……...Tetracycline repressor

TGF-β……Transforming growth factor-beta

VEGF……....Vascular endothelial growth factor

VEGFR-2…….Vascular endothelial growth factor receptor-2

TABLE OF CONTENTS

CHAPTER 2. MATERIALS AND METHODS

CHAPTER 1.

LITERATURE REVIEW

1.1. Oesophageal cancer

Oesophageal cancer highly contributes to the global burden of cancer worldwide. According to the latest epidemiological reports, oesophageal cancer rates as the sixth major cause of cancer-related deaths and the seventh most common cancer worldwide [1]. The incidence of oesophageal cancer is higher among men (11% in high/very high human developmental index (HDI) and 5.5% in low/medium HDI regions) than women (3.7 in high/very high HDI and 3% in low/medium HDI regions) [1]. HDI is a composite measure based on three determinant indexes including life expectancy, education and Gross National Index (GNI) per capita. Oesophageal cancer incidence is frequent in Eastern and Southern African countries, with the urgent need to elucidate risk factors in these regions. Similarly, the incidence rates of oesophageal cancer are high in Eastern Asia countries [1].

Two major histological subtypes of oesophageal cancer, oesophageal squamous cell carcinoma (OSCC) and oesophageal adenocarcinoma (OAC) account for approximately 99% of all oesophageal cancers, with the remainder being small cell carcinomas [2], sarcomas, lymphomas, carcinoids, melanomas [3] and gastrointestinal stromal tumours [4] of the oesophagus. Anatomically, OSCC frequently arises from dysplastic squamous epithelium lining the proximal to middle oesophagus, whereas OAC develops from a columnar metaplasia known as Barrett's oesophagus in the distal oesophagus. The major risk factors associated with the development of OSCC include heavy alcohol consumption and tobacco use [5, 6], whilst gastro-oesophageal reflux disease (GERD), obesity and tobacco use represent the major risk factors for the development of OAC [6-9].

Overall, OSCC and OAC exhibit quite distinctive geographic distributions. Although, the predominant type of oesophageal cancer worldwide is OSCC, the incidence of OAC has surpassed OSCC in the regions of North America, Australia and Europe over the last five decades [10] (**Figure 1.1.**). The increased incidence of OAC has been primarily associated with increased obesity and GERD [10], whereas decreased incidence of OSCC in these regions has been associated with reduction of tobacco use and alcohol consumption, particularly in Western societies [11-13]. Due to rapid

increase in the incidence [14] and high mortality [1] among OAC patients, this thesis is mostly focused on OAC.

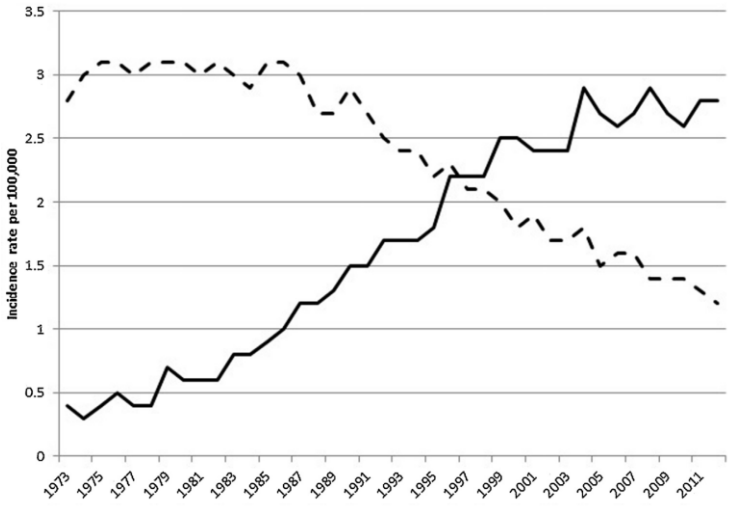

Figure 1.1. The incidence rate of OSCC (dashed line) and OAC (full line) from 1973 to 2011. Adopted from Thrift, 2016 [10].

1.1.1. Current treatment strategies for OAC

Accurate diagnosis and staging of OAC as well as assessment of patients' medical co-morbidities are essential for choosing appropriate therapy. Endoscopy is a widely used first line investigation for OAC detection and early diagnosis. It allows biopsy sampling for tissue diagnosis, as well as assessment of the tumour length and location that determines surgical approaches and the extent of radiation field.

The tumour stage is classified according to the Tumour/Node/Metastasis (T/N/M) classification system of the American Joint Committee on Cancer (AJCC) and the International Union Against Cancer [15]. High resolution multi-slice computer-aided tomography (CT) scan of chest, abdomen and pelvis is widely available so often used as a first line staging tool to determine if the patient has a locally advanced and potentially curable tumour or incurable metastatic disease. Diagnostic performance of CT scan has been shown to be highly specific, but has poor sensitivity in the detection of nodal and distant organ metastasis [16, 17]. On the other hand, positron emission tomography (PET) scan has been shown to be more sensitive and specific in detection

of metastatic disease [16, 18-21]. However, due to limitation in resolution, PET has poor sensitivity in the detection of small lesions less than 1cm in diameter [16]. Endoscopic ultrasound (EUS) is the best tool for assessing tumour invasion or T stage, with the additional ability of sampling of locoregional lymph node via fine needle aspiration [16].

OAC treatment depends on tumour (T/N/M) stage and patient's fitness. Patients with early superficial OAC disease (T1a-1b stage) can be treated by either with endoscopic mucosal or submusocal reseaction or radical resection of involved segment of the oesophagus (oesophagectomy). The main benefits of endoscopic techniques being minimally invasive so better tolerated by patients with preservation of the integrity of the oesophagus. However, endoscopic tumour resection does not treat potentially malignant associated lymph nodes. Although, the proportion of patients diagnosed with T1a-1b stage tumours is increasing, partially due to screening of Barrett's oesophagus, these patients still represent less than 10% of total OAC patients [22, 23].

T2-T4a staged tumours with or without nodal metastasis are considered locally advanced. These tumours constitute 20-30% of total OAC cancers based on Surveillance, Epidemiology, and End Results Program (SEER) (SEER fact sheet, 2016), and are approached with curable intent and treated with multimodality therapy combining surgery, chemotherapy and radiotherapy [15].

Patients with metastatic disease represent over 50% of OAC cancers. They are considered incurable and are offered palliative chemotherapy and/or radiotherapy (SEER fact sheet, 2016).

1.1.2. Molecular targeted therapy

Considering that targeted therapy has been yielding positive outcomes in cancers such as lung, breast, colorectal, ovarian or acute myeloid leukemia with significant improvement in patient survival [24, 25], there are several clinical studies assessing molecular targeted therapy in gastric and gastroesophageal junction cancers [26-28]. For example, the ToGA phase III clinical study of anti-HER2 monoclonal antibody trastuzumab in combination with chemotherapy demonstrated increased overall survival (OS) for gastric and gastroesophageal adenocarcinoma patients with HER2 overexpression (confirmed by immunohistochemistry and/or fluorescence in-situ hybridization) [29]. The ToGA clinical study results have been supported by other randomized studies [30, 31].

In addition to success with trastuzumab, two independent phase III clinical studies, RAINBOW and REGARD have demonstrated that ramucirumab, an anti-vascular endothelial growth factor receptor-2 (VEGFR-2) monoclonal antibody in combination with chemotherapy or as monotherapy, respectively, also provides modest survival benefit in patients with advanced gastric or gastroesophageal cancers [32, 33]. Given that ramucirumab represents the first efficient molecular targeted therapy as a single agent in previously treated patients with gastric and gastroesophageal cancers [33], additional clinical trials have been undertaken [28]. As a result of these clinical studies, trastuzumab or ramucirumab are administered in combination with chemotherapy as a first line or second line treatment for patients with metastatic gastric or gastro-oesophageal cancer in some countries.

However, multimodality treatment combining chemotherapy with molecular targeted therapy only moderately improves OS. For example, the addition of trastuzumab and ramucirumab to standard chemotherapy has improved OS for patients with gastric and gastroesophageal junction cancer only by 2.7 and 2.2 months, respectively [29, 33]. More recent phase II randomized trial comparing chemotherapy with and without ramucirumab showed no difference in progression free survival (PFS) between the two groups [34]. A phase III trial (RAINFALL) showed no significant association with improved OS after adding ramucirumab to the first line chemotherapy in patients with gastric and gastroesophageal junction adenocarcinomas. However, in the same trial,

ramucirumab showed a 25% reduction in the risk of disease progression or death in the primary end point of PFS [35]. Due to these mixed trial results, ramucirumab is still not an approved drug for the treatment of gastric and gastroesophageal junction cancers in some countries like Australia.

In the best case scenario, OAC patients treated with multimodality therapy including molecular targeted therapy are having moderate benefit with extended PFS and OS for several months. Unfortunately, the majority of patients exhibit only partial response or stable disease. These data suggest additional events that have compensatory effects through their intrinsic presence within cells, may contribute to the treatment resistance. In addition to intrinsic resistance, it is likely that acquired resistance plays an important role through up-regulation of oncogenic drivers, as a result of cancer cells response on molecular targeted therapy. The characterization of these secondary oncogenic alterations and their subsequent inhibition in combination with existing targeted therapy have substantial clinical implications as biomarker defined and effective multi-targeted therapies [36].

In order to develop more effective treatment, we need to better understand how OAC develops at the cellular and molecular level.

1.2. Barrett's oesophagus development and characteristics

Barrett's oesophagus is a metaplastic condition characterized by the replacement of the normal squamous epithelium with specialized columnar epithelium in the distal oesophagus [37]. OAC is considered to develop from Barrett's oesophagus through subsequent stages of low grade and high grade dysplasia [38]. The annual risk of the development of OAC from Barrett's oesophagus is low, ranging from 0.12 to 0.65% [39, 40]. Although endoscopic surveillance of patients with Barrett's oesophagus has decreased mortality rate [41] and significantly improved OAC outcome [42], compared to patients outside endoscopic surveillance programmes, the majority of patients with Barrett's oesophagus remain undiagnosed [43]. Consequently, most OAC cancers arise outside surveillance programs, and typically present at an advanced stage. This inability to detect all patients with Barrett's oesophagus, makes effective clinical management of this condition challenging. Therefore, there is a need to develop cost-

effective screening strategies in combination with clinical, blood and tissue markers for early Barrett's oesophagus detection.

1.2.1. Cellular origin of Barrett's oesophagus

A large proportion of research is focused on elucidating the cell of origin and initial mechanisms of Barrett's oesophagus development in order to detect this premalignant lesion early and prevent subsequent transition towards OAC. The pathogenesis of Barrett's oesophagus and its putative cell(s) of origin have been recently reviewed in detail [44]. Taken together, there are four major theories regarding the cellular origin of Barrett's oesophagus: oesophageal squamous cell epithelium [45, 46], oesophageal submucosal glands [47], residual embryonic cells at the gastro-oesophageal junction [48] and stem cells in the gastric cardia [49]. Given the complex network of genetic and epigenetic alterations, physiological environment and epidemiological risk factors contributing to the pathogenesis of Barrett's oesophagus, it is challenging to uniquely model its development from a single cell population.

1.2.2. GERD and molecular pathogenesis of Barrett's

It is widely appreciated that Barrett's oesophagus arises as a response to prolonged GERD [37]. The initial mechanism implicated in the development of Barrett's oesophagus is the up-regulation of certain signalling pathways and transcription factors, such as caudal-regulated homeobox (CDX) 1 and CDX2 by gastric acid and bile salts in the settings of chronic GERD [50-52]. The CDX2 transcription factor is responsible for intestinal cell differentiation and proliferation [53-56]. Importantly, CDX2 is abundantly expressed in Barrett's oesophagus, in contrast to normal squamous epithelium, and represents a marker of intestinal metaplasia in the upper gastrointestinal tract [57, 58]. In addition, it has been shown that the Hedgehog pathway can be aberrantly reactivated in normal oesophageal squamous epithelium by gastric acid or bile salts [59]. The Hedgehog pathway is active during embryonic development of the oesophagus but is normally silenced in the developed normal squamous epithelium [60]. The proposed mechanism of initiation of Barrett's oesophagus involves bone morphogenetic protein 4 (BMP4), as a Hedgehog signalling target gene, which induces expression of SOX9, an intestinal crypt

transcription factor [59]. Of importance, SOX9 has been shown to play a role in the development of Barrett's oesophagus via driving intestinal differentiation of oesophageal squamous epithelium [61].

Further, it has been shown that acid and bile salts are able to induce reactive oxygen species, oxidative stress and DNA damage [62-65]. In support of this, several studies have reported the presence of DNA damage in GERD exposed tissue and Barrett's oesophagus [66-68]. In addition, bile salts have been shown to negatively regulate DNA damage repair (DDR) enzymes, adenine DNA glycosylase (MUTYH) and N-glycosylase/DNA lyase (OGG1) in oesophageal cells [69]. Together, oxidative stress and increased DNA damage within oesophageal tissue due to exposure to acid and bile salts could contribute to the development of Barrett's oesophagus.

Notably, epigenetic regulation is likely to play a role in Barrett's oesophagus development. A higher level of CpG island methylation was observed in Barrett's oesophagus than in normal squamous epithelium [70, 71]. As such, O-6-Methylguanine-DNA Methyltransferase (MGMT) gene, encodes for a protein that is involved in DNA repair, is downregulated by promoter hyper-methylation in Barrett's oesophagus [72]. Moreover, hyper-methylation of CpG islands in promoter regions of tumour suppressor genes has been reported as a mechanism of initiation of pathogenesis, including Barrett's oesophagus, through negative regulation of these genes [70, 73, 74]. Therefore, this negative epigenetic gene regulation of key DNA repair genes or tumour suppressor genes could potentially contribute to the development of Barrett's oesophagus.

Somatic mutations present in Barrett's oesophagus have been thoroughly elucidated across different studies. Thus, inactivation of tumour suppressor gene *CDKN2A* that encodes for cyclin dependent kinase inhibitor 2A ($p16^{INK4A}$) has been frequently reported in Barrett's oesophagus [75, 76]. Furthermore, epigenetic silencing of *CDKN2A* through methylation of the promoter region has also been reported as a predominant mechanism of $p16^{INK4A}$ inactivation [77, 78], in addition to gene mutations [79] and deletions [80]. Aside from frequent mutations of *CDKN2A* in Barrett's oesophagus, mutations of other genes are less frequent. It is likely that presence of GERD predisposes cells to enter initial metaplastic processes within normal

oesophageal squamous epithelium, through increased DNA damage, leading to the eventual development of Barrett's metaplasia.

This hypothesis also links to the fact that somatic mutations present within normal oesophageal tissue are the most strongly associated with age [81], but also with heavy smoking and alcohol consumption [82]. This emphasizes the importance of epidemiological factors in initiation of carcinogenesis, besides somatic mutations. As such, the presence of clones of cells carrying somatic mutations in normal tissues might challenge the belief that somatic mutations are required for the development of metaplasia, although the frequency of these mutations per cell within normal tissue is very low, as most of the cells carry no or one driver mutation. Together, it is unclear whether certain process such as DNA damage caused by bile acids, presence of mutations, or epigenetic changes is required for the development of metaplasia, it is rather the combination of processes that are contributing to the development.

1.3. Progression from non-dysplastic Barrett's towards dysplasia and OAC

Considering that the majority of OAC patients are diagnosed at the later stages of disease progression, mostly with advanced metastatic disease (SEER fact sheet, 2016), the prognosis for this patient group is poor. However, given that the majority of patients with non-dysplastic Barrett's oesophagus are not going to progress to OAC, or even dysplasia [83], the value of endoscopic biopsy surveillance of Barrett's oesophagus has been challenged. In respect of that, novel molecular and physiological biomarkers of Barrett's oesophagus progression towards OAC are needed to efficiently stratify patients that are likely to progress.

The risk of progression towards OAC increases with diagnosis of dysplastic Barrett's oesophagus. Thus, the relative risk of progression from Barrett's oesophagus with low grade dysplasia (LGD) towards OAC is 3.47-4.8%/year [39, 84]. The progression rate towards OAC increases to up to 16-25% per year within patients diagnosed with high grade dysplasia (HGD) [85, 86]. However, certain limitations should be considered when interpreting these results, due to different histological characterization and diagnosis of non-dysplastic Barrett's oesophagus, Barrett's oesophagus with LGD vs HGD, and cancer. Although still confronting a significant gap towards effective clinical

management, the diagnosis of patients with LGD and HGD is the only determinant in predicting increased risk of progression in clinic. Hence, there is a need to better stratify these group of patients, including patients with non-dysplastic Barrett's.

To address this highly important demand, studies have shown higher risk of progression to cancer within 5 years in Barrett's oesophagus patients with increased tetraploid (4N) cell population, aneuploidy and HGD compared to patients with negative, indefinite or LGD presentation [87]. Tetraploid cells exhibit twice the normal DNA content and they are a relatively common characteristic of cancer cells. It has been suggested that aneuploidy can arise during the proliferation of unstable tetraploid cells developed as a result of whole genome doubling [88, 89]. Consistent with this, Li *et al*. characterized the genome of Barrett's oesophagus in patients who had never progressed as relatively stable, whereas the genome of Barrett's oesophagus in patients who subsequently progressed was characterized by initial chromosomal instability with gains and losses and high genome doubling during the 20,425 patient-months of follow up [90]. This concept of genome doubling leading to aneuploidy and increased risk of progression to cancer is consistent with genomic studies into OAC that describe of two theoretical models of Barrett's oesophagus progression: the slow accumulation of mutations in tumour suppressor genes leading to eventual oncogenic amplification vs. the rapid progression due to genomic doubling, leading to genomic instability and aneuploidy [91].

In addition to large genomic aberrations, methylation of single genes has also been associated with increased risk of Barrett's oesophagus progression towards OAC. Thus, promoter hypermethylation of *CDKN2A*, *RUNX3* or *HPP1* was confirmed as an independent risk factor of Barrett's oesophagus progression towards HGD and cancer [92, 93]. Similarly, hypermethylation of *APC*, *TIMP3* or *TERT* was characterized as a predictive biomarker of Barrett's oesophagus progression in another study [94]. Taken together, these data open a potential window for stratifying Barrett's oesophagus progressors. Of note, several studies have suggested that DNA methylation might be used as a predictive biomarker of Barrett's oesophagus progression towards OAC [93-95]. Therefore, characterisation of epigenetic features has been suggested as one of the risk stratification markers of Barrett's oesophagus progression towards malignancy, besides endoscopic surveillance. Although promising, clinical application

of these epigenetic alterations as biomarkers of Barrett's oesophagus progression first needs confirmation in large-scale prospective clinical trials. Therefore, we still have limited knowledge and diagnosis of dysplasia remains the only accepted marker of increased risk.

Altogether, OAC is considered to develop from Barrett's metaplasia, which is known to be caused by GERD. However, we are still unveiling the molecular drivers of this disease. Large genomic studies are now providing insights into genetic drivers of this disease.

1.4. Genomic landscape: Barrett's oesophagus vs. OAC

Whole exome and genome sequencing of matched non-dysplastic Barrett's oesophagus, dysplasia and OAC have shown high clonal heterogeneity within disease stages [91, 96]. In contrast to non-dysplastic Barrett's oesophagus, five out of six Barrett's oesophagus with high grade dysplasia shared common clonal evolution with OAC [91]. These results indicate significant clonal heterogeneity between non-dysplastic Barrett's oesophagus and OAC.

Further genomic analyses have shown high somatic mutation burden already present in non-dysplastic Barrett's oesophagus, even higher than in many human invasive cancers [91, 96]. In contrast to point mutations, structural genomic changes such as CNAs are increased during the progression from non-dysplastic Barrett's oesophagus, to dysplasia to OAC [91]. On the other hand, Ross-Innes *et al*. have reported scarce CNAs across Barrett's oesophagus with low and high grade dysplasia compared to OAC patients [96]. Together, research into the genomic landscape of Barrett's oesophagus and OAC has revealed high clonal heterogeneity and somatic mutational burden of both, whereas CNAs were significantly increasing during the progression from Barrett's oesophagus towards OAC. These findings suggest that CNAs are likely to represent an essential determinant in disease development and progression, particularly within a stage specific manner.

1.4.1 Tumour heterogeneity

Heterogeneity has been identified as significant barrier in successful treatment of cancers [97, 98], including colorectal cancers [99], gastroesophageal adenocarcinomas [100-102], and oesophageal squamous cell carcinomas [103]. One of the important determinants of heterogeneity is the presence of increased genomic instability that precedes intra-tumour heterogeneity. Of note, the presence and significance of heterogeneity in non-dysplastic Barrett's oesophagus and OAC has become evident. Firstly, heterogeneity was identified in an early stage of OAC development - non-dysplastic Barrett [96]. Secondly, the presence of heterogeneity within OAC provides a biological rationale for the low efficacy of current multimodality treatment for the OAC patients with lymph node and distant metastasis. Thus, increased heterogeneity at the level of single nucleotide mutations, insertion/deletions (indel) and amplifications between primary and metastatic tumour sites of gastro-oesophageal cancer contributes to failure of current treatments [104]. Additionally, clonal evolution of OAC cells was observed following neo-adjuvant chemotherapy [100]. Clonal evolution was based on widespread genome doublings, altered mutational spectrum, somatic CNAs and sub-clonal *NOTCH1* mutations [100, 101]. Together, tumour heterogeneity within the primary site and heterogeneity between primary and metastatic sites, as well as high clonality following neo-adjuvant treatment, predetermines relatively poor response and poor outcome for patients. Thus, capturing a more detailed molecular background of the tumour, including heterogeneity, and monitoring the molecular changes during the treatment might aid clinical management of OAC.

1.4.2. Copy number alterations (CNAs)

CNAs are frequently seen across cancers and are highly associated with disease development, progression and aggressiveness. This association is likely due to close regulation of gene expression changes via alterations in DNA copy numbers across different types of solid cancers, including breast [105, 106], prostate [107] or colorectal cancer [108].

Large scale data analyses of somatic CNAs within untreated gastrointestinal adenocarcinomas has revealed the remarkably higher prevalence of focal CNAs within gastric and oesophageal cancers than in colorectal adenocarcinomas [109]. This prevalence seemed to be independent of deletion events across the genome, meaning that higher prevalence of focal CNAs observed in gastric and oesophageal cancers are predominantly due to the amplifications, although a modest increase of focal deletions was observed in oesophageal adenocarcinomas compared to gastric and colorectal. Significantly recurrent whole arm amplifications were present across gastrointestinal adenocarcinomas of colon, stomach and oesophagus at 7p, 8q, 20p and 20q chromosomes. Likewise, these CNAs were reported from individual genomic studies [108, 110-116]. Loss of 5q, 9p and 21q were significant in OAC, whereas loss of 17p was significant in both oesophageal and gastric, but not in colorectal adenocarcinomas. Notably, the presence of these particular CNAs in OAC is not surprising, as chromosomal regions 9p, 21q and 17p contain well known tumour suppressor genes *CDKN2A*, *RUNX1* and *TP53*, respectively [109].

In addition, high copy number gain at chromosomal regions 7p11.2 (containing *EGFR* gene), 8q24.21 (*MYC*), 12p12.1–p11.23 (*KRAS*), 13q22 (*KLF5*), 13q22.3–13q31.1 (*MYCBP2 and EDNRB*), 17q12 (*ERBB2, GRB7, and CDK12*), and 19q12 (*CCNE1*) was detected in 11% of OAC, suggestive of potential oncogenic activation of amplified genes within the particular regions [110]. In support to these results, application of the genomic identification of significant target genes in cancer (GISTIC) method [117] on the same OAC dataset has identified 24 and 28 significant regions of loss and gain, respectively. Most of the GISTIC significant regions were already reported as recurrently altered, such as gained regions encoding for known oncogenes *EGFR*, *MYC*, *KRAS*, and *ERBB2* and lost regions encoding for previously reported tumour suppressor genes *CDKN2A*, *CDKN2B*, *PDE4D*, *PTPRD* [110]. Due to the low sampling size in this study, there are no CNAs with statistically significant effect on survival. Although, patients who present with gain or diploid chromosome 8: 11471452–11891169 and high gain or gain of chromosome 3:122769467–122831829 have poorer survival compared to the patients with CN loss or copy neutral LOH and diploid or CN loss, respectively [110]. Interestingly, gain of 12p chromosome has been reported as an independent prognostic determinant for relapse-free survival following oesophagectomy in OSCC [118].

Given the presence of differential and frequent CNAs across gastrointestinal cancers, including OAC, it is likely that no single CNA, either gain or loss, is associated with overall survival of the patients, but rather the combination of CNAs. Overall, CNAs present in OAC are likely to be highly contributing to the aggressiveness of this disease.

1.4.3. Mutational signatures

In addition to being a highly heterogeneous cancer dominated by copy number alterations, OAC has been characterized by six different mutational signatures with a potential for therapeutic relevance. The three prevalent mutational signatures on a per patient basis are the highly mutagenic S17, known as a hallmark of OAC with T>G substitutions, the S18 aging signature and S3, the impaired homologous recombination (HR) signature driven by *BRCA1/BRCA2* mutations, also known as the DNA Damage Repair impaired (BRCA) signature [119]. Although the BRCA signature is present in OAC patients, only few patients exhibit mutations in *BRCA1/2* genes [119], suggestive of other genetic alterations in homologous recombination pathways that predispose to this signature. Of interest, HR deficiency renders sensitivity to platinum based chemotherapy and poly(adenosine diphosphate ribose) polymerase (PARP) inhibitors in breast and ovarian cancers [120-122], and more recently reported in gastric cancer [123]. Little is known about the HR deficiency and potential application of PARP inhibitors as a treatment option in OAC. In order to utilize PARP inhibitiors in OAC, it will be essential to determine HR activity and characterize biomarkers in the patients with this DNA damage repair impaired (BRCA) signature.

Similarly, it has been suggested that OAC patients with the mutagenic S17 signature could be treated with a synthetic lethality approach in combination with radiotherapy or p53 reactivating drugs [119]. In addition, it has been suggested that these tumours might be treated with a combination of current molecular targeted therapy against overexpressed receptor tyrosine kinases (RTKs) or RTK and downstream signalling molecules considering their frequent amplification/activation. Overall, insights into OAC mutational signatures provide potential for future therapeutic interventions.

1.4.4. Genomic catastrophes

Due to advances in sequencing technology and genetic analyses over the last decade, researchers have been able to gain further detailed insights into complex genomic structural variations that occur in OAC. As such, the new phenomenon called chromothripsis that involves large scale chromosomal rearrangements occurring all at the same time has been reported in cancers [124, 125]. Of note, chromothripsis has been reported in up to 32% of OAC [126], whereas it has been less frequent in OSCC [127]. The proposed mechanisms of chromothripsis have been reviewed elsewhere [128]. Of importance, chromothripsis leads to formation of gene fusion, tumour suppressor disruption and/or oncogenic activation predetermining cell survival [125, 129].

Additionally, it has been suggested that chromosomes that underwent chromothripsis could be reassembled into formations called double minutes (DM). These structures are circular and, in contrast to normal chromosomes, lack telomeres and centromeres. However, during the S phase of the cell cycle, DM structures undergo replication, resulting in the presence of cells with double DM structures [128]. Of importance, chromosome 8 that contains the gene *MYC* has been reported to form DM structures in OAC [126]. Similarly, chromosomes 12, 13 and 20 exhibited high level of structural variations that is suggestive of chromothripsis events in OAC [126]. Therefore, these large scale chromothriptic events might underlie potent oncogene amplification, such as *MYC,* in OAC. Subsequently, cells with structural rearrangements and high copy number changes gain selective advantages and likely enter uncontrolled proliferation, leading to tumorigenesis.

1.4.5. Epigenetic regulation in Barrett's oesophagus and OAC

The main epigenetic alterations such as DNA methylation, post-translational modifications of histones, chromatin remodelling and microRNAs patterns have been implicated in the development and progression of different cancers [130]. Epigenetic alterations across Barrett's oesophagus and OAC have previously been overviewed [131, 132]. In addition, a distinctive DNA methylation signature was observed between normal squamous epithelium and Barrett's oesophagus with significantly higher levels

of methylation present in Barrett's oesophagus. Likewise, patients with HGD and OAC exhibited distinctive and significantly higher levels of DNA methylation than patients with non-dysplastic Barrett's oesophagus or normal squamous epithelium of oesophagus [71]. Interestingly, differential DNA methylation patterns subclassify colorectal tumours into groups with differential phenotypic and clinical manifestations [133, 134]. Moreover, this subclassification of the colorectal tumours opens the rationale for directing treatment based on DNA methylation pattern. In contrast, due to limited knowledge into methylation signatures in OAC, the treatment options based on methylation are significantly challenged. So far, overall goals of studies into epigenetics of OAC cancers have been defining useful biomarkers of precancerous stage and stage specific disease development.

1.4.6. Somatic mutations in OAC

OAC has one of the highest somatic mutational burdens across cancers, following lung [135] and melanoma cancers [136]. Although there is high mutational burden in OAC, clear and characterized genetic drivers of OAC as a result of mutations are still lacking. Genomic studies have revealed the landscape of significantly recurrent somatic mutations in 26 genes across OAC. Some of the significantly mutated genes in OAC include *TP53, CDKN2A*, *ARID1A*, *PIK3CA* and *SMAD4*. *TP53* is by far the most commonly mutated gene with 72% of OAC tumours exhibiting *TP53* mutations [137].

Although at a lower frequency, other significantly altered genes in OAC are *ELMO1* and *DOCK2*, which activate the intracellular mediator of Rho family GTPase, RAC1 [138, 139]. Aberrant activation of RAC1 has been associated with malignant features, including cellular motility [140, 141]. Furthermore, ELMO1 and some of the DOCK family members have been associated with invasion and migration in cancer cells [142, 143]. In line with increased invasiveness of cancer cell lines [144], genes encoding for AKAP6, HECW1*, and* AJAP1, which mediate signalling at adherens junctions, are significantly mutated in OAC [137]. Given that the majority of OAC patients present with metastatic disease at the moment of diagnosis, it is not surprising that molecules involved in regulation of cellular motility and adherens junctions are mutated and potentially contribute to invasiveness and metastasis of cancer cells.

Further, OAC harbor mutations in the genes encoding for SWI-SNF chromatin-remodelling factors including *ARID1A*, *SMARCA4* and *ARID2* [137]. Overall, these factors are acting as tumour suppressor genes across cancers [145, 146]. In contrast to the mutual exclusivity of mutations within DNA damage response genes such as *TP53* and *MDM2*, mutations in SWI-SNF genes are co-occurring, thus suggesting a synergistic effect in OAC tumourigenesis and/or progression [147].

1.4.7. Disruption of cell cycle in non-malignant and malignant cells

Dysregulation of cell cycle control is a frequently reported oncogenic mechanism in gastrointestinal adenocarcinomas [109], including OAC [137, 147]. In response to DNA damage and stress, normal cells undergo cell cycle arrest to enable DNA repair and maintain genomic integrity and stability. However, in the settings of cancer cells, the main cell cycle positive effectors, cyclin dependent kinase (CDK) 2 or CDK 4/6 and their regulatory subunit cyclins E or D1-3 [148], are commonly amplified or activated by mutation. This allows cancer cells to progress without DNA repair, leading to increased genomic instability [149, 150]. For instance, Cyclin D1 is the main positive regulator of cell cycle progression in G1 phase [148, 151, 152], and may function as an oncogene in OAC due to recurrent amplification [147]. Furthermore, the cyclin D1 polymorphism G870A has been associated with increased risk for OAC [153, 154].

CDK/cyclin effectors negatively regulate retinoblastoma protein through phosphorylation, which allows cells to progress through the cell cycle. Oesophageal cancer is characterized by overexpression of cyclin D1 and loss of retinoblastoma expression, and these alterations appear to be mutually exclusive [155]. In addition, mutually exclusive relationships between mainly oncogenic amplifications within cyclin genes (*CCNE1*, *CCND1* and *CCND3*) have been recently observed in OAC [147]. On the other hand, the direct negative regulators of CDKs and cell cycle, such as INK4 ($p16^{INK4A}$, $p15^{INK4B}$), WAF1/KIP (p21, p27, p57), p53 and Rb [149], are commonly depleted in OAC [147, 156-158].

Similarly, in the context of premalignant Barrett's oesophagus cells, dysregulated cell cycle regulation allows cells with DNA damage to divide. Given that $p16^{INK4A}$ functions

as one of the main negative regulators of cell cycle, its inactivation is likely to allow DNA damaged cells to enter uncontrolled proliferation and subsequent malignant transformation [159]. Indeed, Barrett's oesophagus cells with $p16^{INK4A}$ loss are more likely to progress towards dysplasia than cells with $p16^{INK4a}$ wild-type function [160]. Recent data has shown increased risk of the development of OAC in patients with $p16^{INK4A}$ inactivation [161]. It is clear that uncontrolled cell cycle serves as a fuel for cell growth without DNA damage repair, introducing increased genomic instability and leading to malignancy in the oesophagus.

1.5. Aberrant cancer cell growth and receptor tyrosine kinases

Since cancer cells rely on outgrowth over normal cells, it justifies the presence of multiple genetic alterations in the pathways enhancing cellular proliferation, survival, angiogenesis, invasion and metastasis. Thus, aberrant amplifications and activating mutations within RTKs comprise a large proportion of genetic alterations in OAC [137]. RTKs represent the first stage of cell interaction with the extracellular compartment through binding growth factors and activation of downstream signalling pathways. Taken together, the majority of the OAC tumours present with at least one or two amplifications/mutations in RTKs, including *EGFR*, *ERBB2* (*HER2*), *ERBB3*, *ERBB4, MET*, *FGFR2*, *NTRK1*, *IGF1R*, *RET* and *PTK2*.

Although at a lower frequency of activational mutation/amplification compared to RTKs, OAC cancer cells also aberrantly utilize signalling molecules downstream of RTKs. For example, two major signalling pathways aiding cancer cell progression and survival include mitogen-activated protein kinase (MAPK) and phosphatidylinositol 3-kinase (PI3K). Mutations in MAPK-pathway and its main effectors BRAF, KRAS and HRAS are present in ~3% of OAC, whereas PIK3CA, PIK3R1 and PTEN as a part of the PI3K pathway are mutated in up to 13% OAC tumours [137].

Based on research insights into molecular alterations within signalling pathways, numerous clinical trials have been undertaken to molecularly target gastroesophageal adenocarcinomas [24, 26, 127, 162-164]. As mentioned earlier in Section 1.1.2., there has been some success in targeting VEGFR-2 with ramucirumab and HER2 with

trastuzumab, that resulted in using these inhibitors as a first line therapy for the patients with advanced metastatic disease.

1.5.1. VEGFR-2 inhibition

Monoclonal antibody, ramucirumab is used against VEGFR-2 and is the only molecular targeted therapy that has shown significant improvements for gastric and gastroesophageal junction cancer patients when applied as a single agent [33]. The vascular endothelial growth factor (VEGF) signalling pathway is closely associated with providing nutrients for tumour growth and enabling invasion and metastasis through its known role in regulating angiogenesis and lymphangiogenesis. Therefore, it is known from long ago that tumour angiogenesis, as a hallmark of cancer, represents an important predictor of survival in lung, breast and prostate cancers [165-167].

Importantly, it is appreciated that early lymphatic spread and consequent early lymph node metastasis are characteristic of OAC, more so than in other gastrointestinal cancers [168]. Indeed, high tumour neovascularisation is associated with lymph node metastasis and poor prognosis in patients with OAC [169]. Similarly, positive CD31 staining to determine lymphatic vascular density (LVD) has been associated with lymph node metastasis, lymphovascular invasion, tumour stage and shorter disease free survival (DFS) in OAC [170]. Furthermore, it has been shown that even Barrett's oesophagus is neovascularized, with strong expression of VEGFR-2 on endothelial cells of new angiogenic blood vessels [171], suggestive of the involvement of VEGF pathway in the early pathogenesis of Barrett's oesophagus and OAC. In addition, VEGF cytokine is commonly upregulated in OAC [172, 173]. In patients with stage 1 OAC, positive expression of VEGF was significantly correlated with DFS and OS [170]. Similarly, high levels of VEGF-C expression, a member of VEGF pathway and high values of LVD are associated with shorter DFS in the patients with gastroesophageal junction adenocarcinomas [174].

Together, the research evidence supports the involvement of VEGF pathway, including its ligands and receptors, in aggressiveness of gastroesophageal

adenocarcinoma, including OAC, giving the rationale to improve current treatment by targeting this pathway.

1.5.2. HER2 inhibition

As mentioned earlier, besides ramucirumab, trastuzumab is used to inhibit HER2 overexpressing gastroesophageal adenocarcinomas, in addition to chemoradiotherapy +/- surgery treatment regimen. Overall, the addition of trastuzumab to current therapy results in only partial response and moderate improvements on overall patient survival [29].

Molecular biology underlying partial response and only moderate improvements upon treatment with trastuzumab in OAC is essential to be answered. Drawing parallels with breast cancer, where trastuzumab has been commonly used, several mechanisms of resistance have been proposed, including the presence of a truncated intracellular HER2 form, p95-HER2. This truncated HER2 retains kinase activity and ability to associate with other epidermal growth factor receptors (EGFR)s, whereas it lacks the trastuzumab binding site. Elevated expression of p95-HER2 truncated form was reported in tumours with trastuzumab resistance and associated with worse outcome in breast cancer [175, 176].

Additionally, HER2 expression levels seem to have tremendous impact on response to HER2 inhibition with trastuzumab. As such, the benefit of the trastuzumab addition to lapatinib (a small molecule that inhibits intracellular kinase domain of HER2) in neoadjuvant settings in the patients with operable breast cancer, was directly correlated with HER2 expression levels [177].

Importantly, it has been indicated that the mechanism of resistance to HER2 inhibition with trastuzumab in gastroesophageal adenocarcinoma might involve aberrant mutational inactivation of the tumour suppressor gene, *PTEN* [178] or oncogenic activation of RTKs, such as *MET* or *EGFR* [179].

In fact, complex HER2 biology, current methods of testing HER2 expression levels and tumour heterogeneity are likely to significantly contribute to the poor or just

moderately improved OAC patient outcomes upon HER2 inhibition. Therefore, we still need to develop novel and more effective therapeutic approaches.

1.6. *GRB7* gene amplification/overexpression in OAC

HER2 gene amplification and overexpression is commonly seen in OAC [180-182]. It has been shown that *HER2* gene amplification is associated with shortened patient survival and independently predicts poor outcome of patients with OAC [183].

Crucially, additional genomic analysis has identified that the amplicon containing *HER2* (17q12) also includes the *GRB7* gene encoding for growth factor receptor bound protein 7 (GRB7) and this locus is amplified in 16-32% of OAC [184-186]. In contrast to *HER2* [187-189], little is known about the functional role of *GRB7* gene amplification and overexpression and its potential as a therapeutic target in OAC and other cancers.

1.6.1. GRB7 signalling interactions

GRB7 belongs to the GRB7 adaptor family of molecules (consisting of GRB7, 10 and 14). Like other adaptor molecules, GRB7 has been shown to mediate signal transduction from distinct cell surface receptors to specific downstream signalling pathways [190]. GRB7 protein is composed of an amino-terminal proline rich domain, followed by a central domain known as the GM (Grb and Mig) domain and carboxylterminal src-holomogy 2 (SH2) domain (**Figure 1.2.**). The GM domain contains a Ras-associating (RA) domain, a central pleckstrin homology (PH) domain, and a BPS domain (between the PH and SH2 domains). GRB7 contains PXXPs motifs for binding to src-homology 3 (SH3) domain-containing proteins. The central GM region of human GRB7 protein has approximately 50% sequence homology with the *C. elegans* gene product, Mig-10, which is involved in migration of neuronal cells during embryonic development, indicating the potential role of GRB7 in cell migration. By these featured domains, GRB7 interacts with numerous signalling molecules and receptors (**Figure 1.2.**). Most of these interactions are through the SH2 domain of GRB7 protein with phospho-tyrosine sites of its binding partners [191]. Thus, GRB7 interacts with upstream receptor tyrosine kinases (e.g. EGFR/HER2/ERBB3/ERBB4,

Ret, PDGFR, c-Kit and IR), the serine-threonine kinase, Raf-MAPK, and PI3K, known to promote cell growth. In addition, GRB7 interacts with FAK, Rnd1, EphB1 and caveolin, which regulate migration [190-192]. As a result of these interactions, GRB7 is a central molecule in numerous signalling pathways that control cell growth and migration. Therefore, the amplification of GRB7 may suggest a possible role of GRB7 by itself in tumour growth, invasion and migration, independent of HER2.

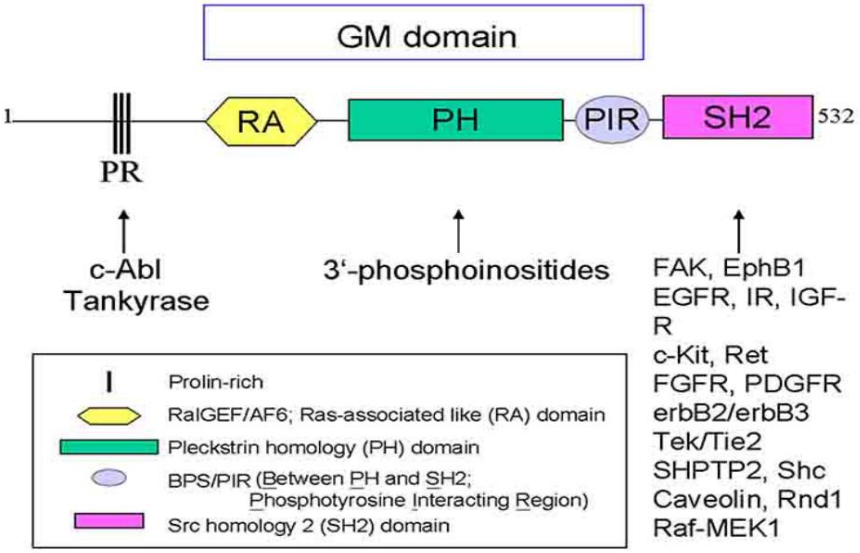

Figure 1.2. Human GRB7 domain structure and interacting proteins. Adapted from Shen and Guan, 2004 [190].

1.6.2. The functional role of GRB7 gene amplification/overexpression in cancers

The functional involvement of GRB7 either in cell proliferation, growth or migration in oesophageal cancer has not been examined. Although GRB7 expression is not detected in normal oesophageal tissue [193], GRB7 is overexpressed in approximately 47% of oesophageal squamous cell carcinomas and is significantly related to extramucosal tumour invasion [193-195]. In addition, GRB7 co-overexpression with HER2 is reported in OAC and OSCC [185, 193], gastric [196], pancreatic [197], ovarian [198] and breast cancer [199]. Most of the knowledge about GRB7 oncogenic function comes from research into breast cancer. It has been shown that signal transduction and tumour development mediated by HER2 are enhanced by GRB7

overexpression [200]. Moreover, studies have shown that GRB7 plays an independent role in tumour proliferation and migration in breast cancer [201-203]. Additionally, in a proportion of breast cancer patients, high expression levels of GRB7 do not always reflect high HER2 levels. Of interest, Ramsey et al. observed that breast cancer patients with high levels of GRB7, but low levels of HER2 have the lowest survival rate indicating the potential importance of GRB7, by itself, in tumourigenesis [203].

1.6.3. GRB7 inhibition

Based on the presented evidence of the oncogenic role of GRB7, a compound named G7-18NATE to target GRB7 overexpressing cancers has been developed [204]. G7-18NATE is a non-phosphorylated peptide compound and lacks cell permeability capacity. Thus, the addition of cell penetrating peptides (Penetratin or Tat) to G7-18NATE are required to enable its cell permeability [205]. Upon development of cell permeable G7-18NATE with penetratin (G7-18NATE-P), initial studies have shown that inhibition of GRB7 in combination with either chemotherapy or trastuzumab, results in synergistic inhibition of proliferation in breast cancer, suggesting the possible benefit of combination targeted therapy with the GRB7 inhibitor [205]. In addition, G7-18NATE-P significantly attenuated metastatic pancreatic cells in an *in vivo* mouse model system [197, 205].

Given that initial studies demonstrate potent GRB7 oncogenic function, additional pre-clinical models of functional and mechanistic characterization of GRB7 role, as well as GRB7 inhibition are necessary to improve current treatment options for patients with 17q12 amplification and consequently GRB7 overexpression in OAC and other cancers.

1.7. Driver mutations during OAC development

The development of OAC is considered to be multistep process involving loss of tumour suppressor genes leading to increased genomic instability, particularly in early stages of disease development. Increased genomic instability leads to genomic changes at the larger scale, such as genomic amplifications, that in combination with oncogenic activations allow dysplastic cells to become malignant. Together, these

events result in the development of invasive and metastatic cancer. Recent genomic studies have strongly supported this concept regarding OAC development and progression [91].

Given the numerous somatic mutations present during OAC development and progression, research is highly challenged to identify and characterize driver gene mutations from passenger mutations. Considering that most of the somatic mutations occur early in OAC development, including non-dysplastic Barrett's oesophagus [206], deciphering the functional role of mutations happening at the disease stage boundaries such as progression from non-dysplastic Barrett's to dysplastic or from HGD to cancer is fundamental to identify and characterize driver gene mutations. Essentially, this evidence would help to understand how OAC develops and subsequently provide insights into how to treat this tumour entity.

Crucially, mutations of tumour suppressor genes *TP53* and *SMAD4* occur predominantly in high grade dysplasia and cancer, respectively [206]. *TP53* encodes for p53 protein that primarily maintain cell homeostasis via regulation of cell cycle progression, apoptosis, autophagy, differentiation, senescence, metabolism and DNA repair [207]. Given that mutations in *TP53* particularly arise during the progression of non-dysplastic Barrett's to LGD and subsequently HGD, most of the patients with HGD are going to have dysfunctional p53 protein [206]. Having dysfunctional p53 protein during early Barrett's oesophagus carcinogenesis is likely to increase genomic instability [208, 209]. *TP53* mutations are most common in dysplastic tissue and OAC and present in more than 70% of patients [206]. In addition, besides losing p53 wild-type tumour suppressive function due to somatic mutations, mutant p53 protein demonstrates strong oncogenic activity through gain of function [210]. It is evident that p53 mutational dysfunction is contributing to OAC tumorigenesis through increasing genomic instability and this happens early in Barrett's carcinogenesis. However, not all patients with Barrett's oesophagus are going to progress to cancer and there is still a significant number of patients that do not require p53 mutations to develop cancer.

Of importance, the key transition from Barrett's oesophagus towards cancer is not well studied. Therefore, deciphering the key transition from Barrett's towards early cancer is essential to recapitulate the disease development and find better treatment options.

Remarkably, the only significantly altered gene at the progression from non-malignant stage towards malignancy is SMAD4. Thus, understanding the functional role of *SMAD4* tumour suppressor gene mutations at this critical stage of OAC progression is of utmost importance.

SMAD4 acts as tumour suppressor and it is a part of the TGF-β signalling pathway that has been frequently reported as altered in gastrointestinal cancers, including OAC [211]. It is well known that inactivating mutations in components of the TGF-β signalling pathway, including SMAD4, result in uncontrolled proliferation in many human cancers. Overall, these tumour suppressing or promoting effects of TGF-β on both the tumour cells and the surrounding stromal cells potentially enables TGF-β to play a role in the initiation, malignant progression and metastasis of human cancers [212].

Among other signalling pathways altered in cancer, TGF-β signalling has been difficult to approach with targeted therapy due to its dual role as a tumour suppressor and tumour promoter in cancer development and progression [213]. In this thesis, TGF-β signalling pathway and its targeted therapy in gastrointestinal cancers has been reviewed.

1.8. TGF-beta signaling and its targeted therapy in gastrointestinal cancers

(This Section contains published review paper with the title: TGF-beta signaling and its targeted therapy in gastrointestinal cancers**)**

DISCOVERY MEDICINE®
www.discoverymedicine.com
ISSN: 1539-6509; eISSN: 1944-7930

TGFβ Signaling and Its Targeted Therapy in Gastrointestinal Cancers

JOVANA RANKO GOTOVAC, KENJI MARK FUJIHARA, WAYNE ALLEN PHILLIPS, AND NICHOLAS JAMES CLEMONS

Abstract: The transforming growth factor β (TGFβ) signaling pathway governs physiological homeostasis in the gastrointestinal system and its deregulation can lead to a diverse range of human pathologies including juvenile polyposis syndrome and tumor initiation, progression, and metastasis. In gastrointestinal malignancies, tumor cells evade the known tumor suppressive effects of TGFβ signaling through frequent inactivation of the pathway. Paradoxically, tumor cells utilize TGFβ-mediated regulation of epithelial-mesenchymal transition and immunomodulation to facilitate the invasive and migratory phenotype of gastrointestinal cancers and avoid immunosurveillance. The dichotomous role of TGFβ as both a tumor suppressor and tumor promoter has highly challenged research efforts to specifically target TGFβ signaling as a cancer therapy. The current preclinical approach is to inhibit TGFβ-mediated generation of a favorable microenvironment for tumor growth, invasion, and metastasis. Here, we overview the alterations of TGFβ signaling and its fundamental biological relevance in gastrointestinal tumorigenesis. We further discuss future perspectives for efficacious molecular targeted treatment of contextual TGFβ tumor-promoting effects in gastrointestinal cancers.
[*Discovery Medicine* 26(142):103-112, September 2018]

Jovana Ranko Gotovac, [1,2], ***Kenji Mark Fujihara***, [1,2], ***Wayne Allen Phillips***, [1,2,3], *and* ***Nicholas James Clemons***, *Ph.D.*, *
1 Division of Cancer Research, Peter MacCallum Cancer Centre, Parkville, Victoria 3010, Australia.
2 Sir Peter MacCallum Department of Oncology, The University of Melbourne, Parkville, Victoria 3010, Australia.
3 Department of Surgery (St Vincent's Hospital), The University of Melbourne, Parkville, Victoria 3010, Australia.

** Corresponding Author: Nicholas James Clemons, Ph.D. (nicholas.clemons@petermac.org)*

Introduction

The transforming growth factor β (TGFβ) pathway transcriptionally regulates target genes in a cell context dependent manner (Massagué, 2012). For example, TGFβ up-regulates expression of the activating protein-1 (AP-1) transcription factor, cJUN, in epithelial cells, whereas it up-regulates the AP-1 transcription factor junB in mesenchymal cells (Verrecchia *et al.*, 2001). TGFβ plays a crucial role in embryonic development, tissue regeneration and homeostasis, cell differentiation, and regulation of inflammatory processes and the immune system. Moreover, TGFβ represents one of the major morphogens that regulate self-renewal and differentiation of embryonic stem cells, as well as somatic stem cells in the gastrointestinal tract (Mishra *et al.*, 2005). TGFβ transduction maintains homeostasis in differentiated cells through effects on multiple biological processes such as proliferation, motility, and extracellular matrix assembly (Roberts *et al.*, 2006).

Given the central role of the TGFβ pathway in these processes, it is not surprising that deregulation of this pathway is a feature of gastrointestinal cancers, as well as other cancers, where it plays a dual role, either as a highly potent tumor suppressor or a promoter of invasion and metastasis of cancer cells. Overall, these tumor suppressing or promoting effects of TGFβ on both the tumor cells and the tumor microenvironment potentially enable TGFβ to play a role in the initiation, malignant progression, and metastasis of cancers (Akhurst and Derynck, 2001).

TGFβ Signal Transduction

TGFβ exists in three isoforms in humans (TGFβ1-3) that belong to the transforming growth factor β superfamily of structurally related cytokines that also includes the bone morphogenic proteins (BMPs), growth and differentiation factors (GDFs), activins,

inhibins, and anti-mullerian hormone (AMH) (Kingsley, 1994). TGFβ is secreted in a latent form that is activated via a number of mechanisms, such as cleavage by proteases to form active homodimers. Activated TGFβ ligands bind to TGFβ type II cell surface receptor dimers, which are serine/threonine kinases (Morikawa *et al.*, 2016; Weiss and Attisano, 2013). This leads to type II-mediated recruitment and phosphorylation of type I receptors and subsequent activation of downstream TGFβ signaling (Weiss and Attisano, 2013).

Depending on the type of TGFβ receptors activated, the signal propagates through recruitment and phosphorylation of two main lines of regulatory SMADs (R-SMADs), either SMAD2/3 or SMAD1/5/8. TGFβ, activins, and nodal and some GDF ligands mainly activate SMAD2/3, while BMP, AMH, and other GDF ligands stimulate SMAD1/5/8. On the other hand, negative feedback to the pathway is maintained by inhibitory SMADs (I-SMADs), such as SMAD6 and SMAD7, which compete with R-SMADs to bind receptors or indirectly aid ubiquitination and degradation of receptor complexes (Inoue and Imamura, 2008; Itoh and Itoh, 2011). Following activation, phosphorylated R-SMAD dimers associate with the common mediator of TGFβ signaling, co-transcription factor SMAD4 (SMAD4). This R-SMAD/SMAD4 trimer complex is considered to be the major functional unit of canonical TGFβ/SMAD signaling that shuttles into the nucleus and alters gene transcription (Massagué, 2012; Morikawa *et al.*, 2016; Weiss and Attisano, 2013).

In addition to SMAD-dependent canonical signaling, TGFβ can also drive intracellular signaling through mitogen-activated protein kinase (MAPK), Rho-like GTPase, and phosphatidylinositol-3-kinase (PI3K)/AKT pathways, known as non-canonical TGFβ signaling (Zhang, 2009). The ability of TGFβ receptors to activate non-canonical TGFβ signaling, in addition to SMAD-dependent canonical signaling, shapes the final downstream effects on the cell growth, apoptosis, epithelial-mesenchymal transition (EMT), migration, and extracellular matrix assembly (Itoh *et al.*, 2003; Zhang, 2009).

Tumor Suppressive Activity of TGFβ

TGFβ tumor suppressive activity is exerted through its growth inhibitory, pro-apoptotic, and immune-modulatory effects, and it is well known that inactivating mutations in components of the TGFβ signaling pathway result in uncontrolled proliferation in many human cancers, including gastrointestinal cancers. Growth inhibition by TGFβ signaling is mainly induced through canonical SMAD-dependent down-regulation of the proto-oncogene c-Myc and up-regulation of p15 and p21, which are negative regulators of G1 phase cyclin-dependent kinases (Massagué, 2008). However, it is now known that the tumor suppressive ability of TGFβ is highly contextual and includes both canonical and non-canonical TGFβ mechanisms. For instance, non-canonical TGFβ-induced activation of the p38 MAPK pathway induces cells to undergo programmed cell death through activation of caspase 8 (Schrantz *et al.*, 2001). Moreover, the TGFβ pathway has an important tumor suppressive activity via its physiological effect on immune cell function. It has been observed that disruption of SMAD4-dependent TGFβ signaling by specific deletion of SMAD4 within T cells can promote tumorigenesis in the gastrointestinal tract (Kim *et al.*, 2006). Therefore, intact SMAD4-dependent TGFβ signaling is mandatory for the maintenance of homeostasis within the gastrointestinal microenvironment and, more importantly, for suppression of gastrointestinal cancer (Kim *et al.*, 2006). It is now clear that premalignant cells of the gastrointestinal tract tend to overcome TGFβ suppressive effect through inactivation of core components of this pathway.

Disrupted TGFβ Signaling and Juvenile Polyposis Syndrome

The importance of TGFβ tumor suppressor activity in gastrointestinal cancers is highlighted by the familial syndrome known as Juvenile Polyposis Syndrome (JPS). This is an autosomal dominant disease characterized by the formation of juvenile polyps in the gastrointestinal tract and by an increased risk for the development of gastrointestinal malignancies, predominantly colorectal (Brosens *et al.*, 2007) and gastric cancers (Aytac *et al.*, 2015). The development of JPS is associated with germline mutations in the TGFβ signaling pathway. As such, germline mutations of the *SMAD4* gene have been frequently found in patients with JPS across the gastrointestinal system (Jee *et al.*, 2013; Soer *et al.*, 2015). Indeed, recent clinicopathologic data has indicated the importance of implementing SMAD4 immunohistochemistry as an additional diagnostic test in suspected JPS within the stomach (Lawless *et al.*, 2017). Another member of the TGFβ pathway with germline mutations in a subset of JPS cases is *BMPR1A,* which encodes the BMP receptor type I (Howe *et al.*, 2001). Therefore, these data highlight the prominent preventive role of TGFβ in the genesis of gastrointestinal polyps and cancer.

Somatic Inactivation of TGFβ Signaling Across Gastrointestinal Cancers

Inactivation of the tumor suppressor activity of the TGFβ pathway also occurs frequently in sporadic gastrointestinal cancers, often through somatic genetic alterations including mutation and gene loss. For example, inactivating mutations of TGFβ signaling pathway components, including *TGFBR1, TGFBR2, ACVR1B, ACVR2A, SMAD2, SMAD3,* and *SMAD4*, occur in approximately 30% of non-hypermutated and 90% of hypermutated colorectal cancers (Cancer Genome Atlas Network, 2012). Similarly, frequent functional inactivation of SMAD4 (25%) and loss of SMAD4 (17.4%) are found in small intestine adenocarcinomas (Bläker *et al.*, 2002; Schrock *et al.*, 2017). In addition to a low frequency of mutations within SMAD4 (13%) (Weaver *et al.*, 2014), loss of heterozygosity of SMAD4 was found in 45% of esophageal adenocarcinoma (EAC) cases (Onwuegbusi *et al.*, 2006). Furthermore, comprehensive genomic analyses have revealed that 47% of pancreatic cancers exhibit mutations in TGFβ signaling molecules including *SMAD4*, *SMAD3*, *TGFBR1*, *TGFBR2*, *ACVR1B*, and *ACVR2A* (Bailey *et al.*, 2016). SMAD4 (also called DPC4, deleted in pancreatic cancer 4) is a well-known tumor suppressor in pancreatic cancers, and is also frequently inactivated in pancreatic cancer by homozygous deletion (Hahn *et al.*, 1996). The frequency of genetic alterations in TGFβ signaling components across gastrointestinal cancers is summarized in Figure 1.

Mouse Models Support a TGFβ Tumor Suppressive Role in Gastrointestinal Cancers

Further understanding of the involvement of the TGFβ signaling pathway in tumorigenesis across the gastrointestinal tract has been gathered from mouse models. In a mouse model of ulcerative colitis-associated colorectal cancer, TGFβ1 knockout was shown to promote hyperplasia and cancer following the introduction of pathogens residing in enteric flora (Engle *et al.*, 2002). These data suggest that development and progression of colorectal cancer involve dysregulation of major compartments of the TGFβ pathway and the presence of enteric microbial content, in shaping the final tumorigenic outcome. Furthermore, depletion of SMAD4 in $Apc^{\Delta 716}$ knockout mice leads to the development of malignant and invasive adenocarcinomas of the intestine (Takaku *et al.*, 1998), while homozygous deletion of SMAD3 alone results in the development of invasive colorectal adenocarcinomas (Zhu *et al.*, 1998).

Interestingly, there is also evidence from mouse models that inactivation of one allele of SMAD4 (haploinsufficiency) is sufficient to initiate tumorigenesis. For instance, mice with deletion of one SMAD4 allele initially develop gastrointestinal polyps, which subsequently progress to adenocarcinoma without inactivation of the remaining wild-type allele (Xu *et al.*, 2000). Further studies have reported that SMAD4 haploinsufficiency causes a dose-dependent inhibition of TGFβ and BMP regulated transcriptional targets, such as SMAD7 and TGFβ1 ligand (Alberici *et al.*, 2008). Overall, this emphasizes the need to elucidate the molecular mechanisms of SMAD4 haploinsufficiency initiated gastrointestinal cancers in the context of TGFβ disrupted signaling.

Negative Regulation of TGFβ Signaling in Gastrointestinal Cancers by Adaptors and Inhibitors

In addition to gene mutation and loss of canonical TGFβ pathway components, TGFβ tumor suppressor activity has also been shown to be negatively impacted by deregulation of adaptor proteins and pathway inhibitors. For example, the adaptor protein, ELF, a β-spectrin, is down-regulated in gastric cancers and plays an important role in the functional specificity and modulation of TGFβ transduction (Katuri *et al.*, 2005). In ELF knockout mice, SMAD3/4 are mislocalized and subsequently, TGFβ signaling is disrupted (Tang *et al.*, 2003), which may promote the development of early stages of colorectal cancer via increased cell proliferation and impaired apoptosis (Tang *et al.*, 2003; 2005).

In addition, TGFβ signaling is negatively regulated through the interaction of inhibitors, such as BMP activin membrane-bound inhibitor (BAMBI), with type-II TGFβ receptors, thus preventing active receptor complex formation (Onichtchouk *et al.*, 1999). In gastric cancer, activation of BAMBI in co-operation with SMAD7 has been proposed to be a mechanism of escaping TGFβ tumor suppressive activity leading to invasion and metastasis (Sasaki *et al.*, 2004; Zhang *et al.*, 2014). In contrast, inhibition of BAMBI activates canonical TGFβ signaling and decreases cell growth *in vitro* and *in vivo* (Yu and Chai, 2017). Moreover, upregulated BAMBI levels have been associated with shorter survival of patients with colorectal (Fritzmann *et al.*, 2009; Togo *et al.*, 2008) and gastric cancer (Zhang *et al.*, 2014). Therefore, BAMBI, as a negative regulator of SMAD-dependent TGFβ signaling, presents a novel potential therapeutic target in colorectal cancer.

Inhibition of TGFβ Signaling Via Transcriptional and Post-transcriptional Regulation in Gastrointestinal Cancers

Recent data have also revealed that TGFβ signaling can be inhibited by targeting expression of pathway components. For example, suppression of SMAD4 expression by promoter methylation was reported in 70% of EAC cases (Onwuegbusi *et al.*, 2006). In gastric cancer models, down-regulation of SMAD3 by miR-424-5p (Wei

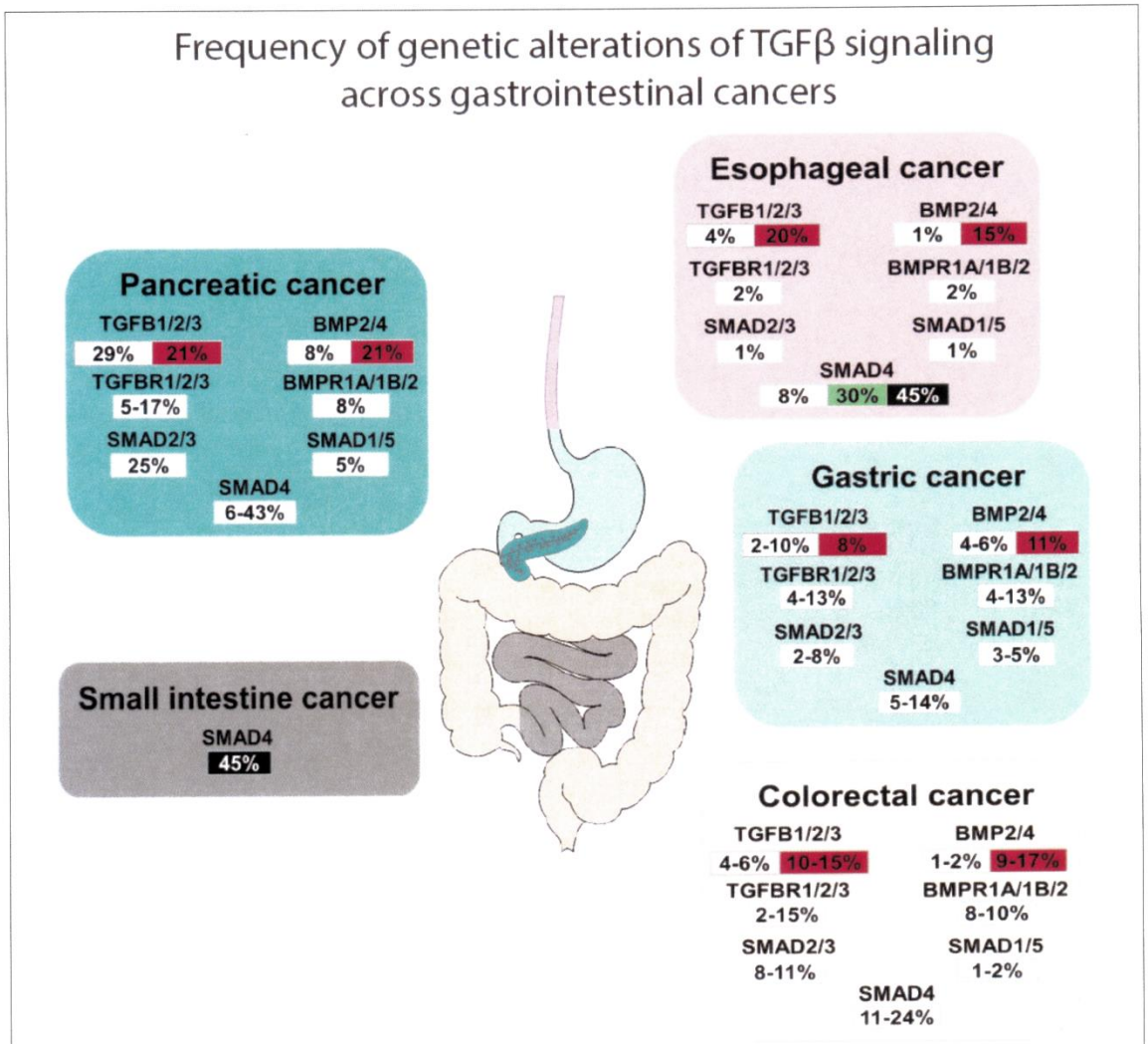

Figure 1. Frequency of genetic alterations in TGFβ pathway related genes across gastrointestinal cancers. Data has been compiled using the cBioPortal software and includes large-scale cancer genomics datasets available for each cancer: **A**) esophageal cancer (Dulak *et al.*, 2013); **B**) gastric cancer (Chen *et al.*, 2015; Cancer Genome Atlas Research Network, 2014; Wang *et al.*, 2014); **C**) colorectal cancer (Brannon *et al.*, 2014; Giannakis *et al.*, 2016; Cancer Genome Atlas Network, 2012; Seshagiri *et al.*, 2012); **D**) pancreatic cancer (Bailey *et al.*, 2016; Biankin *et al.*, 2012; Witkiewicz *et al.*, 2015). Genomic alterations including mutations, deep deletions, amplification, and multiple alterations (as defined by cBioPortal software) have been included to obtain the reported frequency for each gene (white squares). Up-regulated (red squares) and down-regulated (green squares) mRNA expressions have been reported for particular genes (where data were available). Black squares indicate frequency of genomic alterations reported in individual studies (as cited in the text) where no data were available in cBioPortal.

et al., 2016) or SMAD4 by miR-324-3p (Sun *et al.*, 2017) promotes cancer cell proliferation, emphasizing the prominent function of SMAD3 and SMAD4 as independent tumor suppressors in gastric cancer. Moreover, both miRNAs are upregulated in gastric cancer (Sun *et al.*, 2017; Wei *et al.*, 2016). Also, downregulation of TGFβR2 expression by miR-17-5p increases the proliferative capacity and migratory potential of gastric cancer cell lines (Qu *et al.*, 2016). Taken together, these data indicate that development of inhibitors of these miRNAs could be beneficial for the treatment of deregulated TGFβ pathway in gastric cancer.

The TGFβ Paradox: Tumor-promoting Functions of TGFβ Signaling

In embryonic development, TGFβ signaling regulates EMT, one of the main processes directing gastrulation. The main mechanism of TGFβ-induced EMT involves upregulation of the mesenchymal protein vimentin and downregulation of E-cadherin and other components of the epithelial cell junction (Miettinen *et al.*, 1994), thereby promoting cell motility. Thus, paradoxically, whilst the TGFβ signaling pathway undoubtedly has tumor suppressive activity that is inactivated in gastrointestinal cancers, there is also evidence that the pathway can have a tumor-promoting role, primarily through promoting tumor cell EMT and subsequent invasion and metastasis (Valcourt *et al.*, 2005).

In addition to the canonical TGFβ pathway, atypical SMAD-dependent TGFβ signaling has also been shown to regulate EMT. Recent data has shown that TGFβ-induced EMT involves activation of the SMAD1/5 branch of the signaling pathway, rather than typical SMAD2/3 activation (Ramachandran *et al.*, 2018). Previous studies demonstrated that TGFβ can phosphorylate SMAD1/5 independently of the BMP canonical pathway (Wrighton *et al.*, 2009) and this signaling requires type-I TGFβ receptors (Liu *et al.*, 2009), which were previously considered to specifically activate the SMAD2/3 branch of the signaling pathway. Also, in contrast to the paradigm of TGFβ signaling through hetero-tetramerization of type-I with type-II receptors, the TGFβ-induced EMT transcriptional response through SMAD1/5 phosphorylation requires kinase activity between two type-I receptors, TGFβR1 and ACVR1 (Ramachandran *et al.*, 2018). Importantly, activation of SMAD1/5 appears to be necessary for the pro-migratory TGFβ switch (Liu *et al.*, 2009). Moreover, TGFβ-induced EMT is highly dependent on the up-regulation of ID1, the common target gene of SMAD1/5 signaling (Ramachandran *et al.*, 2018).

Non-canonical, SMAD-independent TGFβ signaling may also have a role in EMT. For instance, TGFβ-induction of EMT involves the engagement of extracellular responsive kinase (ERK)/MAPK independent of SMADs to regulate integrin-based cell-matrix adhesion and enhance cell motility in epithelial cells (Zavadil *et al.*, 2001). To elucidate the mechanisms of non-canonical, SMAD-independent TGFβ signaling in EMT, Itoh *et al.* (2003) and Yu *et al.* (2002) generated a mutant TGFβR1 unable to activate SMADs, but with the ability to activate c-jun N-terminal kinase (JNK)/p38 MAPK pathways. By comparing cells expressing the mutant versus wild-type TGFβR1, activation of p38 MAPK was shown to be necessary but not sufficient for TGFβ-induced EMT (Yu *et al.*, 2002). In contrast, in the same cells, p38 MAPK activation is sufficient for TGFβ-induced apoptosis (Yu *et al.*, 2002). Moreover, inhibition of p38 MAPK significantly abrogates TGFβ-induced EMT, while not interfering with phosphorylation of SMAD2 (Bakin *et al.*, 2002), further suggesting that non-canonical TGFβ signaling is required for EMT.

These data give insights into the complex network of EMT regulation through both SMAD-dependent and non-canonical, SMAD-independent TGFβ signaling. Furthermore, it suggests that TGFβ may retain tumor promoting activity through non-canonical pathways when tumor suppressor function is lost through inactivation of SMADs, such as SMAD4 mutation. For example, in *in-vitro* models of the esophageal metaplasia-dysplasia-adenocarcinoma sequence, loss of SMAD4 expression leads to impaired TGFβ anti-proliferative signaling and a switch to SMAD independent activation of kinase pathways such as PI3K, ERK, and JNK (Onwuegbusi *et al.*, 2006; 2007). Consequently, through activation of kinase pathways, TGFβ promotes invasive properties of EAC cells through upregulation of plasminogen activator inhibitor 1 and urokinase proteinase activator expression (Onwuegbusi *et al.*, 2007). Thus, additional research is of utmost importance to understand the clinical relevance of TGFβ dependent transcriptional reprogramming of epithelial cancer cells into mesenchymal-like cells, thereby enhancing tumor metastasis and invasion in gastrointestinal malignancies.

TGFβ Immunosuppressive Role

Another mechanism of TGFβ-driven tumor promotion is via its potent immunosuppressive role. TGFβ1

expression is increased in a subset of cancers throughout the gastrointestinal tract (Bierie and Moses, 2006). In contrast to its tumor suppressive activity in the early stages of cancer development, high serum and tumor tissue levels of TGFβ1 correlate with poor prognosis in patients with colorectal (Lampropoulos *et al.*, 2012) and gastric cancers (Hu *et al.*, 2014). TGFβ can inhibit proliferation and function of CD8+ cytotoxic T-lymphocytes (CTL). For instance, TGFβ induces the expression of inhibitory receptors CD94/NKG2A in tumor-infiltrating CD8+ CTL and subsequently decreases CD8+ CTL cytotoxicity (Sheu *et al.*, 2005). Further, TGFβ1 produced by monocytes/macrophages impairs natural killer (NK) cell function in gastric cancer microenvironment (Peng *et al.*, 2017). NK cells present a vital anti-tumor immune response, and, importantly, reduced tumor-infiltrating NK cells correlate with poor survival and disease progression in gastric cancer (Peng *et al.*, 2017). Recent data has shown a significant association between high infiltration of macrophages and expression levels of TGFβ1 with poor prognosis in gastric cancer (Yan *et al.*, 2016). However, the exact mechanism driving the aggressive gastric cancer phenotype in these settings remains to be elucidated. Overall, regulation of TGFβ signaling may be critical in preventing tumor escape from immune surveillance (Thomas and Massagué, 2005).

Clinical Development of TGFβ Targeted Therapy

The dual tumor suppressive and promoting effects of the TGFβ signaling pathway have long been a major barrier to the development of efficacious molecular targeted therapies. Nevertheless, given that clinical studies have demonstrated that high levels of TGFβ in tumor tissues and serum are associated with worse prognosis in gastrointestinal cancers, the predominant focus for targeting TGFβ in the clinic has been through inhibition of this pathway (Katz et al., 2016). Whilst more comprehensive analyses of the therapeutics aimed at targeting TGFβ signaling can be found elsewhere (de Gramont *et al.*, 2017; Katz *et al.*, 2013), here we have focused our attention on the latest clinical advances in small molecules and biologicals. There are several druggable targets of TGFβ synthesis and signaling currently in clinical development for gastrointestinal cancers. Among these, the therapeutics most actively under clinical investigation include adoptive cell therapies, antisense molecules that prevent TGFβ synthesis, and TGFβ receptor kinase inhibitors.

Adoptive cell therapy

Following on from the success of T-cell based immunotherapies in hematological malignancies, major trials in solid tumors have been attempted, but have yielded limited efficacy, which was predominately attributed to inadequate T-cell migration to tumor sites (Yong *et al.*, 2017). Nevertheless, based on the high propensity for TGFβR2 frameshift mutations in metastatic colorectal cancer, a phase I/II trial has recently been initiated investigating adoptive cell therapy targeting mutant TGFβR2 expressing tumors with patient-derived, mRNA-engineered T-cells (NCT03431311, 2018). This therapeutic approach employs autologous T-cells by re-directing their T-cell receptors to target tumor cells expressing mutant TGFβR2. The results generated from this trial will inform whether targeting TGFβ signaling with T-cell therapies will be able to overcome the shortcomings noted in previous trials.

Trabedersen: TGFβ2 RNA interference

Trabedersen (AP 12009) is an antisense oligodeoxynucleotide designed to target the mRNA of *TGFβ2* and induce its degradation (Jaschinski *et al.*, 2011). Trabedersen, as a monotherapy, was successfully tested in a phase I/II dose escalation study in patients with advanced tumors known to overproduce TGFβ2, including pancreatic neoplasms (NCT00844064, 2011). The survival analysis from pancreatic cancer patients (N=9) reported promising efficacy with a median overall survival of 13.4 months (Oettle *et al.*, 2012). It was reported that the investigators would follow up on this study with further examination of trabedersen as a 2nd-line therapeutic avenue for patients with pancreatic cancers; however, no trials in gastrointestinal cancers are currently listed on clinicaltrials.gov at this time.

Galunisertib: TGFβ receptor kinase inhibitor

Galunisertib is an orally active small molecule inhibitor of TGFβR1 currently under clinical investigation in several tumor streams, including pancreatic cancer, colorectal cancer, and hepatocellular carcinoma. It binds to the intracellular ATP binding site of TGFβR1 and prevents its capacity to phosphorylate and activate R-SMADs (Bueno *et al.*, 2008). Results from a phase I study in advanced stage solid tumors concluded that galunisertib was well tolerated and optimal dosages can be achieved without cardiovascular toxicity (Fujiwara *et al.*, 2015). Similarly, combination therapy of galunisertib and gemcitabine was studied in advanced pancreatic cancer patients and some clinical responses in a phase Ib study were reported (Ikeda *et al.*, 2017). Additional trials in metastatic pancreatic cancer patients investigating galunisertib in combination with the anti-

PD-L1 antibody durvalumab have been initiated (NCT02734160, 2018). Galunisertib is also being studied in advanced colorectal cancer in combination with standard-of-care capecitabine (NCT03470350, 2018).

Conclusion

Given the importance of TGFβ pathway in the regulation of self-renewal and differentiation of stem cells in the gastrointestinal system, it is not surprising that deregulation of this pathway is associated with the development of severe pathological conditions, including cancer. Notwithstanding the evidence supporting TGFβ tumor suppressor activity in different stages of tumor development and progression, it becomes obvious that cancer cells take advantage of the complexity of the pathway. In fact, intact or deregulated TGFβ signaling can be utilized by cancer cells to promote EMT, invasion, and metastasis, and suppress the host immune response in cancers of the gastrointestinal tract. Given the variety of genetic and epigenetic aberrations found across the TGFβ/SMAD pathway among the different gastrointestinal cancers, a tremendous level of specificity regarding patient selection for upcoming trials will be required in order to pinpoint molecular vulnerabilities that can be exploited for therapeutic advantage. Nevertheless, since all currently available therapeutic approaches for treating gastrointestinal cancers are limited by their propensity for patients to develop resistance, the addition of TFGβ inhibitor therapy to standard-of-care or second-line sequential therapeutic regimens has the potential to provide meaningful efficacy in prolonging clinical response in gastrointestinal cancers.

Acknowledgments

N.J.C. is supported by a Fellowship (MCRF16002) from the Department of Health and Human Services acting through the Victorian Cancer Agency, Victoria, Australia.

Disclosure

The authors declare no potential conflicts of interest.

References

Akhurst RJ, Derynck R. TGF-β signaling in cancer-a double-edged sword. *Trends Cell Biol* 11(11):S44-S51, 2001.

Alberici P, Gaspar C, Franken P, Gorski MM, De Vries I, Scott RJ, Ristimäki A, Aaltonen LA, Fodde R. Smad4 haploinsufficiency: a matter of dosage. *Pathogenetics* 1(1):2, 2008.

Aytac E, Sulu B, Heald B, O'Malley M, Laguardia L, Remzi F, Kalady M, Burke C, Church J. Genotype-defined cancer risk in juvenile polyposis syndrome. *Br J Surg* 102(1):114-118, 2015.

Bailey P, Chang DK, Nones K, Johns AL, Patch A-M, Gingras M-C, Miller DK, Christ AN, Bruxner TJ, Quinn MC. Genomic analyses identify molecular subtypes of pancreatic cancer. *Nature* 531(7592):47-52, 2016.

Bakin AV, Rinehart C, Tomlinson AK, Arteaga CL. p38 mitogen-activated protein kinase is required for TGFβ-mediated fibroblastic transdifferentiation and cell migration. *J Cell Sci* 115(15):3193-3206, 2002.

Biankin AV, Waddell N, Kassahn KS, Gingras M-C, Muthuswamy LB, Johns AL, Miller DK, Wilson PJ, Patch A-M, Wu J. Pancreatic cancer genomes reveal aberrations in axon guidance pathway genes. *Nature* 491(7424):399-405, 2012.

Bierie B, Moses HL. Tumour microenvironment: TGFβ: the molecular Jekyll and Hyde of cancer. *Nat Rev Cancer* 6(7):506-520, 2006.

Bläker H, Von Herbay A, Penzel R, Groß S, Otto HF. Genetics of adenocarcinomas of the small intestine: frequent deletions at chromosome 18q and mutations of the SMAD4 gene. *Oncogene* 21(1):158-164, 2002.

Brannon AR, Vakiani E, Sylvester BE, Scott SN, Mcdermott G, Shah RH, Kania K, Viale A, Oschwald DM, Vacic V. Comparative sequencing analysis reveals high genomic concordance between matched primary and metastatic colorectal cancer lesions. *Genome Biol* 15(8):454, 2014.

Brosens LA, Van Hattem A, Hylind LM, Iacobuzio-Donahue C, Romans KE, Axilbund J, Cruz-Correa M, Tersmette AC, Offerhaus GJA, Giardiello FM. Risk of colorectal cancer in juvenile polyposis. *Gut* 56(7):965-967, 2007.

Bueno L, De Alwis DP, Pitou C, Yingling J, Lahn M, Glatt S, Troconiz IF. Semi-mechanistic modelling of the tumour growth inhibitory effects of LY2157299, a new type I receptor TGF-beta kinase antagonist, in mice. *Eur J Cancer* 44(1):142-150, 2008.

Cancer Genome Atlas Network. Comprehensive molecular characterization of human colon and rectal cancer. *Nature* 487(7407):330-337, 2012.

Cancer Genome Atlas Research Network. Comprehensive molecular characterization of gastric adenocarcinoma. *Nature* 513(7517):202-209, 2014.

Chen K, Yang D, Li X, Sun B, Song F, Cao W, Brat DJ, Gao Z, Li H, Liang H. Mutational landscape of gastric adenocarcinoma in Chinese: implications for prognosis and therapy. *Proc Natl Acad Sci U S A* 112(4):1107-1112, 2015.

De Gramont A, Faivre S, Raymond E. Novel TGF-beta inhibitors ready for prime time in onco-immunology. *Oncoimmunology* 6(1):e1257453, 2017.

Dulak AM, Stojanov P, Peng S, Lawrence MS, Fox C, Stewart C, Bandla S, Imamura Y, Schumacher SE, Shefler E. Exome and whole-genome sequencing of esophageal adenocarcinoma identifies recurrent driver events and mutational complexity. *Nat Genet* 45(5):478-486, 2013.

Engle SJ, Ormsby I, Pawlowski S, Boivin GP, Croft J, Balish E, Doetschman T. Elimination of colon cancer in germ-free transforming growth factor beta 1-deficient mice. *Cancer Res* 62(22):6362-6366, 2002.

Fritzmann J, Morkel M, Besser D, Budczies J, Kosel F, Brembeck FH, Stein U, Fichtner I, Schlag PM, Birchmeier W. A colorectal cancer expression profile that includes transforming growth factor β inhibitor BAMBI predicts metastatic potential. *Gastroenterology* 137(1):165-175, 2009.

Fujiwara Y, Nokihara H, Yamada Y, Yamamoto N, Sunami K, Utsumi H, Asou H, Takahash IO, Ogasawara K, Gueorguieva I, Tamura T. Phase 1 study of galunisertib, a TGF-beta receptor I kinase inhibitor, in Japanese patients with advanced solid tumors. *Cancer Chemother Pharmacol* 76(6):1143-1152, 2015.

Giannakis M, Mu XJ, Shukla SA, Qian ZR, Cohen O, Nishihara R, Bahl S, Cao Y, Amin-Mansour A, Yamauchi M. Genomic correlates of immune-cell infiltrates in colorectal carcinoma. *Cell Rep* 15(4):857-865, 2016.

Hahn SA, Schutte M, Hoque AS, Moskaluk CA, Da Costa LT, Rozenblum E, Weinstein CL, Fischer A, Yeo CJ, Hruban RH. DPC4, a candidate tumor suppressor gene at human chromosome 18q21. 1. *Science* 271(5247):350-353, 1996.

Howe JR, Bair JL, Sayed MG, Anderson ME, Mitros FA, Petersen GM, Velculescu VE, Traverso G, Vogelstein B. Germline mutations of the gene encoding bone morphogenetic protein receptor 1A in juvenile polyposis. *Nat Genet* 28(2):184-187, 2001.

Hu W-Q, Wang L-W, Yuan J-P, Yan S-G, Li J-D, Zhao H-L, Peng C-W, Yang G-F, Li Y. High expression of transform growth factor beta 1 in gastric cancer confers worse outcome: results of a cohort study on 184 patients. *Hepatogastroenterology* 61(129):245-250, 2014.

Ikeda M, Takahashi H, Kondo S, Lahn MMF, Ogasawara K, Benhadji KA, Fujii H, Ueno H. Phase 1b study of galunisertib in combination with gemcitabine in Japanese patients with metastatic or locally advanced pancreatic cancer. *Cancer Chemother Pharmacol* 79(6):1169-1177, 2017.

Inoue Y, Imamura T. Regulation of TGF β family signaling by E3 ubiquitin ligases. *Cancer Sci* 99(11):2107-2112, 2008.

Itoh S, Itoh F. Inhibitory machinery for the TGF-β family signaling pathway. *Growth Factors* 29(5):163-173, 2011.

Itoh S, Thorikay M, Kowanetz M, Moustakas A, Itoh F, Heldin C-H, Ten Dijke P. Elucidation of Smad requirement in transforming growth factor-β type I receptor-induced responses. *J Biol Chem* 278(6):3751-3761, 2003.

Jaschinski F, Rothhammer T, Jachimczak P, Seitz C, Schneider A, Schlingensiepen KH. The antisense oligonucleotide trabedersen (AP 12009) for the targeted inhibition of TGF-beta2. *Curr Pharm Biotechnol* 12(12):2203-2213, 2011.

Jee MJ, Yoon SM, Kim EJ, Choi H-J, Kim J-W, Sung RH, Han JH, Chae HB, Park SM, Youn SJ. A novel germline mutation in exon 10 of the SMAD4 gene in a familial juvenile polyposis. *Gut Liver* 7(6):747-751, 2013.

Katuri V, Tang Y, Marshall B, Rashid A, Jogunoori W, Volpe EA, Sidawy AN, Evans S, Blay J, Gallicano GI. Inactivation of ELF/TGF-β signaling in human gastrointestinal cancer. *Oncogene* 24(54):8012-8024, 2005.

Katz LH, Li Y, Chen JS, Munoz NM, Majumdar A, Chen J, Mishra L. Targeting TGF-beta signaling in cancer. *Expert Opin Ther Targets* 17(7):743-760, 2013.

Katz LH, Likhter M, Jogunoori W, Belkin M, Ohshiro K, Mishra L. TGF-beta signaling in liver and gastrointestinal cancers. *Cancer Lett* 379(2):166-172, 2016.

Kim B-G, Li C, Qiao W, Mamura M, Kasperczak B, Anver M, Wolfraim L, Hong S, Mushinski E, Potter M. Smad4 signalling in T cells is required for suppression of gastrointestinal cancer. *Nature* 441(7096):1015-1019, 2006.

Kingsley DM. The TGF-beta superfamily: new members, new receptors, and new genetic tests of function in different organisms. *Genes Dev* 8(2):133-146, 1994.

Lampropoulos P, Zizi-Sermpetzoglou A, Rizos S, Kostakis A, Nikiteas N, Papavassiliou AG. TGF-beta signalling in colon carcinogenesis. *Cancer Lett* 314(1):1-7, 2012.

Lawless ME, Toweill DL, Jewell KD, Jain D, Lamps L, Krasinskas AM, Swanson PE, Upton MP, Yeh MM. Massive gastric juvenile polyposis: a clinicopathologic study using SMAD4 immunohistochemistry. *Am J Clin Pathol* 147(4):390-390, 2017.

Liu IM, Schilling SH, Knouse KA, Choy L, Derynck R, Wang XF. TGFβ stimulated Smad1/5 phosphorylation requires the ALK5 L45 loop and mediates the pro migratory TGFβ switch. *EMBO J* 28(2):88-98, 2009.

Massagué J. TGFβ in cancer. *Cell* 134(2):215-230, 2008.

Massagué J. TGFβ signalling in context. *Nat Rev Mol Cell Biol* 13(10):616-630, 2012.

Miettinen PJ, Ebner R, Lopez AR, Derynck R. TGF-beta induced transdifferentiation of mammary epithelial cells to mesenchymal cells: involvement of type I receptors. *J Cell Biol* 127(6):2021-2036, 1994.

Mishra L, Shetty K, Tang Y, Stuart A, Byers SW. The role of TGF-β and Wnt signaling in gastrointestinal stem cells and cancer. *Oncogene* 24(37):5775-5789, 2005.

Morikawa M, Derynck R, Miyazono K. TGF-β and the TGF-β family: context-dependent roles in cell and tissue physiology. *Cold Spring Harb Perspect Biol* 8(5):a021873, 2016.

NCT00844064. Safety and Tolerability of AP 12009, Administered I.V. in Patients With Advanced Tumors Known to Overproduce TGF-beta-2. Available online at: https://clinicaltrials.gov/ct2/show/NCT00844064 (accessed 21/05/2018). 2011.

NCT02734160. A Study of Galunisertib (LY2157299) and Durvalumab (MEDI4736) in Participants With Metastatic Pancreatic Cancer. Available online at: https://clinicaltrials.gov/ct2/show/NCT02734160 (accessed 25/05/2018). 2018.

NCT03431311. T Cell Receptor Based Therapy of Metastatic Colorectal Cancer (TCR-CRC-001). Available online at: https://clinicaltrials.gov/ct2/show/NCT03431311 (accessed 30/05/2018). 2018.

NCT03470350. Galunisertib and Capecitabine in Advanced Resistant TGF-beta Activated Colorectal Cancer (EORTC1615). Available online at: https://clinicaltrials.gov/ct2/show/NCT03470350 (accessed 25/05/2018). 2018.

Oettle H, Seufferlein T, Luger T, Schmid RM, Wichert GV, Endlicher E, Garbe C, Kaehler KK, Enk A, Schneider A, Rothhammer-Hampl T, Grosser S, Kiessling P. Final results of a phase I/II study in patients with pancreatic cancer, malignant melanoma, and colorectal carcinoma with trabedersen. *J Clin Oncol* 30(15_suppl):4034-4034, 2012.

Onichtchouk D, Chen Y-G, Dosch R, Gawantka V, Delius H, Massague J, Niehrs C. Silencing of TGF-β signalling by the pseudoreceptor BAMBI. *Nature* 401(6752):480-485, 1999.

Onwuegbusi BA, Aitchison A, Chin S-F, Kranjac T, Mills I, Huang Y, Lao-Sirieix P, Caldas C, Fitzgerald RC. Impaired transforming growth factor β signalling in Barrett's carcinogenesis due to frequent SMAD4 inactivation. *Gut* 55(6):764-774, 2006.

Onwuegbusi BA, Rees JR, Lao-Sirieix P, Fitzgerald RC. Selective loss of TGFβ Smad-dependent signalling prevents cell cycle arrest and promotes invasion in oesophageal adenocarcinoma cell lines. *PLoS One* 2(1):e177, 2007.

Peng L-S, Zhang J-Y, Teng Y-S, Zhao Y-L, Wang T-T, Mao F-Y, Lv Y-P, Cheng P, Li W-H, Chen N. Tumor-associated monocytes/macrophages impair NK-cell function via TGFb1 in human gastric cancer. *Cancer* 5(3):248-256, 2017.

Qu Y, Zhang H, Duan J, Liu R, Deng T, Bai M, Huang D, Li H, Ning T, Zhang L. MiR-17-5p regulates cell proliferation and migration by targeting transforming growth factor-β receptor 2 in gastric cancer. *Oncotarget* 7(22):33286-33296, 2016.

Ramachandran A, Vizan P, Das D, Chakravarty P, Vogt J, Rogers KW, Müller P, Hinck AP, Sapkota GP, Hill CS. TGF-β uses a novel mode of receptor activation to phosphorylate SMAD1/5 and induce epithelial-to-mesenchymal transition. *Elife* 7:e31756, 2018.

Roberts AB, Tian F, Byfield SD, Stuelten C, Ooshima A, Saika S, Flanders KC. Smad3 is key to TGF-β-mediated epithelial-to-mesenchymal transition, fibrosis, tumor suppression and metastasis. *Cytokine Growth Factor Rev* 17(1-2):19-27, 2006.

Sasaki T, Sasahira T, Shimura H, Ikeda S, Kuniyasu H. Effect of Nma on growth inhibition by TGF-βa in human gastric carcinoma cell lines. *Oncol Rep* 11(6):1219-1223, 2004.

Schrantz N, Bourgeade M-F, Mouhamad S, Leca G, Sharma S, Vazquez A. p38-mediated regulation of a Fas-associated death domain protein-independent pathway leading to caspase-8 activation during TGFβ-induced apoptosis in human Burkitt lymphoma B cells BL41. *Mol Biol Cell* 12(10):3139-3151, 2001.

Schrock AB, Devoe CE, Mcwilliams R, Sun J, Aparicio T, Stephens PJ, Ross JS, Wilson R, Miller VA, Ali SM. Genomic profiling of small-bowel adenocarcinoma. *JAMA Oncol* 3(11):1546-1553, 2017.

Seshagiri S, Stawiski EW, Durinck S, Modrusan Z, Storm EE, Conboy CB, Chaudhuri S, Guan Y, Janakiraman V, Jaiswal BS. Recurrent R-spondin fusions in colon cancer. *Nature* 488(7413):660-664, 2012.

Sheu B-C, Chiou S-H, Lin H-H, Chow S-N, Huang S-C, Ho H-N, Hsu S-M. Up-regulation of inhibitory natural killer receptors CD94/NKG2A with suppressed intracellular perforin expression of tumor-infiltrating CD8+ T lymphocytes in human cervical carcinoma. *Cancer Res* 65(7):2921-2929, 2005.

Soer E, Tot Nederveen WHDV, Ligtenberg MJ, Moll F, Pierik RG, Vecht J, Vasen HF, Flierman A. Massive gastric polyposis associated with a germline SMAD4 gene mutation. *Fam Cancer* 14(4):569-573, 2015.

Sun G-L, Li Z, Wang W-Z, Chen Z, Zhang L, Li Q, Wei S, Li B-W, Xu J-H, Chen L. miR-324-3p promotes gastric cancer development by activating Smad4-mediated Wnt/beta-catenin signaling pathway. *J Gastroenterol* 1-15, 2017.

Takaku K, Oshima M, Miyoshi H, Matsui M, Seldin MF,

Taketo MM. Intestinal tumorigenesis in compound mutant mice of both Dpc4 (Smad4) and Apc genes. *Cell* 92(5):645-656, 1998.

Tang Y, Katuri V, Dillner A, Mishra B, Deng C-X, Mishra L. Disruption of transforming growth factor-β signaling in ELF β-spectrin-deficient mice. *Science* 299(5606):574-577, 2003.

Tang Y, Katuri V, Srinivasan R, Fogt F, Redman R, Anand G, Said A, Fishbein T, Zasloff M, Reddy EP. Transforming growth factor-β suppresses nonmetastatic colon cancer through Smad4 and adaptor protein ELF at an early stage of tumorigenesis. *Cancer Res* 65(10):4228-4237, 2005.

Thomas DA, Massagué J. TGF-β directly targets cytotoxic T cell functions during tumor evasion of immune surveillance. *Cancer Cell* 8(5):369-380, 2005.

Togo N, Ohwada S, Sakurai S, Toya H, Sakamoto I, Yamada T, Nakano T, Muroya K, Takeyoshi I, Nakajima T. Prognostic significance of BMP and activin membrane-bound inhibitor in colorectal cancer. *World J Gastroenterol* 14(31):4880-4888, 2008.

Valcourt U, Kowanetz M, Niimi H, Heldin C-H, Moustakas A. TGF-β and the Smad signaling pathway support transcriptomic reprogramming during epithelial-mesenchymal cell transition. *Mol Biol Cell* 16(4):1987-2002, 2005.

Verrecchia F, Tacheau C, Schorpp-Kistner M, Angel P, Mauviel A. Induction of the AP-1 members c-Jun and JunB by TGF-β/Smad suppresses early Smad-driven gene activation. *Oncogene* 20(18):2205-2211, 2001.

Wang K, Yuen ST, Xu J, Lee SP, Yan HH, Shi ST, Siu HC, Deng S, Chu KM, Law S. Whole-genome sequencing and comprehensive molecular profiling identify new driver mutations in gastric cancer. *Nat Genet* 46(6):573-582, 2014.

Weaver JM, Ross-Innes CS, Shannon N, Lynch AG, Forshew T, Barbera M, Murtaza M, Ong C-aJ, Lao-Sirieix P, Dunning MJ. Ordering of mutations in preinvasive disease stages of esophageal carcinogenesis. *Nat Genet* 46(8):837-843, 2014.

Wei S, Li Q, Li Z, Wang L, Zhang L, Xu Z. miR-424-5p promotes proliferation of gastric cancer by targeting Smad3 through TGF-β signaling pathway. *Oncotarget* 7(46):75185-75196, 2016.

Weiss A, Attisano L. The TGFbeta superfamily signaling pathway. *Wiley Interdiscip Rev Dev Biol* 2(1):47-63, 2013.

Witkiewicz AK, Mcmillan EA, Balaji U, Baek G, Lin W-C, Mansour J, Mollaee M, Wagner K-U, Koduru P, Yopp A. Whole-exome sequencing of pancreatic cancer defines genetic diversity and therapeutic targets. *Nat Commun* 6:6744, 2015.

Wrighton KH, Lin X, Paul BY, Feng X-H. Transforming growth factor β can stimulate Smad1 phosphorylation independently of bone morphogenic protein receptors. *J Biol Chem* 284(15):9755-9763, 2009.

Xu X, Brodie SG, Yang X, Im Y-H, Parks WT, Chen L, Zhou Y-X, Weinstein M, Kim S-J, Deng C-X. Haploid loss of the tumor suppressor Smad4/Dpc4 initiates gastric polyposis and cancer in mice. *Oncogene* 19(15):1868-1874, 2000.

Yan Y, Zhang J, Li J-H, Liu X, Wang J-Z, Qu H-Y, Wang J-S, Duan X-Y. High tumor-associated macrophages infiltration is associated with poor prognosis and may contribute to the phenomenon of epithelial-mesenchymal transition in gastric cancer. *Onco Targets Ther* 9:3975-3983, 2016.

Yong CSM, Dardalhon V, Devaud C, Taylor N, Darcy PK, Kershaw MH. CAR T-cell therapy of solid tumors. *Immunol Cell Biol* 95(4):356-363, 2017.

Yu L, Hébert MC, Zhang YE. TGF¯β receptor¯activated p38 MAP kinase mediates Smad_independent TGF□β responses. *EMBO J* 21(14):3749-3759, 2002.

Yu W, Chai H. Inhibition of BAMBI reduces the viability and motility of colon cancer via activating TGF-β/Smad pathway in vitro and in vivo. *Oncol Lett* 14(4):4793-4799, 2017.

Zavadil J, Bitzer M, Liang D, Yang Y-C, Massimi A, Kneitz S, Piek E, Böttinger EP. Genetic programs of epithelial cell plasticity directed by transforming growth factor-β. *Proc Natl Acad Sci USA* 98(12):6686-6691, 2001.

Zhang Y, Yu Z, Xiao Q, Sun X, Zhu Z, Zhang J, Xu H, Wei M, Sun M. Expression of BAMBI and its combination with Smad7 correlates with tumor invasion and poor prognosis in gastric cancer. *Tumor Biol* 35(7):7047-7056, 2014.

Zhang YE. Non-Smad pathways in TGF-β signaling. *Cell Res* 19(1):128-139, 2009.

Zhu Y, Richardson JA, Parada LF, Graff JM. Smad3 mutant mice develop metastatic colorectal cancer. *Cell* 94(6):703-714, 1998.

1.9. Overall summary and focus of thesis

The prognosis for all patients diagnosed with oesophageal cancer is relatively poor, with 5 year survival rates ranging from 15 to 22% [10, 214]. Unfortunately, the majority of the patients present with advanced, incurable disease and palliative therapy is the only option. Crucially, we need to develop better treatment options.

OAC is considered to develop from Barrett's metaplasia. Based on the studies into Barrett's oesophagus, the linear model of Barrett's oesophagus progression towards OAC has been supported. This model depicts OAC development from Barrett's oesophagus through increasing grades of dysplasia.

Notwithstanding clinical and basic research efforts in seeking for useful biomarkers for early detection of OAC, the only validated biomarker of Barrett's oesophagus progression towards cancer is the presence of dysplasia. Unfortunately, the detection of dysplasia is not sufficient, and we still lack defined molecular drivers of disease progression. One of the main barriers in defining molecular drivers is the fact that the majority of recurrent mutations in OAC are also present across earlier stages of the disease development. Indeed, the only two mutations identified to arise in a stage specific manner are mutations in *TP53* and *SMAD4*, in HGD and cancer, respectively. One of the main goals of this thesis is to define the driver(s) of progression from HGD to OAC. Thus, this essential stage of malignant progression from HGD towards OAC is the primary focus.

In addition, current treatment options including chemo-radio therapy with/without surgery, are confronting significant challenges, mostly due to intrinsic and/or acquired resistance. Promisingly, implementing molecular targeted therapy as a line of therapy for HER2+ metastatic OAC patients has improved overall patient survival by several months. Nevertheless, despite these improvements, we still need to characterize novel oncogenic molecular drivers of this disease, and more importantly, develop long term effective therapies. Given that oncogenic amplifications represent potent drivers of disease development, particularly at the later stages, thus this thesis will examine the effect of frequent GRB7 amplification in OAC.

Importantly, this doctorate thesis focuses on critical characterization of SMAD4 loss on tumour development and progression and the role of GRB7 amplification in OAC.

1.10. Research hypotheses and aims:

Overall research hypothesis 1: SMAD4 loss drives the progression of Barrett's oesophagus towards OAC

Research aim 1.1: To determine the effect of SMAD4 loss on tumourigenicity of Barrett's oesophagus cells
Hypothesis 1.1: Hypothesis: Loss of SMAD4 enhances initiation of tumourigenesis in Barrett's oesophagus

Research aim 1.2: To determine the effects of SMAD4 loss on TGF-β signalling in OAC
Hypothesis 1.2: SMAD4 loss switches TGF-β and BMP4 signalling from anti-tumourigenic to tumour promoting in Barrett's oesophagus

Overall research hypothesis 2: *GRB7* gene amplification and overexpression is a driver of tumour progression in OAC

Research aim 2.1. Characterize gene copy number/expression status (mRNA, protein) of GRB7 and HER2 in OAC patient cohort and panel of OAC cell lines

Research aim 2.2. Characterize the functional role of GRB7 gene amplification/overexpression in OAC

Research aim 2.3. To establish GBR7 as a potential therapeutic target in oesophageal cancer alone or in combination with current chemo/targeted therapy

CHAPTER 2.

MATERIALS AND METHODS

2.1. CP-B cell line characteristics and culture

CP-B cells (also identified as CP52731 or ChTERT) are human epithelial cells immortalized with exogenous expression of human telomerase reverse transcriptase protein [215]. The primary cells from which this line was derived were obtained from a region of human Barrett's oesophagus containing high grade dysplasia, which makes them a suitable cell model system for studying Barrett's tumourigenesis. Karyotypically, CP-B cells are hypodiploid with the tendency to duplicate into tetraploid (4N) cells. The approximate percentage of the cells with 4N DNA content within the whole CP-B cell population was reported as 24.9% [215]. A slight increase in the proportion of tetraploid cells was observed in the stock of cells used in this thesis (data not shown).

CP-B parental cells were grown in MCDB-153 medium containing 0.4 µg/mL hydrocortisone, 20 ng/mL recombinant human epidermal growth factor, 20 mg/mL adenine, ITS Liquid Media Supplement (100x for the final concentration: 2.5 µg/mL insulin, 1.4 µg/mL transferrin, 1.3 ng/mL selenium), 140 µg/mL bovine pituitary extract, 10 nmol/l cholera toxin (all obtained from Sigma-Aldrich, St. Louis, Missouri, US), 5% (v/v) fetal bovine serum (FBS) obtained from Gibco, Thermo Fisher, Waltham, Massachusetts, US), 375 ng/mL diflucan (Sigma-Aldrich), and 4 mmol/l L-glutamine (Glutamax, Invitrogen, Castle Hill, Australia) adjusted to a pH of 7.2. Cells were grown in monolayer cultures in humidified incubators at 37°C with 5% CO_2. Cell line authentication was conducted by Short Tandem Repeat (STR) analysis using the PowerPlex® 16 genotyping system (Promega, Wisconsin, US) and cultures were confirmed as mycoplasma free by polymerase chain reaction (PCR) (Cerberus Sciences, Scoresby, Australia).

2.2. Cell viability assay

AlamarBlue® (Life Technologies, Melbourne, Australia) reagent was used to determine cell viability. This assay measures the conversion of non-fluorescent and non-toxic cell permeable resazurin to highly fluorescent resorufin by the reducing power of living cells. For assessing cell viability, cells were seeded in a 96-well format plate, and allowed to adhere overnight. Following treatment or plating only, 20% (v/v)

AlamarBlue® was added to each well, incubated in humidified incubators for 2 h at 37°C, and the intensity of fluorescence measured using a FLUOstar OPTIMA microplate reader 89 (BMG Labtech, Mornington, Australia) at an excitation wavelength of 540 nm and an emission wavelength of 590 nm. The intensity of fluorescence was measured every 24 hours or at the last time point.

2.3. Cellular proliferation (confluency) assay

Cellular proliferation was determined using the IncuCyte Live-Cell Analysis System that automatically captures and analyzes images of living cells based on algorithms for each cell line designed using proprietary software (Incucyte FLR, Essen BioScience, Ann Arbor, Mitchigan, US). For these experiments, cells were seeded in 96-well plates and allowed to adhere overnight. Following treatment or plating only, cells were imaged either every 24 hours or at the last time point.

2.4. Cell cycle analysis

One x 10^6 cells were seeded in 10cm Petri dishes, allowed to adhere and grow for 48 hours, then treated with 10ng/mL TGF-β1 for 24 hours. Following the treatment, all adherent cells were collected, centrifuged and the supernatant removed. Cells were washed in cold phosphate buffered saline (PBS) with 1% FBS, fixed with ice-cold 70% ethanol then stained for 120 minutes at room temperature in the dark with 25µg/mL propidium iodide (Molecular Probes, Eugene, Oregon US) and 40µg/mL RNAse A (Qiagen, Hilden, Germany) dissolved in PBS. At least 1 x 10^4 single cell events were detected by flow cytometry (BD FACSCanto™ II, BD Bioscience, San Jose, Canada) and analyzed using Flowlogic software (Inivai Technologies, Mentone, Australia). The distribution of cells in each cell cycle phase was presented as a percentage of the total cell population.

2.5. Western blot analysis

Whole-cell protein extracts were prepared by lysis at 4°C in RIPA buffer (1 mmol/l EDTA; 1% (v/v) NP40; 0.5% (w/v) sodium deoxycholate; 0.1% (v/v) SDS; 50 mmol/l sodium fluoride; 1 mmol/l sodium pyrophosphate in PBS), containing phosphatase

(PhosphoSTOP, Roche, Hawthorn, Australia) and protease (Complete ULTRA, Roche) inhibitors. Protein quantification was performed using a BioRad DC protein assay (BioRad, Hercules, California, US). Equivalent amounts of total protein lysates were suspended in 5x SDS sample buffer, and RIPA buffer was added to reach final concentration of 1x SDS sample buffer (313 mmol/l Tris HCl pH 6.8, 50% (v/v) Glycerol, 10% (v/v) β-mercaptoethanol, 10% (w/v) SDS, 0.05% (w/v) bromophenol blue), boiled and resolved by SDS-PAGE using 10 to 15% (w/v) polyacrylamide gels. Following SDS-PAGE, proteins were semi-dry transferred to methanol-activated polyvinylidene difluoride membranes. Immunoblots were blocked for 1 hour in 5% (w/v) skim milk dissolved in Tris-buffered saline (TBS) containing 0.1% (v/v) Tween 20 and then probed overnight at 4°C with the primary antibody, followed by incubation with corresponding peroxidase-conjugated secondary antibody (Agilent Technologies, California, US) for 1 hour at room temperature. The primary and secondary antibodies used for western blotting are listed in **Table 2.1**. The horseradish peroxidase (HRP) conjugated secondary antibodies were detected using Western Lightning Enhanced Chemiluminescence (PerkinElmer, MA, US) or ECL Plus western blotting substrate kits (Thermo Scientific, Scoresby, Australia). Membranes were reprobed with anti-β-actin, anti-HSP90 α/β or anti-GAPDH antibodies to assess protein loading. All blots were washed thrice in rinsing buffer (0.1% (v/v) Tween 20 in TBS) for 10 min between different incubations.

Table 2.1. Antibodies for western blotting and immunohistochemistry

Antibody	Origin	Clone	Source	Use
Anti-SMAD4	Rabbit	D3M6U	Cell signalling technology	WB
Anti-p21	Rabbit	12D1	Cell signalling technology	WB
Anti-CDC6	Mouse	sc-9964	Santa-Cruz	WB
Ani-human mitochondrial	Mouse	MAB1273	MilliporeSigma	IHC
Anit-CK7	Mouse	OV-TL 12/30	Agilent Technologies	IHC
Anti-β-actin	Mouse	C4	MP-Biomedical	WB
Anti- GAPDH	Mouse	6C5	MilliporeSigma	WB
Swine anti-rabbit-HRP	Swine	P0217	Agilent Technologies	WB
Goat anti-mouse-HRP	Goat	P0447	Agilent Technologies	WB

WB=Western Blotting; IHC=Immunohistochemistry. Source: Cell signalling Technology (CST), Massachusetts, US; Santa Cruz Biotechnology, Inc., Texas, US; MilliporeSigma, Massachusetts, US and Abcam, Cambridge, UK.

2.6. shRNA mediated stable SMAD4 knockdown

Stable SMAD4 knockdown was performed using microRNA-adapted shRNA with the pGIPZ lentiviral vector (Dharmacon™ GIPZ™ Lentiviral Vector, Dharmacon, Colorado, US) according to manufacturer instructions. The sequences of the four SMAD4 shRNA used are listed in **Table 2.2**.

Table 2.2. SMAD4 shRNA sequences.

Vendor Reagent ID	Sequence
V3LHS_408444	AGAGAAGTTCTCAAAGTTA
V3LHS_359404	ACGAGTTGTATCACCTGGA
V2LHS_37196	CTGCTAAATTCTATGTTAA
V2LHS_37198	GACAATATGTCTATTACGA

2.7. Production of lentiviral particles

HEK293T cells were seeded at low confluency in T75 flasks two days prior to transfection, and fresh media was changed 24 hours prior to transfection. Ten µg of vector DNA plasmid together with 10 µg of Lenti-X packaging mix (Clontech, Mountain view, US) and polyethylenimine (Sigma-Aldrich, 4.5 µg/µg DNA) in DMEM media containing tetracycline free FBS were applied drop-wise onto the HEK293T cells. Culture medium was changed after 24 hours, and viral supernatant collected at 72 and 96 hours after transfection. Supernatant was filtered through a 0.45 µm filter to make cell free supernatant and concentrated using an Amicon Ultra-15 Centrifugal Filtration Unit (Merck Millipore, Bayswater, Australia). Prior to transduction of target cells, 8 µg/mL of polybrene (Sigma-Aldrich) was added to each viral aliquot.

2.8. SMAD4 knockout using CRISPR/Cas9 technology

The experimental work for genomic knockout of SMAD4 was adopted from previously established protocols [216, 217]. Briefly, lentiviral vectors containing constitutive expressing endonuclease Cas9 linked via T2A peptide to mCherry fluorescent protein or tetracycline-inducible single guide RNA (sgRNA) expression constructs with ubiquitin promoter coupled with tetracycline repressor (TetR) linked via T2A peptide to GFP were transduced concomitantly into CP-B cells, or Cas9 only expressing

construct for control cells. sgRNA expression is dependent on an H1 promoter and Tet-operating (TetO) site that are negatively regulated by binding TetR. The promoter activity is positively regulated by Doxycycline (Dox) induction that relieves TetR from TetO site. Following Dox induction (Sigma-Aldrich, 2 µg/mL) for 96 h, expressed sgRNA leads to conformational activation of Cas9 endonuclease and guides Cas9 to the targeted SMAD4 DNA sequence of exon 1 (ATAACAGCTATAACTACAAA), exon 2 (ATGTGATCTATGCCCGTCTC) or exon 3 (GGATTAACACTGCAGAGTAA). This results in DNA cleavage and introduction of double strand breaks within the DNA region of interest. Following successful passages, CP-B cells were sorted by flow cytometry (BD Fusion5™, BD Bioscience) to isolate mCherry and GFP positive cells, containing Cas9 and sgRNA, respectively or Cas9 only. This population was subsequently grown followed by single cell sorting and growth of single cell clones. SMAD4 knockout in cell pools and single cell clones was confirmed using western blotting and Sanger sequencing.

2.9. Sanger sequencing

Genomic DNA was extracted from cells using the DNA Blood® and Tissue Mini kit (Qiagen). The coding regions of exon 1, 2, 3 of the *SMAD4* gene were amplified by PCR and cleaned using ExoSAP-IT (Affymetrix, Santa Clara, CA). Primers and PCR conditions are summarized in **Table 2.3**. Cycle sequencing was performed on a 3130 Genetic Analyzer (Thermo Fisher) using the BigDye® Terminator v3.1 sequencing kit (Thermo Fisher).

Table 2.3. Primers and conditions for Sanger Sequencing

SMAD4 exon	Primers	Annealing Temp (^oC)	$MgCl_2$ (25mmol/l)
1	Forward:5'TGTGCCATAGACAAGGTGGA3' Reverse:5'CTTCCAGAAATTCCCATAATGC3'	60	Yes
2	Forward:5'TCACTGCAGCCTTGACCTACTG3' Reverse:5'AAGTCGCGGGCTATCTTCCA3'	60	Yes
3	Forward: 5'GTGGCTGGTCGGAAAGGATT3' Reverse: 5'TACTGCCTGCCGCTCACAC3'	60	Yes

* Primers designed to sequence InDel mutations for CRISPR/Cas9 induced *SMAD4* knockout.

2.10. Animal experiments

All animal work was conducted according to the regulations of the National Health and Medical Research Council Australian Code of Practice for the Care and Use of Animals for Scientific Purposes and with the consent of the Peter MacCallum Cancer Centre Animal Experimentation Ethics Committee. Female NOD-SCID IL-2Rγ knockout (NSG) mice were bred in-house or obtained from Australian BioResources (Garvan Institute of Medical Research, NSW, Australia).

2.11. Modelling OAC development from high grade dysplasia in *in vivo* mouse model system

Following the establishment of *in vitro* SMAD4 knockdown and knockout CP-B isogenic cell line model systems, $5x10^6$ cells resuspended in 100µl of 1:1 PBS and growth factor reduced Matrigel® Matrix (Corning, New York, US) were subcutaneously injected into the right flank of 6-8 weeks old NSG mice. Tumour formation was attentively observed by palpation. Once palpable, tumours were measured with digital callipers and tumour volume calculated using the formula (length × $width^2$)/2. All mice were euthanised at the first signs of ill health (e.g. laboured breathing, bloated abdomen or excessive weight loss: >10% of baseline body weight) or when the tumours reached ≥1500 mm^3. The tumours were harvested and used for histology and immunohistochemistry, cryopreservation and cell line establishment.

2.12. Histology and immunohistochemistry

Immunohistochemistry was performed on formalin-fixed paraffin embedded tissues of CP-B xenografts following removal of paraffin in xylene and rehydration in graded ethanol. Sections were blocked in high pH Dual Endogenous Enzyme Block (DAKO, CA, US) followed by 10% (w/v) bovine serum albumin (BSA) in TBS containing 0.05% Tween-20 (TBS-T) and incubated with primary antibody diluted in 1% (w/v) BSA in TBS-T for 1 hour at room temperature or overnight at 4^oC. Antibodies against the following proteins were used: human mitochondrial antigen (MAB1273, MilliporeSigma), and CK7 (M7018, Agilent Technologies) listed in **Table 2.1**. Images of stained sections were captured on a BX-51 microscope (Olympus).

2.13. Isolation and establishment of cell lines from CP-B SMAD4 knockdown/knockout tumours developed in in vivo model

Following harvesting and separation from the surrounding parenchyma, tumours were washed with PBS, finely chopped then incubated in a waterbath (RATEK Instruments) for 2 hours at 37ºC in 2 mL of PBS containing 2 mg/mL Collagenase A (Roche) and 4 mg/mL Dispase (Roche). Following addition of 10 mL fresh media, cell suspensions were filtered through 45 µm pore size Membrane Filter (MF-Millipore™, Sigma Aldrich) and pelleted by centrifugation (1200 rpm, 5 minutes). Cell lines were established in Dulbecco's Modified Eagle Medium (DMEM) containing 2.5 mmol/l L-glutamine and 4.5 g/l D-glucose (Life Technologies) culture media with 10% (v/v) FBS, and increased concentration of penicillin (100 U/mL) and streptomycin (100 mg/mL) for at least two passages before reducing to standard concentrations of 50 U/mL penicillin, and 50 mg/mL streptomycin. Cells were grown in monolayer cultures in humidified incubators at 37°C with 5% CO_2. Cells were successfully passaged using 0.25% Trypsin, puromycin selected (SMAD4 shRNA knockdown) or FACS sorted for mCherry (SMAD4 CRISPR knockout) to remove contaminating host mouse cells, expanded and verified by performing STR analyses. For the purpose of the phenotypical and physiological comparison between xenograft derived cell lines and original cell lines, CP-B parental and CP-B SMAD4 knockdown/knockout isogenic cell lines were adapted to grow in DMEM media.

2.14. Reinjection of the established SMAD4 knockdown/knockout cell lines

To assess tumourigenicity of the SMAD4 knockdown or knockout CP-B cells established from tumour xenografts, $5x10^6$ cells resuspended in 100 µl of 1:1 PBS and Matrigel® were injected subcutaneously into the right flank of 6-8 weeks old female NSG mice. Tumours were monitored twice per week and tumour volume measured as described in Section 2.11. Necropsy was performed on all animals in order to harvest the tumours and observe the effects of primary site tumour formation, including macro-metastases.

2.15. DNA purification and analyses

Total DNA from cultured cells was isolated using DNeasy ® Blood and Tissue kit (Qiagen) following the manufacturer's instructions. DNA concentration was determined by Invitrogen Qubit 3 Fluorometer (Fisher Scientific, Hampton, New Hampshire, US) and purity was estimated by a NanoDrop ND1000 spectrophotometer (Thermo Scientific).

2.16. Library preparation and Low Coverage-Whole Genome Sequencing (LC-WGS) workflow

The preparation of indexed DNA libraries was performed using NEBNext Ultra II DNA Library Prep Kit for Illumina, according to manufacturer instructions. The fragmentation of 100 ng of starting DNA material was conducted for 120 s in microtubes (Covaris) using the ultrasonication Covaris LE220 system (Covaris, Inc., Woburn, Massachusetts, US). PCR library amplification was performed using the PCR cycling conditions listed in **Table 2.4**. Following amplification, library DNA concentration was measured using Invitrogen Qubit 3 Fluorometer (Fisher Scientific). The sizing analysis of library DNA was performed using a 2200 Tape Station System (Agilent Technology) and High Sensitivity D1000 Screen Tape Assay (Agilent Technology). The prepared libraries were run on an Illumina Nextseq 500 Sequencer using a NextSeq 500 High Output Kit (75 Paired End). High Output Flow Cells were used in order to pool more than 8 samples and sequencing resulted in genome coverage of 1.07-1.70 x per sample. The operation of the Nextseq 500 was conducted by the Molecular Genomics Core Facility, Peter MacCallum Cancer Centre.

Table 2.4. PCR cycling conditions for DNA library amplification

CYCLE STEP	TEMP	TIME	CYCLES
Initial denaturation	98ºC	30 seconds	1
Denaturation	98ºC	10 seconds	8*
Annealing/Extension	65ºC	75 seconds	
Final Extension	65ºC	5 seconds	1
Hold	4ºC	∞	

*Depends on Input DNA material (optimized for 100ng).

2.17. Data analyses for LC-WGS

Following removal of sequencing primers by Cutadapt (v1.7.1) [218], reads were aligned with bwa mem (v0.7.12-r1039) [219] to hg19 (GRCh37). We used ControlFREEC (version 6.7) [220] to assess copy number from the low-coverage WGS data in 50 kb windows across hg19, with default parameters, no matched normal sample and baseline ploidy set to 2. Blacklisted regions including highly repetitive centromeric regions [221] were filtered out in order to yield genomic profile with scarce noise. LC-WGS data analyses were performed using Nexus (v8, BioDiscovery Inc., Hawthorne, CA).

2.18. Quantitative Real-Time PCR (qRT-PCR)

Total cell RNA was isolated using the RNeasy kit according to manufacturer's protocol (Qiagen) or Macherey Nagel Nucleospin RNA kit (Macherey-Nagel GmbH & Co. KG, Duren, Germany). RNA concentration and purity were measured with a NanoDrop ND1000 spectrophotometer (Thermo Scientific). Complementary DNA (cDNA) was generated from 1ug purified RNA using Transcriptor First Strand cDNA Synthesis Kit (Roche). Gene expression changes were determined by SYBR green qRT-PCR (Lightcycler 480, Roche), analysed using the comparative $\Delta\Delta C_T$ (delta delta cycle threshold) method [222] and normalised against GAPDH. qRT-PCR primer sequences are detailed in **Table 2.5.**

Table 2.5. qRT-PCR primer sequences

Gene	Forward (5'- 3')	Reverse (5'- 3')
$p14^{ARF}$	CCCTCGTGCTGATGCTACTG	CATCATGACCTGGTCTTCTAGGAA
$p15^{INK4B}$	CGGGGACTAGTGGAGAAGGT	CGAAACGGTTGACTCCGTTG
$p16^{INK4A}$	GGGGGCACCAGAGGCAGT	GGTTGTGGCGGGGGCAGTT
ACTA2	TCAATGTCCCAGCCATGTAT	CAGCACGATGCCAGTTGT
CRYAB	CTTTGACCAGTTCTTCGGAG	CCTCAATCACATCTCCCAAC
CDC6	TGGATGTTTGCAGGAGAGCTA	GCTCCTTCTTGGCTCAAGGT
GAPDH	GGTGTGAACCATGAGAAG	CCACAGTTTCCCGGAG

2.19. TGF-β Signaling Targets RT² Profiler PCR Array

Eighty-four TGF-β signalling target genes were analysed using TGF-β Signaling Targets RT² Profiler PCR Array (PAHS-235Z; Qiagen). RT² Profiler PCR Arrays were purchased in Format G 384 (4x96) suitable for use with Roche LightCycler 480 (384-well block). The genes screened in this RT^2 PCR Array are listed in **Table 2.6**. $9x10^5$ cells were seeded into 6 well plates and grown for 72 hours. Following serum starvation for 6 hours, cells were treated with 10 ng/mL human recombinant TGF-β1 in serum-deprived media and harvested at 4 and 16 hours. Literature evidence showed that 6 hours starvation prior to stimulation with TGF-β ligands was sufficient to effectively detect expression changes following activation of TGF-β signalling [223]. In order to obtain high purity RNA samples, RNA extraction was performed using Macherey Nagel Nucleospin RNA kit (Macherey-Nagel GmbH & Co. KG). RNA concentration and purity were measured as indicated in Section 2.16. Preparation of cDNA from 100ng (for RT² Profiler PCR Arrays in presence of serum) and 400 ng (for RT² Profiler PCR Arrays in absence of serum) purified RNA (recommended amount of starting RNA material for RT² Profiler PCR Array Format G) was performed using RT^2 First Strand Kit (Qiagen) suitable for PCR-based gene expression analyses together with RT^2 SYBR Green Mastermix (Qiagen), according to manufacturer instructions.

Real time PCR was performed according to the manufacturer instructions (Qiagen) with the PCR components mix and cycling conditions for Roche LightCycler 480 summarized in **Table 2.7** and **Table 2.8**, respectively. Finally, the data were collected and analysed using the web resource Qiagen GeneGlobe Data Analyses centre (https://www.qiagen.com/au/shop/genes-and-pathways/data-analysis-center-overview-page/). The target gene expression levels were quantified relative to the mean geometric value obtained for housekeeping genes (HKG), *ACTB*, *B2M*, *GAPDH*, *HPRT1* and *RPLPO*. HKGs with small changes in their expression across different sample groups (with differences in C_T values <1) were used for normalization, according to recommendations. The lower limit of detection or C_T cut-off was set to 35. Relative gene expression was calculated using ΔC_T method between gene of interest (GOI) and an average of the HKGs, and subsequent ΔΔCt calculations (ΔC_T (Test group) - ΔC_T (Control Group)). Fold change was obtained using 2^ ($-\Delta\Delta C_T$) formula.

2.20. Statistics

Data were analysed by two tailed Student's *t*-test or ratio paired *t*-test to compare two groups of interest. For analyses of three or more groups, one Way ANOVA with Tukey's multiple comparison test was performed. Statistical analyses were performed in Prism 7 (GraphPad) with $p < 0.05$ considered statistically significant. Data from RT^2 PCR arrays were analysed and plots (scatter and volcano) obtained using online Qiagen data analyses centre available at https://www.qiagen.com/au/shop/genes-and-pathways/data-analysis-center-overview-page/. Venn diagrams were designed using Picture Illustrator. R studio was used to generate PCA and loadings plot and heat-map was generated using R package heatmaply [224].

Table 2.6. List of the TGF-β Signalling target genes screened in RT2 PCR Array. (Part 1)

Position	RefSeq Number	Symbol	Description
A01	NM_001613	ACTA2	Actin, alpha 2, smooth muscle, aorta
A02	NM_001105	ACVR1	Activin A receptor, type I
A03	NM_000020	ACVRL1	Activin A receptor type II-like 1
A04	NM_000029	AGT	Angiotensinogen (serpin peptidase inhibitor, clade A, member 8)
A05	NM_014336	AIPL1	Aryl hydrocarbon receptor interacting protein-like 1
A06	NM_000044	AR	Androgen receptor
A07	NM_001674	ATF3	Activating transcription factor 3
A08	NM_001675	ATF4	Activating transcription factor 4 (tax-responsive enhancer element B67)
A09	NM_001186	BACH1	BTB and CNC homology 1, basic leucine zipper transcription factor 1
A10	NM_138578	BCL2L1	BCL2-like 1
A11	NM_001709	BDNF	Brain-derived neurotrophic factor
A12	NM_003670	BHLHE40	Basic helix-loop-helix family, member e40
B01	NM_005104	BRD2	Bromodomain containing 2
B02	NM_001254	CDC6	Cell division cycle 6 homolog (S. cerevisiae)
B03	NM_004064	CDKN1B	Cyclin-dependent kinase inhibitor 1B (p27, Kip1)
B04	NM_005194	CEBPB	CCAAT/enhancer binding protein (C/EBP), beta
B05	NM_004379	CREB1	CAMP responsive element binding protein 1
B06	NM_004380	CREBBP	CREB binding protein
B07	NM_001885	CRYAB	Crystallin, alpha B
B08	NM_001904	CTNNB1	Catenin (cadherin-associated protein), beta 1, 88kDa
B09	NM_001539	DNAJA1	DnaJ (Hsp40) homolog, subfamily A, member 1
B10	NM_001950	E2F4	E2F transcription factor 4, p107/p130-binding
B11	NM_001423	EMP1	Epithelial membrane protein 1
B12	NM_000118	ENG	Endoglin
C01	NM_001429	EP300	E1A binding protein p300
C02	NM_004442	EPHB2	EPH receptor B2
C03	NM_002026	FN1	Fibronectin 1
C04	NM_005252	FOS	FBJ murine osteosarcoma viral oncogene homolog
C05	NM_002569	FURIN	Furin (paired basic amino acid cleaving enzyme)
C06	NM_015675	GADD45B	Growth arrest and DNA-damage-inducible, beta
C07	NM_005270	GLI2	GLI family zinc finger 2
C08	NM_001518	GTF2I	General transcription factor IIi
C09	NM_014685	HERPUD1	Homocysteine-inducible, endoplasmic reticulum stress-inducible, ubiquitin-like domain member 1
C10	NM_005524	HES1	Hairy and enhancer of split 1, (Drosophila)
C11	NM_012258	HEY1	Hairy/enhancer-of-split related with YRPW motif 1
C12	NM_002133	HMOX1	Heme oxygenase (decycling) 1
D01	NM_002165	ID1	Inhibitor of DNA binding 1, dominant negative helix-loop-helix protein
D02	NM_002166	ID2	Inhibitor of DNA binding 2, dominant negative helix-loop-helix protein
D03	NM_002167	ID3	Inhibitor of DNA binding 3, dominant negative helix-loop-helix protein
D04	NM_001550	IFRD1	Interferon-related developmental regulator 1
D05	NM_000572	IL10	Interleukin 10
D06	NM_005655	KLF10	Kruppel-like factor 10
D07	NM_003188	MAP3K7	Mitogen-activated protein kinase kinase kinase 7
D08	NM_001315	MAPK14	Mitogen-activated protein kinase 14
D09	NM_002750	MAPK8	Mitogen-activated protein kinase 8
D10	NM_015844	MBD1	Methyl-CpG binding domain protein 1

Table 2.6. List of the TGF-β Signalling target genes screened in RT2 PCR Array. (Part 2)

Position	RefSeq Number	Symbol	Description
D11	NM_004530	MMP2	Matrix metallopeptidase 2 (gelatinase A, 72kDa gelatinase, 72kDa type IV collagenase)
D12	NM_002449	MSX2	Msh homeobox 2
E01	NM_002467	MYC	V-myc myelocytomatosis viral oncogene homolog (avian)
E02	NM_002478	MYOD1	Myogenic differentiation 1
E03	NM_005596	NFIB	Nuclear factor I/B
E04	NM_020529	NFKBIA	Nuclear factor of kappa light polypeptide gene enhancer in B-cells inhibitor, alpha
E05	NM_017617	NOTCH1	Notch 1
E06	NM_002607	PDGFA	Platelet-derived growth factor alpha polypeptide
E07	NM_000301	PLG	Plasminogen
E08	NM_005036	PPARA	Peroxisome proliferator-activated receptor alpha
E09	NM_000963	PTGS2	Prostaglandin-endoperoxide synthase 2 (prostaglandin G/H synthase and cyclooxygenase)
E10	NM_002820	PTHLH	Parathyroid hormone-like hormone
E11	NM_005607	PTK2	PTK2 protein tyrosine kinase 2
E12	NM_004103	PTK2B	PTK2B protein tyrosine kinase 2 beta
F01	NM_006265	RAD21	RAD21 homolog (S. pombe)
F02	NM_000964	RARA	Retinoic acid receptor, alpha
F03	NM_002895	RBL1	Retinoblastoma-like 1 (p107)
F04	NM_001664	RHOA	Ras homolog gene family, member A
F05	NM_004040	RHOB	Ras homolog gene family, member B
F06	NM_001754	RUNX1	Runt-related transcription factor 1
F07	NM_012234	RYBP	RING1 and YY1 binding protein
F08	NM_002964	S100A8	S100 calcium binding protein A8
F09	NM_000602	SERPINE1	Serpin peptidase inhibitor, clade E (nexin, plasminogen activator inhibitor type 1), member 1
F10	NM_000193	SHH	Sonic hedgehog
F11	NM_005900	SMAD1	SMAD family member 1
F12	NM_005902	SMAD3	SMAD family member 3
G01	NM_005903	SMAD5	SMAD family member 5
G02	NM_005585	SMAD6	SMAD family member 6
G03	NM_005985	SNAI1	Snail homolog 1 (Drosophila)
G04	NM_003107	SOX4	SRY (sex determining region Y)-box 4
G05	NM_138473	SP1	Sp1 transcription factor
G06	NM_004599	SREBF2	Sterol regulatory element binding transcription factor 2
G07	NM_003238	TGFB2	Transforming growth factor, beta 2
G08	NM_003242	TGFBR2	Transforming growth factor, beta receptor II (70/80kDa)
G09	NM_003246	THBS1	Thrombospondin 1
G10	NM_003810	TNFSF10	Tumor necrosis factor (ligand) superfamily, member 10
G11	NM_006472	TXNIP	Thioredoxin interacting protein
G12	NM_003376	VEGFA	Vascular endothelial growth factor A
H01	NM_001101	ACTB	Actin, beta
H02	NM_004048	B2M	Beta-2-microglobulin
H03	NM_002046	GAPDH	Glyceraldehyde-3-phosphate dehydrogenase
H04	NM_000194	HPRT1	Hypoxanthine phosphoribosyltransferase 1
H05	NM_001002	RPLP0	Ribosomal protein, large, P0
H06	SA_00105	HGDC	Human Genomic DNA Contamination
H07	SA_00104	RTC	Reverse Transcription Control
H08	SA_00104	RTC	Reverse Transcription Control
H09	SA_00104	RTC	Reverse Transcription Control
H10	SA_00103	PPC	Positive PCR Control
H11	SA_00103	PPC	Positive PCR Control
H12	SA_00103	PPC	Positive PCR Control

Table 2.7. Real-Time PCR Components Mix

Array Format "G"	384 (4 x 96) option
2x RT^2 SYBR Green MasterMix	650 µl
cDNA synthesis reaction	102 µl
RNase-free water	548 µl
Total Volume	1300 µl

Table 2.8. Cycling Conditions for Roche LightCycler 480*

	Cycles	Duration	Temperature	Comments
Activation	1	10min	95ºC	HotStart DNA Taq Polymerase is activated by this heating step
Cycling	45	15s	95ºC	
		1 min	60ºC	
Melt Curve	1	1 min	95ºC	
Acquisition		1min	65ºC	
		Continuous	96ºC	Acquisition Mode: Continuous
		10s	40ºC	(5 per ºC)

*The adjusted Ramp Rate was 1.5ºC/s.

CHAPTER 3.

LOSS OF SMAD4 IS SUFFICIENT TO PROMOTE TUMOURIGENESIS IN A MODEL OF DYSPLASTIC BARRETT'S OESOPHAGUS

3.1. Introduction

It has been considered that OAC develops from Barrett's oesophagus through intermediate stages of LGD and high grade dysplasia (HGD). Despite a deeper understanding of the molecular basis of step-wise OAC development (addressed in Chapter 1, Sections 1.3. and 1.4.) through utilizing clinical endoscopic sampling and pathological characterisation of the precancerous stages, patient outcome has still not improved [225]. Successful clinical management of OAC has been at least partially hindered by the fact that it is a highly mutated and heterogeneous disease. The recurrent mutations present in OAC highly replicate the ones present in adjacent Barrett's oesophagus [226]. These data are consistent with OAC developing from Barrett's oesophagus. However, the presence of OAC recurrent mutations already within non-dyplastic Barrett's oesophagus makes it challenging to decipher molecular drivers and biomarkers of Barrett's oesophagus progression towards invasive OAC and metastasis.

Similarly, Weaver *et al*. have shown that the majority of recurrently mutated genes in OAC, are also mutated in non-dysplastic Barrett's oesophagus [206]. Thus, the only stage specific mutations are *TP53* and *SMAD4,* which arise in HGD and cancer, respectively. Therefore, *TP53* and *SMAD4* mutations are likely to have relevance in the development and progression of the disease. The biggest proportion of *TP53* gene mutations are missense and happen in the central gene region interfering with sequence specific DNA binding and consequently leading to loss of p53 wild-type function [137, 227]. Chronologically, *TP53* mutations predominantly arise during the progression of non-dysplastic Barrett's oesophagus to high grade dysplasia [206]. As such, *TP53* gene mutations are already present in the majority of cases with high grade dysplasia and patients diagnosed with OAC. In contrast, *SMAD4* mutations and SMAD4 loss of function are exclusively found in the cancer stage of the disease [206]. Although significant research efforts are focusing on understanding the functional effects of *TP53* mutations and restoring p53 wild-type function [228, 229], herein the focus was on deciphering the effects of *SMAD4* mutations and SMAD4 loss of function in cancer progression from HGD towards OAC.

Mutations in the gene encoding for SMAD4 are present in ~13% of OAC patients samples, whereas SMAD4 protein loss is present in ~10% and 44% of primary and metastatic disease, respectively [206, 230]. Furthermore, SMAD4 loss has been associated with increased susceptibility for OAC recurrence and shorter overall survival [230]. In addition, reduced SMAD4 expression levels have been associated with poor survival outcome in colorectal cancer [231]. However, the functional role of SMAD4 loss in OAC development and progression has not been elucidated.

To address this question, isogenic shRNA mediated SMAD4 knockdown and CRISPR mediated SMAD4 knockout of both alleles in HGD cell lines were generated in order to understand whether SMAD4 loss is sufficient to initiate tumour formation *in vivo* using the NSG mouse model system. CP-B cells [215] were utilised, as this cell line represents a valuable model system of high grade dysplastic Barrett's oesophagus that exhibits an existing mutation in *TP53* but is *SMAD4* wild-type. The effect of SMAD4 loss in HGD cells on tumour initiation and progression was assessed in this model.

3.2. RESULTS

3.2.1. Establishment of an isogenic SMAD4 knockout in a high grade dysplasia cell model system

Despite the identification of numerous mutations arising during the progression from non-dysplastic Barrett's towards OAC, the timing of these mutations is largely not stage specific. As described earlier in introduction, we know that mutations in OAC generally occur early in disease development, including in the non-dysplastic Barrett's lesion, raising the question as to whether they are driver or passenger events. Nevertheless, the only two stage specific genetic changes are mutations in the *TP53* gene mutations and *SMAD4* loss of function, which occur in HGD and cancer, respectively.

To address the question about the functional role of SMAD4 in progression towards OAC, a CRISPR/Cas9 mediated SMAD4 knockout approach was used in a high grade dysplastic Barrett's oesophagus cell line, CP-B, to mimic the SMAD4 loss in high grade dysplastic Barrett's oesophagus (**Figure 3.2.1A**). CP-B cells were simultaneously transduced with dual lentiviral vector system consisting of: constitutively expressing Cas9 endonuclease linked via the T2A peptide to the mCherry fluorescent marker protein; and Dox inducible sgRNA cassette with ubiquitin promoter and TetR linked via T2A peptide to the GFP protein. sgRNA expression targeting exon 1, 2 or 3 of the SMAD4 gene were driven by a H1 promoter that contains TetO site closely regulated by binding TetR. The promoter activity is positively regulated via addition of Dox that binds and relieves TetR from the TetO site. Upon Dox induction, transcribed sgRNAs help conformational activation of Cas9 endonuclease leading to DNA binding and cleavage at the specific gene region **(Figure 3.2.1A**). Dox induction modestly decreased SMAD4 protein levels in bulk CP-B cell pools with sgRNAs when compared to non-induced Cas9 only cells (**Figure 3.2.1B**). The decrease in SMAD4 in these pools of cells was small, presumably due to the presence of non-transduced cells and/or cells in which the knockout was incomplete. However, when single cell clones were generated from the cell pools, SMAD4 protein was absent in a number of clones including Ex1.2B1, Ex2.A1 and Ex2.A4 and truncated in one clone, Ex1.D2 (**Figure 3.2.1C, D**). In addition, Sanger sequencing confirmed the presence of indel mutations in CP-B clones Ex1.2B1, Ex2.A1 and Ex1.D2 (**Figure 3.2.1E-G**). *In vitro* growth of SMAD4 knockout cells was not significantly different to Cas9 control cells (**Figure**

3.2.1H). Based on these results, Ex1.2B1 CP-B SMAD4 knockout clone was chosen for future experiments.

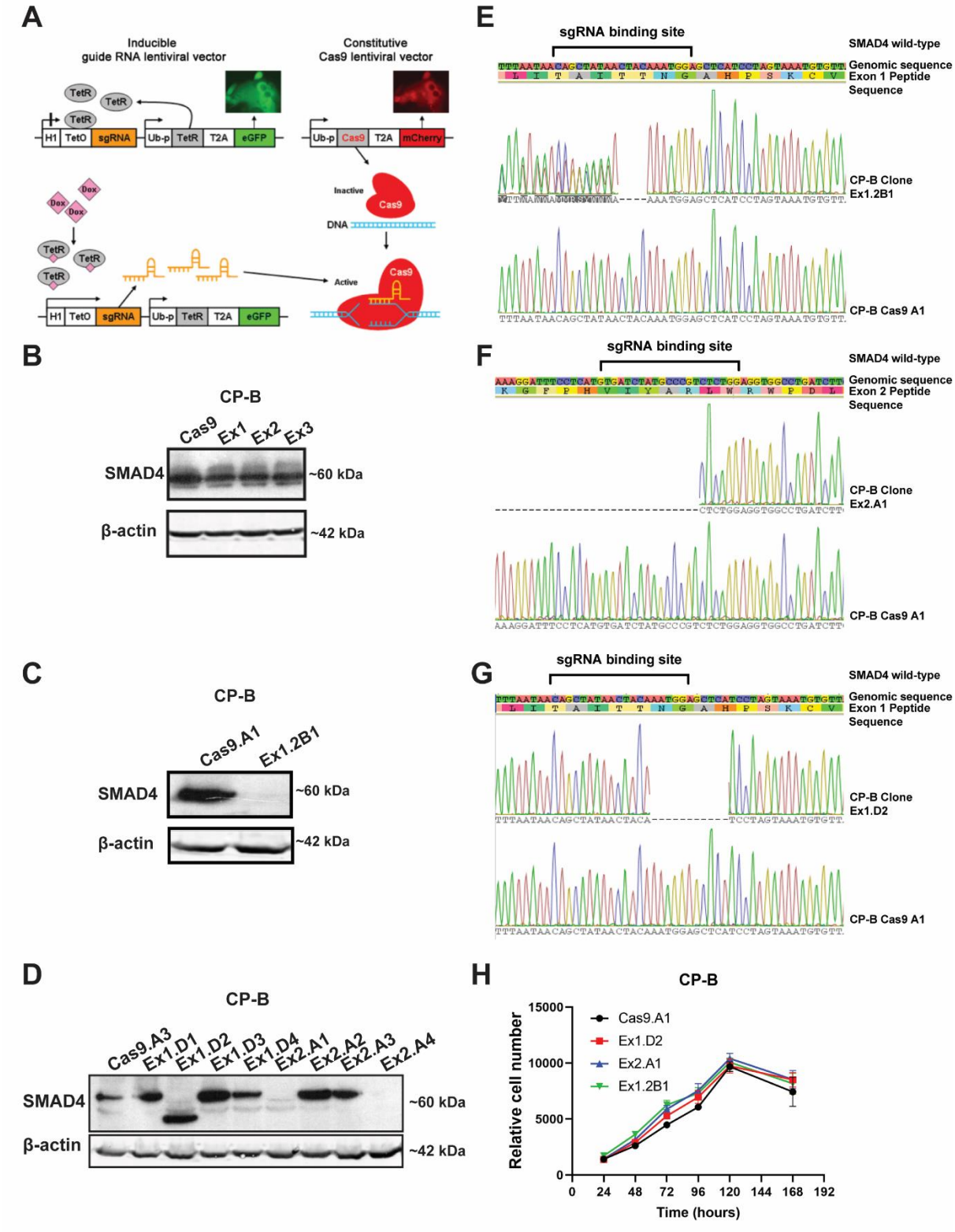

Figure 3.2.1. SMAD4 knockout in human oesophageal high grade dysplasia CP-B cells using CRISPR/Cas9 technology. (A) Schematic representation of sgRNA activation upon Dox induction and

concomitant activation of Cas9 (Schematic acquired from [217]). (B) Western blots for SMAD4 in lentiviral transduced pool of the CP-B control cells with Cas9 only non-induced with Dox (Cas9) and Dox induced (96 hours) sgRNA targeting exon 1, 2 or 3 of SMAD4 gene (Ex1, Ex2, Ex3). (C, D) Western blots for SMAD4 in clonal populations from Dox induced SMAD4 targeted cell pools compared to non-induced Cas9 only control cells (Cas9.A1 and Cas9.A3). (E, F, G) Representative results from Sanger sequencing demonstrating indel mutations within SMAD4 exon 1 and 2 target sequences in 3 separate cell clones. (H) Relative cell number determined by cell viability assay (Alamar Blue®) of $5x10^3$ SMAD4 knockout cells compared to Cas9 control cells. Cell viability assay was performed from 24-168 hours on three independent occasions each with 6 technical replicates. Data shown represent mean±SEM (n=3).

3.2.2. Generating shRNA mediated SMAD4 knockdown in high grade dysplasia CP-B cells

Non-inducible pGIPZ lentiviral vectors expressing different SMAD4 shRNAs were used to constitutively knockdown SMAD4 (**Figure 3.2.2A**). Four different shRNAs targeting different gene regions were tested for SMAD4 knockdown efficiency by western blot in CP-B cells (**Figure 3.2.2B**). Two out of four shRNAs, (sh37196 and sh37198) demonstrated high SMAD4 knockdown efficiency and were chosen for future experiments. *[In order to simplify future labelling, only S96 and S98 were appended to cell line name, with S indicating shRNA and the numbers 96/98 indicating the specific shRNA]*. *In vitro* growth of SMAD4 knockdown cells was not significantly different from pGIPZ empty vector control cells (**Figure 3.2.2C**).

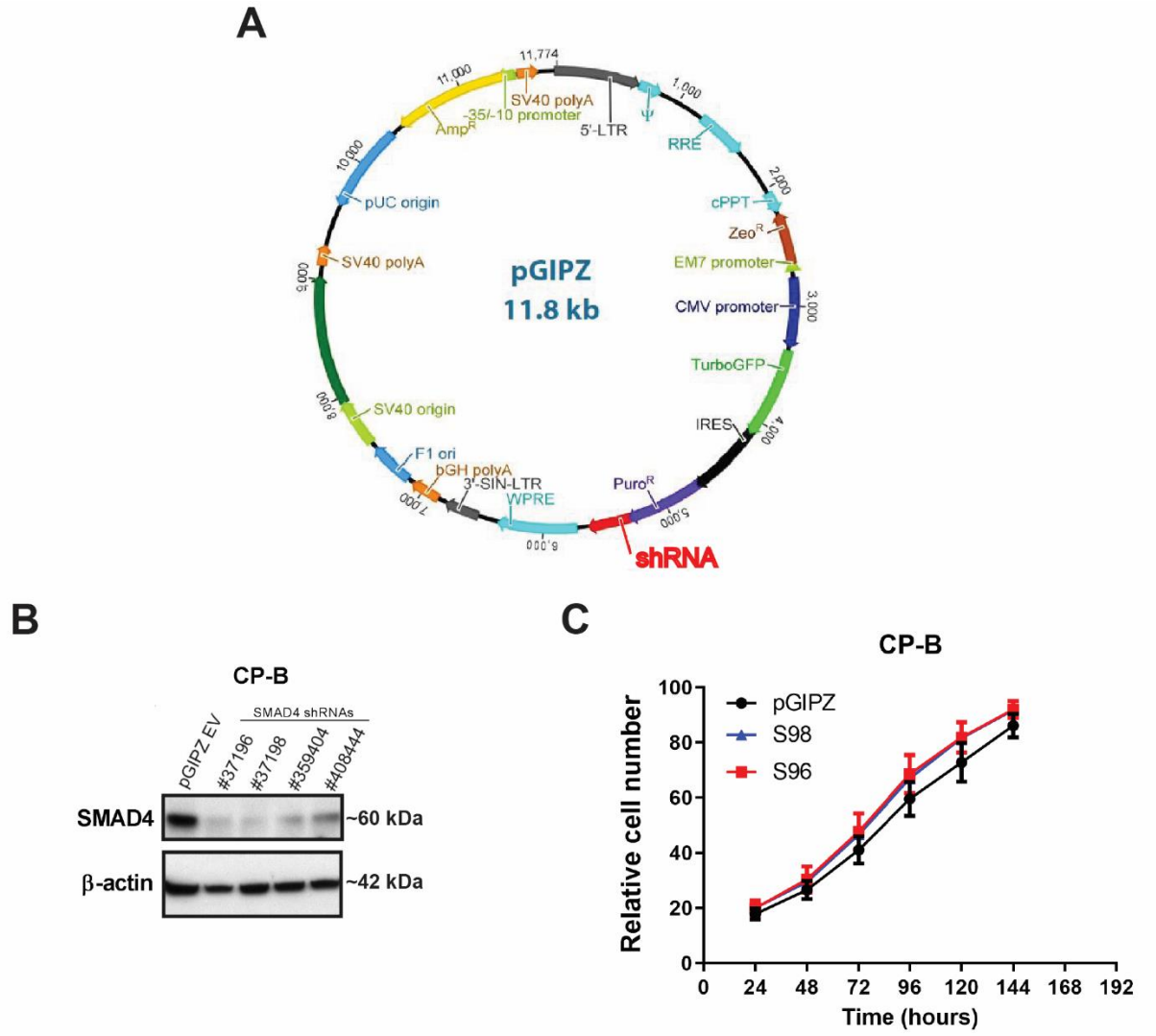

Figure 3.2.2. shRNA mediated SMAD4 knockdown in high grade dysplasia CP-B cells. (A) Map of pGIPZ lentiviral vector. (B) Immunoblotting for SMAD4 protein expression levels in CP-B cells

transduced with pGIPZ empty vector or four different SMAD4 shRNA constructs. (C) Cell confluency assay comparing relative cell numbers from 24-144 hours in $1x10^4$ cells with pGIPZ empty vector or the two most efficient SMAD4 shRNA constructs. All experiments were performed on 3 independent occasions each with three technical replicates. Data shown represent mean±SEM (n=3).

3.2.3. SMAD4 loss initiates tumorigenesis of dysplastic Barrett's oesophagus cells *in vivo*

In order to decipher whether SMAD4 is a functional genetic driver of Barrett's oesophagus progression, *in vivo* xenograft experiments using NSG mice were performed. Schematic representation of the experimental flow is shown (**Figure 3.2.3A**) including subcutaneous injection of isogenic CP-B SMAD4 knockdown or knockout (bulk and clonal) cells into the mice in order to understand the biological effects of SMAD4 depletion or loss on tumour development and progression compared to SMAD4 wild-type control cells (parental, pGIPZ vector only and Cas9 only CP-B cells). All mice injected with either CP-B SMAD4 knockdown or knockout cells, started to form palpable tumours during the time course of the experiments. SMAD4 knockout tumours started to grow around day 150 (**Figure 3.2.3C**), while SMAD4 knockdown tumours started to grow from day 180 (**Figure 3.2.3B**). In addition, injection of bulk SMAD4 knockout cells resulted in tumour formation around day 300 (**Figure 3.2.3C**). On the other hand, subcutaneous injections of SMAD4 wild-type control cells including CP-B parental, pGIPZ vector only and Cas9 only, did not result in tumour formation, apart from one mouse out of seventeen that formed a tumour at day 340 (**Figure 3.2.3B**). This tumour formed in a mouse injected with CP-B parental cells. The tumour frequency following cell injection *in vivo* and time to tumour onset are summarized in **Table 3.2.1**.

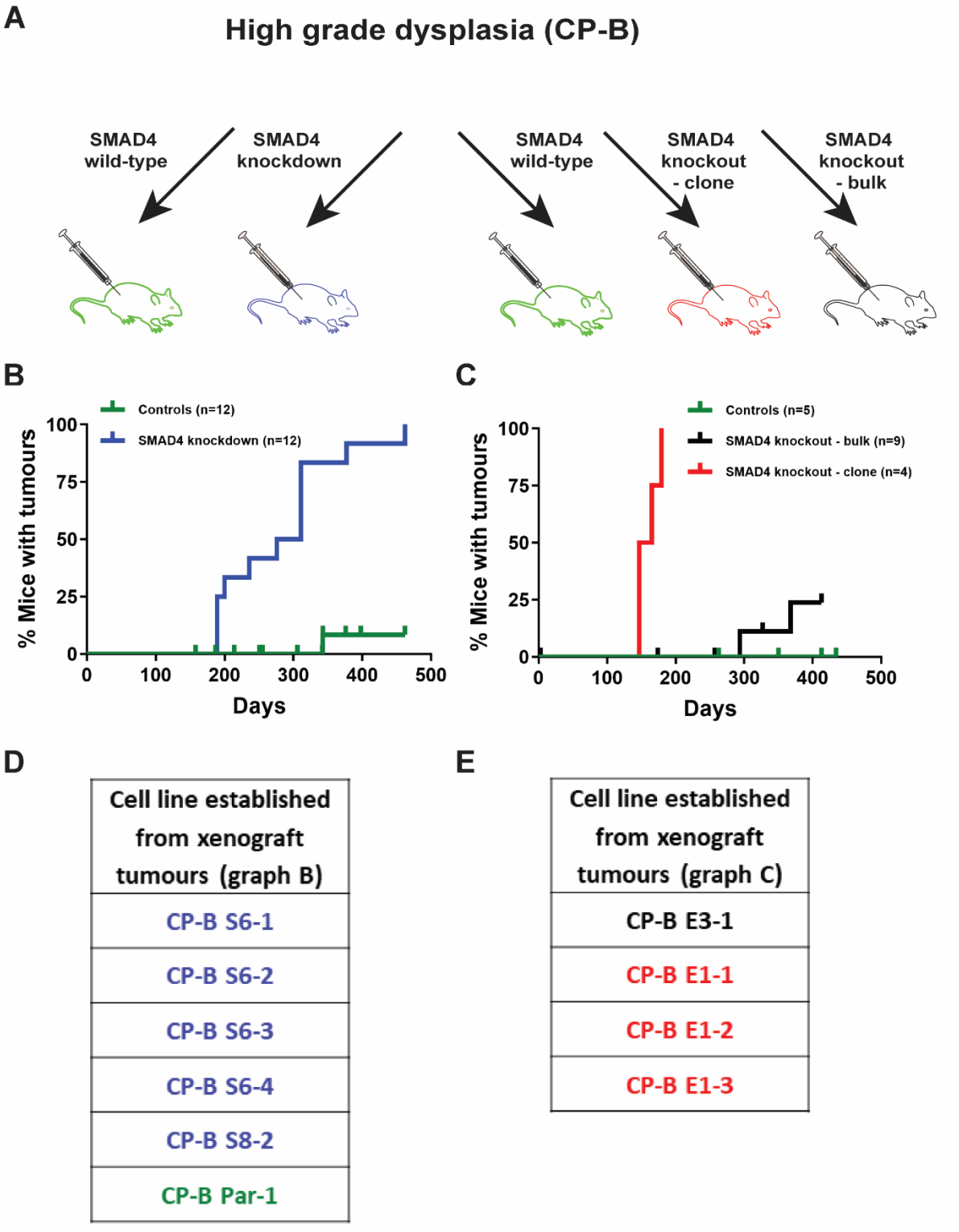

Figure 3.2.3. Tumour formation following SMAD4 knockdown and knockout cells in CP-B cells. (A) Experimental plan of *in vivo* experiment that includes injection of SMAD4 wild-type control cells (parental and pGIPZ vector only CP-B cells), and SMAD4 knockdown (CP-B sh96, CP-B sh98), or SMAD4 wild-type control cells (Cas9 only CP-B cells) and SMAD4 knockout cells (Bulk and Clonal CP-B cells) in 4-8 mice per group. (B, C) Kaplan-Meier curves show the percentage of the mice with detected tumours following injection with (B) CP-B SMAD4 knockdown cells and (C) CP-B SMAD4 knockout cells compared to SMAD4 wild-type cells. Each tick on the graphs represents an animal that

was euthanised at the first signs of ill health but did not have a tumour (confirmed at necropsy). (D, E) list of cell lines re-derived from CP-B xenograft tumours following (D) SMAD4 knockdown and (E) SMAD4 knockout experiment, including controls. The suffixes 'S6/8' and 'E1/E3' appended to a cell line name indicate that these cells have been developed from 96 and 98 shRNA mediated SMAD4 knockdown and SMAD4 knockout (E1-clonal; E3-bulk) tumours, respectively. In addition, suffix '-' with number 1, 2, 3 or 4 appended to the end of cell line name indicate the number of mouse with the xenograft. Par-1 cell line was developed from the only control tumour that arose from an injection of CP-B parental cells.

Table 3.2.1. Tumour frequency *in vivo* and established cell lines

	Cells injected	Tumour frequency	Mean (and range) days to tumour onset	Cell Lines Established	Cell line names (CP-B)
Controls	Parental*	1/6	343	1/1	Par-1
	pGIPZ vector only*	0/6	NA	NA	NA
	Cas9 only*	0/5	NA	NA	NA
shRNA knockdown	SMAD4 shRNA #37196*	6/6	251 (189-311)	4/6	S6-1*, S6-2*, S6-3*, S6-4*; †
	SMAD4 shRNA #37198	6/6	308 (189-462)	1/6	S8-2
CRISPR knockouts	Bulk knockouts	2/9	331 (294-368)	1/2	E3-1
	Ex1.2B1 clone*	4/4	159 (147-179)	3/4	E1-1*; †, E1-2*; †, E1-3*

*LC-WGS performed (Chapter 3. Subheading 3.2.7). †form spontaneous metastases from xenograft (Chapter 3. Subheading 3.2.6).

To decipher molecular and functional features of the developed tumours, tumours were harvested for cell line isolation and establishment (**Figure 3.2.3D, E** and **Table 3.2.1)**. Subsequently, after successful growth *in vitro*, all cell lines were expanded in culture and selected using puromycin for SMAD4 knockdown (**Figure 3.2.3D**) and m-Cherry FACS sorting of SMAD4 knockout (**Figure 3.2.3E**) cell lines. All cell lines were authenticated as being derived from CP-B parental cell line (more than 80% compatibility) using the STR Profile Database Matching algorithm from American Type Culture Collection (ATCC). The STR results are summarized in **Table 3.2.2** and **Table 3.2.3**.

Table 3.2.2. STR analyses of cell lines established from SMAD4 knockdown tumours

Loci	Reference profile	CP-B Par-1	CP-B S6-1	CP-B S6-2	CP-B S6-3	CP-B S6-4
CSF1PO:	8, 12	8, 12	8	8	8	8
D13S317:	8, 12	8, 12	8, 12	8, 12	8, 12	8, 12
D16S539:	10, 13	10,13	10,13	10,13	10,13	10,13
D5S818:	11, 12	11, 12	11	11	11	11
D7S820:	11, 12	11, 12	11, 12	11, 12	11, 12	11, 12
THO1:	8, 9	8, 9	8, 9	8, 9	8, 9	8, 9
TPOX:	8, 9	8, 9	8, 9	8, 9	8, 9	8, 9
vWA:	18, 20	18, 20	18, 20	18, 20	18, 20	18, 20
Amelogenin:	XY	X	X	X	XY	X
Loci Matches with reference profile ≥80%	Yes	Yes	Yes	Yes	Yes	Yes

Reference Profile: CP-B (ATCC CRL-4028). STR= Short Tandem Repeat.

Table 3.2.3. STR analyses of cell lines established from SMAD4 knockout tumours

Loci	Reference profile	CP-B E3-1	CP-B E-1	CP-B E-2	CP-B E-3
CSF1PO:	8, 12	8, 12	8	8	8
D13S317:	8, 12	8, 12	8, 12	8, 12	8, 12
D16S539:	10, 13	10,13	10,13	10,13	10,13
D5S818:	11, 12	11, 12	11	11	11
D7S820:	11, 12	11, 12	12	12	12
THO1:	8, 9	8, 9	8, 9	8, 9	8, 9
TPOX:	8, 9	8, 9	8, 9	8, 9	8, 9
vWA:	18, 20	18, 20	18, 20	18, 20	18, 20
Amelogenin:	XY	X	XY	XY	XY
Loci Matches with reference profile ≥80%	Yes	Yes	Yes	Yes	Yes

Reference Profile: CP-B (ATCC CRL-4028). STR= Short Tandem Repeat.

3.2.4. Functional characterisation of CP-B SMAD4 knockdown or knockout tumour derived cell lines

To further characterise cell lines established from xenograft tumours, SMAD4 protein expression levels were examined. Importantly, cell lines established from SMAD4 knockout clones (E1-1, E1-2 and E1-3) or SMAD4 knockdown (S6-1, S6-2, S6-3, S6-4 and S8-2) tumours still had no SMAD4 protein expression or differential lower levels compared to CP-B parental cells, respectively, with exception of CP-B E3-1 cells, derived from xenograft that arose from bulk knockout cells (**Figure 3.2.4A**). Interestingly, CP-B Par-1 cells, derived from the only xenograft that arose from the injection of control CP-B SMAD4 wild-type cells, had significantly lower SMAD4 protein

levels compared to CP-B parental cells. Moreover, cell proliferation assays were performed to determine the relative growth of the cell lines that have been established from xenograft tumours compared to the original SMAD4 knockdown and SMAD4 knockout CP-B cells that had been grown only in an *in vitro* experimental environment and not *in vivo*. For this purpose, one cell line each derived from SMAD4 knockdown or knockout xenografts and the corresponding two original cell lines grown only *in vitro* were chosen. As expected, relative cell number of CP-B SMAD4 knockdown (CP-B S96) cells grown only in *in vitro* conditions was significantly lower compared to cells that were established from the corresponding tumour xenograft (CP-B S6-2) (**Figure 3.2.4B**). Similarly, CP-B SMAD4 knockout cells established from tumour xenografts (CP-B E1-1) grew faster than the original CP-B SMAD4 knockout cells only grown in *in vitro* conditions (CP-B Ex1.2B1) (**Figure 3.2.4C**). In summary, it is evident that following subcutaneous injection in the *in vivo* mouse model system, CP-B SMAD4 knockdown and knockout cells likely acquired genetic alterations that lead to a functionally altered growth profile compared to the original cells only grown in *in vitro* conditions.

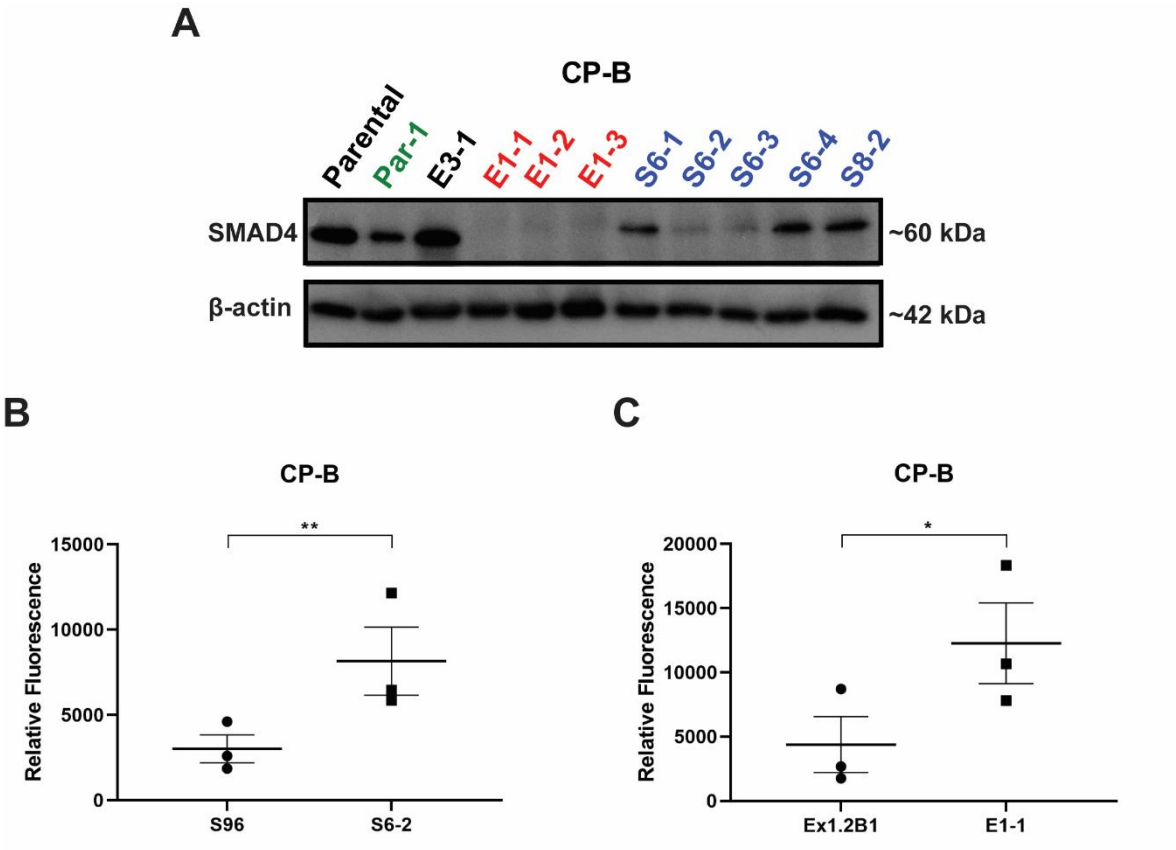

Figure 3.2.4. Functional characterisation of cell lines established from CP-B SMAD4 knockdown or knockout xenograft tumours. (A) Western blot for SMAD4 protein levels across cell lines. (B, C) Cell viability assay (AlamarBlue®) at 144 hours following plating $2x10^3$ cells and comparing relative fluorescence of (B) CP-B S96 SMAD4 knockdown cells (C) or CP-B Ex1.2B1 SMAD4 knockout cells grown *in vitro* versus cells established from corresponding xenografts. The cell viability assay was performed on 3 independent occasions each with 6 technical replicates. *p < 0.05, **p< 0.01: Ratio paired t-test. Shown are means for each individual experiment. Bars represent mean±SEM for all three expreriments.

3.2.5. Histological characterisation of CP-B SMAD4 knockdown or knockout driven tumours

In order to understand the biological background of CP-B SMAD4 knockdown and knockout developed tumours compared to the SMAD4 wild-type cells, the tumours were collected for histological characterization. Hematoxylin and eosin (H&E) counterstaining showed distinctive histological features of SMAD4 knockdown and knockout tumours. Morphologically, SMAD4 knockdown tumours (**Figure 3.2.5A, C, E**) and SMAD4 knockout tumours (**Figure 3.2.6A, C, E**) are largely similar. The tumours are highly cellular comprising sheets of epithelioid to plasmacytoid cells, in areas resembling a “fried egg appearance”, with round prominent nuclei, dispersed

chromatin, moderate amounts of eosinophilic cytoplasm and mild degree of pleomorphism. Although, the SMAD4 knockout tumours are chiefly composed of epithelioid cells, there is a presence of scattered, intervening spindle cells (**Figure 3.2.6A, C, E**), whereas SMAD4 knockdown tumours did not exhibit this morphological feature (**Figure 3.2.5A, C, E**). Interestingly, knockout tumour CP-B E1-3 (**Figure 3.2.6C**) is predominantly composed of spindle cells with interdigitating subcutaneous fat, with both a nodular and septal distribution.

Further, immunohistochemistry using a human specific mitochondrial antibody showed dot-like positivity, consistent with mitochondrial staining pattern in both SMAD4 knockdown (**Figure 3.2.5B, D, F**) and knockout CP-B grown xenografts (**Figure 3.2.6B, D, F**), confirming the human origin of the tumours. Given that cytokeratin 7 (CK7) has been identified as one of the positive markers of OAC, CK7 immunohistochemical staining was performed on SMAD4 knockdown and knockout developed xenografts (**Figure 3.2.7**). As expected, SMAD4 knockdown (**Figure 3.2.7A, B**) and knockout (**Figure 3.2.7C, D**) xenografts demonstrated CK7 positivity, indicating that these tumours have particular immunohistochemical features present in OAC.

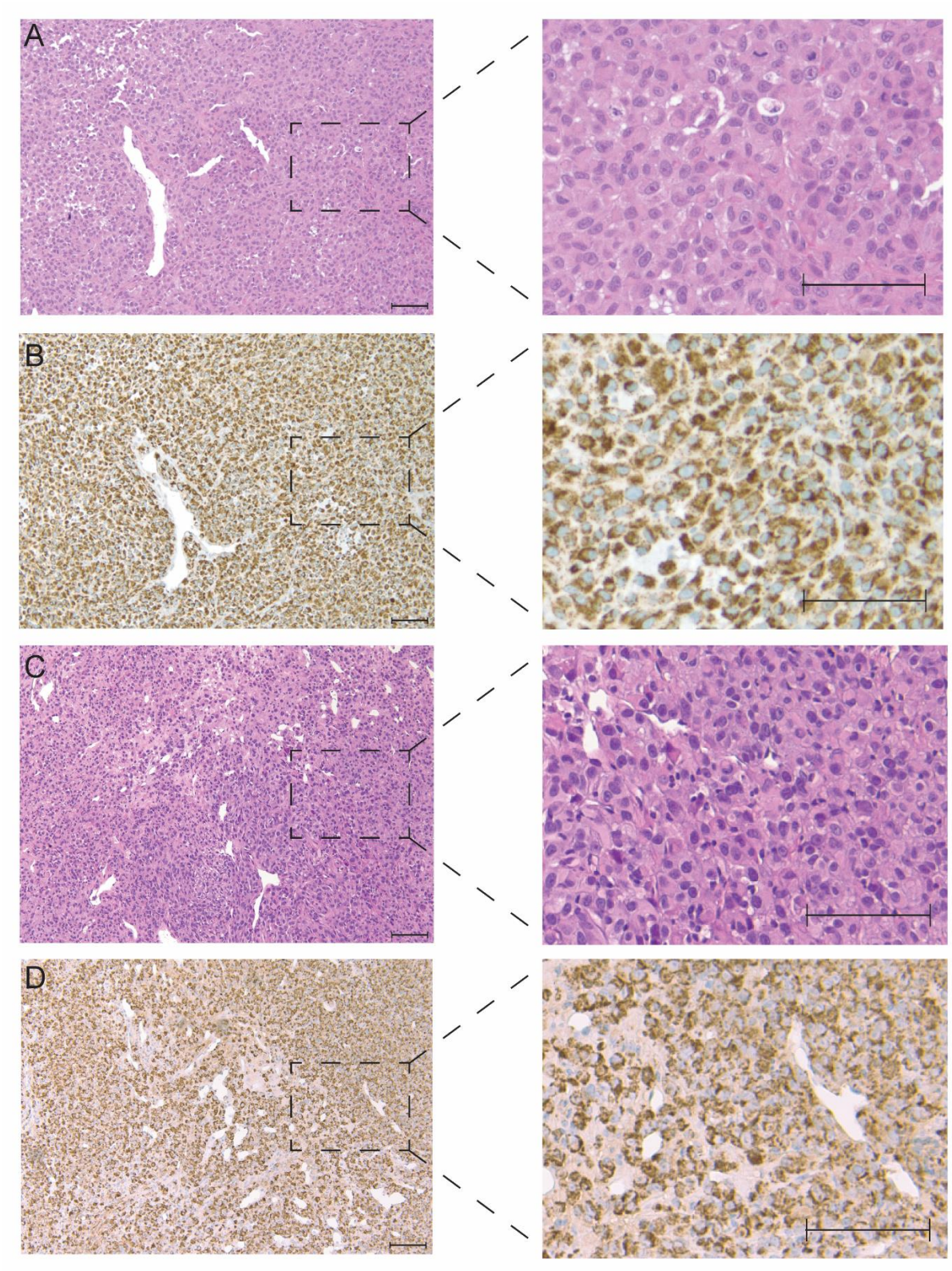
A
B
C
D

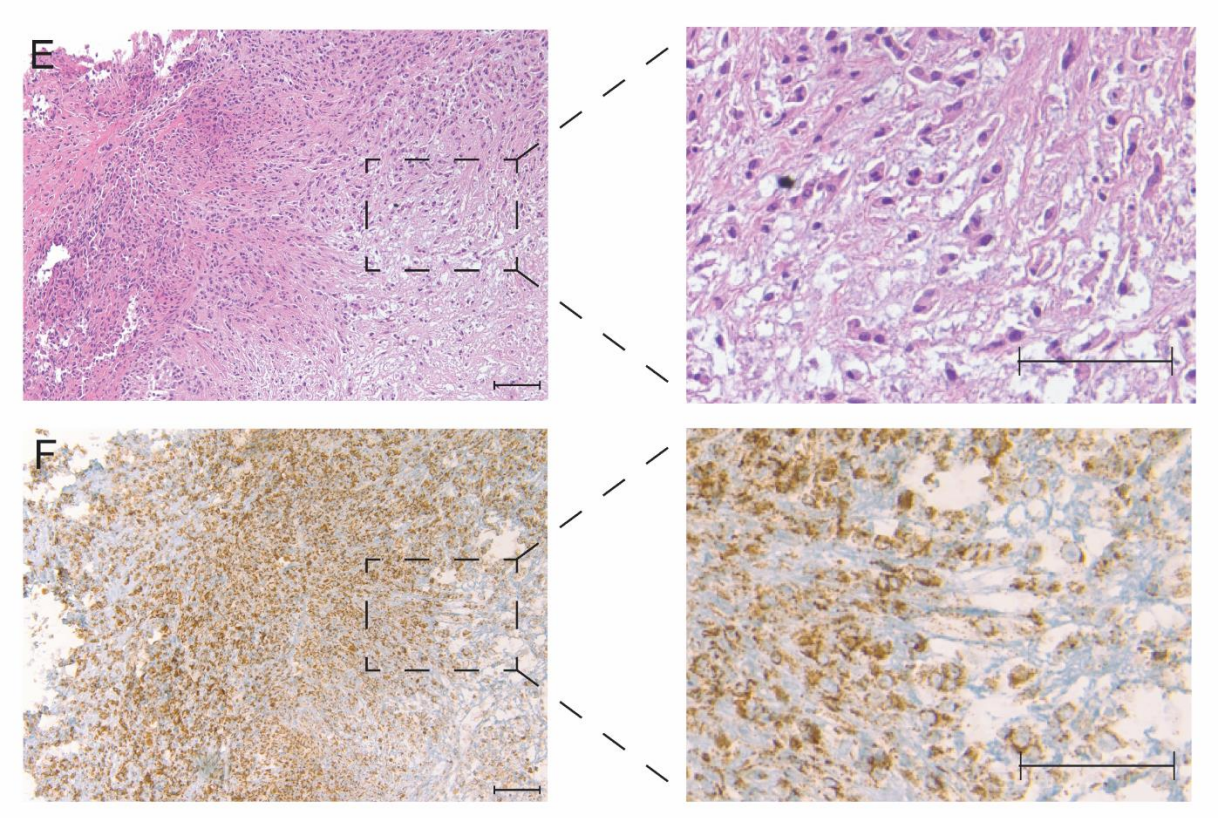

Figure 3.2.5. SMAD4 knockdown driven tumours and their immunohistological features. Representative H&E (Upper panels) and human specific mitochondrial staining (lower panels) of SMAD4 knockdown induced tumour xenografts including (A, B) CP-B S8-2; (C, D) CP-B S8-1; (E, F) CP-B S6-4, respectively. Scale bars represent 100µm.

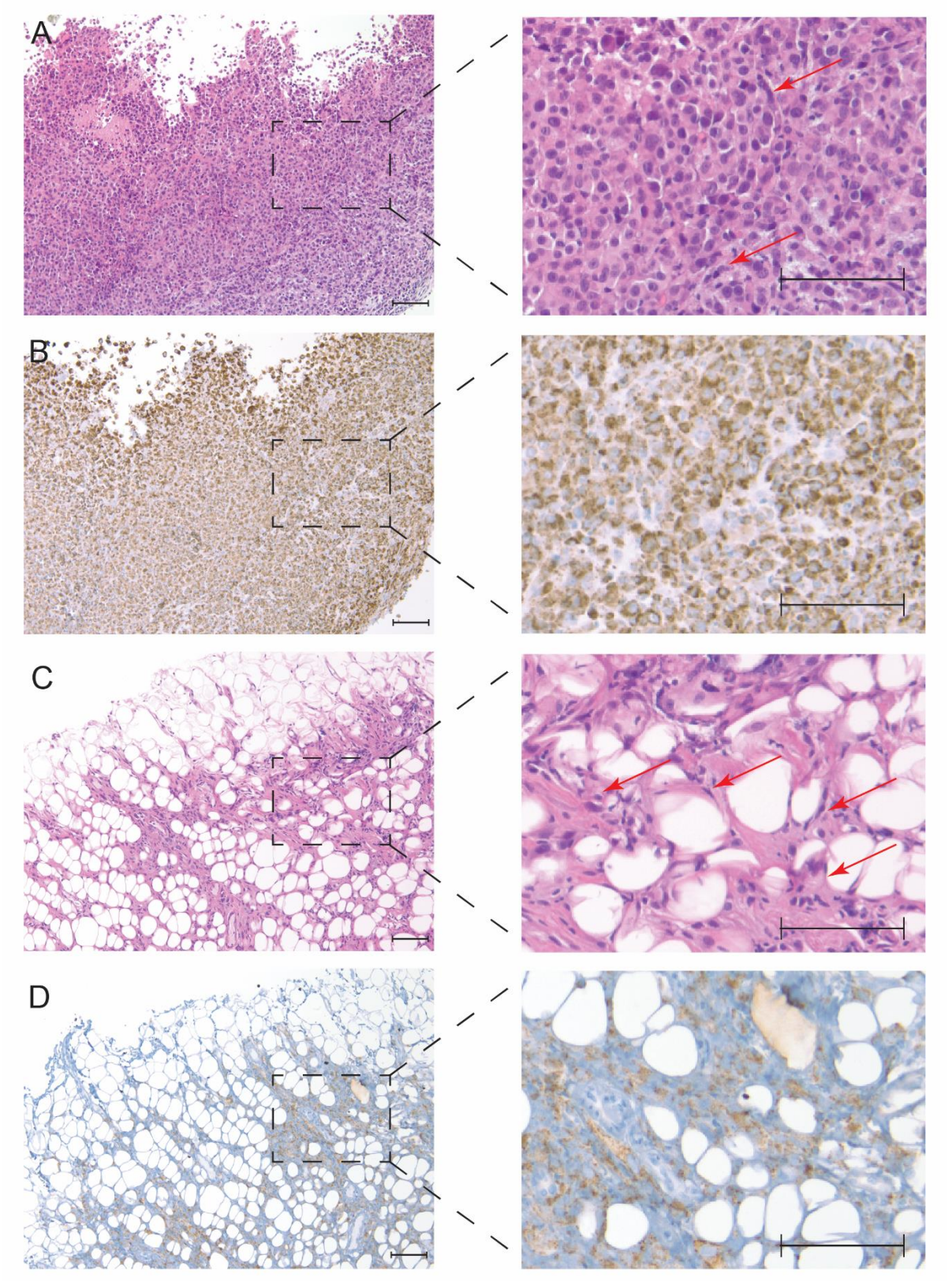
A
B
C
D

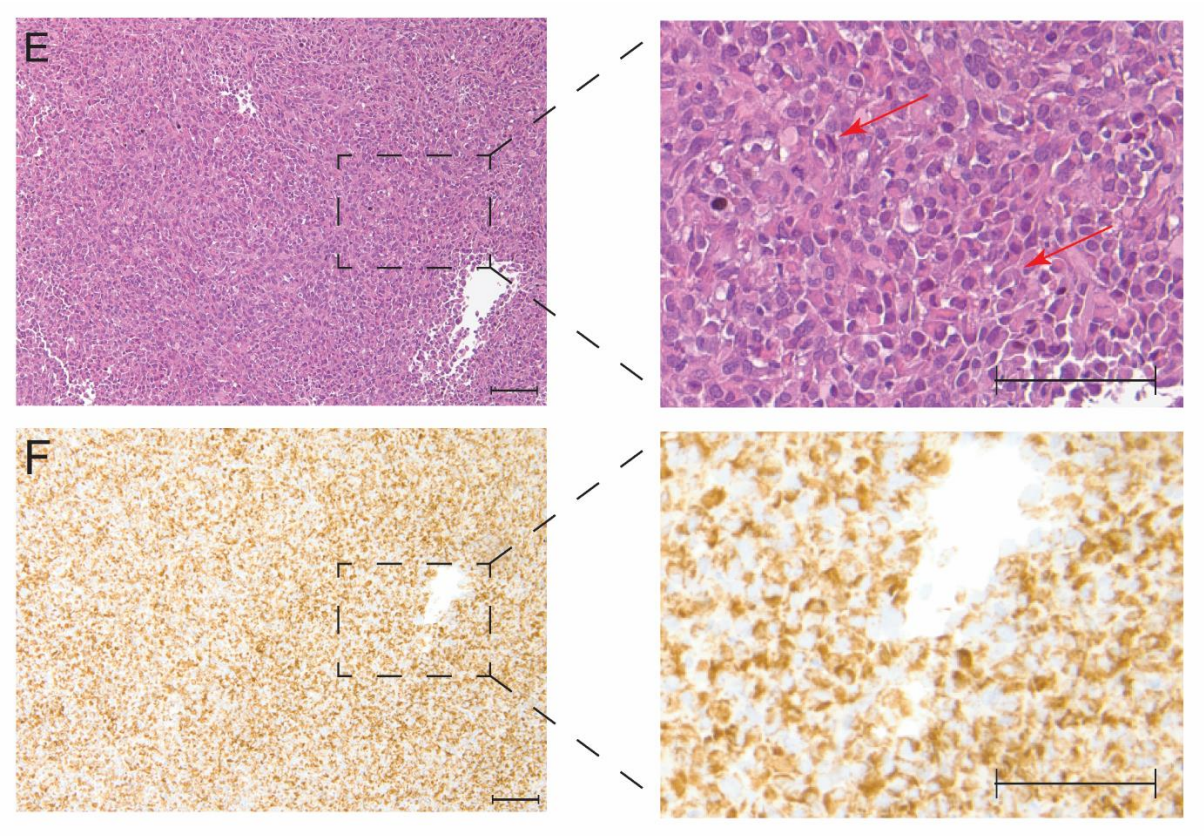

Figure 3.2.6. SMAD4 knockout driven tumours exhibit scattered, intervening spindle cell like morphology. Representative H&E (upper panels) and human specific mitochondrial immunohistochemistry staining (lower panels) of SMAD4 knockout induced tumour xenografts including (A, B) CP-B E1-1; (C, D) CP-B E1-3; and (E, F) CP-B E3-1 xenografts. Red arrows point to cells with spindle like morphology. Scale bars represent 100µm.

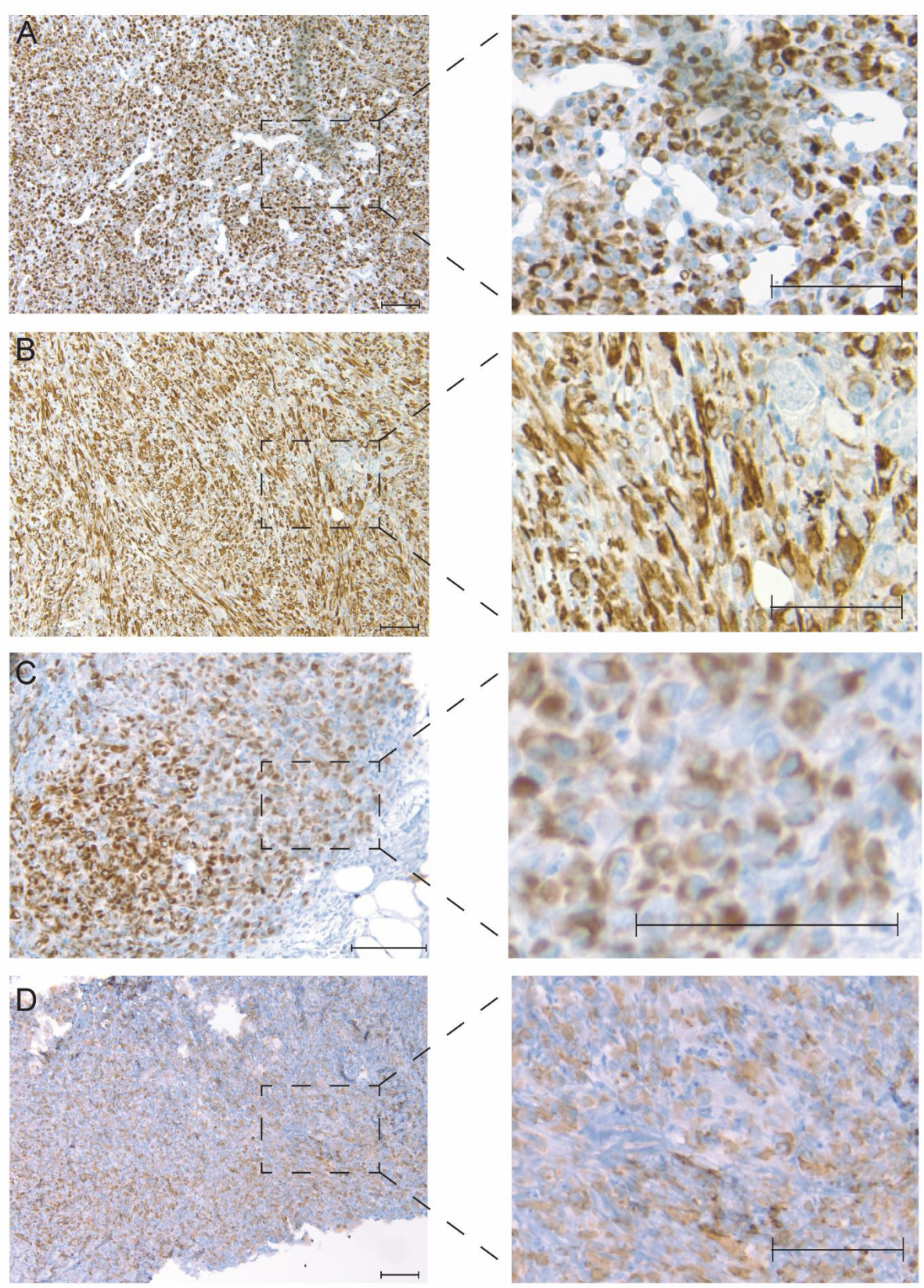

Figure 3.2.7. SMAD4 knockdown and knockout xenografts demonstrate OAC histological characteristics. Representative CK7 immunohistochemistry staining across SMAD4 knockdown (A) CP-B S8-1; (B) CP-B S6-1; and SMAD4 knockout (C) CP-B E3-1; (D) CP-B E1-2 tumour xenografts. Scale bars represent 100µm.

3.2.6. Cell lines re-derived from CP-B SMAD4 knockdown and knockout xenografts acquired potent tumorigenic and metastatic capabilities

Given that SMAD4 knockdown or knockout leads to the increased tumorigenic potential of dysplastic Barrett's cells and eventual formation of tumours *in vivo* in mice, it was hypothesized that cell lines re-established from the tumours would show enhanced tumourigenicity. To address this hypothesis, established cell lines were reinjected into mice, which confirmed that these cells lines are indeed tumourigenic, and that they reached ethical size limits in an accelerated time frame compared to the initial tumours (**Figure 3.2.8A**). The tumour growth rates *in vivo* were variable between cell lines and there was no consistent relationship between SMAD4 knockdown vs. knockout cells and the growth rate. These results suggest that the tumour growth rates are dependent on additional genetic changes that likely arose during tumour initiation and growth *in vivo*. Additionally, following reinjection of cells lines, it was observed that CP-B E1-1, E1-2 and S6-4 cells acquired spontaneous macro-metastatic potential to the lungs and ipsilateral axillary lymph node within 8-12 weeks, two of the main metastatic sites in OAC patients (**Figure 3.2.8B-D, Table 3.2.1**). We performed histological characterization of primary xenograft tumour CP-B S6-4 (**Figure 3.2.8E**) and its corresponding metastatic lesions within lung tissues (**Figure 3.2.8F-J**). H&E counterstaining showed distinctive histological features of metastatic sites containing tumour cells vs. normal lung tissue (**Figure 3.2.8F-J**). Immunohistochemistry using a human specific mitochondrial antibody showed dot-like positivity, consistent with mitochondrial staining pattern in metastatic sites, in opposite to non-stained normal lung tissue (**Figure 3.2.8K-N**), confirming the human origin of the metastatic cells.

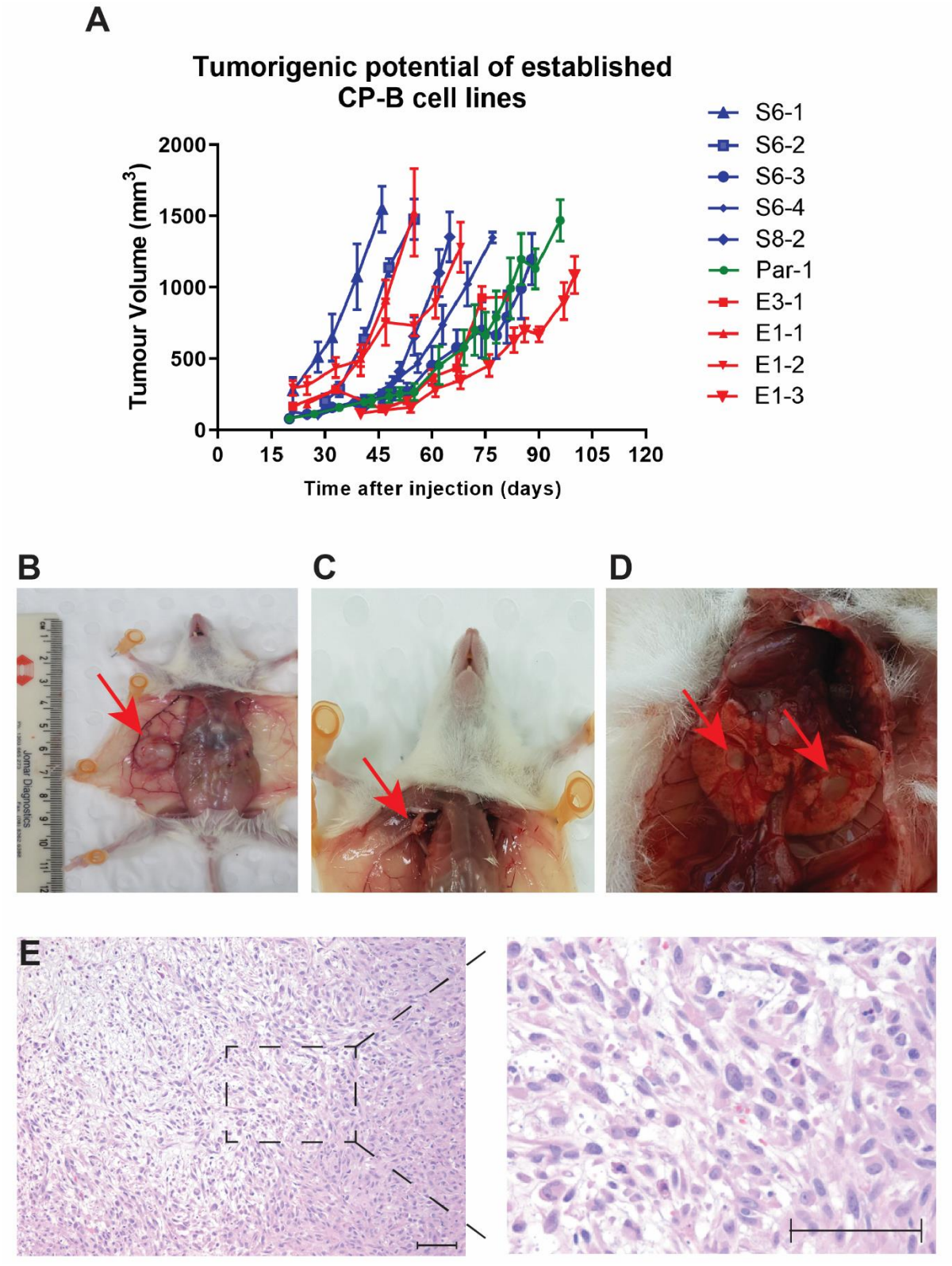
A
Tumorigenic potential of established CP-B cell lines
Tumour Volume (mm3)
2000
1500
1000
500
0
0
15
30
45
60
75
90
105
120
Time after injection (days)
S6-1
S6-2
S6-3
S6-4
S8-2
Par-1
E3-1
E1-1
E1-2
E1-3
B
C
D
E

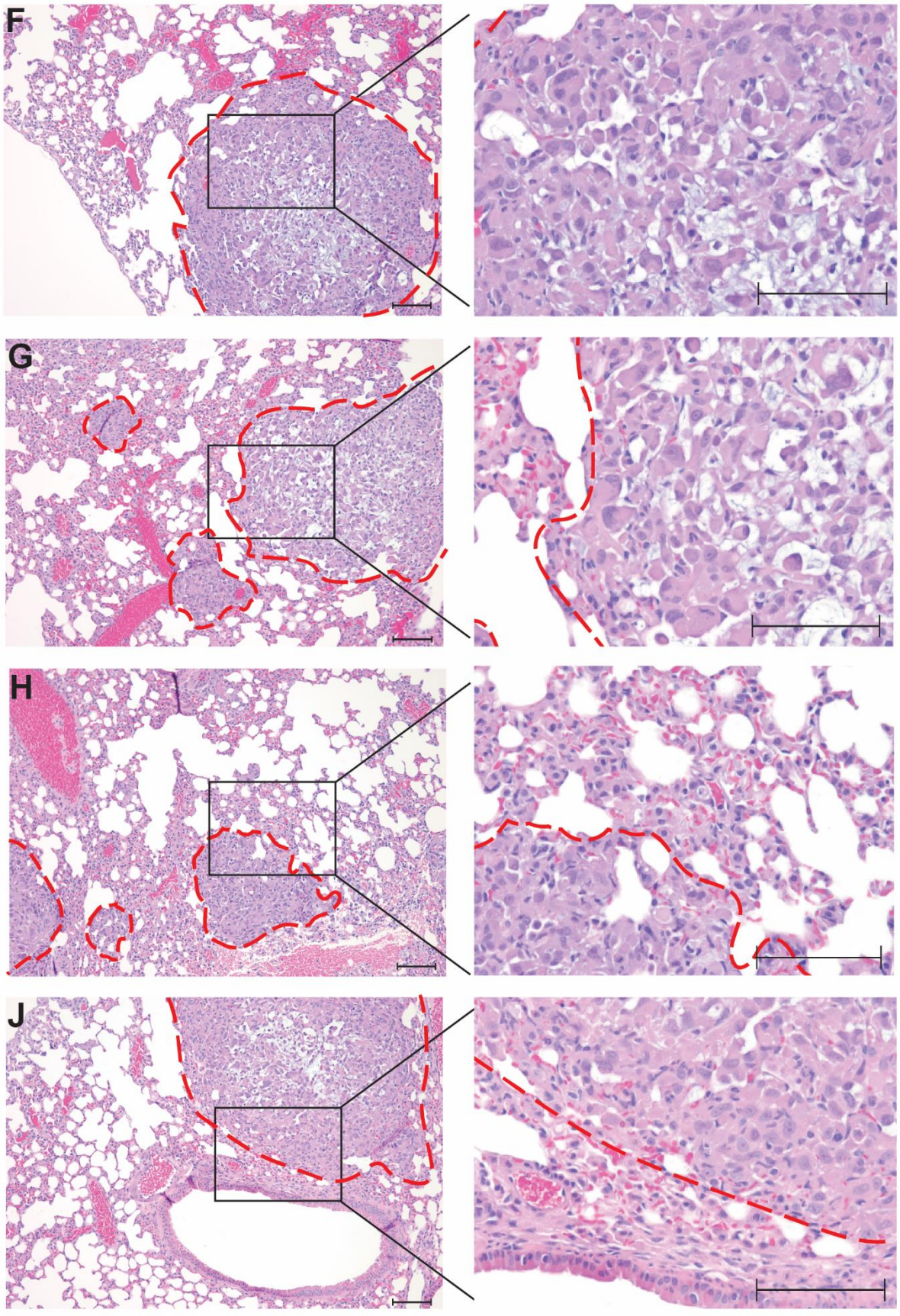
F
G
H
J

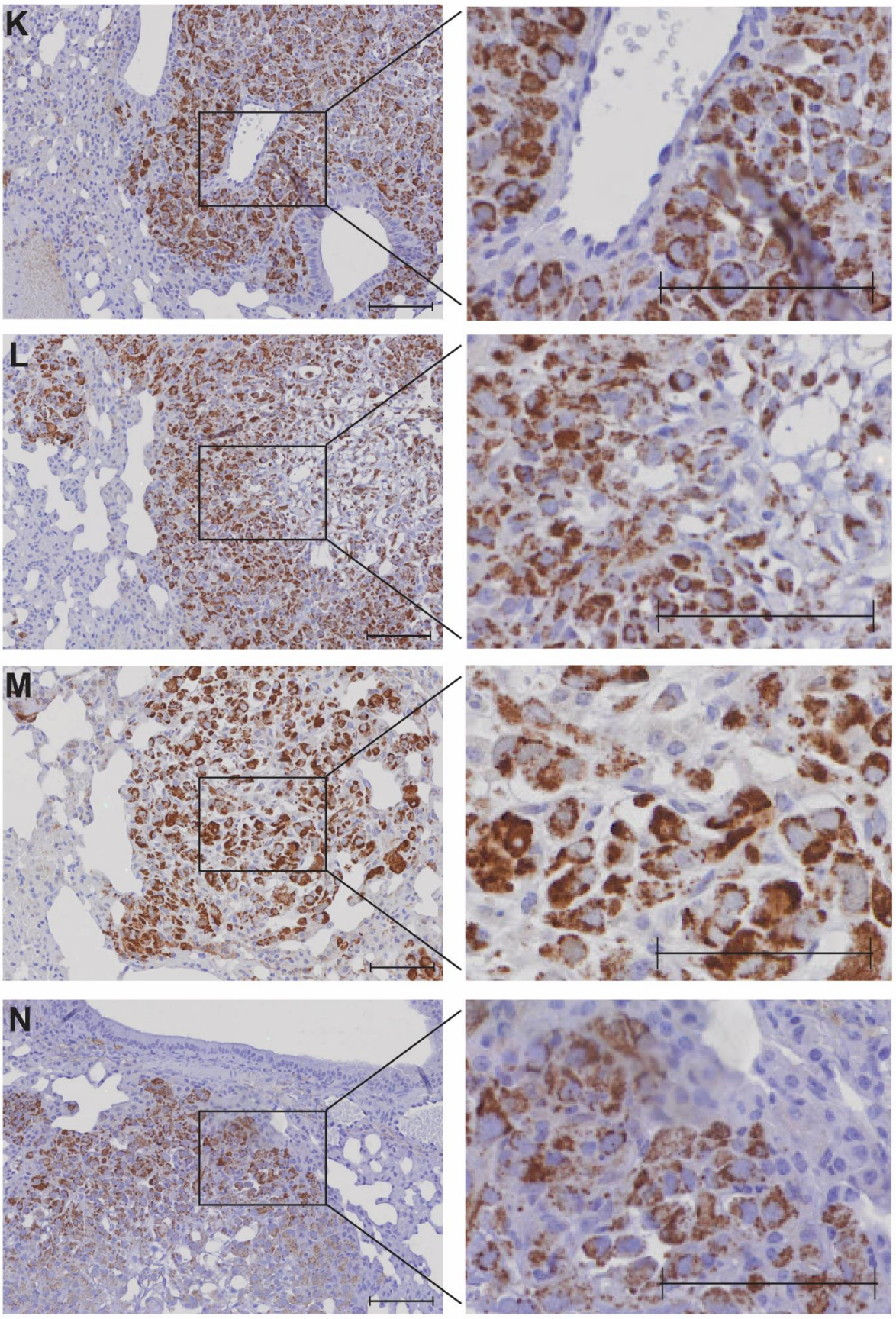

Figure 3.2.8. Potent tumorigenic and metastatic features of CP-B cell lines established from SMAD4 knockdown and knockout xenografts. (A) Tumour growth following reinjection of CP-B

SMAD4 knockdown (blue lines) or knockout (red lines) tumour derived cell lines *in vivo*. Data represent mean±SEM, n=4 per group. (B-C) Representative necropsy examination at ethical endpoint of representative NSG mice with primary tumour (B, red arrow), with widespread right axillary lymph node (C, red arrow) and lung (D, red arrows) macroscopic metastases, respectively. (E) H&E counterstaining of primary tumour (CP-B S6-4) and (F-J) metastatic sites within lungs (CP-B S6-4). Dashed red lines demarcate the border between the normal lung tissue and metastatic tumors cells. (K-N) Human specific mitochondrial immunohistochemistry staining of metastatic sites within lungs. Scale bars represent 100µm.

3.2.7. Distinctive copy number aberrations characterise tumourigenesis in CP-B cells upon SMAD4 loss

Summarizing the results up to this point of this chapter, it has been shown that CP-B parental SMAD4 wild-type cells are rarely tumorigenic in the *in vivo* mouse model system, whereas SMAD4 knockdown or knockout promoted tumourigenicity of CP-B cells. However, taking into consideration the latency between injection of the cells and formation of palpable tumours (**Figure 3.2.3B and C**), it is likely that additional genetic alterations, besides initial SMAD4 depletion or loss, happened over time to contribute to the tumour growth. As shown earlier in this chapter, cell lines re-derived from SMAD4 knockdown and knockout xenografts exhibit potent tumorigenic and metastatic capabilities (**Figure 3.2.8A-D**). Given that there is no clear difference in the *in vivo* growth rate of SMAD4 knockdown and knockout tumour cell lines (**Figure 3.2.8A**), it is suggestive of additional genetic changes that likely arose during the *in vivo* latency period and tumour growth.

The predominant mechanism of SMAD4 loss driven tumorigenesis from high grade dysplasia is not clear. In order to acquire a deeper understanding of the molecular mechanisms that underlie tumour progression from HGD towards OAC following SMAD4 depletion or loss, LC-WGS was performed to detect copy CNAs that occurred during the tumourigenic conversion of the cells *in vivo* in mice. The rationale for performing this kind of analysis was based on previously published genomic studies, which showed that CNAs are more frequently found in OAC than in Barrett's oesophagus with low and high grade dysplasia, when comparing paired patient samples [91, 96]. Therefore, the level of CNAs represents an important distinguishing feature between dysplastic Barrett's and OAC.

LC-WGS was performed on CP-B SMAD4 wild-type control cells (parental, pGIPZ vector only and Cas9 only), SMAD4 knockdown (CP-B S96) and SMAD4 knockout (CP-B Ex1.2B1) cells that have only been grown *in vitro,* and tumorigenic cell lines that were established from SMAD4 knockdown (CP-B S6-1, S6-2, S6-3, S6-4) and SMAD4 knockout (CP-B E1-1, E1-2, E1-3) tumour xenografts (**Table 3.2.1**). Initially, the presence of pre-existing CNAs within high grade dysplastic CP-B SMAD4 wild-type control cells was noticed, such as heterozygous loss of whole copy of chromosome 4, 8p and 21q arms and gain of whole copy of chromosome 20 (**Figure 3.2.9**).

More importantly, LC-WGS data showed that the majority of tumorigenic SMAD4 knockdown or knockout CP-B cells exhibited distinctive and consistent CNA alterations when compared to CP-B SMAD4 wild-type cells (**Figure 3.2.9**). These alterations largely happened within the same regions of the genome, suggestive of a specific relationship between the observed alterations and loss of SMAD4 expression. The multiple CN gains and losses across all sequenced cell lines are listed in **Table 3.2.4**. Consistent copy number gain of chromosome 8q arm was observed across all tumour xenograft derived cell lines, but not in parental CP-B and control cell lines (**Table 3.2.4.**). Furthermore, SMAD4 knockout, but not knockdown cells that have only been cultured *in vitro*, exhibited 8q gain. CNAs specific to SMAD4 knockout *in vitro* also included 6q 22.31-23.3 loss. On the other hand, 5p chromosome gain was noted across 70% of tumour derived cell lines, 100% of SMAD4 knockdown and SMAD4 knockout cell lines grown *in vitro*, as well as in pGIPZ vector only control cells, suggesting that CP-B cells are pre-disposed to 5p gain, with noticeable enhancement occurring when SMAD4 is depleted or lost in the cells. Tumorigenic cell lines exhibited distinctive CNAs such as focal gain of 12q and loss of 14q21.1-24.3 chromosome regions. Overall, the above listed CNAs were observed across 100% of SMAD4 knockout and 25-75% SMAD4 knockdown tumorigenic cell lines. These data could be explained by the fact that SMAD4 knockdown cells still express residual levels of SMAD4 that is likely having partial effect in these cells, while the SMAD4 knockout cells are completely prevented in utilizing SMAD4.

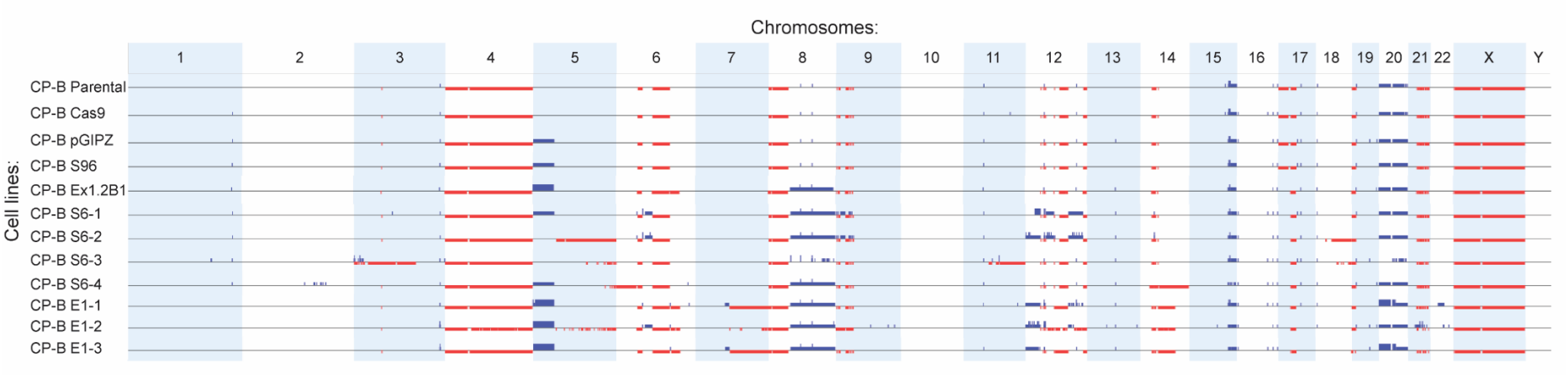

Figure 3.2.9. Copy number alterations. LC WGS across; SMAD4 wild-type cells (CP-B Parental; CP-B Cas9; CP-B pGIPZ); SMAD4 knockout (CP-B Ex1.2B1) and SMAD4 knockdown (CP-B S96) cells grown *in vitro*; tumorigenic SMAD4 knockdown (CP-B S6-1, S6-2, S6-3, S6-4) and knockout (CP-B E1-1, E1-2, E1-3) cells derived from xenograft tumours. Summary of the gains (blue) and losses (red) for individual cell lines across all chromosomes compared to reference genome (Human HG19).

Table 3.2.4. Summary of consistent copy number alterations observed in CP-B SMAD4 knockdown/knockout driven tumours

	SMAD4 wild-type Control			SMAD4 knockdown (in vitro)	SMAD4 knockout (in vitro)	Tumorigenic SMAD4 knockdown				Tumorigenic SMAD4 knockout		
	Parental	Cas9	pGIPZ	S96	Ex1.2 B1	S6-1	S6-2	S6-3	S6-4#	E1-1#	E1-2#	E1-3
Chromosome												
5			5q	5q	5q	5q			5q	5q	5q	5q
6					6q22.31-23.3	6p12.1-11.2	6p12.1-11.2			6q22.31-23.3 6q22.1	6q22.31-23.3 6q22.1 6p12.1-11.2	6q22.31-23.3 6q22.1
7										7q11.22-11.23 7q11.23-36.3	7q11.23-36.3 partial	7q11.22-11.23 7q11.23-36.3
8					8q	8q	8q	8q partial	8q	8q	8q	8q
12						12p12.2-11.21	12p13.33-11.21			12p13.33-11.21	12p13.33-11.21	12p13.33-11.21
14									14q21.1-24.3	14q21.1-24.3	14q21.1-24.3	14q21.1-24.3
17					17p	17p	17p	17p	17p	17p	17p	17p
20										20p		20p

Blue text represents gains, red text represents losses. #Metastatic cell lines.

Besides tumorigenic potential acquired following SMAD4 knockdown and knockout, some CP-B cells exhibited metastatic features. In order to find distinctive CNAs characteristic for metastatic cells, tumorigenic and metastatic CP-B cells were compared with cells that were only tumorigenic. Data showed no distinctive CNAs when comparing metastatic and non-metastatic CP-B cells (**Table 3.2.4**).

The fraction of the genome that was altered was also analysed (**Figure 3.2.10**). The output of this analysis is the percentage of the genome that has been affected by copy number gains or losses. Crucially, tumorigenic SMAD4 knockdown or knockout cells exhibited significantly higher fraction of the genome with CNAs compared to the CP-B SMAD4 wild-type control cells (**Figure 3.2.10**). Interestingly, when comparing metastatic and non-metastatic cell lines, metastatic cell lines exhibited a higher percentage of the genome altered compared to non-metastatic SMAD4 knockout tumour cell lines (Metastatic cell lines are marked by larger size symbols).

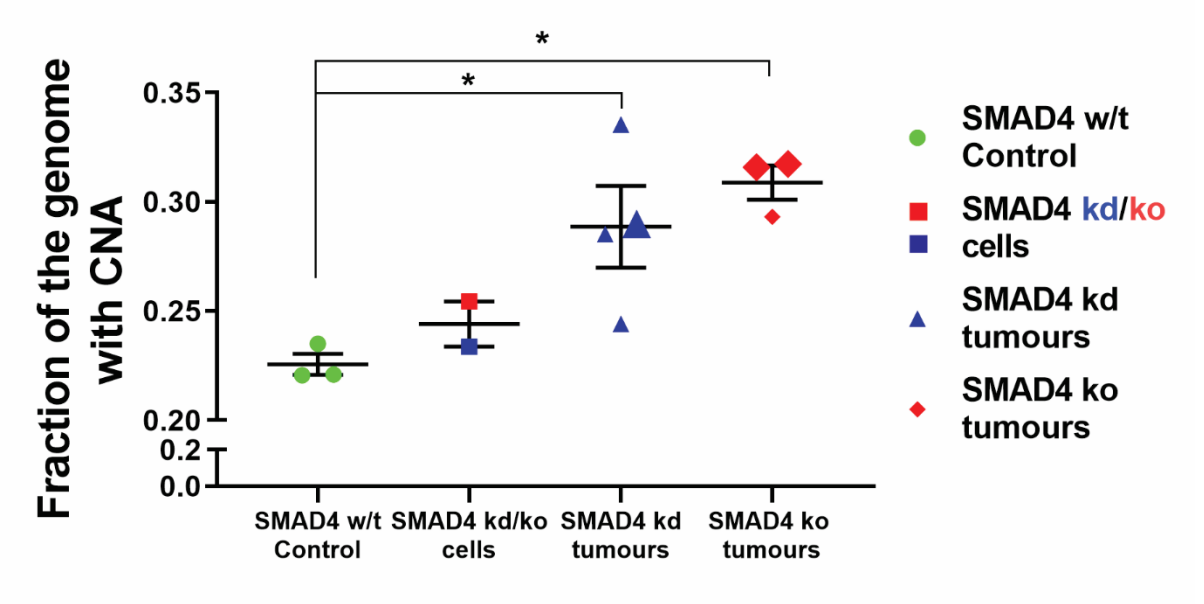

Figure 3.2.10. Fraction of the genome altered in tumorigenic cells established from SMAD4 knockdown or knockout tumour xenografts and CP-B SMAD4 wild-type controls. CP-B cells compared are SMAD4 wild-type cells, parental, pGIPZ vector only and Cas9 only (SMAD4 w/t Control), original SMAD4 knockdown or knockout (SMAD4 kd/ko cells) only grown in *in vitro* conditions and tumorigenic SMAD4 knockdown (SMAD4 kd tumours) or knockout (SMAD4 ko tumours) cells derived from xenograft tumours. Shown are data for individual cell lines. Metastatic cell lines are marked by larger size symbols. Horizontal bars indicate mean (long bars) and SEM (short bars), *p < 0.05: One Way ANOVA with Tukey's multiple comparison test.

3.3. Discussion

In contrast to colorectal cancer that is characterized by well-established oncogenic activations and tumour suppressor gene losses that drive disease progression in a step-wise fashion, OAC is lacking defined molecular drivers of disease development and progression. In addition, genomic studies have revealed that most of the recurrent mutations in OAC are already present at similar frequencies in non-dysplastic Barrett's oesophagus, with the exception of mutations in *TP53* and *SMAD4* tumour suppressor genes, which arise characteristically in high grade dysplasia and cancer, respectively [206]. Therefore, focusing on deciphering the role of stage specific mutations and the importance of the mutations not present in Barrett's oesophagus, but only in OAC, such as *SMAD4* mutations, could provide useful clinical targets [226].

The association between *SMAD4* gene inactivation and tumorigenesis has been reported in neoplasms, such as gastric [232], pancreatic and colorectal adenocarcinomas [233-236]. However, the association of SMAD4 gene inactivation and OAC disease stage specific development and progression has not yet been studied. Of importance, SMAD4 knockdown and SMAD4 knockout model systems were developed in precancerous Barrett's HGD cells to investigate the role of SMAD4 in OAC disease development and progression *in vivo*. This study provides the first evidence in preclinical models of OAC development, that SMAD4 inactivation is sufficient to initiate tumorigenesis in high grade dysplastic Barrett's oesophagus cells, CP-B, *in vivo*.

In order to understand the biology responsible for Barrett's oesophagus tumorigenesis that has been initiated following SMAD4 knockdown or SMAD4 knockout, the histopathological features of the resultant tumours were assessed. Taking into consideration the lack of reliable and specific markers for OAC [237], CK7 (observed in 89-92% of OAC cases) staining was used to histologically characterise established tumours. The results showed strong tumour CK7 reactivity, indicating the OAC histological features of established tumours *in vivo*. Further, a key strength of this study is the re-derivation of cell lines from the xenograft tumours that arose following SMAD4 knockdown or knockout. Initially, no SMAD4 protein expression or differential lower levels were detected across re-derived cell lines, with exception of cells re-

derived from bulk SMAD4 knockout grown tumour (CP-B E3-1) and sequencing analyses are needed to decipher biology undergoing growth of this tumour. Further, re-derivation of cell lines allowed us to characterize SMAD4 knockdown or knockout xenograft tumours at the functional and genomic levels. Of importance, before performing any functional and genomic studies on established cell lines, the tumourigenicity of these cells was confirmed by reinjection *in vivo* and rapid tumour formation was observed. Interestingly, there was no difference in rate of tumour growth between SMAD4 knockdown and knockout tumour derived cell lines.

Together, it is likely that in some cases, progression from high grade dysplastic Barrett's oesophagus toward OAC is initiated by loss of the tumour suppressor gene, SMAD4. In addition, the tumour formation following SMAD4 knockdown (as opposed to knockout) in our model could be explained by earlier described model of SMAD4 haploinsufficiency [232], where gene dosage plays the crucial role in the prolonged, but eventual tumour formation. Interestingly, in contrast to Alfred Knudson's 'two-hit' model that states the necessity of inactivation of both tumour suppressor alleles for tumour formation, a minority of tumour suppressor genes only require inactivation of a single allele to successfully initiate tumorigenesis [238]. This condition is known as haploinsufficiency, with the ability to develop malignancy in the presence of the remaining wild-type allele. As such, SMAD4 haploinsufficency is sufficient to initiate gastric polyposis and cancer in a mouse model [232]. Conclusively, SMAD4 knockdown and knockout aids the high grade dysplasia cells in increasing tumorigenic potential that results in the tumour formation *in vivo*. Understanding the tumour initiation processes in the settings of depleted or loss of SMAD4 in precancerous cells is of high importance for discovering mechanisms and clinically discriminatory markers implicated in progression towards OAC.

In addition, spontaneous metastatic potential was detected in some of the established cell lines. Metastases represent the major cause of cancer related deaths [239]. Of note, the median survival time for the patients with advanced or metastatic oesophageal cancer who receive palliative chemo-radiotherapy is still poor (<1 year) [240]. Unfortunately, over 70% of OAC patients present with de novo metastasis or develop metastasis after diagnosis [241]. Hence, there is an urgent need to

understand the molecular and cellular mechanisms leading to metastasis in order to improve current treatment options for this patient cohort.

Current research is confronting two major obstacles in order to successfully treat this cancer patient group including poorly understood molecular mechanisms underlying metastatic processes, which is exacerbated by a limited number of preclinical *in vivo* metastastic model systems. In addition, the model systems that are available exhibit several confinements, such as technically challenging orthotopic transplants, low rate of metastasis and long duration of the experiment until the first detectable micro-metastasis [242-244]. Hence, the development of effective spontaneous OAC metastatic model systems would provide tools for better understanding the molecular mechanisms and potential novel therapeutic intervention for the majority of OAC patients.

Recently, it has been reported that SMAD4 loss is present in ~44% of patients with loco-regional and distant metastasis, suggesting an important role of SMAD4 loss in driving the invasive and metastatic potential of OAC [230]. The same study has reported that SMAD4 loss is present in ~10% patients with surgically resectable disease. In support of this study, in the models developed in this chapter, an increased metastatic potential was observed for established tumorigenic SMAD4 knockdown and SMAD4 knockout cell lines to specifically spread to two frequently observed OAC metastatic sites [245], the lungs and axillary lymph node. Hence, these new metastatic models are a useful addition to the recently described highly aggressive OAC Flo1^{LM} metastatic model system that spreads to multiple sites including the liver, lungs and mediastinal lymph nodes [246]. Importantly, these SMAD4 knockdown and knockout metastatic model systems are overcoming challenges of currently used metastatic OAC preclinical models. First of all, macro-metastases were detected within 8-12 weeks following subcutaneous injection, whereas another study reports detectable metastases after 40 weeks [244]. In addition, the technical challenges, morbidity and mortality are significantly decreased when using the subcutaneous model system developed in this thesis compared to orthotopic OAC models that have been shown to metastasise [243, 244].

Further, large scale sequencing of paired Barrett's oesophagus and OAC samples has provided insight into the genetic landscape of both entities. Primarily, patients with LGD and HGD Barrett's oesophagus have not exhibited significantly different number of mutations compared to non-dysplastic Barrett's. In addition, the results have shown less than 20% overlap when comparing spectra of single-nucleotide variants (SNVs) in OAC with paired LGD and HGD Barrett's tissue, suggestive of increasing genetic heterogeneity during disease development [96]. Contrastingly, large scale sequencing has revealed increased CNAs in OAC, while Barrett's oesophagus with either LGD or HGD exhibited few CNAs [96], indicating that structural chromosomal rearrangements play a critical role in the transition from HGD towards OAC. Based on these results, the focus was on deciphering the role of SMAD4 loss on histological and physiological changes, as well as genetic alterations with the main interest in CNAs at this critical transition stage from HGD toward OAC.

Given that CNAs are frequent at the later stages of the malignant progression of OAC, CNAs were explored across the tumours that developed upon SMAD4 knockdown or knockout in comparison to SMAD4 wild-type high grade dysplasia cells. In previously published data, CNAs were scarce across Barrett's oesophagus with high grade dysplasia [96], whereas the data in this chapter show the presence of distinctive CNAs already present in CP-B high grade dysplasia cell model system. Therefore, studies of CNAs in a patient cohort that includes a larger proportion of samples with HGD as well as multiple HGD xenograft models of progression towards OAC would provide a better understanding of the sequence of CNAs arising and the effect on disease progression. Indeed, Stackler et al., have reported that CNAs increase during the progression from non-dysplastic to dysplastic Barrett's. More importantly, in support of the results in this chapter, CNAs significantly increase during the progression from Barrett's oesophagus with dysplasia to OAC [91].

The distinctive CNAs that were present in high grade dysplastic parental CP-B cells overlapped with the most frequently reported CNAs across adenocarcinomas of the oesophagus, stomach and colon [109]. As such, parental CP-B cells already displayed 20p, 20q chromosome arm gain and 8p arm loss, which are frequently amplified across common adenocarcinomas of the gastrointestinal tract, including OAC. Likewise, CNAs that were significant only in OAC, including focal 9p, 5q and 21q arm

loss, were already present in parental CP-B cells. The 5p chromosome harbours genes such as BASP1, TARS, PAIP1, BRD9, RAD1, SKP2, and POLS that are involved in regulation of DNA repair and cell cycle regulation and their deregulation has been suggested to contribute to colorectal cancer progression [109]. Interestingly, significant losses in OAC, such as 9p and 21q arm that contain tumour suppressor genes including *CDKN2A* and *RUNX1* are observed in parental CP-B cells. Overall, given that CP-B cells are rarely tumourigenic (1/17 injections, **Table 3.2.1**) the above mentioned CNAs already present in CP-B cells are unlikely to be sufficient for disease progression towards cancer, although they might contribute together with other genetic alterations. In summary, CP-B or high grade dysplasia cells exhibited loss of whole copy of chromosome 4, 8p and 21q arm or gain of whole copy of chromosome 20, some of the most common CNAs that are present in OAC patient samples [96].

More importantly, distinctive CNAs were detected that were present only in cells derived from SMAD4 knockout/knockdown tumour xenografts, but not in CP-B parental cells. Firstly, 8q amplification was detected, which is frequently seen in OAC patient samples [109]. Importantly, these data indicate that distinctive chromosomal structural rearrangements including 8q gain loss are leading towards disease progression from HGD towards cancer following SMAD4 loss or prolonged depletion. It is not surprising that the process of OAC tumorigenesis relies on gain of chromosome 8q considering the presence of the gene encoding the well-known oncogene, c-myc. Interestingly, given that 8q gain in isogenic CP-B SMAD4 knockout cells was observed, it is likely that gain of 8q happened during *in vitro* culturing conditions, as a direct consequence of complete SMAD4 loss. Similarly, 6q 22.31-23.3 loss was detected upon SMAD4 knockout in vitro. Considering that 8q chromosome gain was detected across all tumour derived SMAD4 knockdown CP-B cells, these data suggest that prolonged SMAD4 depletion also leads to this particular chromosomal aberration. Secondly, distinctive chromosomal rearrangements were observed that happened following growth of SMAD4 knockdown or knockout cells *in vivo*. These CNAs include partial gain of 12q and loss of 14q21.1-24.3 chromosomes. Of note, oncogenes such as CDK4 and MDM2 are positioned within 12q chromosome [247] and their amplification and overexpression have been implicated in tumourigenesis, including oesophageal cancer [248-251]. Taken into consideration the driver events present in OAC, the most recent genomic studies have suggested

on potential benefit of using CDK4/6 inhibitors is OAC [147]. It is likely that this subset of CNAs is responsible for progressive capacity of SMAD4 knockdown and knockout high grade dysplasia cells towards cancer and subsequent acquiring invasive and migratory characteristics. In support of these results, Passelo *et al*., have reported a correlation between the total number of chromosomal aberrations and poor survival outcome in OAC [252].

Given that acquisition of spontaneous metastatic potential was observed in some of the established tumorigenic SMAD4 knockdown and SMAD4 knockout cell lines, the acquisition of concomitant distinctive CNAs was investigated. Although, distinctive CNAs were not observed, SMAD4 knockout metastatic cell lines derived from tumour xenografts had a higher percentage of the genome with CNAs. Considering that OAC has been characterized as highly mutated, it is possible that metastatic ability is not acquired by distinct CNAs, but rather characterized by high percentage of the genome with CNAs, in combination with group of genetic mutations including SNVs, small indels and single nucleotide polymorphisms. Furthermore, epigenetic regulation plays an important role in Barrett's oesophagus progression towards cancer [77, 78], but also in metastasis across different cancers [253], opening a new area to investigate epigenetic regulation in OAC, in order to understand its metastatic potential.

Of high importance, it was observed that CNAs in tumorigenic SMAD4 knockdown and knockout CP-B cells (LC WGS) were consistent with common CNAs found in OAC patient samples. Taken together, this high genomic instability, characterized by structural chromosomal rearrangements within the tumours following SMAD4 loss, implicates SMAD4 as a protector of genome integrity in OAC development and progression. Given the evidence, it is likely that not the single alteration, but more the combination of CNAs leads to the progression of high grade dysplasia towards OAC following deregulation of SMAD4 expression.

CHAPTER 4.

DECIPHERING THE BIOLOGICAL EFFECTS OF SMAD4 LOSS ON TGF-β SIGNALLING IN OAC: *IN VITRO STUDIES*

4.1. Introduction

In Chapter 3, it was shown that SMAD4 knockdown and knockout dysplastic Barrett's cells have increased tumorigenic potential compared to SMAD4 wild-type cells. Moreover, increased tumorigenic potential upon SMAD4 knockdown and SMAD4 knockout was accompanied by a significantly increased fraction of the genome with copy number alterations. Rationally, these results suggested that the functional effect of SMAD4 loss as a part of TGF-β signalling in dysplastic Barrett's cells, should be explored.

The SMAD4 tumour suppressor gene is located on the q arm of chromosome 18 and encodes a common intracellular effector of the TGF-β superfamily signalling pathway. Normally, this pathway is initiated through activation of type I and type II trans-membrane serine/threonine kinase receptors upon binding of TGF-β or BMP ligands such as TGF-β1 and BMP4 (among numerous other ligands), leading to phosphorylation of SMAD2/3 or SMAD1/5/8 arm of the signalling and downstream association with SMAD4 [254]. The anti-proliferative effects of TGF-β are achieved through transcriptional down-regulation of myc and up-regulation of CDK inhibitors 2B ($p15^{INK4B}$) and 1A (p21), which leads to cell cycle arrest in normal epithelial cells [255]. However, impaired TGF-β signalling due to genetic alterations within members of this signalling pathway is important in the pathogenesis of cancer [212]. As reviewed in Chapter 1.8, gastrointestinal malignancies frequently display inactivating mutations within TGF-β signalling cascade, including SMAD4 loss.

The functional role of SMAD4 loss in development and progression of OAC has not been elucidated. In *in vitro* models, loss of SMAD4 expression in the metaplasia-dysplasia-adenocarcinoma sequence correlates with impaired TGF-β anti-proliferative signalling and a switch to SMAD independent activation of kinase pathways such as PI3K, ERK and JNK [256, 257]. Consequently, through activation of kinase pathways, TGF-β promotes invasive properties of OAC cells. Overall, it appears that TGF-β has growth suppressor activity in the early stages of tumour development, but at the later stages it promotes EMT and metastasis [258, 259]. In order to utilize TGF-β signalling pathway for anti-cancer therapy, we still need to understand TGF-β mediated

oncogenic mechanisms that emerge when this signalling pathway is switched through SMAD4 loss.

Initial studies into SMAD4 dependent and independent mechanisms of action in the context of TGF-β signalling have shown an indispensable role of SMAD4 in the regulation of a subset of target genes in normal human keratinocyte cells and pancreatic cancer cells [260]. In addition, it has been shown that in the absence of SMAD4 some of the TGF-β target genes are still induced [261]. However, the precise mechanism of SMAD4 dependent and independent regulation of gene expression within TGF-β signalling in the development and progression of OAC is not well known.

On the other hand, TGF-β1 has been frequently reported to be abundantly expressed across cancers and positively contributing to tumour progression, metastasis, angiogenesis and poor outcome. Its role among other members of TGF-β signalling in gastrointestinal malignancies has been reviewed in Chapter 1.8. Overall, we have limited knowledge about TGF-β signalling upon activation with TGF-β1 ligand once SMAD4 is lost.

Herein, the focus of this chapter is on the functional characterisation of the cell response to TGF-β signalling, when its key mediator, SMAD4, is lost in dysplastic Barrett's cells. Further, the effect of SMAD4 loss on the differential gene expression profile of TGF-β specific target genes upon stimulation with TGF-β1 cytokine compared to basal conditions was investigated. Therefore, this chapter is concentrated on the differential regulation of genes following SMAD4 loss and the effects of SMAD4 loss as a part of TGF-β signalling on the pathophysiology of OAC.

4.2. RESULTS

4.2.1. TGF-β1 induces Go/G1 cell cycle arrest through SMAD4-dependent signalling and up-regulation of p21

To better understand TGF-β mediated tumorigenic mechanisms following SMAD4 loss, the expression of G1/S cyclin-dependent kinase inhibitor p21 was examined in the response to TGF-β1 and BMP4 ligands in SMAD4 wild-type and SMAD4 knockout cells (**Figure 4.2.1 A**). In cells with wild-type SMAD4 (CP-B parental and Cas9 only expressing cells), TGF-β1 and BMP4 induced p21 protein expression. Contrastingly, CP-B SMAD4 knockout cells (Ex1.2B1) failed to increase p21 expression levels in both treatment settings (**Figure 4.2.1 A**). Furthermore, cell cycle analyses were performed 24 hours following treatment in order to functionally determine the effect of TGF-β1 (**Figure 4.2.1 B, C**). TGF-β1 induced Go/G1 cell cycle arrest in SMAD4 wild-type cells, whereas SMAD4 knockout cells did not respond with Go/G1 cell cycle arrest. Taken together, this suggests that TGF-β1 induces cell cycle arrest through SMAD4 dependent signalling and deregulation of SMAD4 signalling results in complete blocking of TGF-β1 mediated cell cycle arrest.

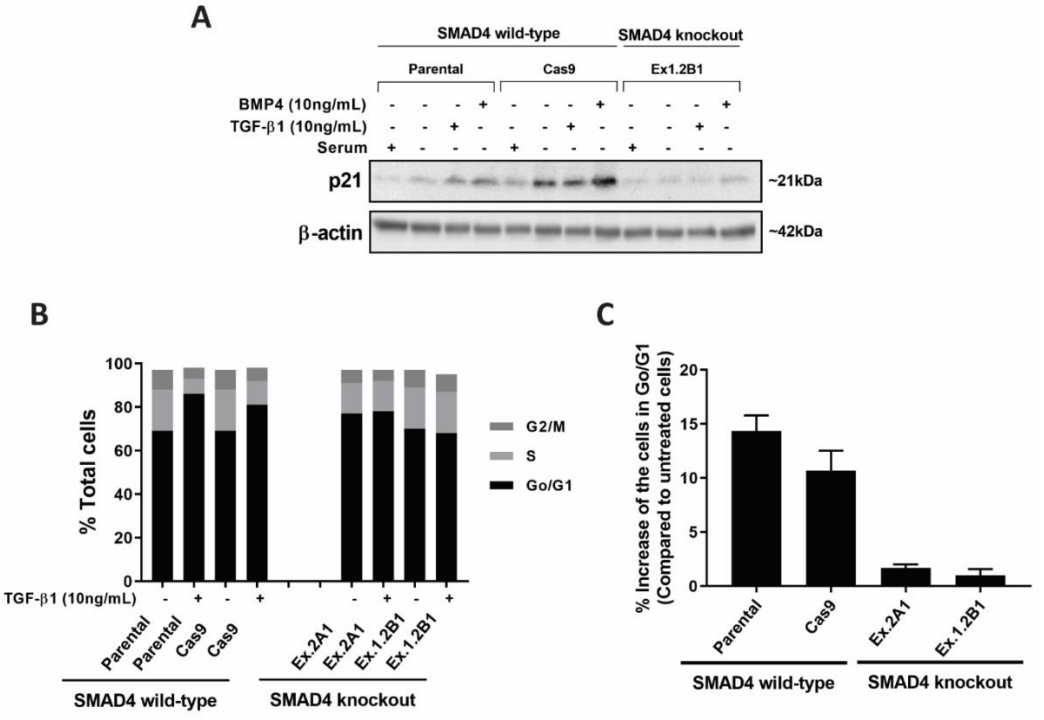

Figure 4.2.1. TGF-β1 induces cell cycle arrest in SMAD4 wild-type, but not in SMAD4 knockout cells. (A) Representative protein immunoblot of G1/S checkpoint inhibitor p21 following treatment of CP-B SMAD4 wild-type (Parental and Cas9) and SMAD4 knockout (EX1.2B1) isogenic cells with 10ng/mL TGF-β1 and 10ng/mL BMP4 for 16 hours. (B) Representative histogram of cell cycle analyses

(PI staining) in CP-B SMAD4 wild-type (Parental and Cas9) and SMAD4 knockout (Ex2.A1 and Ex1.2B1) cells following the treatment with 10ng/mL TGF-β1 over 24 hours. (C) Percentage of the cells arrested in Go/G1 following the treatment with TGF-β1.n=3 independent experiments, data represent mean±SEM.

4.2.2. Differential gene expression profile in SMAD4 knockout cells and in SMAD4 wild-type cells upon treatment with TGF-β1

RT^2 Profiler PCR Arrays were performed to decipher the expression profile of human TGF-β signalling target genes following the loss of SMAD4. Firstly, the effect of human recombinant TGF-β1 cytokine on the expression profile of TGF-β signalling target genes in the SMAD4 wild-type and SMAD4 knockout cells was assessed. In order to avoid gene expression changes due to the presence of serum components, the cells were grown for 6 hours in serum-free conditions prior to treatment with TGF-β1 (also in serum free conditions) for 16 hours (late response). CP-B Parental and Cas9, as SMAD4 wild-type cells, were treated with TGF-β1. Complementary CP-B Ex2.A1 and Ex1.2B1 SMAD4 knockout cells underwent the same treatment. Gene expression profiling of SMAD4 wild-type cells following treatment with TGF-β1 and complete serum deprivation showed up-regulated genes including *HEY1*, *HMOX1*, *SERPINE1*, *SNAI1*, *PTHLH*, *ID1*, *EPHB2*, *ID3*, *GADD45B*, *PDGFA* and *SOX4* and down-regulated genes *PTGS2*, *AGT*, *SP1*, *SHH*, *RBL1*, *TXNIP*, *E2F4*, *NOTCH1*, *NFKBIA*, *BCL2L1*, *CDKN1B*, *CTNNB1*, *PTK2B* and *BRD2* (**Figure 4.2.2 A** and **Table 4.2.1)**. On the other hand, there were limited changes in the gene expression profile of SMAD4 knockout cells with up-regulation of only *PTHLH*, *SNAI1*, *MSX2*, *ID1*, *SERPINE1* and *RUNX1* and down-regulation of *AIPL1* and *AGT* following treatment with TGF-β1 and complete serum deprivation in this particular gene set (**Figure 4.2.2 B** and **Table 4.2.2)**. Graphs for representative up- or down-regulated genes in either SMAD4 wild-type or SMAD4 knockout cells following stimulation with TGF-β1 are shown (**Figure 4.2.3 A-D**) or representative upregulated gene in both, SMAD4 wild-type and SMAD4 knockout cells (**Figure 4.2.3 E**). In addition, data is presented via a Venn diagram in order to compare the differences in gene regulation following stimulation with TGF-β1 for 16 hours in SMAD4 wild-type vs. SMAD4 knockout cells (**Figure 4.2.3. F**).

These data suggest that SMAD4 is required for Barrett's cells to up-regulate a sub-set of genes in response to TGF-β1, such as *HEY1*, *HMOX1*, *EPHB2*, *ID3*, *GADD45B*,

PDGFA and *SOX4* or to down-regulate *PTGS2*, *SP1*, *SHH*, *RBL1*, *TXNIP*, *E2F4*, *NOTCH1*, *NFKBIA*, *BCL2L1*, *CDKN1B*, *CTNNB1*, *PTK2B* and *BRD2*, indicating SMAD4 dependent regulation of these genes. In contrast, SMAD4 knockout cells maintain the ability to up-regulate *PTHLH*, *SNAI1*, *ID1* and *SERPINE1* or down-regulate *AGT*, suggestive of SMAD4 independent regulation of these genes, likely through SMAD2/3 transcription factor activity upon stimulation with TGF-β1. In addition, TGF-β1 treatment of SMAD4 knockout cells leads to up-regulation of *MSX2* and *RUNX1* and down-regulation of *AIPL1*, suggesting that SMAD4 inhibits TGF-β1 mediated changes in expression of these genes

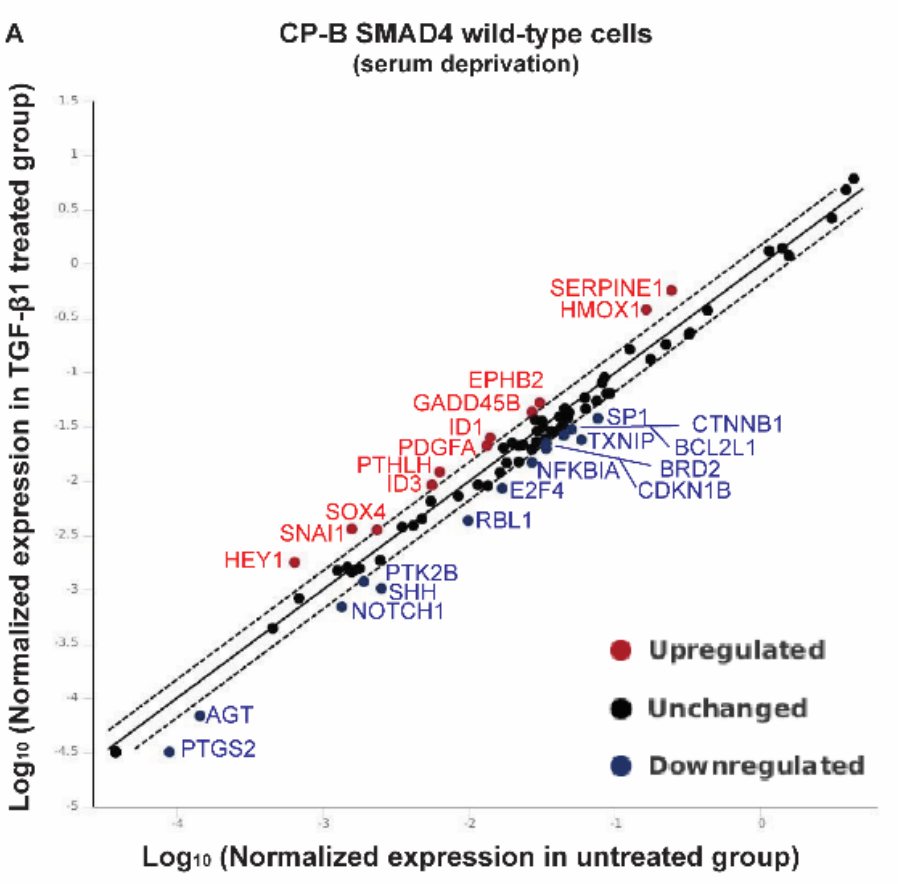

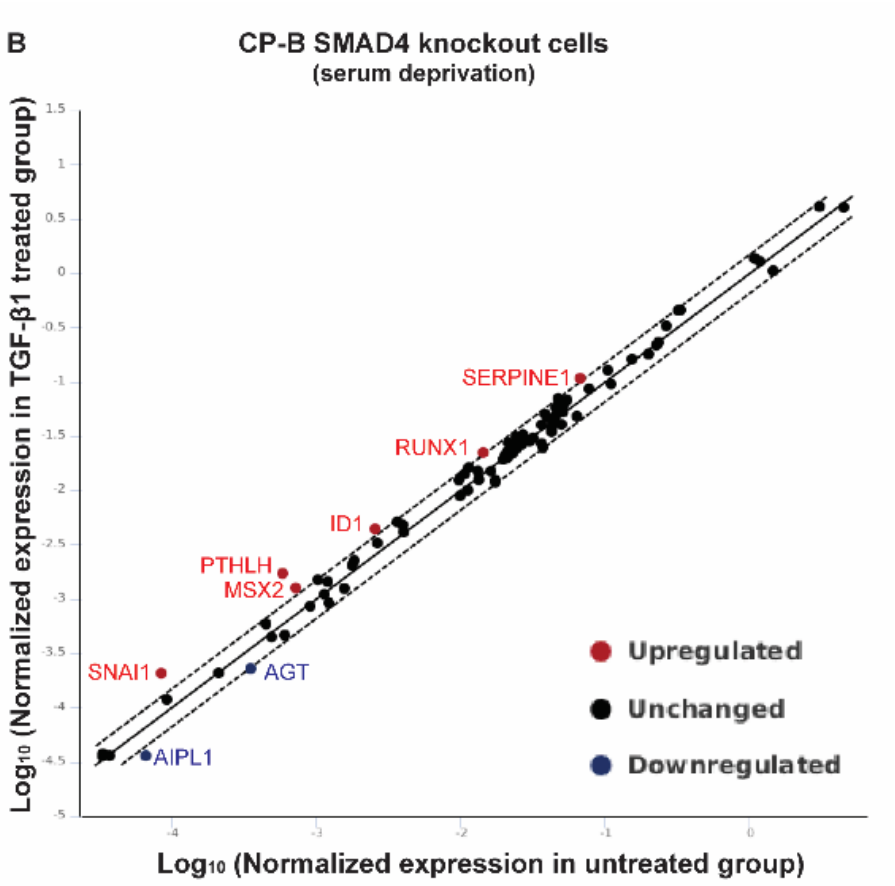

Figure 4.2.2. TGF-β signalling target gene expression in CP-B SMAD4 wild-type and SMAD4 knockout cells following the treatment with TGF-β1 under serum deprivation for 16 hours. A RT^2 Profiler PCR Array was used to determine transcript expression levels of TGF-β1 signalling targets in (A) SMAD4 wild-type cells (CP-B Parental and CP-B Cas9) and (B) SMAD4 knockout cells (CP-B Ex2.A1 and CP-B Ex1.2B1) upon treatment with TGF-β1 for 16 hours compared to respective untreated cells. The scatter plot compares the normalized expression of every gene on the TGF-β signalling targets RT^2 Profiler PCR array (**Table 2.6**) between TGF-β1 treated group vs untreated. The average geometric mean of five HKG genes, *ACTB*, *B2M*, *GAPDH*, *HPRT1* and *RPLPO* was used for normalization within each group. The solid line indicates unchanged gene expression, whereas the broken lines indicate a 1.5 fold regulation (2^(- Delta Delta C_T)) cut-off threshold. Fold- regulation values greater than 1.5 or less than -1.5 are indicated in red or blue, respectively. CP-B Parental and CP-B Cas9 or CPB Ex2.A1 and CP-B Ex1.2B1 are considered as biological replicates. Each dot on the graph represents the mean of pooled data from (A) CP-B Parental and CP-B Cas9 (SMAD4 wild-type) or (B) CPB Ex2.A1 and CP-B Ex1.2B1 (SMAD4 knockout) cells treated with TGF-β1 compared to untreated cells, respectively.

Table 4.2.1. Genes up- or down-regulated upon TGF-β1 treatment of SMAD4 wild-type cells

RefSeq	Gene Symbol	Gene Full Name	Fold Regulation[a]
NM_012258	HEY1	Hairy/enhancer-of-split related with YRPW motif 1	2.76
NM_002133	HMOX1	Heme oxygenase (decycling) 1	2.32
NM_000602	SERPINE1	Serpin peptidase inhibitor, clade E (nexin, plasminogen activator inhibitor type 1), member 1	2.31
NM_005985	SNAI1	Snail family transcriptional repressor 1	2.28
NM_002820	PTHLH	Parathyroid hormone-like hormone	1.92
NM_002165	ID1	Inhibitor of DNA binding 1, dominant negative helix-loop-helix protein	1.80
NM_004442	EPHB2	EPH receptor B2	1.72
NM_002167	ID3	Inhibitor of DNA binding 3, dominant negative helix-loop-helix protein	1.63
NM_015675	GADD45B	Growth arrest and DNA-damage-inducible, beta	1.61
NM_002607	PDGFA	Platelet-derived growth factor alpha polypeptide	1.58
NM_003107	SOX4	SRY (sex determining region Y)-box 4	1.50
NM_000963	PTGS2	Prostaglandin-endoperoxide synthase 2 (prostaglandin G/H synthase and cyclooxygenase)	-2.80
NM_138473	SP1	Sp1 transcription factor	-2.49
NM_000193	SHH	Sonic hedgehog	-2.48
NM_002895	RBL1	Retinoblastoma-like 1 (p107)	-2.29
NM_000029	AGT	Angiotensinogen (serpin peptidase inhibitor, clade A, member 8)	-2.12
NM_006472	TXNIP	Thioredoxin interacting protein	-2.02
NM_001950	E2F4	E2F transcription factor 4, p107/p130-binding	-1.98
NM_017617	NOTCH1	Notch 1	-1.95
NM_020529	NFKBIA	Nuclear factor of kappa light polypeptide gene enhancer in B-cells inhibitor, alpha	-1.82
NM_138578	BCL2L1	BCL2-like 1	-1.71
NM_004064	CDKN1B	Cyclin-dependent kinase inhibitor 1B (p27, Kip1)	-1.71
NM_001904	CTNNB1	Catenin (cadherin-associated protein), beta 1, 88kDa	-1.69
NM_004103	PTK2B	PTK2B protein tyrosine kinase 2 beta	-1.62
NM_005104	BRD2	Bromodomain containing 2	-1.53

[a] Fold regulation in mRNA expression levels as assessed by RT^2 Profiler PCR Array. Genes labelled in red and blue colour are up-regulated and down-regulated, respectively, in SMAD4 wild-type cells treated with TGF-β1 and complete serum deprivation for 16 hours compared to untreated (serum deprivation only) cells.

Table 4.2.2. Genes up- or down-regulated upon TGF-β1 treatment of SMAD4 knockout cells

RefSeq	Gene Symbol	Gene Full Name	Fold Regulation[a]
NM_002820	PTHLH	Parathyroid hormone-like hormone	2.94
NM_005985	SNAI1	Snail family transcriptional repressor 1	2.44
NM_002449	MSX2	Msh homeobox 2	1.76
NM_002165	ID1	Inhibitor of DNA binding 1, dominant negative helix-loop-helix protein	1.72
NM_000602	SERPINE1	Serpin peptidase inhibitor, clade E (nexin, plasminogen activator inhibitor type 1), member 1	1.6
NM_001754	RUNX1	Runt-related transcription factor 1	1.55
NM_014336	AIPL1	Aryl hydrocarbon receptor interacting protein-like 1	-1.83
NM_000029	AGT	Angiotensinogen (serpin peptidase inhibitor, clade A, member 8)	-1.53

[a] Fold regulation in mRNA expression levels as assessed by RT^2 Profiler PCR Array. Genes labelled in red and blue color are up-regulated and down-regulated, respectively, in SMAD4 knockout cells treated with TGF-β1 and complete serum deprivation for 16 hours compared to untreated cells (serum deprivation only) cells.

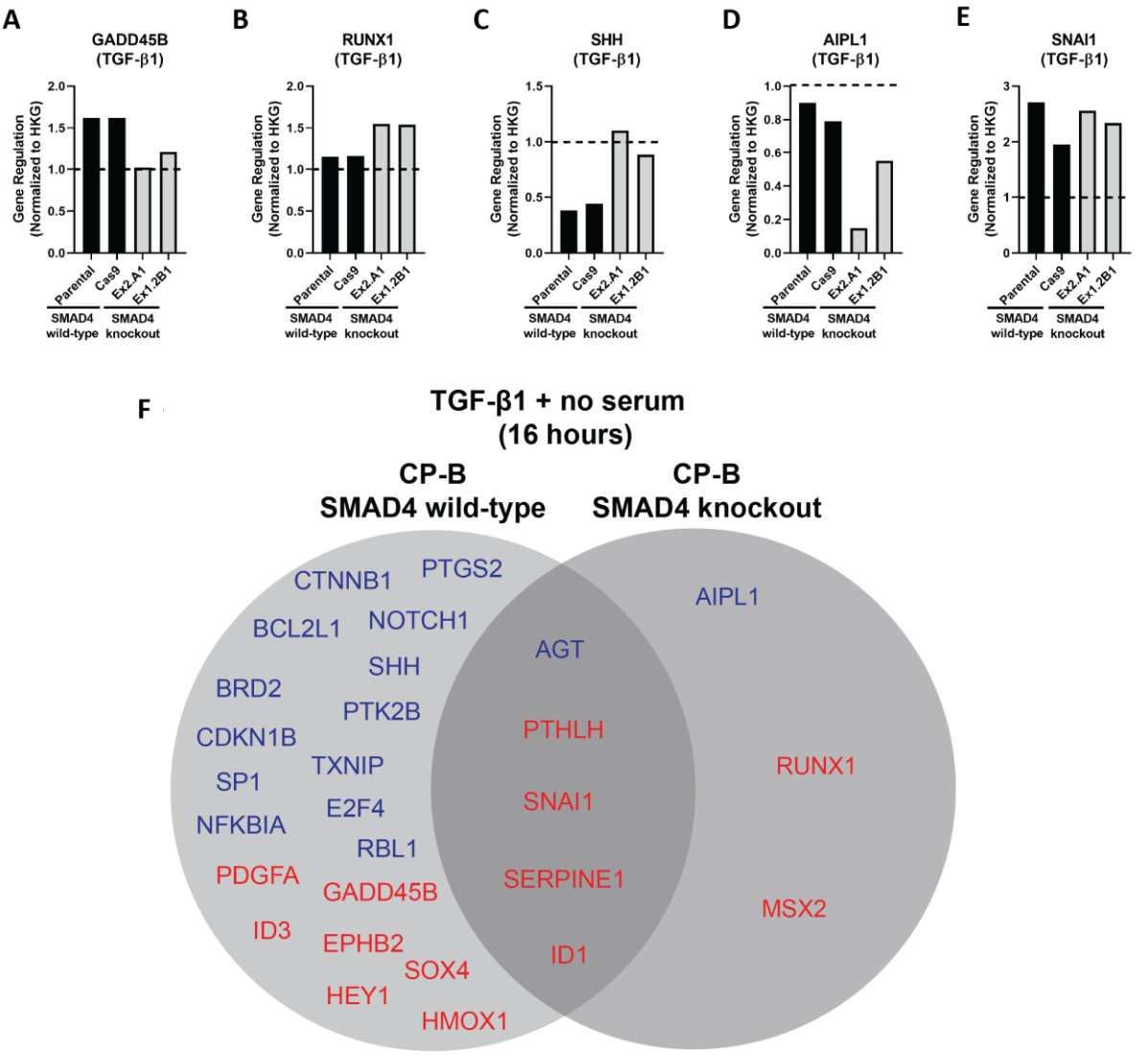

Figure 4.2.3. Individual gene regulation in SMAD4 wild-type and SMAD4 knockout cells in response to TGF-β1 in the absence of serum. Graphs were generated by using RT^2 Profiler PCR Array data output. Transcript expression levels of TGF-β1 signalling targets (A) GADD45B, (B) RUNX1, (C) SHH, (D) AIPL1, (E) SNAI1 were determined in SMAD4 wild-type (CP-B Parental and CP-B Cas9) and SMAD4 knockout (CP-B Ex2.A1 and Ex1.2B1) cells upon treatment with 10ng/mL TGF-β1 for 16 hours in the absence of serum and normalised to untreated cells (n=1 biological replicate per each cell line). The average geometric mean of five HKG genes, *ACTB*, *B2M*, *GAPDH*, *HPRT1* and *RPLPO* was used for normalization within each sample. (F) Venn diagram representing the TGF-β1 signalling target genes regulated in SMAD4 wild-type and/or SMAD4 knockout cells in response to TGF-β1. Genes labelled in red and blue colour represent up- and down-regulated genes, respectively.

4.2.3. Early and late response to TGF-β1 in SMAD4 wild-type and SMAD4 knockout cells under presence of serum

Although there is differential gene expression profile of TGF-β signalling target genes following treatment with TGF-β1 in either SMAD4 wild-type or SMAD4 knockout cells in the serum deprivation conditions for 16 hours, the majority of genes were

unchanged (**Figure 4.2.2. A, B**). It was hypothesised that this may be because of a general lack of cellular activity due to the absence of serum or regulation of a subset of genes happened at an earlier time point, in response to TGF-β1. Therefore, TGF-β1 treatment of SMAD4 wild-type and SMAD4 knockout cells was also performed in the presence of serum. Furthermore, in order to decipher whether the expression profile of TGF-β signalling target genes differs between early and late responses, stimulation with TGF-β1 was performed for either 4 or 16 hours. Differential gene expression of TGF-β signalling target genes was obtained for SMAD4 wild-type (**Figure 4.2.4 A, B and Table 4.2.3)** and SMAD4 knockout cells (**Figure 4.2.5. A, B and Table 4.2.4**). Indeed, in the presence of serum, a larger proportion of the target genes were differentially expressed at both time points, particularly in SMAD4 wild-type cells.

Among the down-regulated genes at both 4 and 16 hour time points in SMAD4 wild-type cells are *SMAD3* and *SHH* (**Figure 4.2.4 C**). ID3 was down-regulated at 4 hours but had returned to basal levels at 16 hours, whereas *ATF3*, *FOS* and *AR* were down-regulated only after 16 hours treatment with TGF-β1. The early response of SMAD4 wild-type cells to TGF-β1 treatment involved up-regulation of *IFRD1*, *NOTCH1*, *PTGS2*, *SOX4*, *PTK2B* and *FOS* genes, which had returned to basal levels at 16 hours, whereas the late response was characterized by positive regulation of *AGT*, *IL10* and *EPHB2*. The genes up-regulated at both time points upon treatment of SMAD4 wild-type cells with TGF-β1 include *HEY1*, *BHLHE40*, *FURIN*, *GADD45B*, *GLI2*, *HMOX1*, *SNAI1*, *PDGFA*, *PTHLH*, *RHOB* and *SERPINE1* (**Figure 4.2.4 C**) and their level of up-regulation was not noticeably different between the two time points. The details of the up- and down-regulated genes in SMAD4 wild-type cells at early and late time points following treatment with TGF-β1 are listed in **Table 4.2.3**.

Similar to serum-free conditions, the differential gene expression profile of TGF-β signalling target genes in SMAD4 knockout cells was markedly different to the response of SMAD4 wild-type cells to treatment with TGF-β1 in the presence of serum. In particular, far fewer target genes were differentially regulated in SMAD4 knockout cells than in SMAD4 wild-type cells following TGF-β1 treatment for 4 hours in the presence of serum (**Figure 4.2.5 A).** Furthermore, there was very little overlap in the differentially regulated genes at the two time points in SMAD4 knockout cells, with only

AGT being up-regulated at both early and late time points. As such, the early response of SMAD4 knockout cells to TGF-β1 treatment was characterised by up-regulation of *SHH* and down-regulation of *SOX4*, *PTHLH*, *HEY1* and *FOS* (**Figure 4.2.5 A** and **Table 4.2.4**). SMAD4 knockout cells respond to TGF-β1 treatment with up-regulation of *AR*, *PLG*, *AIPL1*, *SNAI1*, *PDGFA*, *SMAD1*, *GLI2*, *ACTA2*, *HEY1*, *PTK2* and *ID2* and down-regulation of *MSX2* at the late time point (**Figure 4.2.5 B** and **Table 4.2.4**). Up - and down regulated genes in SMAD4 knockout cells at an early and late time point or at both time points are presented via Venn diagram (**Figure 4.2.5 C**).

In addition, gene expression following treatment with TGF-β1 for 16 hours in the absence or presence of serum was compared in SMAD4 wild-type vs. SMAD4 knockout cells. A 4-way Venn diagram was created to visualize gene sets that are regulated in response to TGF-β1 in SMAD4 wild-type cells and/or SMAD4 knockout cells in the absence and/or presence of serum (**Figure 4.2.6**).

In particular, these findings show that SMAD4 loss leads to significant alterations in gene expression profile of TGF-β signalling target genes in response to TGF-β1 cytokine and suggest the importance of future research to understand the complex network of TGF-β signalling upon SMAD4 loss. Further, differential gene expression profile of TGF-β signalling target genes was observed between the absence and presence of serum in SMAD4 wild-type as well as SMAD4 knockout cells. It is likely that presence of cytokines other than TGF-β1 in serum dictate changes in gene expression of TGF-β signalling target genes in SMAD4 wild-type, but also in SMAD4 knockout cells.

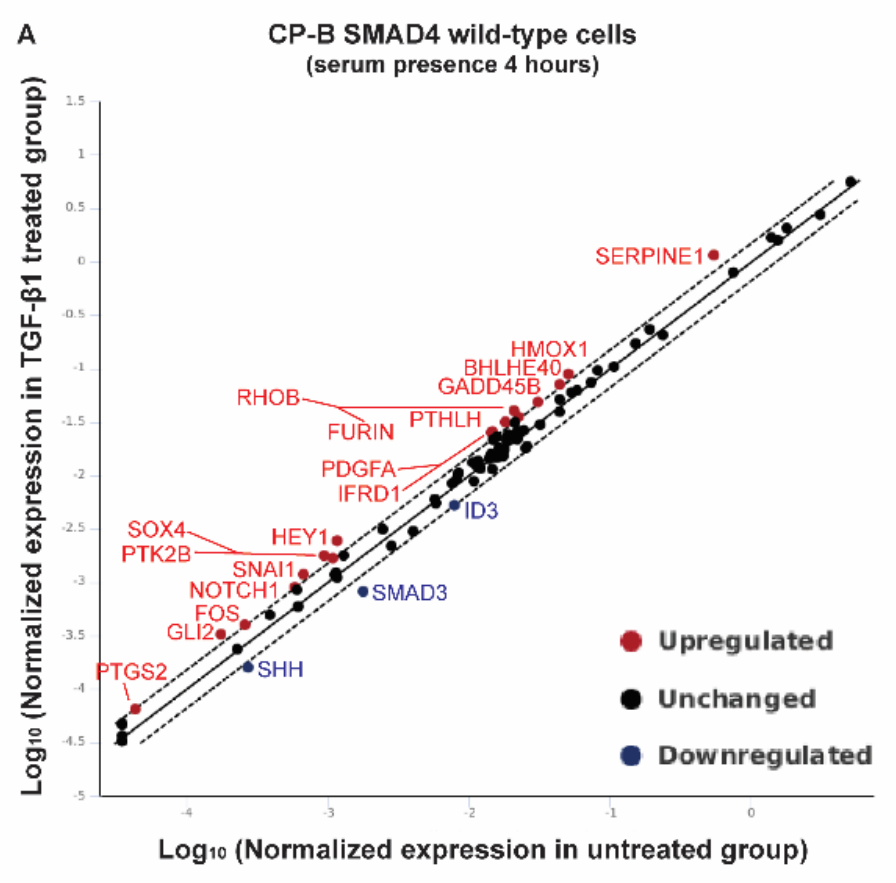
A
CP-B SMAD4 wild-type cells
(serum presence 4 hours)
Log10 (Normalized expression in TGF-β1 treated group)
Log10 (Normalized expression in untreated group)
SERPINE1
HMOX1
BHLHE40
GADD45B
RHOB
FURIN
PTHLH
PDGFA
IFRD1
ID3
SOX4
PTK2B
HEY1
SNAI1
NOTCH1
SMAD3
FOS
GLI2
PTGS2
SHH
Upregulated
Unchanged
Downregulated

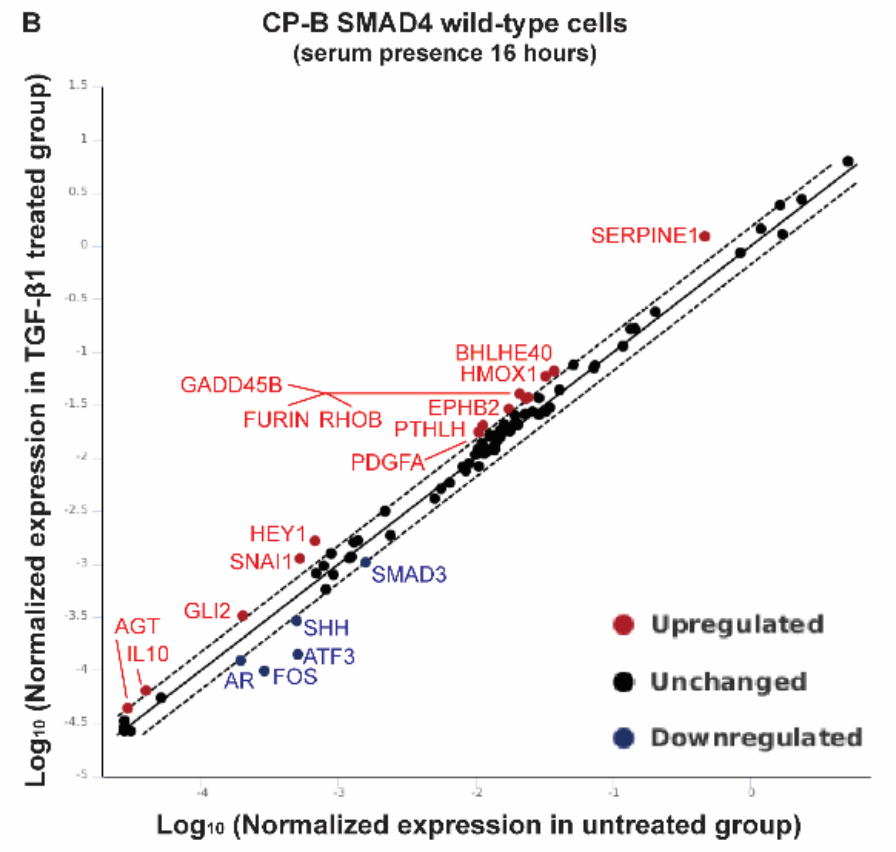
B
CP-B SMAD4 wild-type cells
(serum presence 16 hours)
Log10 (Normalized expression in TGF-β1 treated group)
Log10 (Normalized expression in untreated group)
SERPINE1
BHLHE40
HMOX1
GADD45B
EPHB2
FURIN
RHOB
PTHLH
PDGFA
HEY1
SNAI1
SMAD3
GLI2
AGT
SHH
IL10
ATF3
AR
FOS
Upregulated
Unchanged
Downregulated

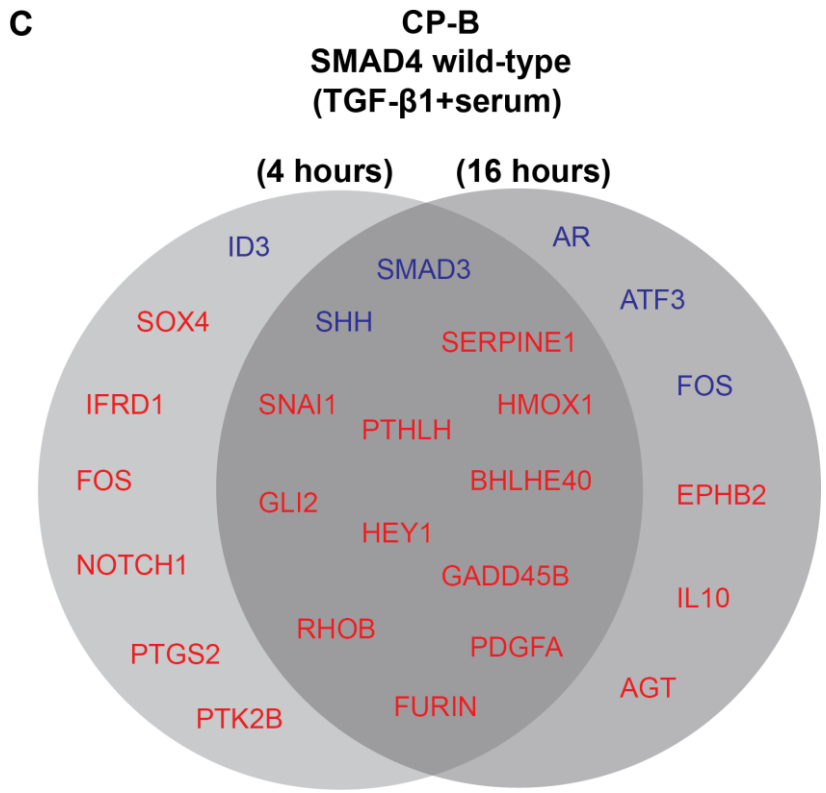

Figure 4.2.4. TGF-β signalling target gene expression in CP-B SMAD4 wild-type cells following the treatment with TGF-β1 for 4 or 16 hours in the presence of serum. . RT^2 Profiler PCR Array to determine transcript expression levels of panel of human TGF-β1 signalling targets in SMAD4 wild-type (CP-B Parental and CP-B Cas9) cells upon treatment with TGF-β1 for (A) 4 hours and (B) 16 hours in the presence of serum compared to untreated cells. The scatter plots compare the normalized expression of every gene (delta C_T for each gene within groups of interest) on the TGF-β signalling targets RT^2 Profiler PCR array between TGF-β1 treated and untreated group by plotting them against each other. The average geometric mean of five HKG genes, *ACTB*, *B2M*, *GAPDH*, *HPRT1* and *RPLPO* was used for normalization within each sample. The solid line indicates unchanged gene expression, whereas the broken lines indicate the 1.5 fold regulation threshold. CP-B Parental and CP-B Cas9 are considered as biological replicates. Each dot on the graph represents pooled data from CP-B Parental and CP-B Cas9 cells treated with TGF-β1 compared to untreated cells. (C) Venn Diagram representing the TGF-β1 signalling target genes regulated at early (4 hours) and/or late (16 hours) time point in SMAD4 wild-type cells in response to TGF-β1 in the presence of serum. Genes labelled in red and blue colour represent up- and down-regulated genes, respectively.

Table 4.2.3. Genes up- or down-regulated in SMAD4 wild-type cells upon TGF-β1 treatment in the presence of serum for 4 hours and 16 hours

RefSeq	Gene Symbol	Gene Full Name	Fold Regulation[a] 4 hours	Fold Regulation[a] 16 hours
NM_000029	AGT	Angiotensinogen (serpin peptidase inhibitor, clade A, member 8)	-	1.51
NM_003670	BHLHE40	Basic helix-loop-helix family, member e40	1.61	1.78
NM_004442	EPHB2	EPH receptor B2	-	1.68
NM_005252	FOS	FBJ murine osteosarcoma viral oncogene homolog	1.53	-
NM_002569	FURIN	Furin (paired basic amino acid cleaving enzyme)	1.56	1.58
NM_015675	GADD45 B	Growth arrest and DNA-damage-inducible, beta	1.56	1.92
NM_005270	GLI2	GLI family zinc finger 2	1.84	1.64
NM_012258	HEY1	Hairy/enhancer-of-split related with YRPW motif 1	2.09	2.44
NM_002133	HMOX1	Heme oxygenase (decycling) 1	1.73	1.83
NM_001550	IFRD1	Interferon-related developmental regulator 1	1.73	-
NM_000572	IL10	Interleukin 10	-	1.63
NM_017617	NOTCH1	Notch 1	1.55	-
NM_002607	PDGFA	Platelet-derived growth factor alpha polypeptide	1.77	1.68
NM_000963	PTGS2	Prostaglandin-endoperoxide synthase 2 (prostaglandin G/H synthase and cyclooxygenase)	1.51	-
NM_002820	PTHLH	Parathyroid hormone-like hormone	1.75	1.79
NM_004103	PTK2B	PTK2B protein tyrosine kinase 2 beta	1.55	-
NM_004040	RHOB	Ras homolog gene family, member B	1.93	1.55
NM_000602	SERPINE 1	Serpin peptidase inhibitor, clade E (nexin, plasminogen activator inhibitor type 1), member 1	2.09	2.62
NM_005985	SNAI1	Snail family transcriptional repressor 1	1.74	2.17
NM_003107	SOX4	SRY (sex determining region Y)-box 4	1.89	-
NM_001950	AR	E2F transcription factor 4, p107/p130-binding	-	-1.55
NM_001674	ATF3	Activating transcription factor 3	-	-3.60
NM_005252	FOS	FBJ murine osteosarcoma viral oncogene homolog	-	-2.91
NM_002167	ID3	Inhibitor of DNA binding 3, dominant negative helix-loop-helix protein	-1.51	-
NM_000193	SHH	Sonic hedgehog	-1.71	-1.70
NM_005902	SMAD3	SMAD family member 3	-2.2	-1.51

[a] Fold regulation in mRNA expression levels as assessed by RT^2 Profiler PCR Array. Genes labelled in red and blue color are up-regulated and down-regulated in SMAD4 wild-type cells treated with TGF-β1 (4 and 16 hours), respectively. Dash line indicates fold regulation of the gene at that time point was below the set threshold of 1.5.

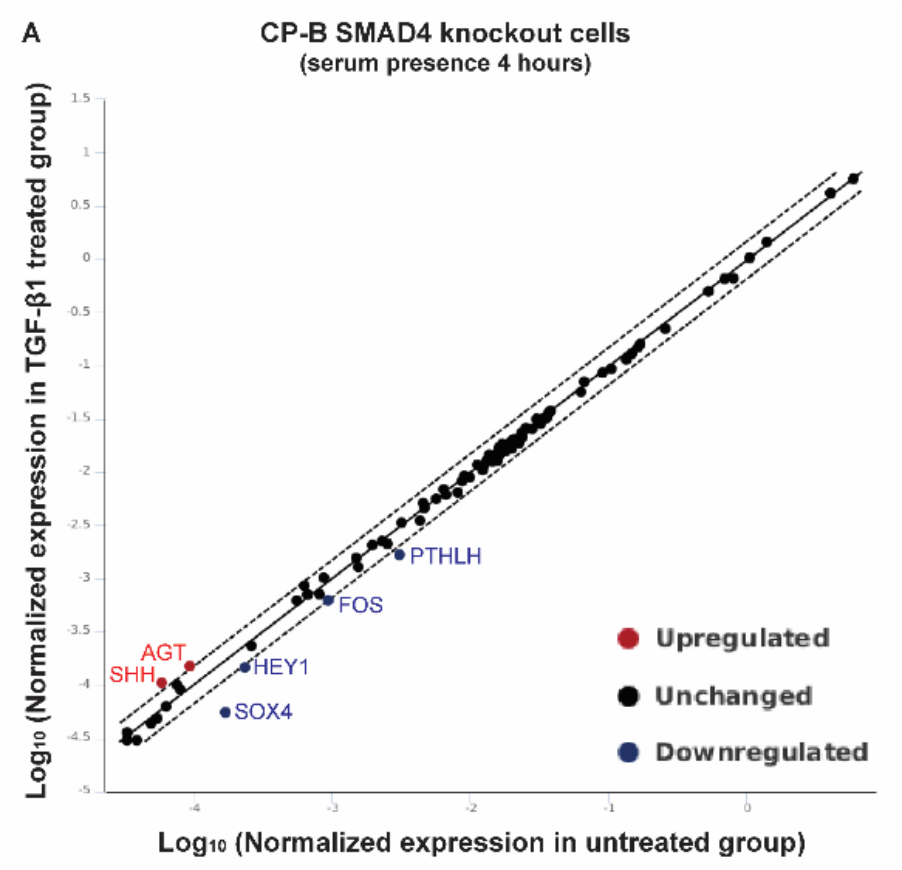
A
CP-B SMAD4 knockout cells
(serum presence 4 hours)
Log10 (Normalized expression in TGF-β1 treated group)
Log10 (Normalized expression in untreated group)
PTHLH
FOS
AGT
SHH
HEY1
SOX4
Upregulated
Unchanged
Downregulated

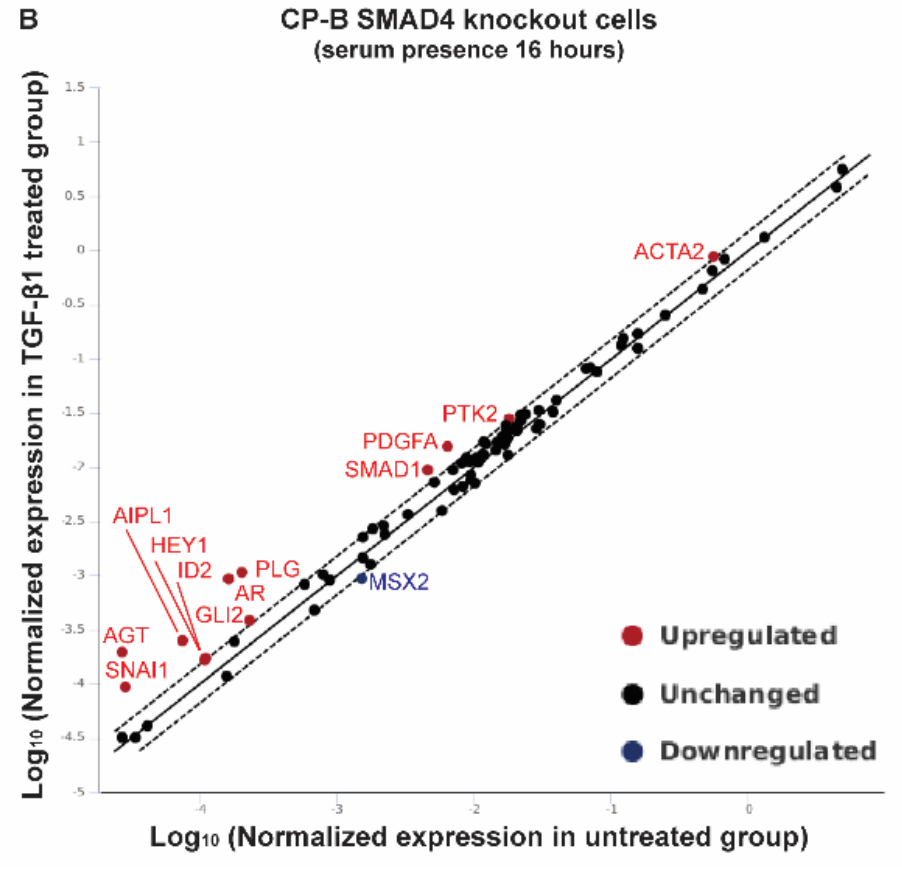
B
CP-B SMAD4 knockout cells
(serum presence 16 hours)
Log10 (Normalized expression in TGF-β1 treated group)
Log10 (Normalized expression in untreated group)
ACTA2
PTK2
PDGFA
SMAD1
AIPL1
HEY1
ID2
PLG
AR
GLI2
MSX2
AGT
SNAI1
Upregulated
Unchanged
Downregulated

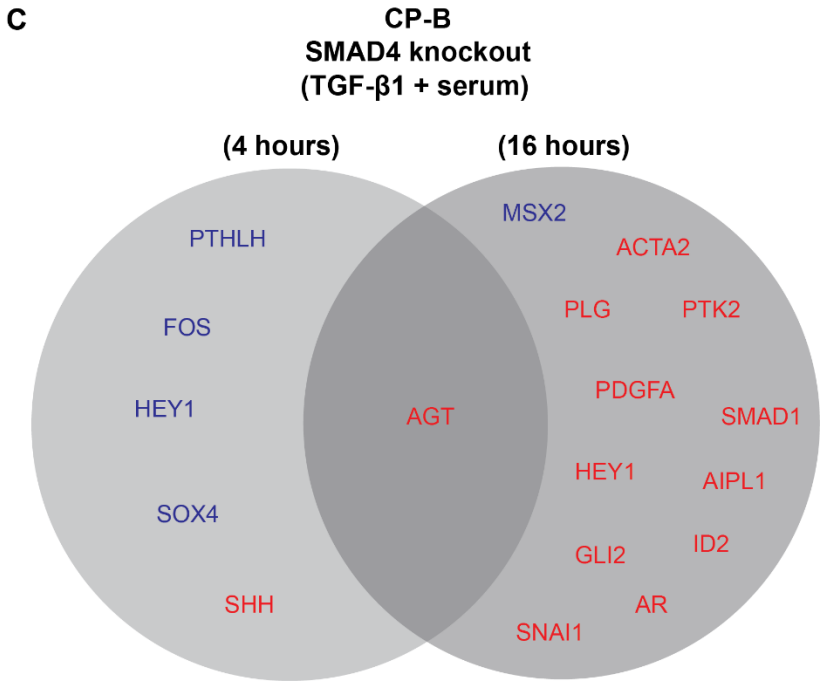

Figure 4.2.5. TGF-β signalling target gene expression in CP-B SMAD4 knockout cells following the treatment with TGF-β1 for 4 or 16 hours in the presence of serum. RT^2 Profiler PCR Array to determine transcript expression levels of panel of human TGF-β1 signalling targets in SMAD4 knockout (CP-B Ex2.A1 and CP-B Ex1.2B1) cells upon treatment with TGF-β1 for (A) 4 hours and (B) 16 hours in the presence of serum compared to untreated cells. The scatter plots compare the normalized expression of every gene (delta C_T per each gene within groups of interest) on the TGF-β signalling targets RT^2 Profiler PCR array between TGF-β1 treated group vs. untreated group by plotting them against each other. The average geometric mean of five HKG genes, *ACTB*, *B2M*, *GAPDH*, *HPRT1* and *RPLPO* was used for normalization in each sample. The solid line indicates unchanged gene expression, whereas the broken lines indicate the 1.5 fold regulation threshold. CP-B Ex2.A1 and CP-B Ex1.2B1 are considered as biological replicates. Each dot on the graph represents pooled data from CP-B Ex2.A1 and CP-B Ex1.2B1 cells treated with TGF-β1 compared to untreated CP-B Ex2.A1. Untreated SMAD4 knockout CP-B Ex1.2B1 sample had relatively lower C_T values than the rest of the samples and was excluded from the analyses. (C) Venn Diagram representing the TGF-β1 signalling target genes regulated at early (4 hours) and/or late (16 hours) time point in SMAD4 knockout cells in response to TGF- β1 in the presence of serum. Genes labelled in red and blue colour represent up- and down-regulated genes, respectively.

Table 4.2.4. Genes up- or down-regulated in SMAD4 knockout cells upon TGF-β1 treatment in the presence of serum for 4 and 16 hours

RefSeq	Gene Symbol	Gene Full Name	Fold Regulation[a] 4 hours	Fold Regulation[a] 16 hours
NM_001613	ACTA2	Actin, alpha 2, smooth muscle, aorta	-	1.56
NM_000029	AGT	Angiotensinogen (serpin peptidase inhibitor, clade A, member 8)	1.6	7.18
NM_014336	AIPL1	Aryl hydrocarbon receptor interacting protein-like 1	-	3.36
NM_000044	AR	Androgen receptor	-	5.69
NM_005270	GLI2	GLI family zinc finger 2	-	1.67
NM_012258	HEY1	Hairy/enhancer-of-split related with YRPW motif 1	-	1.56
NM_002166	ID2	Inhibitor of DNA binding 2, dominant negative helix-loop-helix protein	-	1.51
NM_002607	PDGFA	Platelet-derived growth factor alpha polypeptide	-	2.41
NM_000301	PLG	Plasminogen	-	5.28
NM_005607	PTK2	PTK2 protein tyrosine kinase 2	-	1.54
NM_000193	SHH	Sonic hedgehog	1.79	-
NM_005900	SMAD1	SMAD family member 1	-	2.03
NM_005985	SNAI1	Snail family transcriptional repressor 1	-	3.26
NM_002449	MSX2	Msh homeobox 2		-1.62
NM_005252	FOS	FBJ murine osteosarcoma viral oncogene homolog	-1.51	-
NM_012258	HEY1	Hairy/enhancer-of-split related with YRPW motif 1	-1.62	-
NM_002820	PTHLH	Parathyroid hormone-like hormone	-1.85	-
NM_003107	SOX4	SRY (sex determining region Y)-box 4	-3.08	-

[a] Fold regulation in mRNA expression levels as assessed by RT^2 Profiler PCR Array. Genes labelled in red and blue color are up-regulated and down-regulated in SMAD4 knockout cells treated with TGF-β1 (4 and 16 hours), respectively. Dash line indicates fold regulation of the gene at that time point was below the set threshold of 1.5.

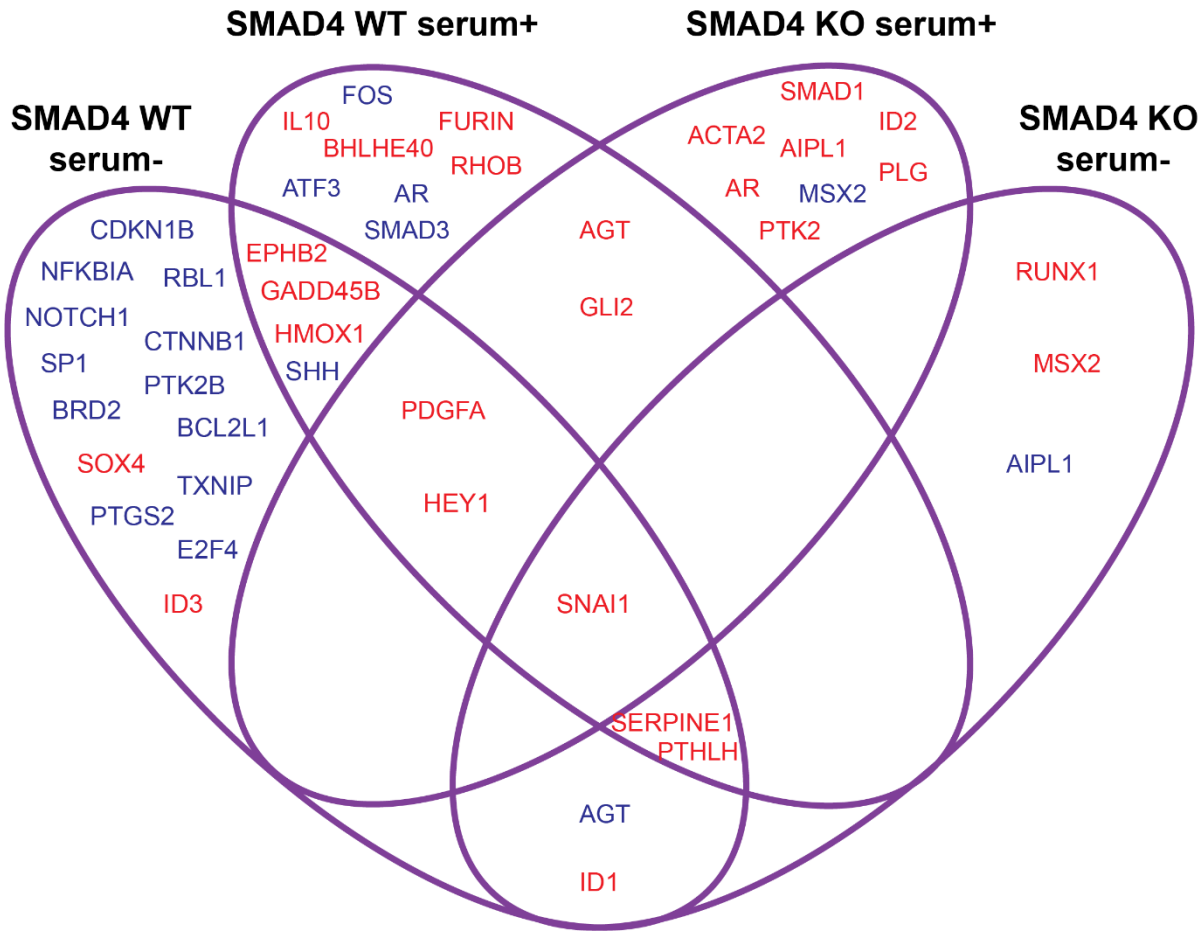

Figure 4.2.6. Comparison of differentially regulated target genes following TGF-β1 treatment in the presence or absence of serum. 4 way Venn diagram representing the set of differentially regulated genes following treatment with TGF-β1 in the presence (serum+) or absence of serum (serum-) for 16 hours in SMAD4 wild-type (SMAD4 WT) and SMAD4 knockout cells (SMAD4 KO). Genes labelled in red and blue colour represent up- and down-regulated genes, respectively. The online tool used to generate 4 way Venn Diagram is available at http://bioinformatics.psb.ugent.be/webtools/Venn/.

4.2.4. High extent of differential gene expression profile in SMAD4 knockout cells compared to SMAD4 wild-type cells

In order to look specifically at the effect of TGF-β1 on gene regulation, unsupervised hierarchical clustering was performed to identify gene-clusters based on differential expression between TGF-β1 treated and untreated SMAD4 wild-type and SMAD4 knockout cells in the absence of serum (**Figure 4.2.7**). Of note, SMAD4 wild-type cells treated with TGF-β1 clustered apart from untreated cells. These observations support the results observed in **Figure 4.2.2A.**, indicating the differential gene regulation of TGF-β signalling target genes in SMAD4 wild-type cells upon treatment with TGF-β1. On the other hand, the two knockout cell lines, CP-B Ex2.A1 and Ex1.2B1, clustered

separately upon treatment with TGF-β1, indicating the degree of difference in response to TGF-β1 between two SMAD4 knockouts. These data reflect the results already seen in **Figure 4.2.2B,** that treatment with TGF-β1 in SMAD4 knockout cells, does not affect the expression of TGF-β signalling target genes, as much as in SMAD4 wild-type cells. More strikingly, SMAD4 knockout cells cluster apart from SMAD4 wild-type cells, irrespective of TGF-β1, indicating the differential gene expression profile under basal conditions between SMAD4 wild-type and SMAD4 knockout cells.

To improve the visualization of the individual genes contributing to the differences, principal component analyses (PCA) was performed. PCA simplifies the complexity of high dimensional data while still retaining the trends and patterns of individual genes contribution. This analysis clusters together and visualizes the genes that contribute in the same pattern to the differences between two entities, in this case SMAD4 wild-type and SMAD4 knockout cells, and their response to TGF-β1 (**Figure 4.2.8 A**). Overall, genes positioned in the centre of the graph are not contributing to the differences, whereas genes positioned outside of the centre are highly contributing to the differences in gene expression between SMAD4 wild-type and SMAD4 knockout cells in response to TGF-β1. In addition, the loadings plot (**Figure 4.2.8 B**) shows strong positive correlation of gene expression profile between individual SMAD4 knockout variables (both untreated and TGF-β1 treated), but also between SMAD4 wild-type variables (both untreated and TGF-β1 treated). Only moderate shifts in the variables were observed comparing TGF-β1 treatment vs. control in either SMAD4 wild-type or SMAD4 knockout cells. Importantly, loadings of SMAD4 wild-type vs. SMAD4 knockout variables positioned in adjacent quadrants and loadings reaching the correlation circle are indicative of significant differential gene expression between clusters independent of TGF-β1 treatment. In other words, the greatest difference in gene expression is between SMAD4 knockout vs. SMAD4 wild-type cells, irrespective of TGF-β1. However, this significant difference comes from few genes as reflected by loading angles less than 90 degrees between clusters, leading to a large proportion of the gene expression being unchanged, which is also shown in the clustering heat map (**Figure 4.2.7**).

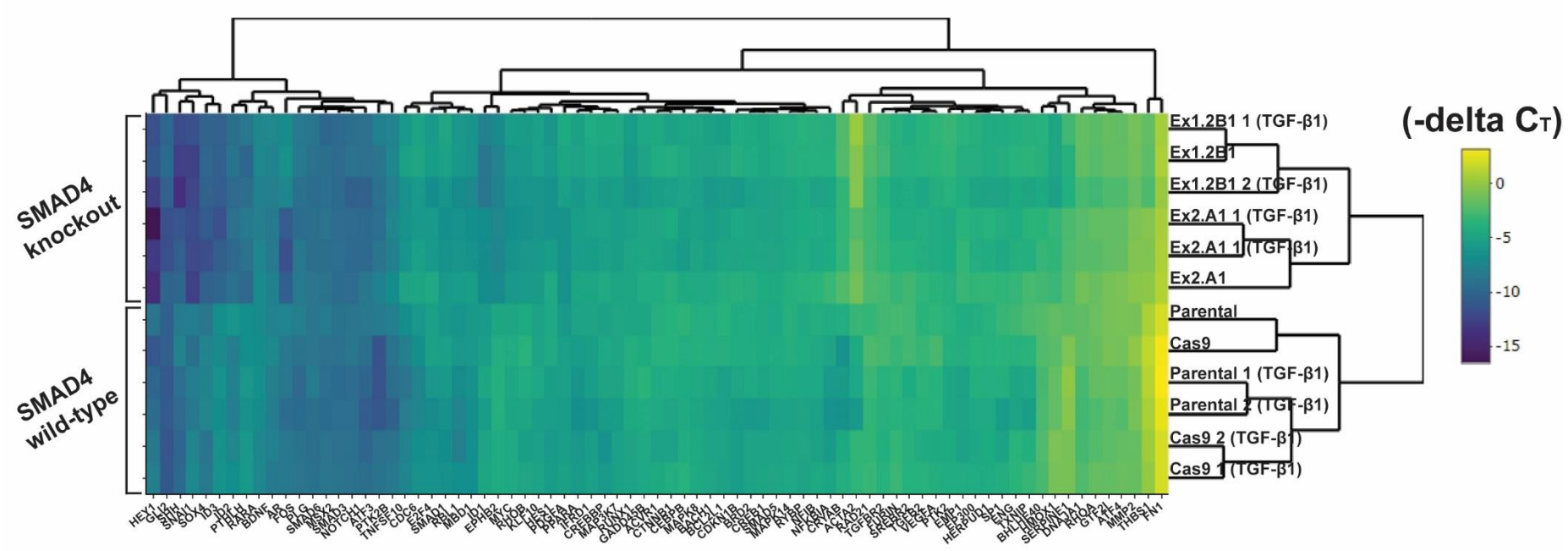

Figure 4.2.7. Clustergram of TGF-β1 specific target genes expression for SMAD4 wild-type and knockout CP-B cells. Clustergram was based on unsupervised hierarchical clustering of the entire dataset, including clustering individual samples and genes. Clustergram displays a heat map with dendograms indicating co-regulated genes across individual samples, including 2 independent replicates per each, CP-B Parental and Cas9 (SMAD4 wild-type), and Ex2.A1 and Ex1.2B1 (SMAD4 knockout) cells at 16 hour time point (under TGF-β1 treatment) and 1 independent group of untreated cells. Normalized gene expression (-delta C_T) within SMAD4 wild-type and SMAD4 knockout group of cells per each gene was used to generate clustergram with heatmap. The colour scale indicates -delta CT values. The geometric mean of HKG genes *ACTB*, *B2M*, *GAPDH*, *HPRT1* and *RPLPO* was used to calculate deltaCT values for each gene.

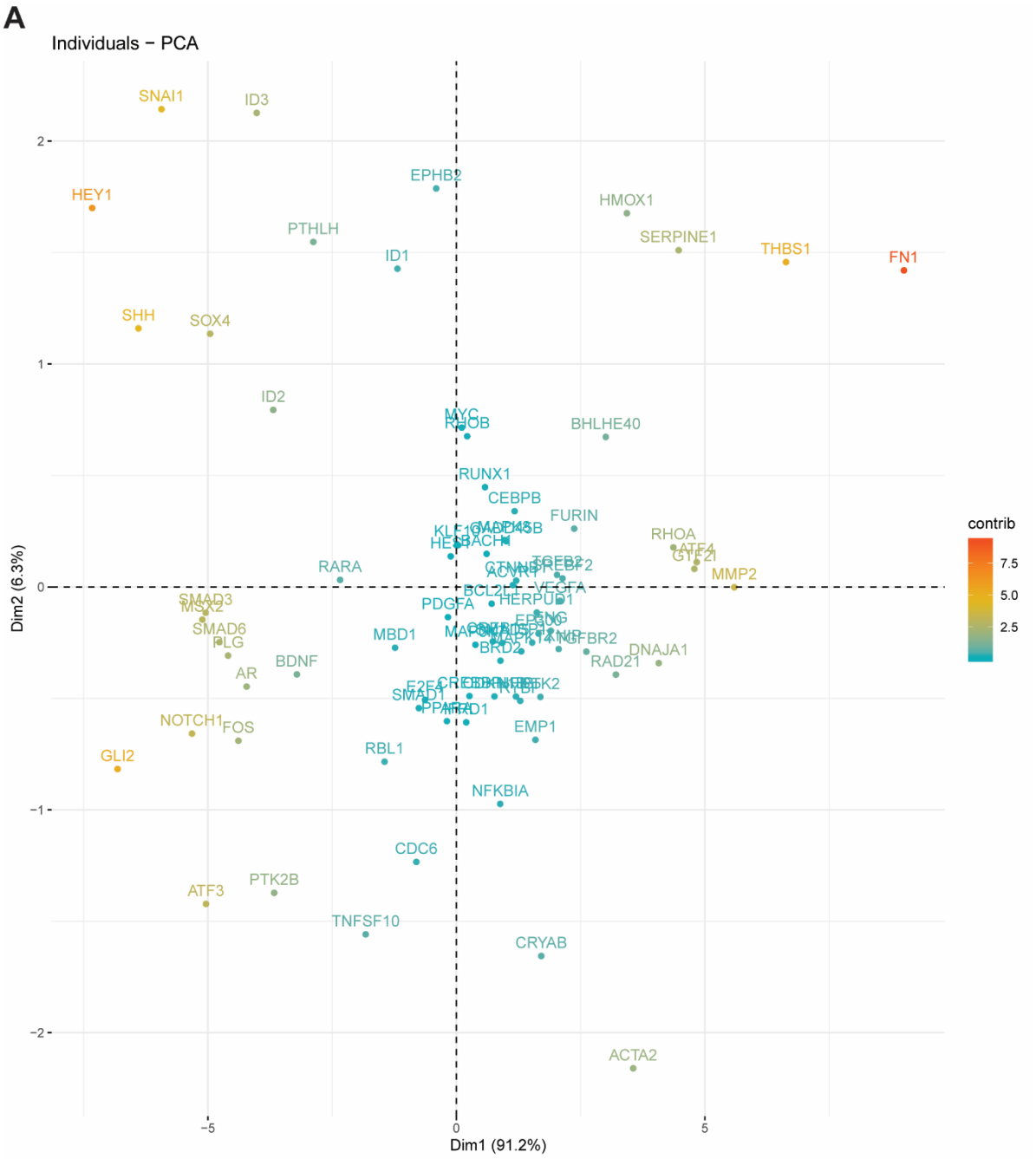
A
Individuals − PCA
SNAI1
ID3
EPHB2
HEY1
HMOX1
PTHLH
SERPINE1
THBS1
FN1
ID1
SHH
SOX4
ID2
BHLHE40
RUNX1
CEBPB
FURIN
RHOA
ATF4
GTF2I
RARA
MMP2
SMAD3
SMAD6
PDGFA
MBD1
BDNF
AR
DNAJ1
RAD21
NOTCH1
FOS
EMP1
GLI2
RBL1
NFKBIA
CDC6
PTK2B
ATF3
TNFSF10
CRYAB
ACTA2
contrib
7.5
5.0
2.5
Dim2 (6.3%)
Dim1 (91.2%)
2
1
0
−1
−2
−5
0
5

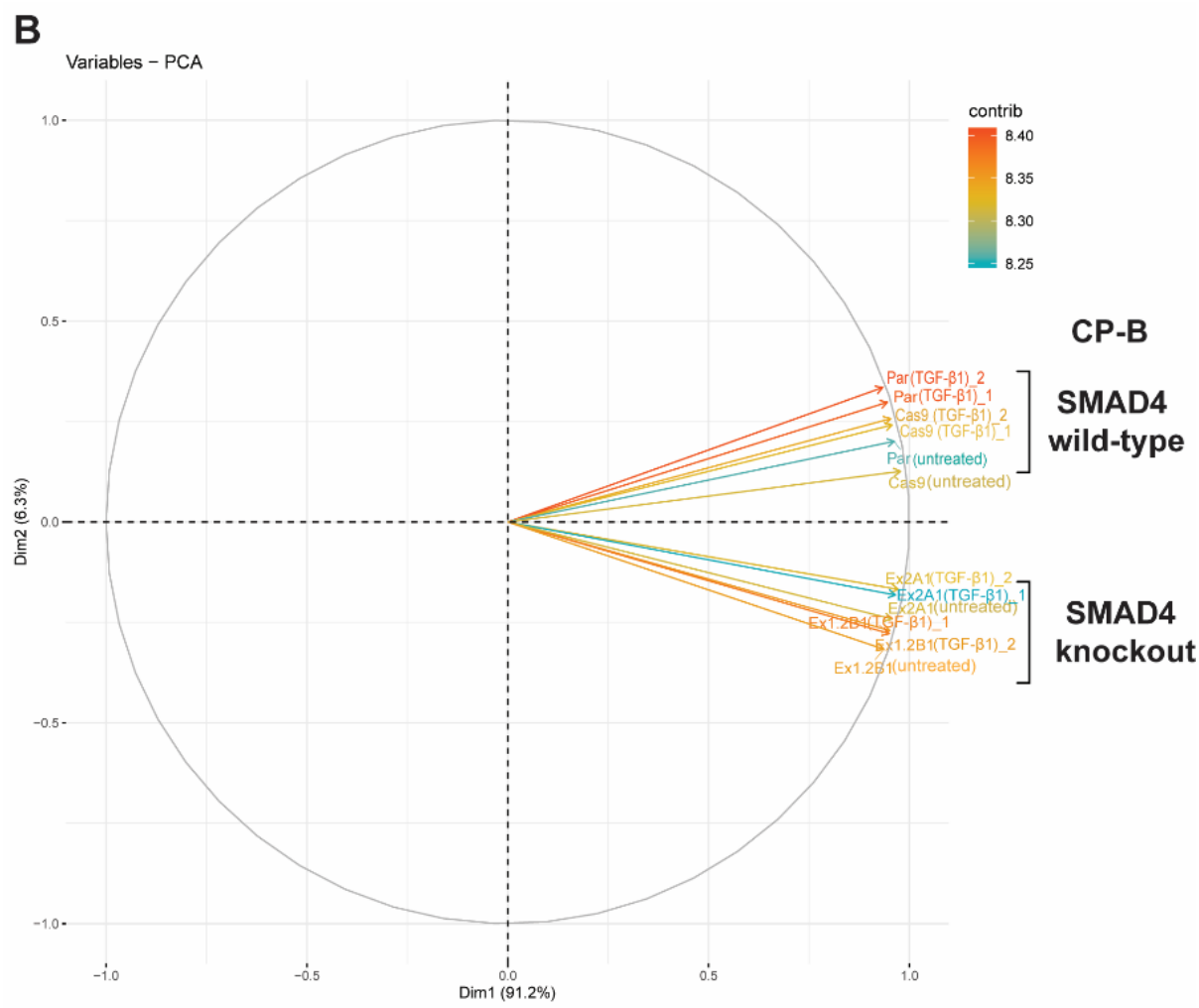

Figure 4.2.8. Principal component analyses (PCA) of differential gene expression between SMAD4 wild-type and SMAD4 knockout CP-B cells. (A) PCA comparing normalized individual gene expression (delta C_T) in SMAD4 wild-type (Parental and Cas9) and SMAD4 knockout (Ex2.A1 and Ex1.2B1) CP-B cells treated with TGF-β1 compared to untreated cells. The normalization of the data was performed using geometric mean of HKG genes *ACTB*, *B2M*, *GAPDH*, *HPRT1* and *RPLPO* within each group. Colour scale indicates the contribution level (in percentage) of individual variables (genes) towards differences in expression profile (principal component). The contribution of a variable (in percentage) to a given principal component is calculated with formula (variable cos2*100)/(total cos2 of the principal component). (B) Loadings plot representing the correlation of gene expression profile between different variables, including CP-B Parental, Cas9, Ex2.A1 and Ex1.2B1 treated with TGF-β1 and untreated control cells. Positively correlated variables are grouped together, whereas negatively correlated variables are positioned on opposite sides of the plot origin. Colour scale of arrows represents the contribution (in percentage) of individual variables (samples) to the differences with respect to the whole dataset.

Of high importance, in order to determine if SMAD4 loss itself dictates differences in gene expression, gene expression profiles were compared between SMAD4 wild-type and SMAD4 knockout CP-B cells in serum deprivation conditions without any additional treatment (**Figure 4.2.9** and **Table 4.2.5)**. Importantly, the difference in gene expression was confirmed between SMAD4 wild-type and SMAD4 knockout cells in basal conditions (serum deprivation). Up-regulated genes in SMAD4 knockout cells compared to SMAD4 wild-type cells are *CRYAB*, *CDC6*, *AGT*, *TNFSF10*, *PTK2B*, *ATF3* and *B2M* and down-regulated are *RHOB*, *SOX4*, *HEY1*, *TSBS1*, *ID2*, *SERPINE1*, *BHLHE40*, *HMOX1*, *SHH*, *SNAI1*, *EPHB2*, *ID1*, *RPLPO*, *PTHLH*, *MYC*, *FN1*, *PTGS2*, *RUNX1* and *ID3*, as summarized in **Table 4.2.5**.

Based on these results, we compared SMAD4 wild-type and SMAD4 knockout cells (both under the treatment with TGF-β1). Finally, significant gene expression changes were identified by volcano plot (**Figure 4.2.10**) and summarized in **Table 4.2.6**. It is clear that the same genes (apart *ACTA2, NFKBIA* and *EMP1*) are differentially expressed between SMAD4 wild-type vs. SMAD4 knockout cells, even in the absence of TGF-β1 (**Figure 4.2.9**). In addition, data is presented via Venn diagram and demonstrates overlapping gene set of SMAD4 knockout vs. SMAD4 wild-type (basal serum starved conditions) with gene set of SMAD4 knockout vs. SMAD4 wild-type cells (under TGF-β1 treatment) and these results suggest that there is little effect of TGF-β1 (**Figure 4.2.11**).

In conclusion, SMAD4 loss dictates gene expression differences in the set of TGF-β signalling target genes under both basal conditions and TGF-β1 treatment. As such, the magnitude of differential gene expression changes was more pronounced when comparing SMAD4 wild-type and SMAD4 knockout cells irrespective of TGF-β1 treatment and time point, or absence or presence of serum. Furthermore, when comparing within SMAD4 wild-type or knockout cells, the response to TGF-β1 cytokine was altered in SMAD4 knockout cells compared to the response in SMAD4 wild-type cells. For instance, SMAD4 knockout cells lost the ability to up-regulate and down-regulate a subset of genes upon addition of TGF-β1, compared to SMAD4 wild-type cells. Together, SMAD4 knockout significantly alters the TGF-β pathway target gene expression profile of CP-B high grade dysplasia cells.

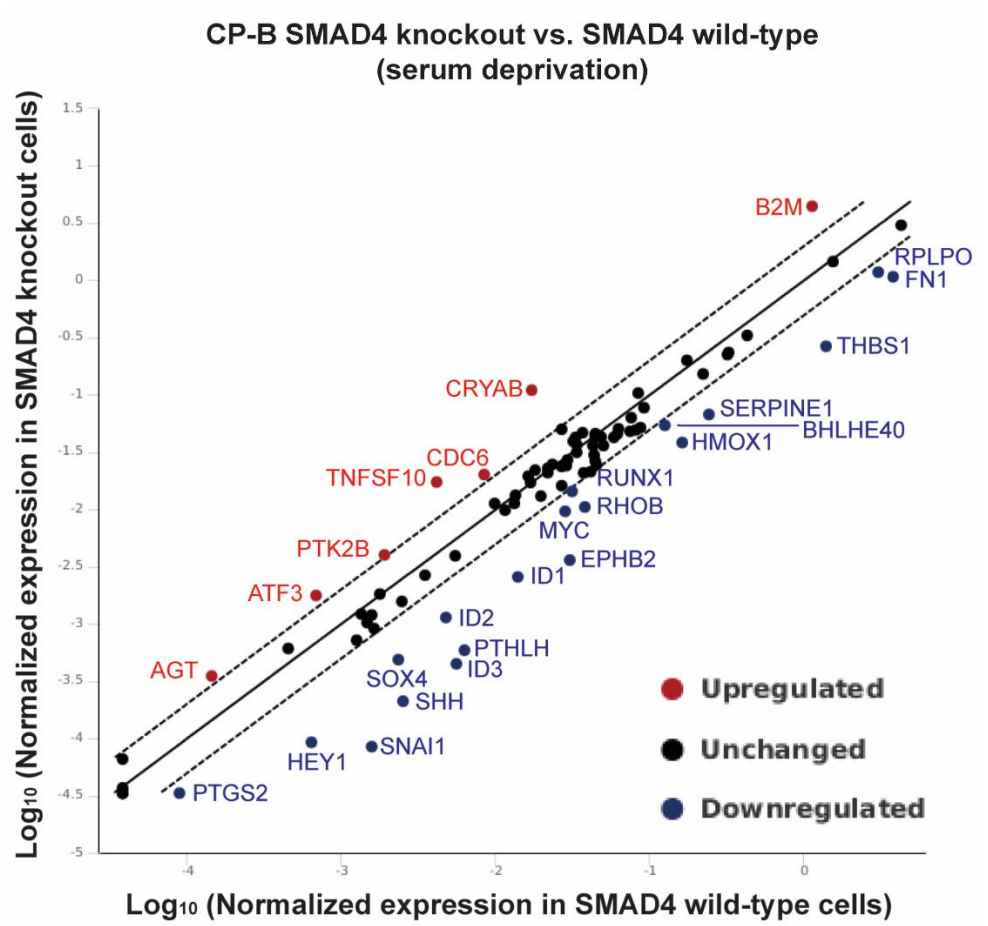

Figure 4.2.9. Basal TGF-β signalling target gene expression in SMAD4 wild-type cells vs. SMAD4 knockout cells. RT^2 Profiler PCR Array was used to determine transcript expression levels of TGF-β1 signalling targets comparing SMAD4 wild-type group (CP-B Parental and CP-B Cas9 cells) and SMAD4 knockout group (CP-B Ex2.A1 and CP-B Ex1.2B1 cells) in the absence of serum. The scatter plot compares the normalized expression of every gene on the TGF-β signalling targets RT^2 Profiler PCR array between SMAD4 wild-type group vs. SMAD4 knockout. The average geometric mean of five HKG genes, *ACTB*, *B2M*, *GAPDH*, *HPRT1* and *RPLPO* was used for normalization within each group. The solid line indicates unchanged gene expression, whereas the broken lines indicate a 2-fold regulation (2^(- Delta Delta C_T)) cut-off threshold. CP-B Parental and CP-B Cas9 or CPB Ex2.A1 and CP-B Ex1.2B1 are considered as SMAD4 wild-type and SMAD4 knockout biological replicates, respectively. Each dot on the graph represents the mean of pooled data from CP-B Parental and CP-B Cas9 (SMAD4 wild-type) compared to CPB Ex2.A1 and CP-B Ex1.2B1 (SMAD4 knockout) cells.

Table 4.2.5. Profiler PCR Array Results in CP-B SMAD4 knockout compared to SMAD4 wild-type cells in basal conditions.

RefSeq	Gene Symbol	Gene Full Name	Fold Regulation[a] -Serum
NM_001885	CRYAB	Crystallin, alpha B	6.42
NM_003810	TNFSF10	Tumor necrosis factor (ligand) superfamily, member 10	4.12
NM_004048	B2M	Beta-2-microglobulin	3.91
NM_001674	ATF3	Activating transcription factor 3	2.57
NM_000029	AGT	Angiotensinogen (serpin peptidase inhibitor, clade A, member 8)	2.41
NM_001254	CDC6	Cell division cycle 6	2.38
NM_004103	PTK2B	PTK2B protein tyrosine kinase 2 beta	2.09
NM_005985	SNAI1	Snail family transcriptional repressor 1	-18.74
NM_002167	ID3	Inhibitor of DNA binding 3, dominant negative helix-loop-helix protein	-12.63
NM_000193	SHH	Sonic hedgehog	-11.99
NM_002820	PTHLH	Parathyroid hormone-like hormone	-10.73
NM_004442	EPHB2	EPH receptor B2	-8.5
NM_012258	HEY1	Hairy/enhancer-of-split related with YRPW motif 1	-7
NM_002165	ID1	Inhibitor of DNA binding 1, dominant negative helix-loop-helix protein	-5.42
NM_003246	THBS1	Thrombospondin 1	-5.29
NM_003107	SOX4	SRY (sex determining region Y)-box 4	-4.83
NM_002133	HMOX1	Heme oxygenase (decycling) 1	-4.27
NM_002166	ID2	Inhibitor of DNA binding 2, dominant negative helix-loop-helix protein	-4.21
NM_004040	RHOB	Ras homolog gene family, member B	-3.68
NM_000602	SERPINE1	Serpin peptidase inhibitor, clade E (nexin, plasminogen activator inhibitor type 1), member 1	-3.65
NM_002026	FN1	Fibronectin 1	-3.61
NM_002467	MYC	MYC proto-oncogene	-2.97
NM_000963	PTGS2	Prostaglandin-endoperoxide synthase 2 (prostaglandin G/H synthase and cyclooxygenase)	-2.68
NM_001002	RPLP0	Ribosomal protein, large, P0	-2.62
NM_003670	BHLHE40	Basic helix-loop-helix family, member e40	-2.35
NM_001754	RUNX1	Runt-related transcription factor 1	-2.19

[a] Fold regulation in mRNA expression levels as assessed by RT^2 Profiler PCR Array. Genes labelled in red and blue colours are up-regulated and down-regulated, respectively, in SMAD4 knockout cells compared to SMAD4 wild-type cells in serum deprivation or in the presence of serum. Dash line represents no change in fold regulation of the gene above the set threshold of 2.

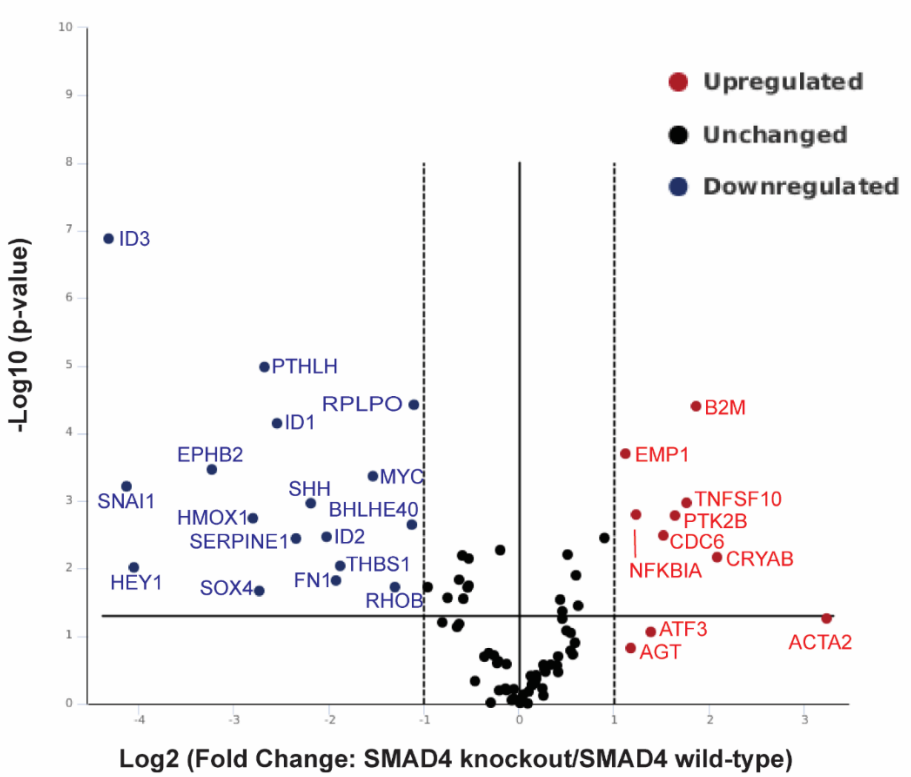

Figure 4.2.10. TGF-β signalling target gene expression in SMAD4 wild-type cells vs SMAD4 knockout cells treated with TGF-β1. Data presented on the volcano plot was acquired by performing an RT^2 Profiler PCR Array to determine transcript expression levels of TGF-β1 signalling targets in CP-B Ex2.A1 and Ex1.2B1 (SMAD4 knockout) vs. CP-B Parental and Cas9 (SMAD4 wild-type) cells following treatment with TGF-β1 for 16 hours in the absence of serum. Normalization was performed using the geometric mean of *ACTB*, *B2M*, *GAPDH*, *HPRT1* and *RPLPO* genes. The volcano plot displays statistical significance (-Log10 p-value) on the y axis vs. Log2 fold change on the x axis. p-values were calculated by Student's t-test of the replicate 2^ (- Delta C_T) values for each gene in the SMAD4 wild-type and SMAD4 knockout groups. Fold-Change (2^ (- Delta Delta C_T)) is the normalized gene expression (2^(- Delta C_T)) in the SMAD4 knockout group divided by the normalized gene expression (2^ (- Delta CT)) in the SMAD4 wild-type group. Each dot on the volcano plot represents the mean of data pooled from 2 biological replicates of each cell line including SMAD4 wild-type cells (CP-B Parental and Cas9) and SMAD4 knockout cells (CP-B Ex2.A1 and CP-B Ex1.2B1). Dashed vertical line represents a Log2 fold change (Log2 fold change) of gene expression, and the horizontal solid line represents a p-value (–Log10 p-value) threshold (p-value<0.05 is considered as threshold for statistical significance).

Table 4.2.6. Genes up- or down-regulated in SMAD4 knockout cells compared to SMAD4 wild-type cells (under TGF-β1 treatment)

RefSeq	Gene Symbol	Gene Full Name	Fold Regulation[a]	p value[b]
NM_001613	ACTA2	Actin, alpha 2, smooth muscle, aorta	9.42	ns
NM_001885	CRYAB	Crystallin, alpha B	4.24	6.81e-03
NM_004048	B2M	Beta-2-microglobulin	3.64	4.00e-05
NM_003810	TNFSF10	Tumor necrosis factor (ligand) superfamily, member 10	3.41	1.07e-03
NM_004103	PTK2B	PTK2B protein tyrosine kinase 2 beta	3.12	1.64e-03
NM_001254	CDC6	Cell division cycle 6	2.87	3.25e-03
NM_001674	ATF3	Activating transcription factor 3	2.63	ns
NM_020529	NFKBIA	Nuclear factor of kappa light polypeptide gene enhancer in B-cells inhibitor, alpha	2.35	1.60e-03
NM_000029	AGT	Angiotensinogen (serpin peptidase inhibitor, clade A, member 8)	2.26	ns
NM_001423	EMP1	Epithelial membrane protein 1	2.17	2.00e-04
NM_002167	ID3	Inhibitor of DNA binding 3, dominant negative helix-loop-helix protein	-19.90	6.21e-06
NM_005985	SNAI1	Snail family transcriptional repressor 1	-17.45	6.09e-04
NM_012258	HEY1	Hairy/enhancer-of-split related with YRPW motif 1	-16.56	9.62e-03
NM_004442	EPHB2	EPH receptor B2	-9.41	3.43e-04
NM_002133	HMOX1	Heme oxygenase (decycling) 1	-6.99	1.81e-03
NM_003107	SOX4	SRY (sex determining region Y)-box 4	-6.64	2.15e-02
NM_002820	PTHLH	Parathyroid hormone-like hormone	-6.4	1.00e-05
NM_002165	ID1	Inhibitor of DNA binding 1, dominant negative helix-loop-helix protein	-5.84	7.10e-05
NM_000602	SERPINE 1	Serpin peptidase inhibitor, clade E (nexin, plasminogen activator inhibitor type 1), member 1	-5.08	3.60e-03
NM_000193	SHH	Sonic hedgehog	-4.55	1.08e-03
NM_002166	ID2	Inhibitor of DNA binding 2, dominant negative helix-loop-helix protein	-4.06	3.40e-03
NM_002026	FN1	Fibronectin 1	-3.8	1.51e-02
NM_003246	THBS1	Thrombospondin 1	-3.69	9.14e-03
NM_002467	MYC	MYC proto-oncogene	-2.9	4.32e-04
NM_004040	RHOB	Ras homolog gene family, member B	-2.48	1.89e-02
NM_003670	BHLHE40	Basic helix-loop-helix family, member e40	-2.19	2.25e-03
NM_001002	RPLP0	Ribosomal protein, large, P0	-2.15	3.80e-05

[a] Fold regulation in mRNA expression levels as assessed by RT^2 Profiler PCR Array. Genes labelled in red and blue color are up-regulated and down-regulated, respectively, in SMAD4 knockout cells compared to SMAD4 wild-type cells.

[b] p value was calculated by performing Student's t-test of 2^ (- Delta C_T) values for each gene between SMAD4 wild-type and SMAD4 knockout cells.

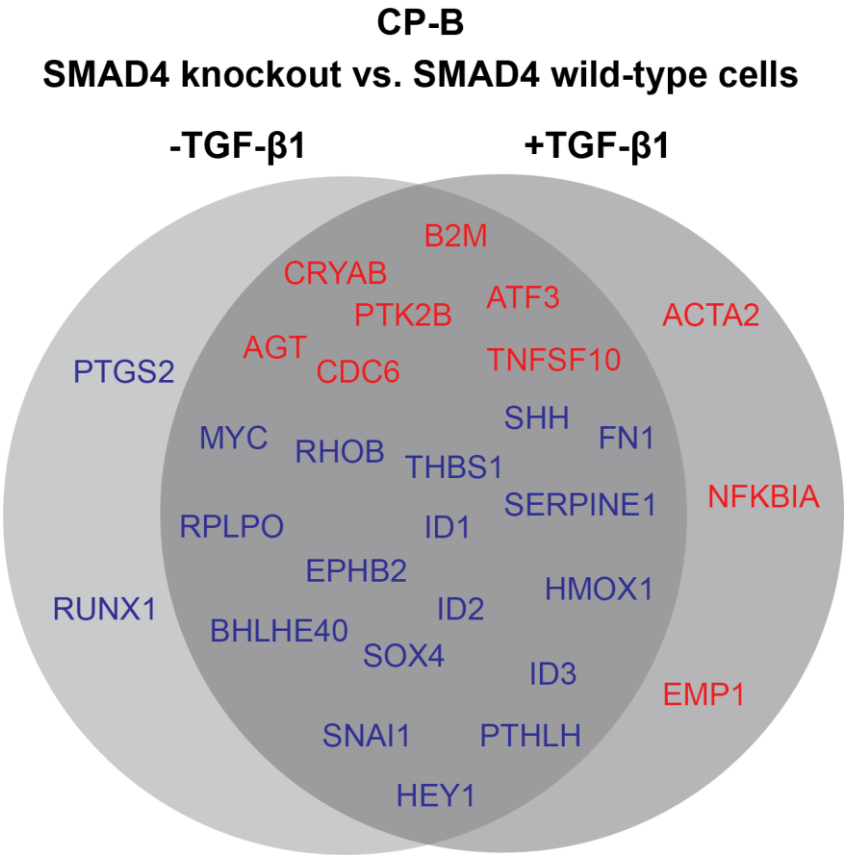

Figure 4.2.11. Comparison of gene regulation between SMAD4 knockout and SMAD4 wild-type cells in basal conditions and/or under the treatment with TGF-β1. Venn diagram representing the set of differentially regulated genes of SMAD4 knockout vs. SMAD4 wild-type cells in the absence of serum without any treatment for 16 hours (serum deprivation) and SMAD4 knockout vs. SMAD4 wild-type cells under TGF-β1 for 16 hours in the absence of serum (under TGF-β1). Genes labelled in red and blue colour represent up- and down-regulated genes, respectively.

4.2.5. Validation of gene expression changes in TGF-β signalling targets genes

Next, gene expression changes identified using RT^2 PCR Arrays were validated. The focus for validation was on the genes *ACTA2*, *CRYAB* and *CDC6* due to literature evidence supporting the overexpression and oncogenic role of these genes in cancers, including gastrointestinal cancers [262-265]. Firstly, the mRNA expression levels of *ACTA2*, *CRYAB* and *CDC6* were validated across CP-B SMAD4 wild-type and SMAD4 knockout cells in response to TGF-β1 treatment in the absence of serum (**Figure 4.2.12A, B, C**). All data were analysed relative to untreated SMAD4 wild-type cells in the absence of serum. It is evident that basal expression levels of *ACTA2*, *CRYAB* and *CDC6* are higher in SMAD4 knockout cells compared to SMAD4 wild-type cells, irrespective of treatment (**Figure 4.2.12A, B, C**). These results strongly support the evidence from RT^2 PCR Arrays that showed a higher magnitude of

differential gene expression in SMAD4 knockout cells compared to SMAD4 wild-type cells (**Figure 4.2.9)**.

SMAD4 wild-type cells did not significantly increase *ACTA2* expression levels upon addition of TGF-β1, whereas, *ACTA2* expression levels were slightly increased in SMAD4 knockout cells following TGF-β1 treatment (**Figure 4.2.12A**). Contrastingly, the mRNA expression levels of *CDC6* did not change in either SMAD4 wild-type or knockout cells upon TGF-β1 treatment (**Figure 4.2.12C**), but we observed a moderate increase of *CRYAB* expression in SMAD4 wild-type cells (**Figure 4.2.12B**).

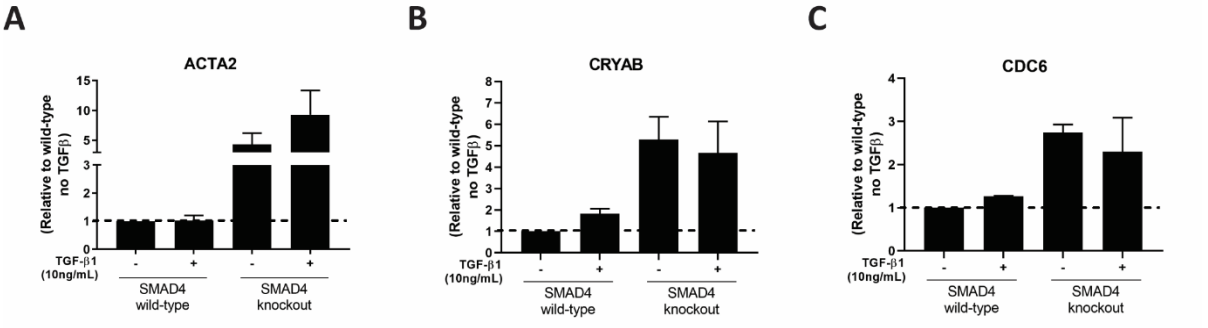

Figure 4.2.12. Validation of RT^2 Profiler PCR Array results. (A, B, C) *ACTA2*, *CRYAB* and *CDC6* mRNA expression in CP-B SMAD4 wild-type and SMAD4 knockout cells was assessed by qRT-PCR following treatment with 10ng/mL TGF-β1 for 16 hours in the absence of serum. For ACTA2 and CRYAB experiments, n=2 independent experiments per each cell line, including (CP-B Parental, Cas9, Ex.2.A1 and Ex1.2B1) and for CDC6 experiment, n=1 for each cell line. Error bars=SEM.

4.2.6. SMAD4 loss renders increased resistance to chemotherapy

Up-regulation of *CDC6* levels in CP-B SMAD4 knockout cells compared to CP-B SMAD4 wild type cells was also validated at the protein level. CDC6 protein expression was almost undetectable in SMAD4 wild-type cells, whereas both SMAD4 knockout cell lines expressed high CDC6 protein levels (**Figure 4.2.13A**). To further investigate the relationship between SMAD4 and CDC6 expression, cell lines derived from CP-B SMAD4 knockdown and knockout xenografts (Chapter 3. Figure 3.2.3 and 3.2.4) were investigated. These cells have different levels of SMAD4 protein depending on the efficiency of different shRNAs (S6-1, S6-2 and S6-3) or knockout of SMAD4 (E1-1, E1-2 and E1-3). Remarkably, cells with down-regulation of SMAD4 by shRNA (but not complete knockout) expressed CDC6 at proportionally lower levels, compared to parental CP-B cells with wild-type SMAD4, whereas SMAD4 knockout

cells expressed high CDC6 levels (**Figure 4.2.13B**). Taken together, these data suggest the close regulation of CDC6 via SMAD4.

CDC6 is involved in the regulation of the early origin of DNA replication, and also in progression of the cell cycle via helping the transition from the S to G2/M phase of the cell cycle [266]. Thus, deregulation of CDC6 expression could lead to aberrations in essential cell processes, including DNA replication and division. Indeed, high CDC6 levels are known to be associated with increased resistance to chemotherapy [265]. Thus, sensitivity of CP-B parental and SMAD4 knockout cells to one of the currently used chemotherapy drugs in OAC, cisplatin, was tested. Notably, CP-B SMAD4 knockout cells demonstrated significantly increased resistance to cisplatin compared to SMAD4 wild-type cells (**Figure 4.2.13C, D**). Whether the increased cisplatin resistance is aided by high CDC6 expression levels in SMAD4 knockout cells, or there is another mechanism of increased resistance is yet to be answered. Together, our data indicates that cells with an absence of SMAD4 exhibit increased resistance to the currently used chemotherapy drug, cisplatin.

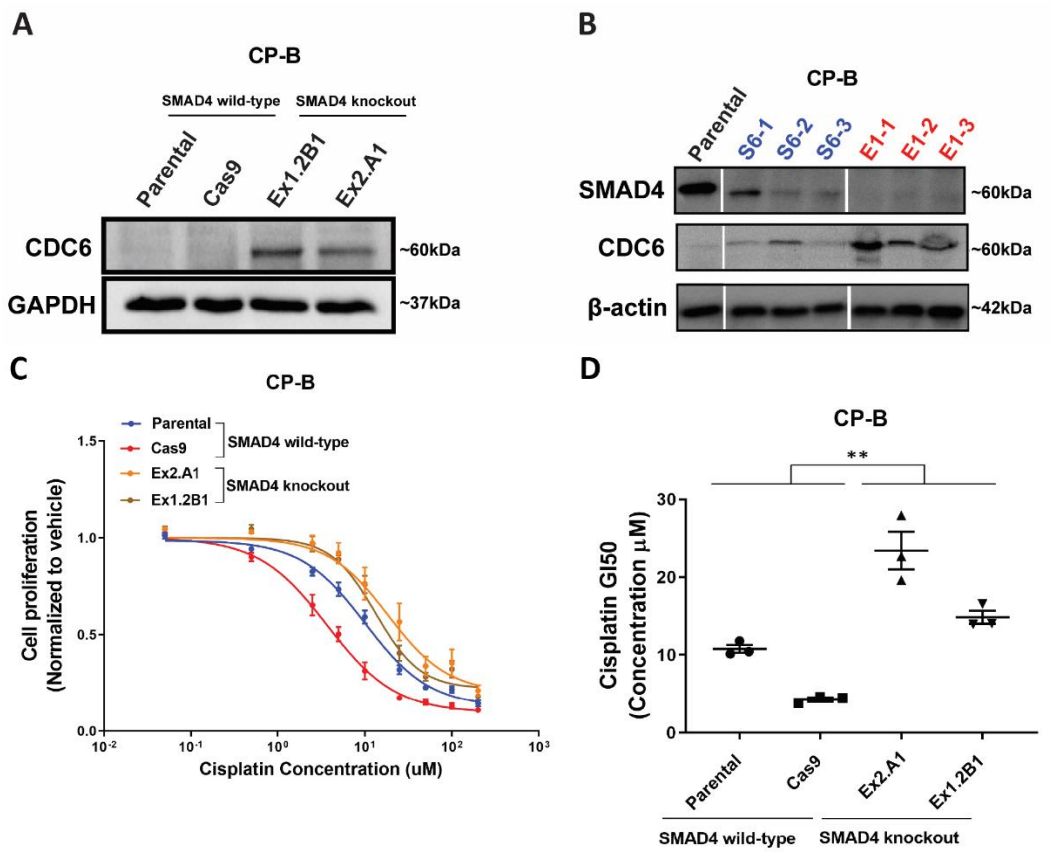

Figure 4.2.13. Up-regulation of CDC6 in CP-B SMAD4 knockout cells is associated with resistance to cisplatin. Western blot of (A) CDC6 protein in CP-B SMAD4 wild-type and knockout cells (without any treatment). (B) CDC6 protein levels across CP-B parental (SMAD4 wild-type) and established tumour cells lines (Chapter 3. Figure 3.2.3 and Table 3.2.1) with SMAD4 knockdown (CP-B S6-1-3, blue) or SMAD4 knockout (CP-B E1-1-3, red). (C) Cell proliferation measured by Incucyte (relative to vehicle) in SMAD4 wild-type and knockout cells following treatment with the indicated doses of cisplatin for 96 hours Data represent mean±SEM, n=3 independent experiments. (D) GI50 values of cisplatin in CP-B SMAD4 knockout versus wild-type cells. Error bars=SEM, **p<0.01, two tailed Student's t-test.

4.2.7. Silencing mechanism of the INK4/ARF tumour suppressor locus upon SMAD4 loss in CP-B high grade dysplasia cells

Previously published data in mouse embryo fibroblasts demonstrated that up-regulation of CDC6 was associated with down-regulated expression of the INK4-ARF tumour suppressor locus genes [267]. Based on these data, the expression of INK4-ARF genes were assessed in SMAD4 knockout/CDC6 high expressing CP-B cells in comparison to SMAD4 wild-type/CDC6 low expressing CP-B parental cells. Indeed, the transcript levels of INK4/ARF genes encoding $p14^{ARF}$, $p15^{INK4B}$ and $p16^{INK4A}$ were decreased in SMAD4 knockout cells versus SMAD4 wild-type cells (**Figure 4.2.14**). These data indicate that the INK4/ARF locus is positively regulated in SMAD4 wild-

type cells. However, the question of whether SMAD4 directly regulates INK4/ARF locus or indirectly through CDC6 or some other mechanism of action, is yet to be answered.

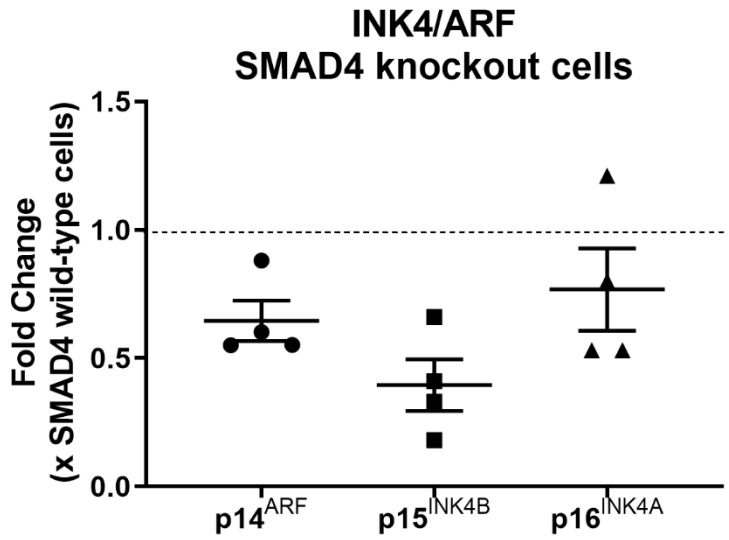

Figure 4.2.14. Negative regulation of INK4/ARF tumour suppressor genes through SMAD4 knockout in CP-B high grade dysplasia cells. mRNA expression (qRT-PCR) of $p14^{ARF}$, $p15^{INK4B}$ and $p16^{INK4A}$ in CP-B SMAD4 knockout cells vs. SMAD4 wild-type cells under basal serum starved conditions. For all experiments, n=2 biological replicates per each cell line, including CP-B Parental, CP-B Cas9, CP-B Ex2.A1 and CP-B Ex1.2B1, error bars=SEM. The comparison was made between CP-B Parental/Ex2.A1 and CP-B Cas9/Ex1.2B1.

4.3. Discussion

The growth inhibitory effects of TGF-β are known to be mediated through transcriptional activation of tumour suppressors *p15^{INK4B}* and *p21* [255, 268, 269]. In this study, it was shown that both TGF-β cytokines, TGF-β1 and BMP4, up-regulate p21 protein expression levels in CP-B high grade dysplasia SMAD4 wild-type cells under serum-starved conditions. In contrast, isogenic CP-B SMAD4 knockout cells were unable to respond with up-regulation of p21 upon treatment with either TGF-β1 or BMP4. These data suggest that p21 expression is regulated by SMAD4 dependent TGF-β signalling and loss of SMAD4 canonical TGF-β pathway prevents CP-B cells responding with up-regulation of p21.

Given that one of the main mediators of TGF-β induced cell cycle arrest is p21, the cell cycle of CP-B SMAD4 wild-type and SMAD4 knockout cells upon TGF-β1 cytokine treatment was compared. Overall, it was found that G1 cell cycle arrest induced by TGF-β1 in SMAD4 wild-type cells is likely to be entirely mediated through SMAD4-dependent pathways, as this effect was absent in CP-B SMAD4 knockout cells. These data indicate that TGF-β mediated cell growth inhibition is dependent on SMAD4, and it is likely that SMAD4 loss might lead to uncontrolled cell growth, one of the features that pre-determines progression from premalignant to malignant cells, and a feature cancer cells rely on. Together, these initial experiments validated CP-B cells as a suitable model to further investigate the effect of SMAD4 loss. Although, these results were expected based on previous literature, it was important to show that SMAD4 loss in CP-B cells leads to altered response to TGF-β signalling.

Taken into account the importance of SMAD4 in TGF-β mediated cell growth inhibition, deciphering the downstream mechanisms of SMAD4 dependent regulation of gene expression within TGF-β signalling might elucidate tumour promoting effects of SMAD4 loss. Indeed, many more genes were up- or down-regulated by stimulation with TGF-β1 in SMAD4 wild-type cells, than in SMAD4 knockout cells. Loss of regulation of these genes within SMAD4 knockout cells could have a tumour promoting effect. Furthermore, a smaller set of genes, such as *RUNX1*, *MSX2* and *AIPL1* were found to be regulated by TGF-β1 specifically in SMAD4 knockout cells. These genes may have a role in promoting tumourigenesis following loss of SMAD4. As such,

literature evidence supports involvement of *RUNX1* in regulation of EMT, migration, invasion and angiogenesis in cancers [270-272]. Therefore, future experiments focusing on understanding the functional role of these genes, primarily *RUNX1* in the settings of premalignant or malignant cells might provide answers about SMAD4-independent, TGF-β downstream tumour promoting mechanisms.

Additionally, it was shown that genes *BHLHE40*, *FURIN*, *PTHLH*, *RHOB* and *SERPINE1* were up-regulated in SMAD4 wild-type cells upon TGF-β1 treatment only in the presence of serum (at both early and late time points), but not in SMAD4 knockout cells. Considering the presence of serum and additional TGF-β cytokines during the stimulation with TGF-β1, these data show regulation of the genes in SMAD4 dependent manner and possibly via its activation with different cytokines, besides TGF-β1.

These findings of SMAD4 dependent regulation of TGF-β target genes are consistent with other studies. Positive regulation of *SERPINE1* and *FURIN* [273], and *BHLHE40* and *GADD45B* [260] gene expression have been reported to be SMAD4-dependent, in response to stimulation with TGF-β cytokines. Similarly, in this study, *FURIN*, *BHLHE40* and *GADD45B* were up-regulated upon TGF-β1 treatment in SMAD4 wild-type cells, whereas SMAD4 knockout cells were unable to up-regulate these genes. In contrast, although SMAD4 dependent positive gene regulation of *SERPINE1* has been reported by others [273], herein SMAD4 knockout cells were also able to up-regulate *SERPINE1* upon treatment with TGF-β1 in serum deprived conditions. These results could be explained by the different experimental set-ups and use of different cytokines, TGF-β1 in this study versus TGF-β3 by Koinuma *et al*. [273].

Among the genes differentially expressed in SMAD4 wild-type and SMAD4 knockout cells in response to cytokine TGF-β1 in the presence of serum, *PTHLH*, *SOX4* and *SHH* gene were found to be inversely regulated in these cells. As such, the expression of the *SHH* gene was down-regulated in SMAD4 wild-type cells and up-regulated in SMAD4 knockout cells. The *SHH* gene encodes for sonic hedgehog cytokine that activates hedgehog (HH) pathway. The HH pathway has an essential role in embryonic development, whereas in adult tissues it continues to signal primarily within stem and progenitor cells and it is responsible for maintaining tissue homeostasis and

repair [274]. However, aberrant activation of the HH pathway has been implicated in cancer development and resistance to chemotherapy in gastrointestinal malignancies [275, 276]. The effect of up-regulation of *SHH* upon SMAD4 loss in oesophageal cancer has not been extensively studied, although HH pathway activation has been associated with chemo-radiotherapy resistance in OSCC [277]. In addition, SHH is also upregulated in Barrett's carcinogenesis [59] and results from this thesis suggest that SHH upregulation in some cases could be due to the SMAD4 loss. Altogether, it is likely that loss of SMAD4 leads to deregulation of TGF-β1 responsive genes that are involved in regulation of stemness, cell differentiation and angiogenesis leading to increased oncogenesis and invasiveness.

To further decipher SMAD4 dependent gene regulation, expression of TGF-β signalling target genes was compared between CP-B SMAD4 wild-type and SMAD4 knockout cells, independent of TGF-β1. Importantly, differential expression of TGF-β signalling target genes was observed when comparing SMAD4 wild-type and SMAD4 knockout cells under basal conditions and irrespective of treatment and time point.

Promoter wide analysis of SMAD4 binding sites has identified that half of the binding sites upon stimulation with TGF-β3 were SMAD4 specific sites, whereas the rest of binding sites were overlapping with SMAD2/3. As such, one of the corresponding target genes, *CDC6*, was down-regulated by SMAD4 transcription factor activity following treatment with TGF-β3 [273]. In support of these data, *CDC6* was up-regulated in SMAD4 knockout cells compared to SMAD4 wild-type cells (**Figure 4.2.9**). It is likely that up-regulated *CDC6* in SMAD4 knockout cells is the result of the loss of negative transcriptional regulation of *CDC6* via wild-type SMAD4.

Given that *CDC6* up-regulation and deregulation of other genes was observed in SMAD4 knockout compared to SMAD4 wild-type cells under serum starvation conditions (**Figure 4.2.9 and 4.2.12**), this evidence raises the discussion about the SMAD4 transcription factor activity mediated via autocrine or paracrine production of TGF-β cytokines by the CP-B cells that induce TGF-β signalling. As such, these changes might reflect SMAD4 dependent loss of autocrine or paracrine signalling effect. An alternative interpretation of this result is that SMAD4 might have transcription factor activity independent of cytokine mediated TGF-β signalling.

CDC6 is involved in pre-replication complex assembly and one of its main roles is regulation of early DNA replication processes [266]. CDC6 has also been implicated in transition from S-G2/M phase of the cell cycle via regulation of S phase DNA replication [278]. Importantly, high CDC6 expression levels have a negative effect on survival outcome in the patients with breast cancer [279]. Overall, the oncogenic effects of CDC6 overexpression in cancer progression are becoming evident. Notwithstanding the essential roles of CDC6 in DNA replication and cell cycle regulation, its deregulation in cancer development and progression has been scarcely studied, including in OAC. This thesis reports the up-regulation of CDC6 upon SMAD4 loss and this transcriptional regulation is likely to be through suppressive activity of SMAD4 and cooperation with other transcription factors.

In support of these results, Kennedy et al. reported that E2F Transcription Factor 1 (E2F1) may act as a major SMAD4 co-transcription factor in regulating cell proliferation in normal cells, whereas this regulation is lost in cancer [280]. In addition, recently published data showed alternative silencing of the INK4/ARF ($p15^{INK4B}$, $p16^{INK4A}$, and $p19^{ARF}$) tumour suppressor locus in E3 ubiquitin ligase E6AP-/- mouse embryo fibroblasts. Of interest, E6AP reduces the E2F1-dependent positive transcription of CDC6, the key repressor gene of $p15^{INK4B}$, $p16^{INKAa}$, and $p19^{ARF}$ locus in mouse fibroblasts [267].

The INK4/ARF locus in humans encodes $p14^{ARF}$ (also known as $p19^{ARF}$ in mouse), $p15^{INK4b}$, and $p16^{INK4b}$ tumour suppressors. $p15^{INK4b}$ and $p16^{INK4a}$ function as inhibitors of CDK4 and CDK6 by their direct binding and interfering with kinase-mediated phosphorylation of retinoblastoma protein leading to eventual G1 cell cycle arrest. In addition, $p14^{ARF}$ tumour suppressor activity is mirrored in its ability to regulate p53 levels through inactivation of the p53 negative regulator MDM2 [281].

Considering up-regulated CDC6 expression levels in our SMAD4 knockout high grade dysplasia model, $p14^{ARF}$, $p15^{INKB}$, and $p16^{INKA}$ expression levels in CDC6 high expressing cells were investigated. Of high importance, expression of INK4/ARF locus genes was found to be significantly down-regulated in CP-B SMAD4 knockout cells with high CDC6 expression levels. Therefore, a deeper understanding of the SMAD4

loss/CDC6 high mechanism driving silencing the INK4/ARF tumour suppressor locus may provide better screening biomarkers and open the possibility for novel therapeutic approaches in cancer treatment through identification of patients with silenced INK4/ARF locus.

Given that $p16^{INK4A}$ mutations are frequent in OAC [75, 76], the correlation between mutations in *SMAD4* and *CDKN2A*, the gene encoding $p16^{INK4A}$ was investigated. Based on the publically available datasets on OAC (cBioPortal database (https://www.cbioportal.org/)), there is a tendency towards mutual exclusivity between mutations in *SMAD4* and *CDKN2A*, and also *CDKN2B*, encoding $p14^{ARF}$ and $p15^{INK4b}$. Thus, there is a possibility that SMAD4 loss represents an additional mechanism of down-regulating not only *CDKN2A*, but also *CDKN2B* in OAC.

Furthermore, high CDC6 expression levels have been associated with increased resistance to the widely used chemotherapy drug, cisplatin [265]. Herein, the response to cisplatin was compared in isogenic CP-B SMAD4 knockout cells expressing high CDC6 levels and SMAD4 wild-type cells. Indeed, CP-B SMAD4 knockout/CDC6 high cells were found to have increased resistance to cisplatin compared to SMAD4 wild-type/CDC6 low expressing cells. Given that the majority of OAC patients are not responding to, or relapsing soon after systemic treatment with chemotherapy drugs, this study highlights the possibility to use SMAD4 mutation or loss as a novel biomarker of increased chemotherapy resistance in OAC and other cancers.

A wealth of evidence raises an intriguing aspect of CDC6 function that involves close regulation of the origin of DNA replication. Origin of DNA replication is tightly regulated during evolution and CDC6 plays an essential role in composing a chromatin-bound multiprotein pre-replicative complex. Oncogene-induced replication stress has been considered as one of the main inducers of genomic instability, particularly during the early stages of tumorigenesis [282]. In this instance, CDC6 oncogenic activation in SMAD4 knockout cells might lead to deregulation of DNA replication licencing leading to increased genomic instability and progression of tumorigenesis.

Besides *CDC6*, *ACTA2* was up-regulated to the highest extent in SMAD4 knockout compared to SMAD4 wild-type cells. *ACTA2* encodes for alpha smooth muscle protein

known as one of the mesenchymal markers in cancer [262]. Up-regulated levels of *ACTA2* in SMAD4 knockout cells might contribute to epithelial mesenchymal transition (EMT) and subsequent acquisition of invasive characteristics of mesenchymal cells. Another interesting oncogenic candidate up-regulated in SMAD4 knockout cells is the *CRYAB* gene. This gene encodes for alpha B-crystallin protein that has been implicated in EMT and promoting invasion and metastasis in gastric and colorectal cancers [263, 264]. The mechanism of *CRYAB* regulation across cancers is unknown. However, this study reports the regulation of *CRYAB* through SMAD4 dependent canonical TGF-β signalling.

Certainly, the gene expression pattern in CP-B cells upon SMAD4 loss is significantly changed, resulting in up-regulation of potential oncogenes and down-regulation of tumour suppressor genes. Indeed, up-regulated genes following SMAD4 loss, such as *ACTA2*, *CRYAB*, *CDC6*, *EMP1* and *PTK2B*, have previously been implicated in oncogenesis across different cancers [262-266, 283]. Overall, the results generated in this chapter provide a rationale for seeking a deeper understanding of the molecular mechanisms downstream of altered TGF-β signalling resulting from SMAD4 loss. Crucially, future studies are required to functionally characterize the role of altered genes in the setting of SMAD4 loss in precancerous cells. Altogether, SMAD4 loss could promote TGF-β mediated tumorigenesis via enhancing some of the tumour promoting effects of TGF-β, while TGF-β tumour suppressive functions are lost.

In addition, it is likely that SMAD4 as a tumour suppressor, represents an essential orchestrator of genomic stability within metaplastic Barrett's cells. SMAD4 loss leads to increased genomic instability through a complex network of inactivation of tumour suppressor genes within the INK4/ARF locus. Also, activation of oncogenes such as *CDC6* following SMAD4 loss is likely to be implicated in tumorigenesis by inducing genomic instability through increased replication stress.

CHAPTER 5.

GRB7 AMPLIFICATION IS AN ONCOGENIC DRIVER INDEPENDENTLY OF HER2 AMPLIFICATION IN OAC

This chapter has been written as a manuscript for submission to a Journal. Materials and Methods and Bibliography used to generate data are included within the manuscript.

Authors: Gotovac JR[1,2], Liu DSH[1,2,3#,4#], Yates MJ[1], , Macpherson AA[1], Simpson KJ[1,2], Eslick GD[3], Mitchell C[1], Duong CP[1,2], Phillips WA[1,2,4], Clemons NJ[1,2]*.

[1] Peter MacCallum Cancer Centre, 305 Grattan St, Melbourne, Victoria, Australia, 3000

[2] Sir Peter MacCallum Department of Oncology, The University of Melbourne, Parkville, Victoria, Australia, 3010

[3] Nepean Clinical School, The University of Sydney, Kingswood, NSW, Australia, 2747

[4] Department of Surgery (St Vincent's Hospital), The University of Melbourne, Parkville, Victoria, Australia, 3010

[#] Current affiliation

[3#] Austin Health, 145 Studley Rd, Heidelberg, Victoria, Australia, 3084

[4#] Northern Health, 185 Cooper St, Epping, Victoria, Australia, 3076

*To whom correspondence should be addressed.

Email: nicholas.clemons@petermac.org

Telephone: +61 3 8559 5273

ABSTRACT

The HER2 proto-oncogene is frequently amplified and overexpressed in oesophageal adenocarcinoma (OAC). However, therapeutic targeting of HER2 in HER2 overexpressing OAC tumours has not proven to be as effective as expected. Herein, we focus on the potential oncogenic role of growth factor receptor bound protein 7 (GRB7), the gene which is also positioned within the known HER2 amplicon (17q12) and often co-amplified with HER2 in OAC.

GRB7 protein expression was analysed by immunohistochemistry in tumours from 88 OAC patients. GRB7 was frequently overexpressed in OAC tumours (36%) and patients with GRB7 overexpressing tumours were found to have poor overall survival relative to patients with GRB7 low/negative tumours. Transient knockdown of GRB7 in OAC cell lines decreased proliferation and clonogenic survival, and induced apoptosis. Furthermore, the GRB7 and HER2 high expressing OAC cell line Eso26 responded to GRB7 knockdown but was insensitive to HER2 inhibition by trastuzumab. Consistent with these *in vitro* findings, mimicking GRB7 inhibition *in vivo* with inducible-shRNA significantly inhibited tumour growth in both OE19 and Eso26 OAC cell line xenograft models. HER2 expression did not predict sensitivity to trastuzumab in these models, with Eso26 xenografts remaining refractory to trastuzumab treatment. Finally, reverse phase protein array analyses revealed a potential role for PI3K, mTOR, MAPK, and receptor tyrosine kinase signalling in the oncogenic action of GRB7.

Our study provides strong evidence for an oncogenic role for GRB7 in OAC and suggests that targeting GRB7 may be a potential therapeutic strategy for this cancer.

Key words: oesophageal adenocarcinoma; GRB7; HER2; trastuzumab; targeted therapy; and 17q12 amplicon.

INTRODUCTION

Cancer of the oesophagus remains the sixth major cause of cancer related deaths worldwide [1]. There are two major histological subtypes of oesophageal cancer: oesophageal squamous cell carcinoma (OSCC) and oesophageal adenocarcinoma (OAC). Although the most common subtype worldwide is OSCC, the incidence of OAC has risen rapidly over the last four decades in North America, Europe and Australia, whereas the incidence of OSCC has decreased [2,3]. The prognosis for OAC is poor with 5-year survival ranging from 14-22% [4,5]. Despite the application of multimodality therapy which consist of chemotherapy, radiotherapy and surgery, the majority of patients are either unresectable, experience early relapse or develop distant disease with limited treatment options. Hence, there is an urgent need for new therapeutic strategies.

In an era of effective molecular targeted therapy in treating solid cancers such as breast [6,7] and lung cancers [8], OAC is still lacking defined oncogenic drivers amenable to therapeutic targeting. The only two FDA approved targeted therapies for the treatment of OAC, trastuzumab (Herceptin) targeting human epidermal growth factor receptor 2 (HER2,) and ramucirumab, targeting vascular endothelial growth factor receptor 2 (VEGFR2), have only shown modest survival benefit [9,10]. This may be partly explained by the activation of multiple oncogenic pathways that maintain tumour survival and mediate therapeutic resistance [11]. Therefore, inhibiting intersecting signalling pathways may have greater therapeutic efficacy.

The HER2 proto-oncogene is positioned within the 17q12 amplicon and its amplification and overexpression have been frequently associated with carcinogenesis [12,13]. Given the frequent HER2 gene amplification and/or overexpression across cancers including gastrointestinal cancers, a wide range of clinical studies are currently underway in order to successfully target HER2 [14]. However, further molecular characterization of the 17q12 amplicon has shown that this region also contains other genes frequently amplified with HER2, including GRB7 [15,16]. The involvement of GRB7 in carcinogenesis has been scarcely studied.

GRB7 is an SH2-domain containing adaptor molecule that mediates cellular signalling through interaction with multiple receptor tyrosine kinases and their downstream

partners [17]. In this way, GRB7 is a central node that connects multiple potential oncogenic drivers to downstream signalling pathways and thus, represents an attractive therapeutic target. High GRB7 expression is associated with decreased survival in patients with breast cancer [18], whereas overexpression of GRB7 and its variant (GRB7v) are correlated with high grade ovarian cancers [19]. Overall, the lack of preclinical evidence with regard to the functional role of GRB7 amplification and/or overexpression in oesophageal cancer is preventing the identification of any potential therapeutic benefits of targeting GRB7 in this disease.

Herein, for the first time, we report the frequency of GRB7 protein expression levels within an OAC patient cohort and correlation with clinico-pathological data and survival outcome. Furthermore, we assayed the functional effects of manipulating GRB7 expression levels in *in vitro* cell line models of OAC. Importantly, we demonstrated the therapeutic value of inhibiting GRB7 in OAC xenografts. In summary, our body of work highlights the potential oncogenic role and therapeutic significance of GRB7 in OAC.

MATERIALS AND METHODS

Oesophageal cancer research cohort

Use of patient samples in this study was approved by the Human Research Ethics Committee of the Nepean Blue Mountains Local Health District. The cohort consisted of OAC patients recruited from January 1, 2000 to January 31, 2013. Information about this patient cohort, including detailed clinico-pathological data and clinical management as well as HER2 status (based on immunohistochemistry (IHC) and silver in sity hybridization (SISH)), has been published previously [20]. Tumour microarrays (TMAs) of patient tumours were assessed for GRB7 positivity. Sufficient tissue and clinico-pathological data were available for 88 patients.

Histology and IHC

TMA sections were obtained from formalin-fixed paraffin embedded (FFPE) tissue TMA blocks and stained with hematoxylin and eosin for histological features. The IHC protocol included blocking sections in Dual Endogenous Enzyme Block (Dako) high pH followed by 10% (w/v) bovine serum albumin (BSA) in tris-buffered saline containing 0.05% Tween-20 (TBS-T) and incubation with primary anti-GRB7 antibody (LS-C138038, LSBio) 1:500 diluted in 1% (w/v) BSA in TBS-T for 1h at room temperature followed by incubation overnight at 4°C. Primary antibodies were probed with horse radish peroxidase (HRP)-conjugated anti-rabbit secondary antibody polymer (Dako) and visualized with 3,3-diaminobenzidine (DAB) using the EnVision+Detection System (DakoCytomation) according to the manufacturer's protocol, and counterstained with hematoxylin. IHC on positive and negative control tissues was performed concurrently. Images of anti-GRB7 stained TMA sections were captured with a VS-120 microscope (Olympus) and scoring was performed by two independent researchers, and in co-operation with an expert pathologist (CM) the final consensus score was obtained. GRB7 IHC was assessed as 3+/positive - strong complete cytoplasmic and basolateral reactivity, 2+/positive - equivocal or moderate complete cytoplasmic and basolateral reactivity, 1+/low - faint incomplete cytoplasmic reactivity, and 0/negative - no cytoplasmic reactivity. A tumour was considered GRB7 high expressing if it showed either 3+ or 2+ by IHC, whereas 1+ and 0 IHC scoring was considered as low/negative expressing (**Figure 1A**). Only staining in tumour cells was scored and homogenous staining was observed in each core across the tumour cell portion.

Cell lines and culture

OE19, OE33 and HEK-293T cells were obtained from the American Type Culture Collection. FLO-1, OACM5.1, Eso26, Eso51, SKGT4, OACP4C and cells were kindly gifted from Rebecca Fitzgerald (University of Cambridge, UK). JH-EsoAd1 cells were provided by James Eshleman (Johns Hopkins University, MD) and immortalized normal human oesophageal squamous (NES) epithelial cells were provided by Rhonda Souza (University of Texas Southwestern Medical Centre, TX). OANC1 cells were developed in our laboratory [21]. Eso51, OE19, OE33, OACM5.1, ESO26, SKGT4, OACP4C and JH-EsoAd1 cells were cultured in Roswell Park Memorial Institute (RPMI) 1640 medium containing 2.5 mmol/L L-glutamine (Life Technologies). HEK-293T, FLO-1 and OANC1 cells were grown in Dulbecco's Modified Eagle Medium (DMEM) containing 2.5 mmol/L L-glutamine and 4.5 g/L D-glucose (Life Technologies). NES cells were grown in MCDB-153 medium containing 400 ng/ml hydrocortisone, 20 ng/ml epidermal growth factor (EGF), 20 mg/ml adenine, 140 µg/ml bovine pituitary extract, ITS Liquid Media Supplement (100X) for the final concentration of 2.5 µg/ml insulin, 1.4 µg/ml transferrin, 1.3 ng/ml selenium (Sigma-Aldrich, Australia), 10 nmol/L cholera toxin, 5% v/v fetal bovine serum (FBS), 375 ng/ml diflucan and 4 mmol/L L-glutamine (Glutamax, Invitrogen) and adjusted to a pH of 7.2. All cell lines were grown at 37°C with 5% CO_2. Unless otherwise specified, all cell culture media contained 10% v/v FBS, 50 U/ml penicillin, and 50 mg/ml streptomycin (Life Technologies). All cell lines were authenticated by Short Tandem Repeats (STR) analyses using the PowerPlex® 16 System and confirmed mycoplasma free by PCR analyses (Cerberus Sciences, Scoresby, Australia).

Transient GRB7 knockdown

For experiments in 96-well plates (cell proliferation assays) $1x10^4$/well OE19, Eso26, OE33, OACP4C, NES or $2x10^4$/well OANC1 cells were transfected with 40 nM ON-TARGETplus non-targeting pool or siNTC (Dharmacon; D-001810-10) or *GRB7* siRNA (siGENOME SMARTpool, Dharmacon; M-012701-01) using Lipofectamine RNAiMax solution (Life Technologies) according to manufacturer's instructions. Six well plates were used for cell cycle, apoptosis and RNA analyses. Six-cm Petri dishes were used for harvesting protein lysates. The cell number and Lipofectamine RNAiMax volume for 6-well plate or 6 cm Petri dish experiments were scaled up from the 96 well

plate format using cell growth surface area multiplication factors as per manufacturer's guidelines.

GRB7 knockdown using shRNA

GRB7-specific shRNAs (**Supplementary Table 1**) and shRenilla control (sh Control) were cloned into the doxycycline inducible LT3GECIR lentiviral expression vector containing the optimized miR-E backbone [22]. The mCherry and turbo-GFP reporters were used to monitor transduction efficiency and induction of the shRNA, respectively. OE19 and Eso26 cells were progressively passaged into larger flasks and induced with doxycycline (Sigma-Aldrich, 2 µg/ml) for 48 hr before cytometric sorting (BD Fusion5™, BD Bioscience) to isolate mCherry and GFP positive cells.

Reverse Transcription Quantitative PCR (RTqPCR)

Total cell RNA was extracted using the RNeasy kit (Qiagen, Doncaster, Australia) according to the manufacturer's protocol and reverse transcribed using the Transcriptor First Strand cDNA Synthesis Kit (Roche, Hawthorn, Australia). Primers used for RTqPCR are summarized in **Supplementary Table 2**. Gene expression changes were determined using SYBR green RT-PCR (Lightcycler 480, Roche), normalised against GAPDH and quantified using the ΔΔCt method.

Cellular proliferation assay

Cellular proliferation was determined using a microscopy based real time live cell imaging system (Incucyte FLR, Essen BioScience). This assay quantifies the cellular confluency per given imaged area based on software algorithms. For these experiments, cells were seeded in 96-well plates with transfection reagents or treated with doxycycline, trastuzumab or vehicle and imaged every 24 h for up to 144 h. For proliferation experiments following GRB7 overexpression $2x10^4$ Flo1, OACP4C and OE33 cells were seeded in 96-well plate and imaged at last time point, as indicated.

Cell viability assays

Cell viability was assayed using AlamarBlue® (Life Technologies) or CellTiter-Glo® (Promega) reagents. Following shRNA induction with doxycycline for 72 h, cell viability was assessed at 120 h with the addition of 20% v/v AlamarBlue® (OE19 cells) or 50% v/v CellTiter-Glo® (Eso26 cells) without removing pre-existing medium

in 96-well plates. Fluorescence intensity (AlamarBlue®) was measured using a FLUOstar OPTIMA plate reader (BMG Labtech, Mornington, Australia) at an excitation of 540 nm and an emission of 590 nm following incubation for 2 h at 37°C. Luminescence (CellTiter-Glo®) was measured using a Cytation 3 Imaging Reader (BioTek) upon incubation for 10 min at room temperature.

Clonogenic survival assay

To investigate the effects of GRB7 knockdown (shRNA) on long term survival, cells were induced with 2 µg/ml doxycycline or vehicle (saline) for 72 h. Then, $5x10^3$ Eso26 and OE19 cells/well were seeded in six-well plates in media with 2 µg/ml doxycycline or saline. Colonies were allowed to form for 10 days (Eso26) or 14 days (OE19) with addition of media (5ml) ± doxycycline after 7 days. To investigate the effect of GRB7 overexpression on colony forming ability, OACP4C, OE33 and FLO1 cells containing constructs expressing GRB7 or RFP were seeded ($1x10^3$/well) in six-well plates in 2ml of media and allowed to form colonies for 10 days with 2ml of fresh media added at day 5. Cell colonies were fixed and stained with crystal violet (0.5% w/v), rinsed in water, air-dried and digitally scanned. Discrete colonies of >50 cells were manually counted using ImageJ Cell Counter and expressed as a total number (OACP4C) or a percentage (Eso26, OE19) of vehicle treated sh Control transduced cells.

Migration Assay

$5x10^5$ Flo1, OACP4C and OE33 cells expressing GRB7 or RFP in serum free media were seeded into the upper chamber of 8 µm pore size Boyden Chambers with media containing 10% serum in the lower chamber and incubated at 37°C with 5% CO_2 for 24 h. The permeable membranes were fixed with 100% methanol for 15 min at -20°C, and stained with crystal violet (0.5% w/v) and removed. Representative photographs were taken with an AMG EVOS FL microscope (Advanced Microscopy Group) and cells that had migrated though the membrane were counted manually using ImageJ Cell Counter.

Apoptosis assay

$2.5x10^5$ OE19 and Eso26 cells/well were seeded into 6 well plates and cultured following transfection with GRB7 siRNA for 144 h or trastuzumab treatment for 120 h. Cells were stained with Annexin V-FITC antibody and propidium iodide (PI) (BD

Pharmigen kit) according to manufacturer's instructions. The extent of apoptosis (percent of Annexin-V positive cells within total cell population) was determined by flow cytometry (BD FACSCanto™ II, BD Bioscience) and analyzed using Flowlogic software (Inivai Technologies).

Cell cycle analysis

$2.5x10^5$ OE19 and Eso26 cells/well were seeded into 6 well plates and following transfection with GRB7 siRNA pool were cultured for 144 h or trastuzumab treatment for 120 h. All cells were collected, spun down and the supernatant removed. Cells were washed in cold PBS with 1% FBS and fixed in 70% ethanol. Following complete ethanol removal cells were stained for 2 h at room temperature in the dark with 25µg/ml propidium iodide (Molecular Probes, Eugene, Oregon USA) and 40µg/ml RNAse A (Qiagen) in PBS. A minimum of 10,000 single cell events were detected by flow cytometry (BD FACSCanto™ II, BD Bioscience) and analyzed using Flowlogic software (Inivai Technologies, Mentone, Australia). The distribution of cells in each cell cycle phase was expressed as a percentage of total cell population.

Western blot analysis

Cells or tissues were lysed at 4°C in RIPA buffer (1 mmol/L EDTA; 1% v/v NP40; 0.5% w/v sodium deoxycholate; 0.1% w/v SDS; 50 mmol/L sodium fluoride; 1 mmol/L sodium pyrophosphate in PBS) with added phosphatase (PhosphoSTOP, Roche) and protease (Complete ULTRA, Roche) inhibitors according to manufacturer's guidelines. Cells were harvested at the indicated time points following transfection with siRNA, or treatment with 2µg/ml doxycycline or vehicle (for shRNA experiments). Tumour tissues were harvested from mice at the indicated time points and homogenised with the PowerLyser™ 24 (MO BIO laboratories, Inc) in tubes containing metallic beads.

Protein concentrations were quantified using a Bradford protein assay (BioRad). Equivalent amounts of protein lysates were boiled, resolved by SDS-PAGE using the range of 7 to 15% w/v acrylamide gels according to the size of the protein of interest, and transferred to polyvinylidene difluoride membranes. Membranes were blocked for 1 h in buffer containing 5% w/v skim milk powder, 0.1% v/v Tween 20 in Tris-buffered saline and probed overnight at 4°C with the primary antibody (**Supplementary Table 3**). Blots were washed three times in rinsing buffer (0.1% v/v Tween 20 in Tris-buffered

saline) for 10 min, followed by incubation with horse radish peroxidase-conjugated secondary antibody (Dako) for 1 hour at room temperature. Proteins were visualised using Western Lightening Enhanced Chemiluminescence (ECL) (PerkinElmer, MA, USA) or ECL Plus Western blotting substrate kit (Thermo Scientific, Scoresby, Australia). Blots were reprobed with anti-β-actin or anti-GAPDH antibody to determine protein loading.

GRB7 overexpression

GRB7 was ectopically expressed in FLO-1, OACP4C and OE33 cells using the Precision LentiORF pLOC lentiviral vector purchased from GE Dharmacon (OHS5898-202620211). In this system, the open reading frame *GRB7* has been cloned downstream of the CMV promoter and contains turbo-GFP as a reporter gene. The turbo-RFP gene was used as a control. GFP positive FLO-1, OACP4C and OE33 cells were sorted by FACS and grown up for future experiments. The expression of *GRB7* was assessed using RT-PCR and western blotting.

Animal experiments

All animal experiments were conducted in accordance with the *National Health and Medical Research Council Australian Code of Practice for the Care and Use of Animals for Scientific Purposes* and approved by the Peter MacCallum Cancer Centre (PMCC) Animal Experimentation Ethics Committee. NOD-SCID IL-2RγKO (NSG) mice were obtained from the Garvan Institute of Medical Research or bred in-house.

Tumour xenografts

To generate OE19 and Eso26 cell line xenografts, $5X10^6$ cells were resuspended in 100µl of 1:1 ice-cold phosphate buffered saline (PBS) and growth factor reduced Matrigel® Matrix (Corning) and kept on ice. Cells were injected subcutaneously into the right flank of 6-8 weeks old female NSG mice. When tumours reached $150mm^3$ volume (calculated using the formula length × $width^2/2$), mice were randomized into groups of 5-8 for treatments. Concomitantly with vehicle, doxycycline and/or trastuzumab treatments, subcutaneous tumour volume was measured with callipers twice per week up to the end of the experiment. All mice were euthanised when subcutaneous tumours reached ≥ 1500 mm^3 or at first signs of ill health or discomfort,

apart from 6 mice that were euthanized at 15, 25 or 30 days to determine GRB7 knockdown efficiency in vivo.

Reverse Phase Protein Array (RPPA)

Protein lysates were prepared from treated tissue culture cells in CLB1 buffer (Zeptosens, Bayer), and quantified using a Pierce™ Coomassie Plus (Bradford) Protein Assay Kit (n=3/treatment). Due to the lower yield, samples including OE19 cells treated with siGRB7 were concentrated using the Amicon Ultra-0.5 Centrifugal Filter Unit (UFC5003, Merck Millipore). Using a Sciclone/Caliper ALH3000 liquid handling robot (Perkin Elmer), samples were prepared in 4 dilutions (100%, 63%, 40% and 25%) in 10% CLB1:90% CSBL1 buffer (Zeptosens, Bayer) and spotted onto ZeptoChips (Zeptosens) in 3-4 technical replicates using a Nano-plotter-NP2.1 non contact microarray system (GeSim). Chips were blocked for 1 h with BB1 buffer (Zeptosens), incubated with pre-validated primary antibodies (1:500, 20 h), and Alexa Fluor® 647 anti-rabbit secondary antibody (1:1000, 4 h) (#Z25308, Thermo Fisher Scientific). Chips were read on a Zeptosens instrument and software version 3.1 used to calculate the Relative Fluorescence Intensity (RFI). All samples were normalised to the background values reported in the secondary antibody-only negative control.

Statistical analysis

Data were analysed by two tailed Student's *t*-test or paired *t*-test to compare two groups of interest. For analyses of three or more groups, parametric one-way ANOVA with Dunnett's multiple comparisons post-test was performed. Statistical analyses were performed in Prism 7 (GraphPad). Contingency table analyses with Chi square or Fisher's exact test were used to compare GRB7 3+, 2+, 1+ and 0 IHC scoring with HER2 positivity (HER2+ tumours) or GRB7 3+ vs. others and HER2 positivity, respectively. Correlation of clinico-pathological variables and GRB7 expression was obtained by performing logistic regression analysis. Odds ratio with 95% CIs were reported. Kaplan-Meier curves were generated for overall survival defined as the time from diagnosis to death from any cause. Statistics for RPPA protein RFI values between treatment and control samples was obtained with Welch *t*-test. For analyses of the cell line xenograft tumour volume over the time course of the treatment, we compared groups of growth curves between different treatments in OE19 and Eso26 xenografts by using CGGC permutation test. This test performs the permutation tests

of the differences between groups of the growth curves for the full time course of the treatment [23,24]. For all statistical analyses, $p<0.05$ was considered statistically significant.

RESULTS

GRB7 expression status in OAC patient samples and correlation with clinico-pathological data

To determine whether GRB7 expression is a prognostic biomarker in OAC, we first evaluated the expression of GRB7 in TMAs from 88 patient samples [20]. Representative images of OAC biopsy cores for different scoring intensities including 3+, 2+, 1+ and 0 are shown in **Figure 1A** and the proportion of samples with each intensity score is summarised in **Table 1**. Given the GRB7 gene is located within 17q12 amplicon and previously reported to be co-amplified and overexpressed (mRNA) with HER2 in OAC [25], the correlation between GRB7 expression (this study) and HER2 status [20] was examined. While it is clear from the data in **Table 1**. that there was a trend for the high GRB7 expressing tumours to be more likely HER2 positive (p=0.03). Nevertheless, there were clearly numerous GRB7 positive tumours that were not HER2 positive. This would suggest that positivity was not necessarily just the result of co-amplification with HER2 and that other mechanisms for increasing GRB7 expression may exist. To investigate associations between GRB7 expression and clinico-pathological characteristics (**Supplementary Table 4**), we compared GRB7 high tumours (IHC3+ and 2+ in 14.8 and 21.6%, respectively) to GRB7 low/negative tumours (IHC1+ and 0 in 31.8 and 31.8%, respectively). Logistic regression analysis showed that GRB7 high tumours were more likely to have a well differentiation grade compared to the GRB7 low/negative tumours. There was no association with vascular, perineural, serosal or lymphatic invasion, although the number of cases that had this information reported was small (data not shown). Importantly, GRB7 high expression was significantly correlated with worse overall survival in patients with OAC (**Figure 1B**).

GRB7 knockdown inhibits cell growth in GRB7 overexpressing OAC cell lines

The transcript and protein expression levels of GRB7 and HER2 were investigated across a panel of ten OAC cell lines and in a normal oesophageal squamous cell line (NES) (**Figure 2A, B**). GRB7 and HER2 mRNA expression was significantly higher in OE19, OE33, OACP4C and Eso26 tumour cell lines compared to NES (**Figure 2A**), consistent with *GRB7* and *HER2* gene amplification in these cell lines (**Table 2**). Similarly, high GRB7 and HER2 protein expression levels were detected in OE19 and Eso26 cell lines (**Figure 2B**), while OE33, OACP4C and the other cell lines expressed GRB7 and HER2 protein at lower levels (**Figure 2B**). OE19 and Eso26 cells also show

the presence of a smaller molecular weight GRB7 protein (**Figure 1B**), which is likely to be GRB7 variant protein [19,26]. To evaluate the functional contribution of GRB7 high expression, GRB7 knockdown was performed using siRNA. Efficient knockdown of GRB7 mRNA and protein levels (**Figure 2C, D**) significantly decreased cell proliferation in GRB7 high expressing OE19 and Eso26 cells (**Figure 2E, F**). In contrast, GRB7 knockdown in representative oesophageal cell lines with low GRB7 protein expression levels, OANC1 and NES cells, did not affect cellular proliferation compared to control siRNA (**Supplementary Figure 1A, B**).

GRB7 knockdown has an advantage over anti-HER2 therapy in decreasing cellular proliferation *in vitro*

Given that GRB7 may act a central node for oncogenic signalling, and is commonly overexpressed in OAC (Table 1), including cell line models (**Figure 2A, B**), GRB7 presents a rational therapeutic target as an alternative, or in addition to current targeting of HER2. Initially, sensitivity to trastuzumab across OAC cell lines was determined in dose response curves (**Supplementary Figure 2A-F**). Interestingly, only OE19 cells (high HER2 expression) were sensitive to trastuzumab with maximum efficacy reached at the concentration of 0.1µM (**Supplementary Figure 2A**). Based on this evidence, the dose of 0.1 µM trastuzumab was selected for subsequent experiments. In contrast, Eso26 and OE33 cells (also high HER2 expressing) were not sensitive to trastuzumab (**Supplementary Figure 2B, C**). We next compared the effect of GRB7 knockdown and HER2 inhibition, alone or in combination, in OE19 and Eso26 cells. Importantly in OE19 cells, GRB7 knockdown significantly decreased cellular proliferation comparable to trastuzumab only treatment. There was, however, no statistically significant additional growth inhibitory effect when combining GRB7 knockdown with trastuzumab (**Figure 3A**). Contrastingly, in HER2 amplified Eso26 cells, trastuzumab alone did not result in any growth inhibitory effect *in vitro*, whilst GRB7 knockdown significantly decreased cellular proliferation. Similar to OE19 cells, the addition of trastuzumab to GRB7 knockdown did not result in further growth inhibition. (**Figure 3B**). These results support our hypothesis that GRB7 functions as a central node for oncogenic signalling, and that its inhibition may achieve a wider therapeutic applicability than targeting HER2. Based on these findings, we proceeded to elucidate the functional role of GRB7 in OAC and its potential as a therapeutic target.

Functional validation of GRB7 knockdown using inducible shRNA

To investigate the long-term effect of GRB7 knockdown, we cloned four GRB7-specific shRNA into a doxycycline inducible lentiviral expression vector (**Supplementary Figure 3A**). The efficiency of each shRNA to knockdown GRB7 protein was assessed in OE19 cells (**Supplementary Figure 3B**). Two out of four constructs with sh1 and sh2 were chosen for further functional validation and analyses. Expression of sh1 or sh2 RNAs effectively decreased GRB7 protein levels in both OE19 and Eso26 (**Figure 4A, B**) cells. To functionally validate the effect of shRNA mediated GRB7 knockdown, we examined the effect on OE19 and Eso26 cell proliferation compared to a sh Control targeting a non-expressed protein (Renilla). Proliferation was significantly decreased following sh2 GRB7 activation in both cell lines, whereas activation of sh1 GRB7 decreased proliferation in Eso26 but not OE19 cells (**Figure 4C, D**). The ineffectiveness of sh1 GRB7 correlated with higher endogenous and residual GRB7 protein levels following sh1 activation in OE19 cells. We next determined long term clonogenic survival following GRB7 knockdown in OE19 and Eso26 cell lines. Consistent with the effects on cell proliferation, GRB7 knockdown using shRNA dramatically reduced colony formation in OE19 cells (**Figure 4E, G**) and Eso26 cells (**Figure 4F, H**). Taken together, these results demonstrate the importance of GRB7 in cell proliferation and clonogenic capacity in GRB7 amplified OAC cell lines.

GRB7 regulates cell growth and apoptosis in OAC cells

We next assessed whether reduced cell growth and clonogenic survival was due to cell cycle arrest and/or apoptosis following GRB7 knockdown or HER2 inhibition. GRB7 knockdown or HER2 inhibition did not lead to G1/S or G2/M arrest in Eso26 and OE19 cells (**Supplementary Figure 4A-C**). However, an increase in the subGo fraction was observed following siGRB7 knockdown in both cell lines or trastuzumab treatment in OE19 cells (**Supplementary Figure 4A-C**), suggesting that these cells are undergoing cell death. To clarify whether GRB7 knockdown or HER2 inhibition induces apoptosis, we quantified the percentage of Annexin-V positive cells at 144h after GRB7 knockdown or 120h following treatment with trastuzumab. In both cell lines, GRB7 knockdown led to apoptosis (**Figure 5A, C**). Consistent with our proliferation assay results, apoptosis was induced in OE19 but not Eso26 cells upon trastuzumab treatment (**Figure 5B, C**).

GRB7 overexpression results in cell line dependent increase in cell growth and migratory capacities

We next examined the consequences of GRB7 overexpression on cell growth, clonogenic survival and migration potential. FLO1 (low GRB7 expression), and OACP4C and OE33 (medium and high mRNA GRB7 expression) cells were transduced with lentiviral vectors containing GRB7 or control red fluorescent protein (RFP) cDNA. GRB7 overexpression (**Figure 6A, B**) increased cell proliferation (trend towards significance) in OACP4C cells (**Figure 6C**) but not FLO1 and OE33 cells (**Supplementary Figure 5A, B**). Consistent with this, GRB7 overexpression significantly increased colony forming ability in OACP4C cells (**Figure 6D**). To extend insights into GRB7 oncogenic function, we performed migration assays in the same cell lines. Of interest, GRB7 overexpression significantly increased migratory potential in FLO1 (**Figure 6E**), but not OACP4C and OE33 cells (data not shown).

GRB7 inhibition displays strong anti-tumour activity in OAC cell line xenografts

We next investigated the anti-tumour activity of GRB7 inhibition and/or trastuzumab *in vivo*. In OE19 xenografts, tumour growth was completely inhibited by trastuzumab alone or in combination with GRB7 knockdown (**Figure 7A**). Importantly, GRB7 knockdown alone also impaired tumour growth compared to vehicle treatment. Noticeably, after an initial lack of tumour growth in the doxycycline GRB7 knockdown only group the tumour volume began to increase around 17 days after commencing treatment with doxycycline (**Figure 7A, red arrow**). Consistent with this, GRB7 protein expression in tumours showed a gradual increase over time despite continued treatment with doxycycline in a separate cohort of 6 mice (**Figure 7B**). This is potentially due to diminished efficacy of the shRNA over time and/or selective outgrowth of clones with higher GRB7 expression. In contrast to the OE19 xenografts, trastuzumab treatment did not significantly inhibit tumour growth of Eso26 tumour xenografts, while GRB7 knockdown alone or in combination with trastuzumab had significant anti-tumour activity compared to the vehicle treatment group (**Figure 7C**). Although, it might appear that trastuzumab is having anti-tumour activity in comparison to the vehicle, this was not statistically significant. As expected, OE19 and Eso26 sh Control xenografts did not respond to doxycycline treatment (**Supplementary Figure 6A, B**).

Deciphering GRB7 mechanism of oncogenic signalling transduction

To explore the potential mechanism underpinning GRB7 oncogenic signalling, we performed RPPA on protein lysates isolated from Eso26 and OE19 cells transiently treated with siRNA targeting GRB7 or control siRNA (**Figure 8 and Supplementary Figure 7**). We specifically looked at the activity of the signalling pathways through detection of phosphorylation of signalling intermediates as well as their total protein. This analysis further supports our hypothesis that GRB7 acts as a central node that mediates oncogenic signalling in OAC. As evidence, Eso26 and OE19 cells with GRB7 knockdown displayed decreased signal intensities in the phospho-kinases that participate in PI3K/mTOR (Akt_P 473, Akt_P308, rsS6_P S240;244and mTOR_P S2448) and MAPK (Erk1/2_P T202/Y204) pathway signalling. This suggests reduced signal transduction leading to decreased cellular proliferation, survival and metabolism. However, OE19 cells demonstrated decreased signal intensities in 4E-BP1_P T37;T46 phosphoprotein, whereas Eso26 cells exhibit increased signal intensities of 4E-BP1_P T37;T46 and 4E-BP1_P S65 (**Figure 8A and Supplementary Figure 7A, B**). Given that mTOR complex 1 phosphorylates 4E-BP1 to induce protein synthesis [27], decreased signal intensity of 4E-BP1_P T37;T46 phosphoprotein could explain decreased cell proliferation following GRB7 knockdown in OE19 cells and indicate positive association of GRB7 overexpression and mTOR complex 1 activity. In contrast, GRB7 knockdown in Eso26 cells is unlikely to decrease proliferation via this mechanism, as these cells demonstrate even increased intensities of 4E-BP1 phosphorylated proteins. More strikingly, we observed reciprocal increase in the total protein in opposite to decreased phosphorylated protein, particularly in Eso26 cells treated with siGRB7, meaning that decrease in signalling is additionally profound. Representative graphs of the ratio of phospho/total protein, irrespective of absolute levels are presented in **Figure 8B**.

On the other hand, we observed enhanced signalling intensities for mediators of apoptosis, such as cleaved caspase 3 (Casp3_Clvd D175), within Eso26 and OE19 cells upon GRB7 knockdown, demonstrating an essential role of GRB7 signalling in promoting cell survival. Moreover, pro-apoptotic Bax was increased in Eso26, whereas OE19 cell displayed decreased Rb_P S807;S811 leading to cell cycle arrest and subsequent cell death, upon GRB7 knockdown (**Figure 8A and Supplementary Figure 7C**). Interestingly, HER2 high expressing and trastuzumab sensitive OE19

cells, displayed decreased phosphorylation of HER2 and HER3 receptors (Her2_P Y1248;Y1173, HER3/ErbB3) and SHP-2 (SHP-2_P Y542), and also cell cycle regulators such as CDC2 (cdc2_P Y15), upon GRB7 knockdown. Contrastingly, Eso26 cells which are HER2 high expressing but insensitive to trastuzumab, exhibited no change of these phosphoproteins and, moreover, increased levels of Her2_P Y1221;Y1222 (**Figure 8A and Supplementary Figure 7D, E**).

DISCUSSION

There is an unmet need for new, effective treatments for OAC. Significant focus has been directed towards targeting the HER2 oncogene in OAC, which is reported to be amplified and overexpressed in approximately 15% of cases [12,15]. However, this approach has largely failed to replicate the success obtained with anti-HER2 therapies in HER2-positive breast cancers, with median overall survival for HER2 positive gastric or gastro-oesophageal junction adenocarcinoma patients receiving trastuzumab showing only modest survival benefit [10]. Furthermore, even in HER2 overexpressing patients treated with trastuzumab, only proportion of this patients respond [14]. It is clear that presence of amplification of HER2 amplicon does not predict the response to trastuzumab. This raises the possibility that targeting other oncogenes than HER2 within 17q12 amplicon might be efficacious in this group of patients.

Molecular dissection of the 17q12 amplicon, wherein the HER2 gene is located, in OAC patient samples has revealed the presence of several additional candidate genes that could also have an oncogenic role, including GRB7 [28]. We report that GRB7 is co-overexpressed, at both the transcript and protein levels, with HER2 across a panel of OAC cell lines. More importantly, we report, for the first time, frequent GRB7 overexpression in an OAC patient cohort based on immunohistochemistry staining. Although a previous study has reported that HER2 and GRB7 co-amplify in OAC samples [25], our data demonstrate that this relationship between HER2 and GRB7 does not translate linearly at the transcript and protein expression levels. Crucially, patients with GRB7 high expressing tumours had significantly shorter overall survival compared to patients with GRB7 low expressing or negative tumours. These data suggest that GRB7 overexpression has a potential oncogenic role in OAC tumourigenesis and is consistent with findings in breast [18] and gastric cancer [29] that support a role for GRB7 in the promotion of cancer growth.

In support of this idea, we show that GRB7 orchestrates OAC tumour cell growth, survival and migration in cell line models. Although, GRB7 has been reported to associate with, and potentially transmit oncogenic signalling through, the HER2 receptor [17], our results indicate that GRB7 plays a role independent of HER2 signalling in OAC. Importantly, aberrantly expressed GRB7 mediates signalling from the numerous receptor tyrosine kinases (RTKs) such as EGFR, HER2, HER3, IR, IGF-R,

PDGFR, FGFR, that are involved in the control of cellular growth and FAK and EphB1 regulated migration processes, to downstream signalling cascades [17]. Importantly, our RPPA results provide a mechanistic basis for the GRB7 orchestrated OAC carcinogenesis. As such, GRB7 likely transmits signalling through PI3K/mTOR, MAPK and receptor tyrosine kinases, but also has a role in apoptosis, enabling cancer cells to proliferate and survive. Taken together, the acquisition of the malignant cancer cell phenotype is enhanced with GRB7 overexpression. Thus, from the functionally important GRB7 interaction partners, it is likely that GRB7 is increasing the oncogenic potential of cancer cells by sustaining cell growth, preventing apoptosis, and either acquiring or potentiating migration capabilities. Hence, overexpression of GRB7 in OAC tumours likely provides oncogenic drive in combination with RTK mutational activation or amplification and overexpression, and may even do so without the need for prominent over-expression of upstream oncogenic RTKs.

Indeed, detailed research into OAC genetics has revealed that individual OAC exhibit oncogenic activation of multiple RTKs, meaning that using multiple drugs would be required in eradicating cancer [30]. Of importance, as demonstrated in this paper, GRB7 functions as a signalling adaptor molecule in multiple oncogenic signalling pathways. Therefore, an alternative may be to use GRB7 as a therapeutic target, as inhibiting GRB7 may weaken cancer cell growth and lead to cell death by blocking multiple oncogenic signalling pathways.

An important finding here is that tumour growth suppression is achieved through depletion of GRB7 in HER2 and GRB7 overexpressed, but trastuzumab insensitive tumour cells. Given that the majority of HER2 overexpressing cancers are intrinsically resistant to HER2 inhibition or acquire resistance following treatment, targeting GRB7 might be a promising therapeutic approach for HER2 resistant cancers. Furthermore, GRB7 has been characterized as a promising therapeutic target in breast cancer treatment, primarily in combination with either doxorubicin or trastuzumab [31]. Interestingly, our results revealed a significant reduction of OAC cell proliferation following GRB7 depletion, but no synergistic effect between GRB7 depletion and trastuzumab treatment. However, using GRB7 depletion in combination with inhibition of other RTKs might be beneficial and further studies are required. Certainly, given the oncogenic functions of GRB7 overexpression in our preclinical *in vitro* and *in vivo*

tumour xenograft models and poor OAC patient survival, we advocate the importance of developing effective and novel inhibitors against GRB7.

Given the high toxicity rates in the patients treated with chemotherapy compared to treatment with molecular targeted therapies [8], it is rational to utilize highly specific GRB7 inhibitors in patient care. As such, recent efforts to target GRB7 have resulted in the development of bicyclic peptide GRB7-SH2 inhibitors that have high specificity as well as high binding affinity [32,33]. In an era of advances in developing molecular targeted therapy against SH2 domains in cancers [34] our preclinical studies endorse the future development of GRB7 inhibitors and their potential clinical use in OAC patient treatment. Altogether, we unveil oncogenic a functional relationship between GRB7 and OAC, which provides a rationale for developing more effective therapies via targeting GRB7 overexpressing cancers.

ACKNOWLEDGEMENTS

We thank the following Peter MacCallum Cancer Centre core facilities: Flow Cytometry, Victorian Centre for Functional Genomics and the ACRF Translational Reverse Phase Protein Array platform.

This research was supported by a National Health and Medical Research Council (NHMRC) of Australia Project Grant (#APP1120293 to WAP and NJC) and the Australian Cancer Research Foundation (for the Peter MacCallum Cancer Centre Flow Cytometry, Victorian Centre for Functional Genomics, and Translational Proteomics RPPA facilities). JRG was supported by a Melbourne International Research Scholarship (University of Melbourne). DSL was supported by Royal Australasian College of Surgeons (RACS) Foundation for Surgery John Loewenthal, Reg Worcester and Eric Bishop Fellowships, Cancer Therapeutics Scholarship (Cancer Therapeutics CRC) and a NHMRC Postgraduate Research Scholarship. NJC is supported by a Fellowship (MCRF16002) from the Department of Health and Human Services acting through the Victorian Cancer Agency, Victoria, Australia.

The Victorian Centre for Functional Genomics (KJS.) is funded by the Australian Cancer Research Foundation (ACRF), the Australian Phenomics Network (APN) through funding from the Australian Government's National Collaborative Research Infrastructure Strategy (NCRIS) program, the Peter MacCallum Cancer Centre Foundation and the University of Melbourne Research Collaborative Infrastructure Program.

MAIN FIGURES:

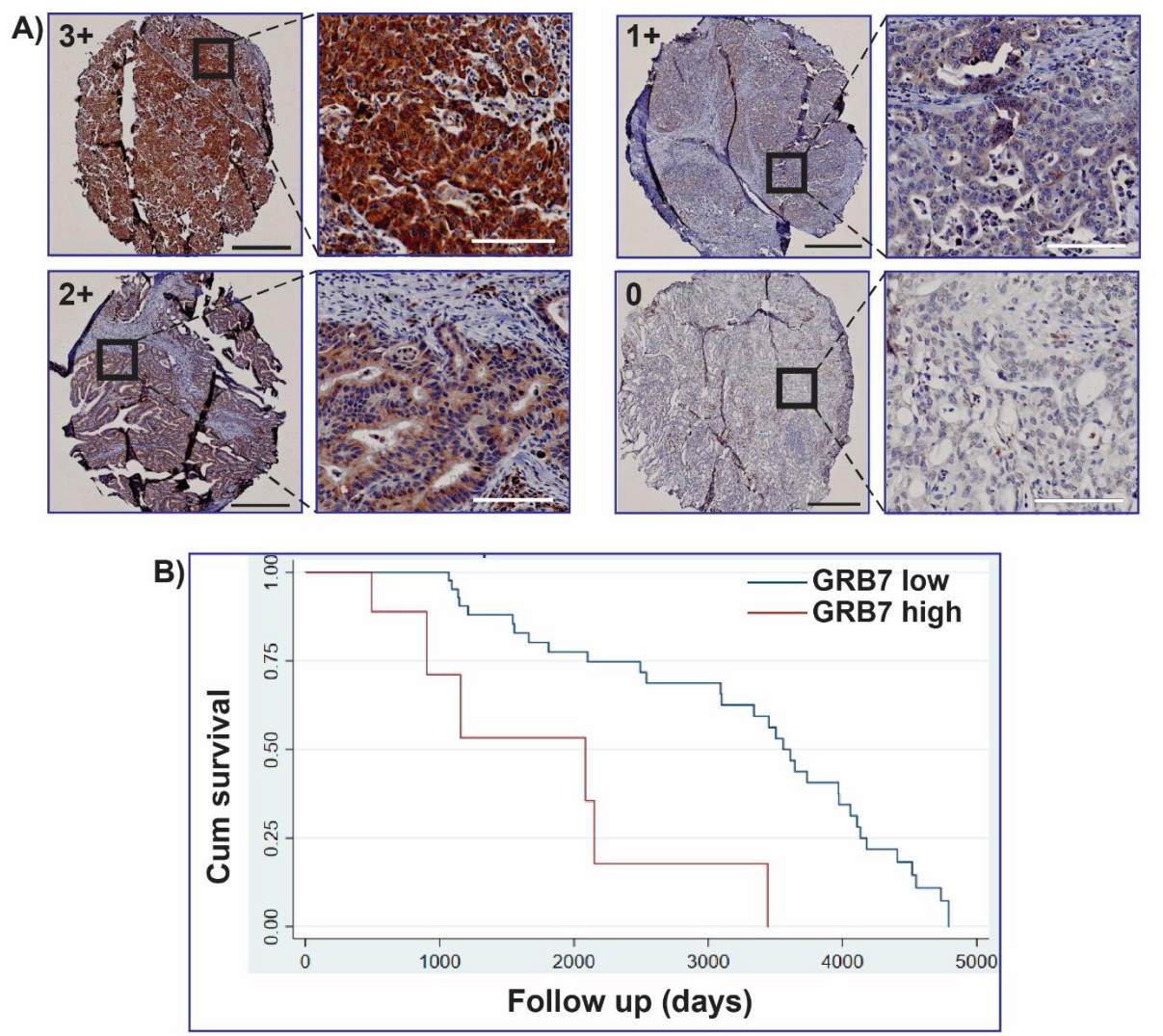

Figure 1. Overexpression of GRB7 correlates with poor OAC patient outcome. (A) Representative images of OAC biopsy cores used as standard for GRB7 IHC scoring system (3+, 2+, 1+ and 0), respectively. Dark colour scale bars represent 500µM, whereas white colour scale bars represent 100µm. (B) Kaplan-Meier curves demonstrating the effect of GRB7 high expression (3+, 2+, red curve) vs. GRB7 low/negative expression (1+, 0, blue curve) on overall survival. Logistic regression analysis was used to compare survival between 32 OAC patients with GRB7 high tumours and 56 patients with GRB7 low/negative tumours.

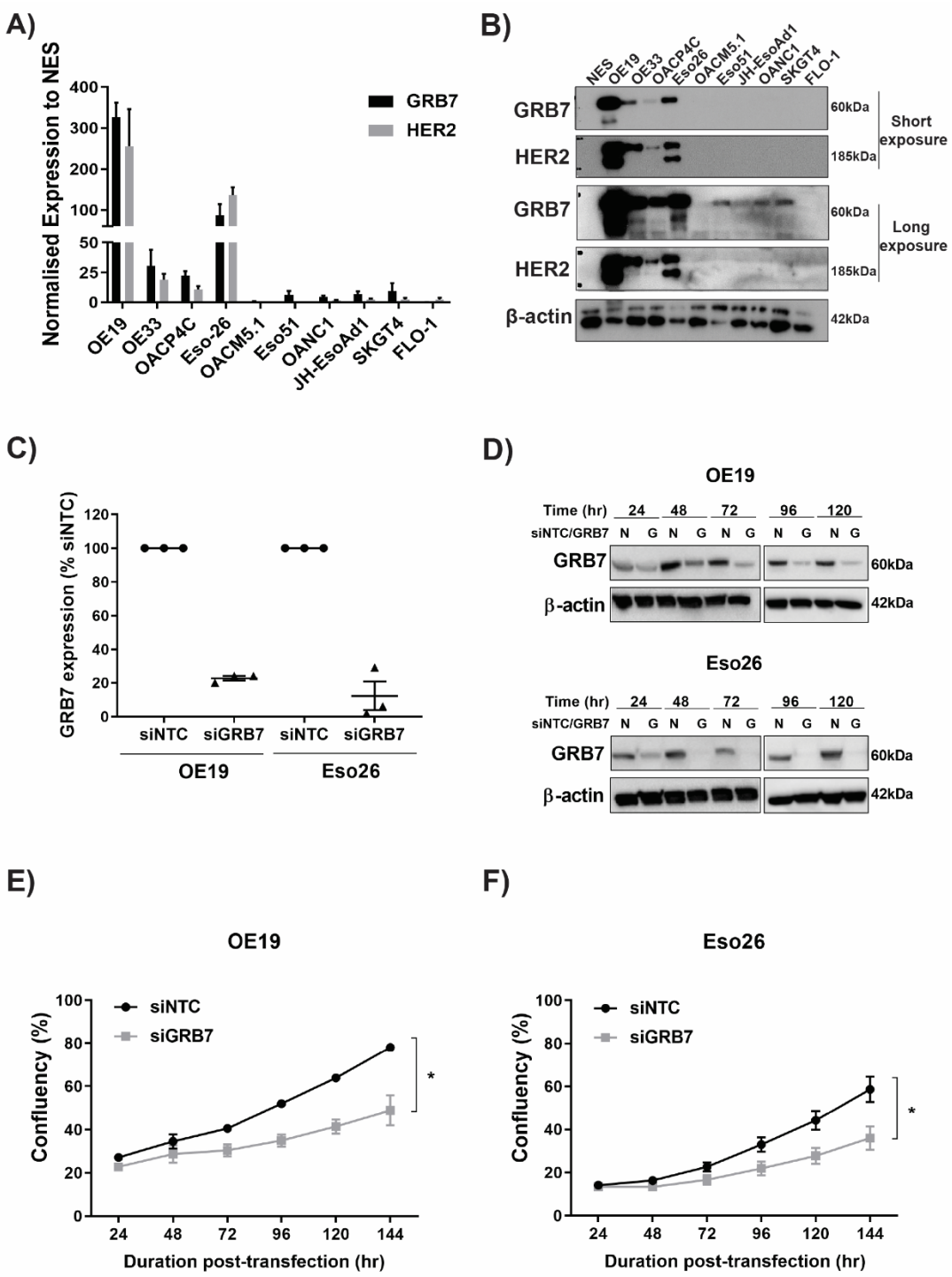

Figure 2. GRB7 knockdown inhibits cell growth in GRB7 overexpressing oesophageal adenocarcinoma cell lines. Basal expression of GRB7 and HER2 in a panel of ten human OAC cell lines and a normal oesophageal squamous cell line (NES) determined by RTqPCR (A) and western blotting (B). Representative western blots imaged at two different exposure times are shown. GRB7 mRNA (C) and protein levels (D) in OE19 and Eso26 cells following knockdown with GRB7 siRNAs (siGRB7 or G) compared with non-targeting control siRNA (siNTC or N). Expression of mRNA was determined by RTqPCR 24 hr after transfection with siRNA. Western blots were performed 24-120 hr after transfection. (E, F) Cell confluency measured with an Incucyte optical scanner from 24-144 hr after transfection with GRB7 siRNA or siNTC in OE19 (E) and Eso26 (F) cells. Data represent mean±SEM from 3 independent experiments (no error bars indicate SEM less than size of symbol), Two tailed Student's *t*-test, *p<0.05 for the last time point.

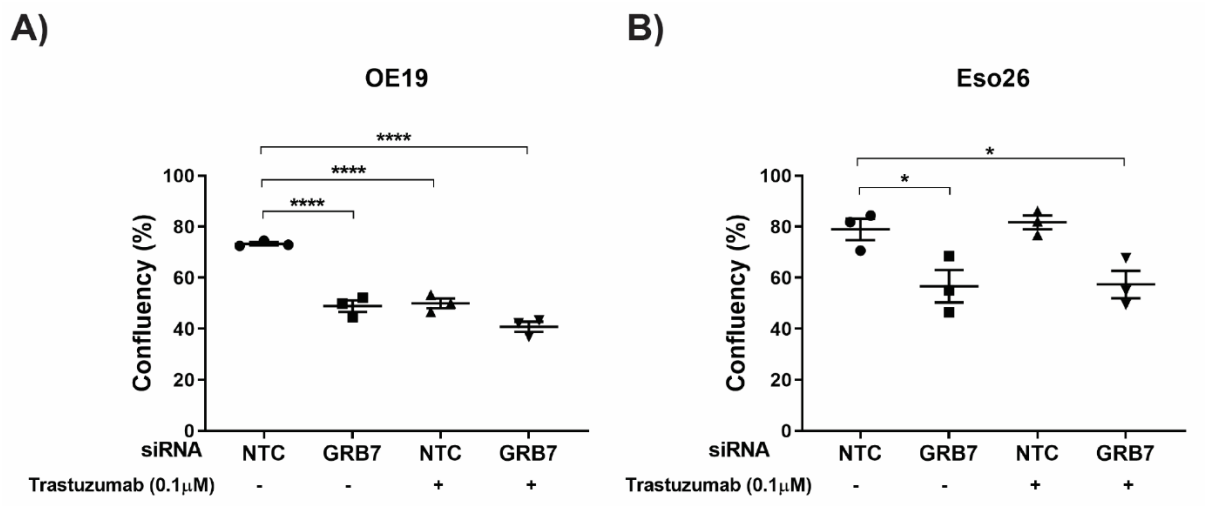

Figure 3. Trastuzumab resistant Eso26 cells respond to the depletion of GRB7 by suppression of cell proliferation. Cell confluency of OE19 (A) and Eso26 (B) cells 144 hr after transfection with siNTC or siGRB7, alone or in combination with trastuzumab (0.1μM). Bars represent overall mean±SEM for 3 independent experiments. Individual data points represent mean for each experiment. One way Ordinary ANOVA with Dunnett's multiple comparisons post-test, *p<0.05, ****p<0.0001.

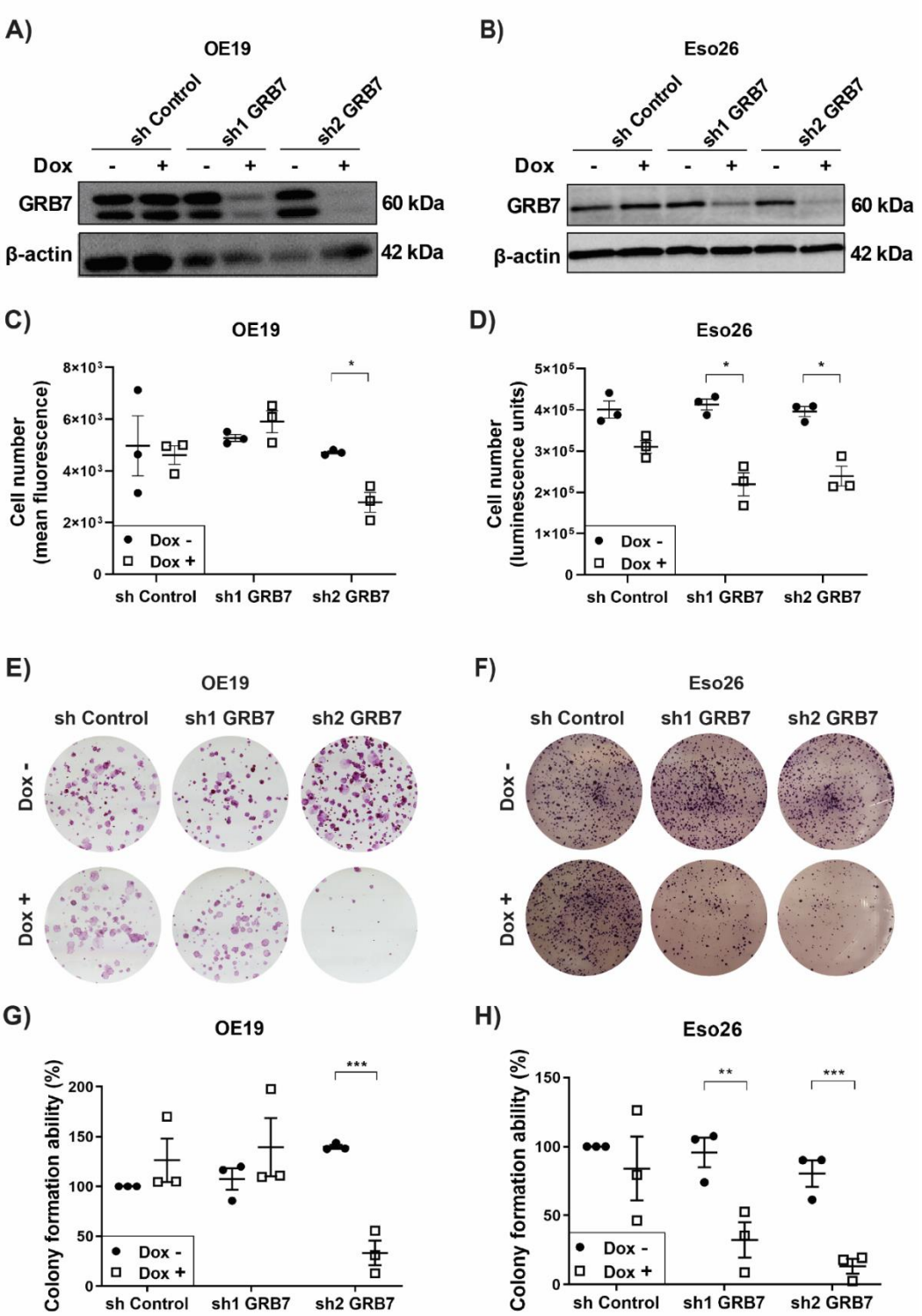

Figure 4. Functional validation of specifically designed shRNAs to target GRB7. The effect of inducible GRB7 shRNA expression for 72 hr (2µg/ml doxycycline (Dox)) on GRB7 protein levels was assessed by western blotting in (A) OE19 and (B) Eso26 cells. Following initial shRNA induction (72 hr 2µg/ml Dox), cells were replated and viability of (C) OE19 and (D) Eso26 cells was assessed at 120 hr. Representative images and quantification of colony formation assays in OE19 (E, G) and Eso26 (F, H) cells following induction of sh Control or sh GRB7. Individual data points represent mean (C, D) or count (G. H) for each experiment. Bars represent overall mean±SEM for all 3 experiments. Statistics: (C, D), Paired *t*-test (two-tailed), *p<0.05 and (E, F) two tailed Student's *t*-test, *p<0.05, **p<0.01, ***p<0.001 compared to no dox treatment.

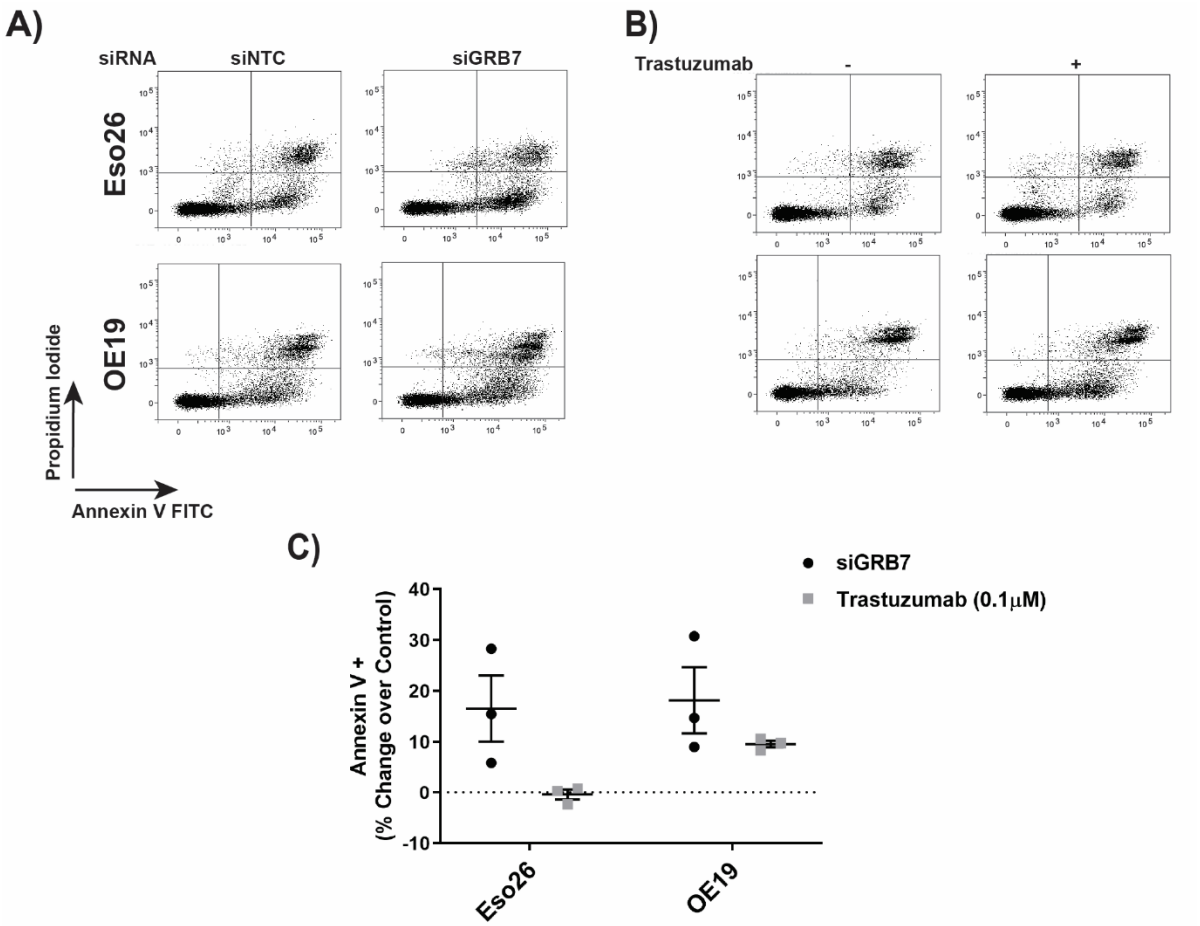

Figure 5. GRB7 knockdown induces apoptosis in high HER2 expressing but trastuzumab resistant Eso26 cells. Representative AnnexinV-FITC/Propidium Iodide (PI) FACS plots of Eso26 and OE19 cells transfected with siNTC or siGRB7 for 144 hr (A) or treated with vehicle or trastuzumab (0.1μM) for 120 hr (B). (C) Quantification of AnnexinV positive cells in Eso26 and OE19 cells treated with siGRB7 and trastuzumab (0.1μM) compared to siNTC and vehicle, respectively. Bars represent mean±SEM for 3 independent experiments.

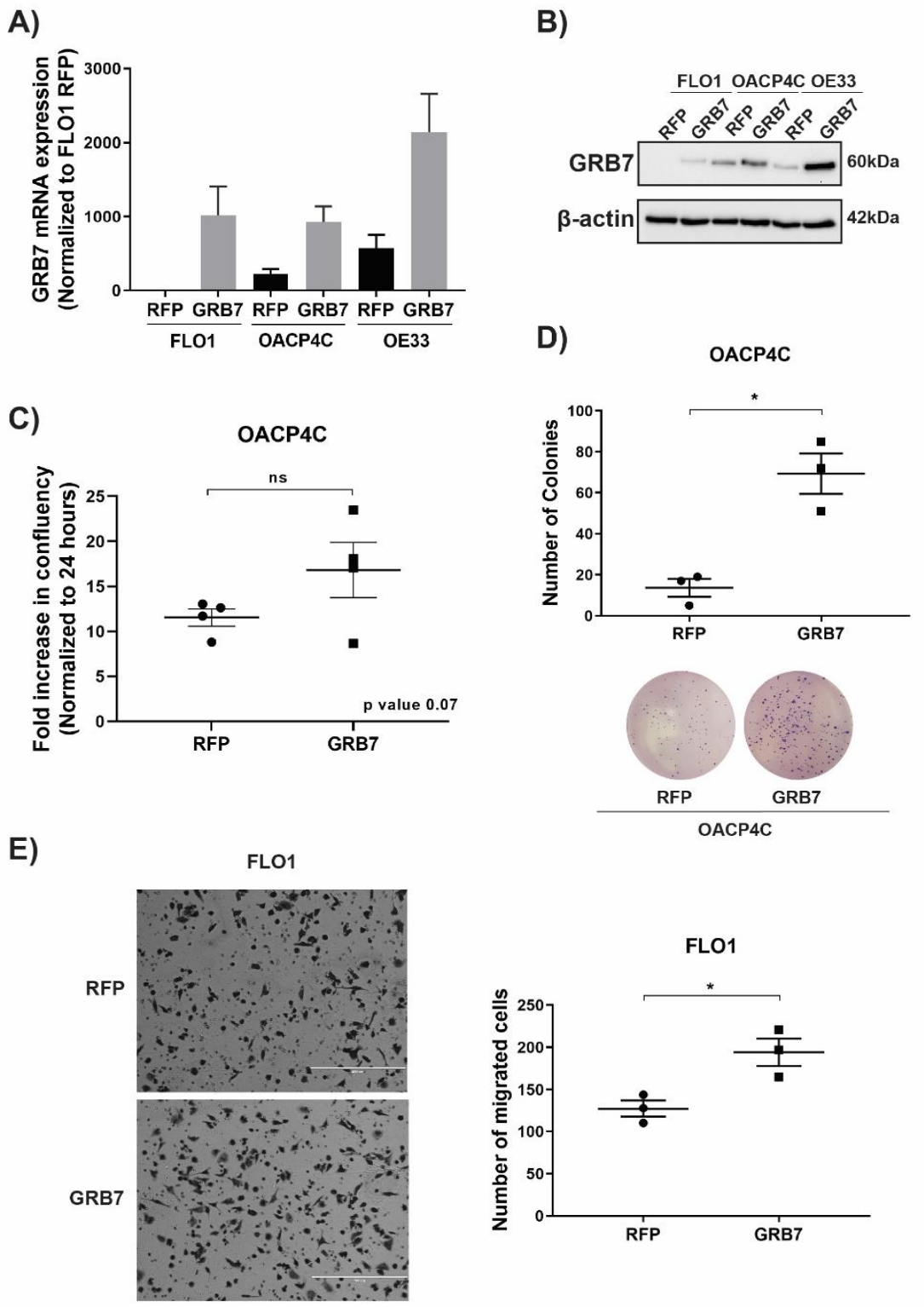

Figure 6. Increased oncogenic potential upon GRB7 overexpression in OAC cell lines. GRB7 mRNA (A) and protein (B) expression levels following overexpression of GRB7 or red fluorescence protein (RFP) control cDNA in FLO1, OACP4C and OE33 cells. (C) Cell confluency measured at 196 hr in OACP4C cells containing GRB7 vs. RFP expression vector and Ratio paired *t*-test was used to test statistical significance, ns=not significant. (D) Clonogenic assay of OACP4C cells following GRB7 overexpression vs. RFP control. (E) Representative image (Left) and cell count (Right) of Boyden Chamber Migration Assay of FLO1 GRB7 overexpressing cells vs. RFP control. Scale bars represent 400μm. Two tailed Student's *t*-test, *p<0.05, bars represent overall mean±SEM for 3 independent experiments.

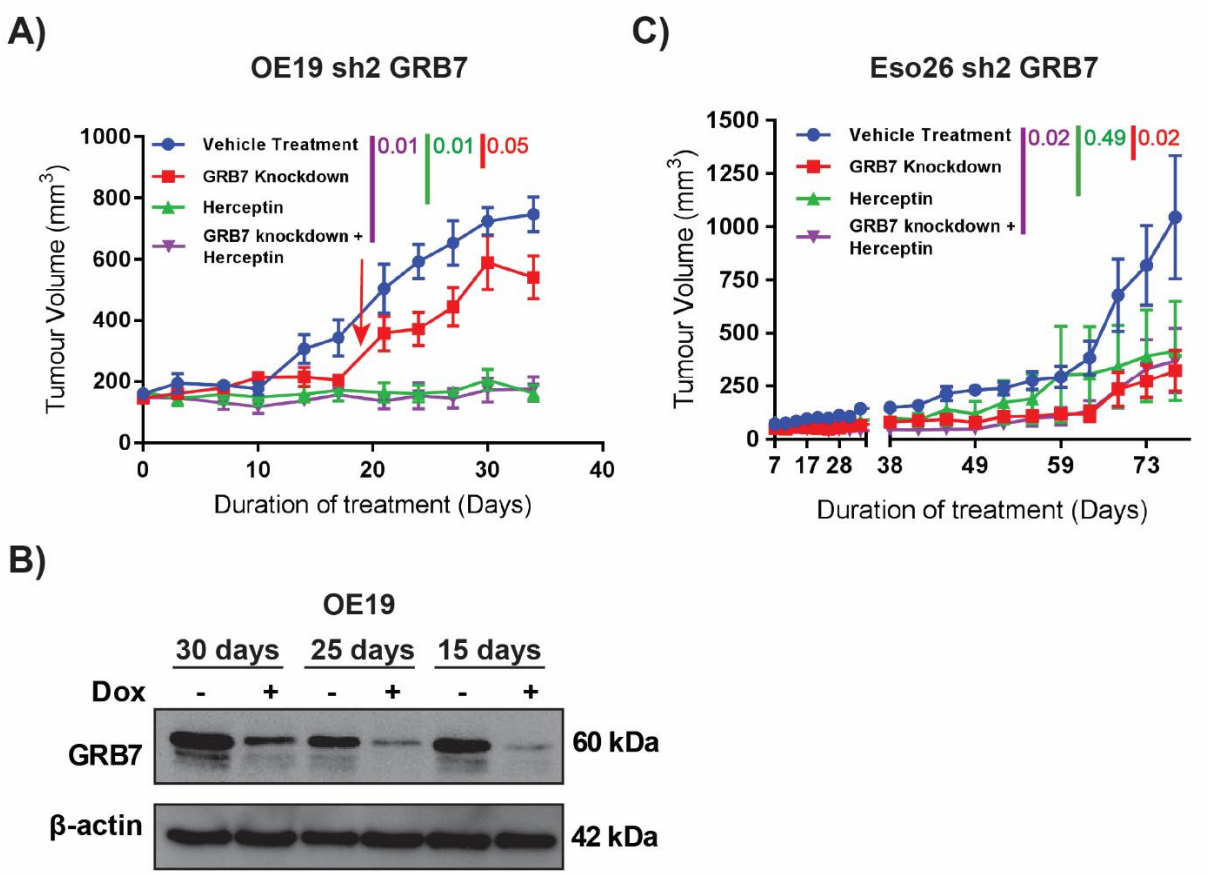

Figure 7. GRB7 knockdown in OAC cell line xenografts attenuates tumour growth. Growth of (A) OE19 and (C) Eso26 cell line xenografts containing GRB7 sh2 construct in NSG mice treated with vehicle (sterile water), doxycycline (GRB7 knockdown), Herceptin (10mg/kg, twice per week) or doxycycline/Herceptin combination (n=5-6 mice per group, data represent mean±SEM). Red arrow in (A) indicates the time point when doxycycline only treated xenograft tumours started to grow. Red, green and purple colour coded numbers represent p-values (CGGC permutation test) of comparison between vehicle treatment vs. GRB7 knockdown, Herceptin and combination of GRB7 knockdown + Herceptin, respectively. The test is available online at http://bioinf.wehi.edu.au/software/compareCurves/. (B) Western blot of OE19 sh504 GRB7 xenografts to determine effectiveness of GRB7 knockdown during the course of *in vivo* shRNA doxycycline (Dox) induction at 15, 25 and 30 days.

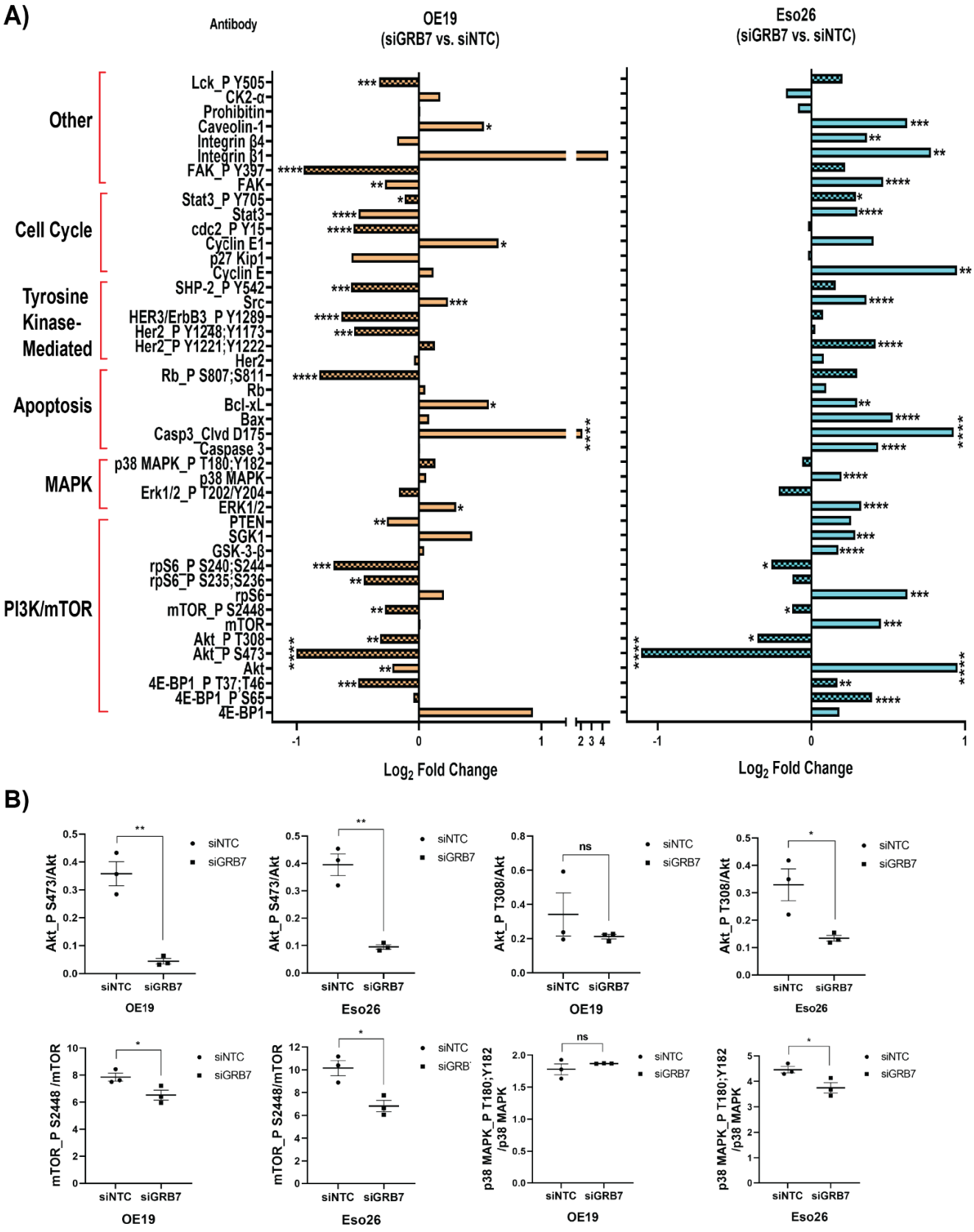

Figure 8. Knockdown of GRB7 leads to decreased activation of pro-growth and survival signalling pathways and upregulation of apoptotic mediators. RPPA analysis was performed on lysates from Eso26 and OE19 OAC cells treated with siGRB7 for 96 hr and compared to siRNA control treated cells. (A) Results are presented as $\log_2$ fold change of mean relative fluorescence intensity (RFI)

for GRB7 knockdown (siGRB7) compared to control (siNTC) calculated from 3 biological replicates, each with 3-4 technical replicates. Positive values represent up-regulation and negative values represent down-regulation. Patterned and solid bars represent phosphorylated and total proteins, respectively. (B) Representative graphs of ratio phospho/total protein for OE19 and Eso26 cells transfected with siNTC Control or siGRB7. Welch's *t*-test: ns-not significant, *p<0.05, **p<0.01, ***p<0.001, ****p<0.0001.

SUPPLEMENTARY FIGURES:

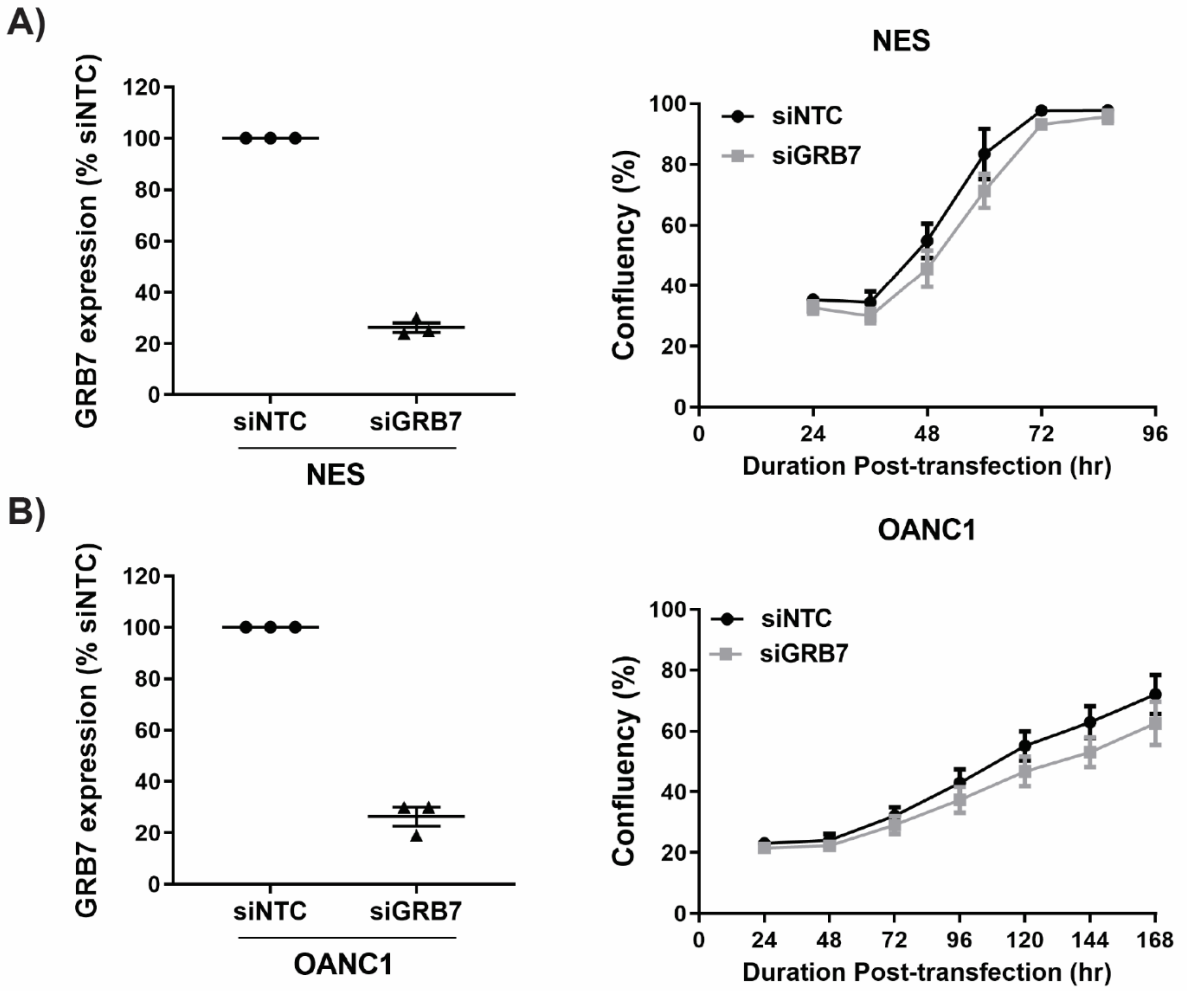

Supplementary Figure 1. Functional characterisation of GRB7 knockdown in low GRB7 expressing OAC cell lines. (A, B) GRB7 transcript expression levels following siRNA knockdown (RTqPCR) and subsequent time course proliferation assay (Incucyte) in NES and OANC1, respectively. For all experiments n=3 independent biological replicates, data represent mean±SEM.

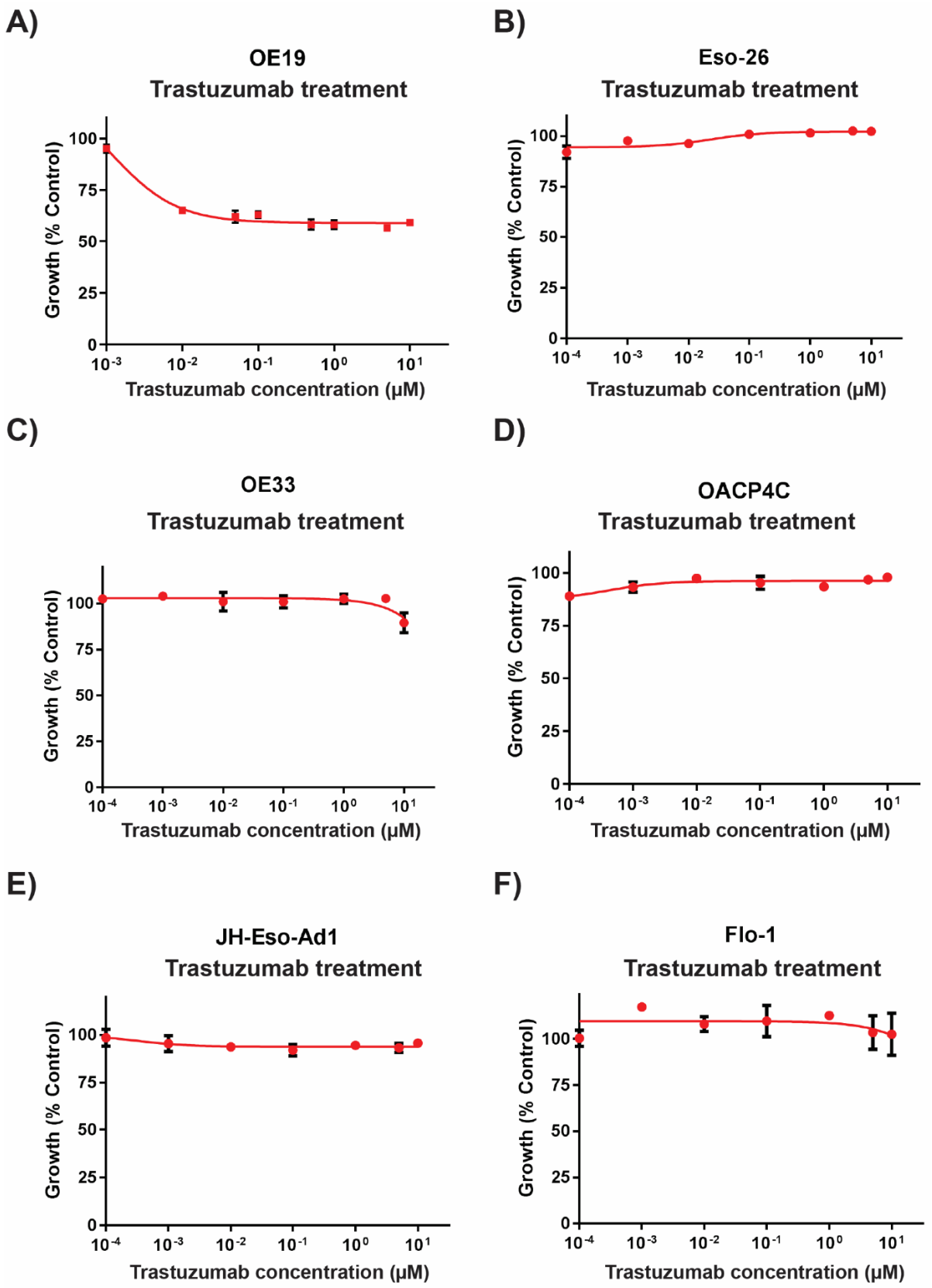

Supplementary Figure 2. The sensitivity to trastuzumab across OAC cell lines. The effect of trastuzumab on cell growth was examined (Incucyte) in six human OAC cell lines. The results represent percentage of the cell growth when treated with trastuzumab compared to control at 120 hr. Bars represent overall mean±SEM for 3 independent experiments.

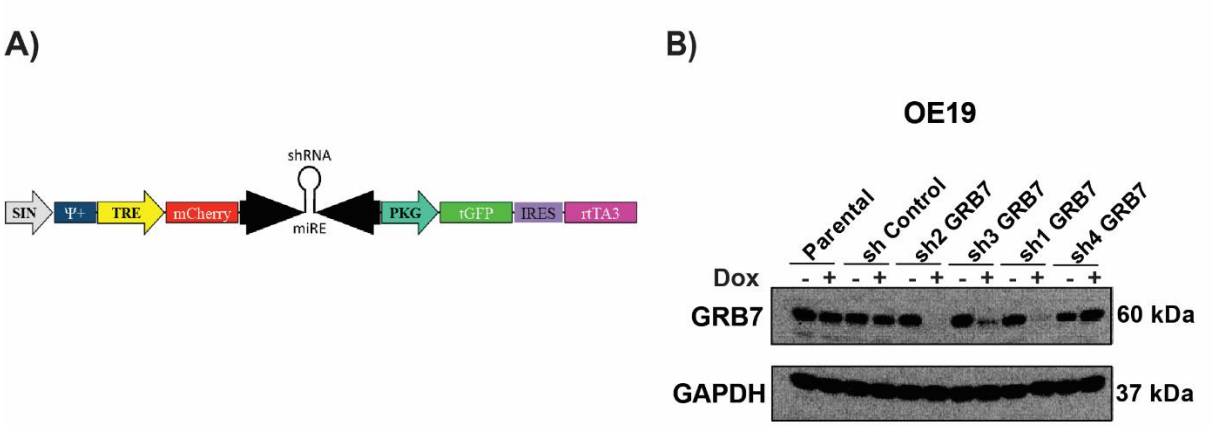

Supplementary Figure 3. Functional validation of shGRB7 in OAC cell lines. (A) Diagram of the LT3GECIR lentiviral doxycycline (Dox)-inducible expression vector with possibility to clone either sh-gene specific RNA or sh Control shRNA. (B) GRB7 western blots after induction of 4 GRB7 specific shRNA constructs with Dox (2µg/ml) for 24 hr in OE19 cells.

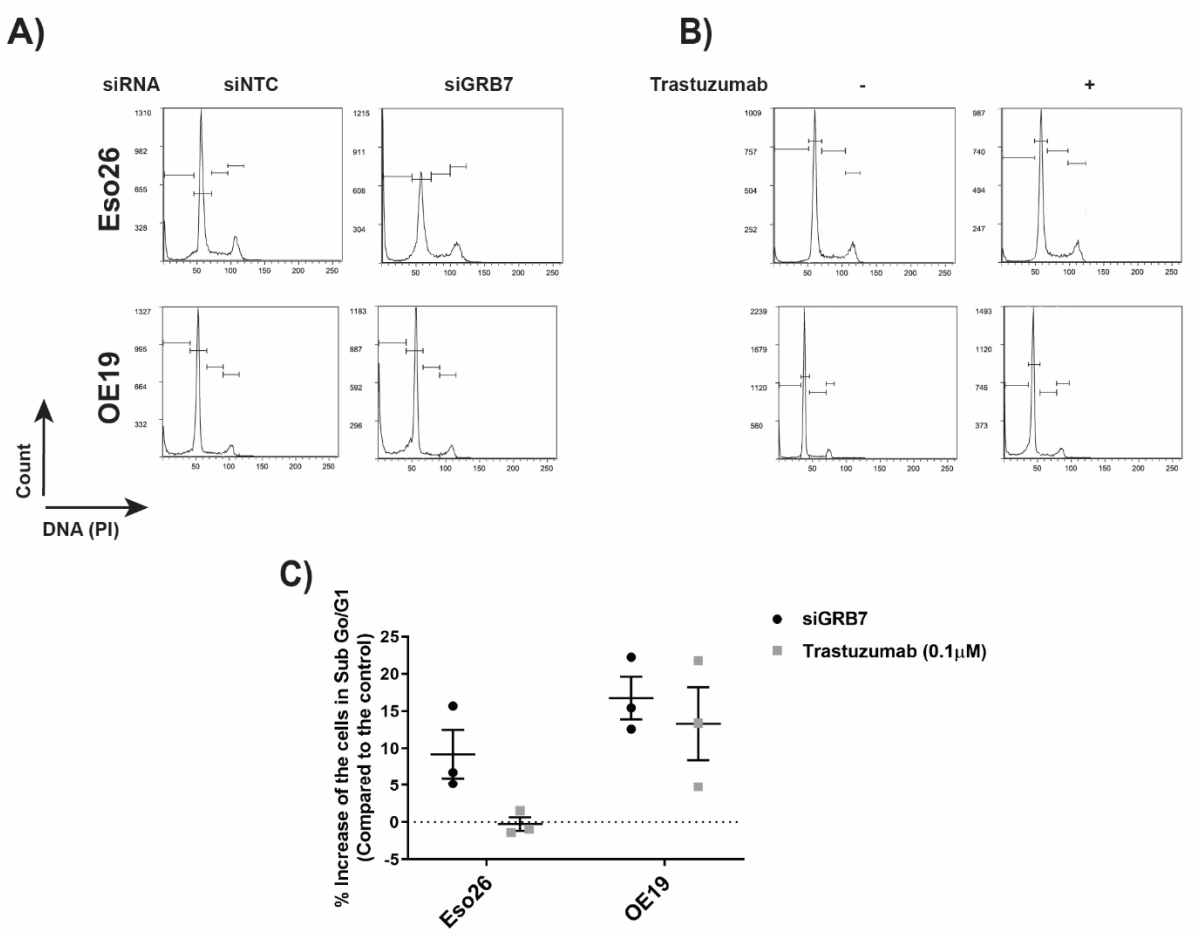

Supplementary Figure 4. GRB7 knockdown induces an increase in SubGo/G1 subpopulation of cell cycle in GRB7 high expression OAC cell lines. Representative DNA (propidium iodide, PI) histograms of cell cycle analyses in Eso26 and OE19 cell lines treated with siGRB7 for 144h (A) or 0.1μM Trastuzumab for 120h (B) compared to siNTC or vehicle, respectively. (C) Percentage increase of SubGo/G1 phase of the cell cycle. Bars represent mean±SEM from 3 independent experiments.

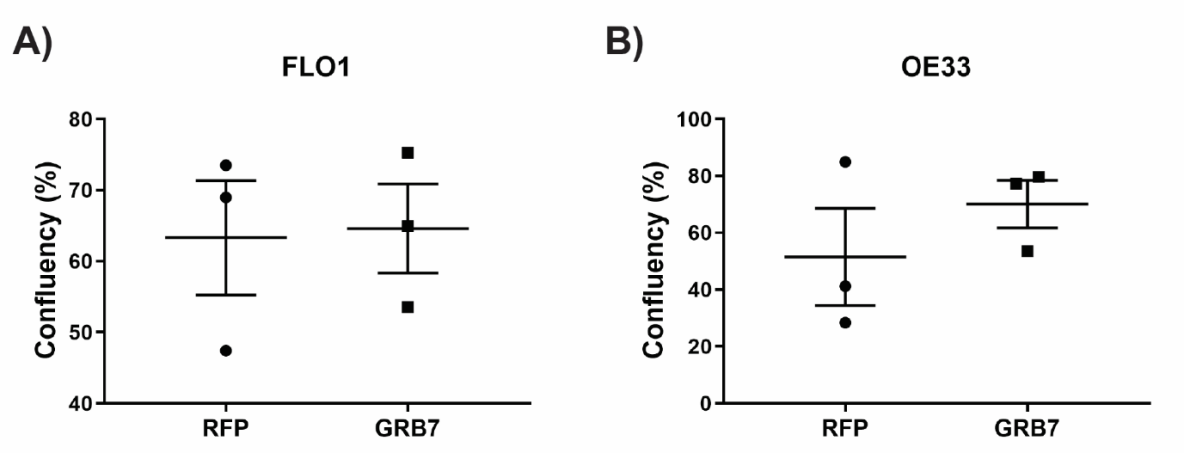

Supplementary Figure 5. Proliferation assay following GRB7 overexpression in OAC cell lines. (A) Confluency (Incucyte) was measured at 144 hr following plating of FLO1 cells and (B) at 96 hr following plating of OE33 cells. Bars represent mean±SEM from 3 independent experiments. Individual data points represent mean for each experiment.

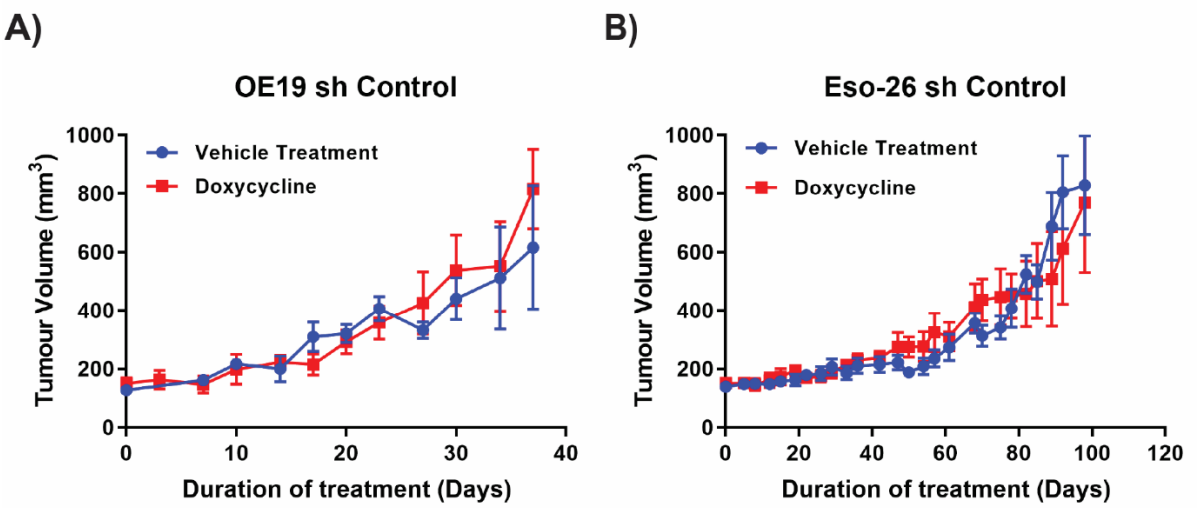

Supplementary Figure 6. The effect of doxycycline on the growth of OE19 and Eso26 sh Control cell line xenograft. (A, B) The effect of doxycycline in chow (600mg/kg) and water (2mg/ml) on growth of OE19 (B) and Eso26 (C) sh Control cell line xenografts. Growth curves represent the average tumour volume for 3 and 6 mice used per group in OE19 and Eso26 xenografts, respectively.

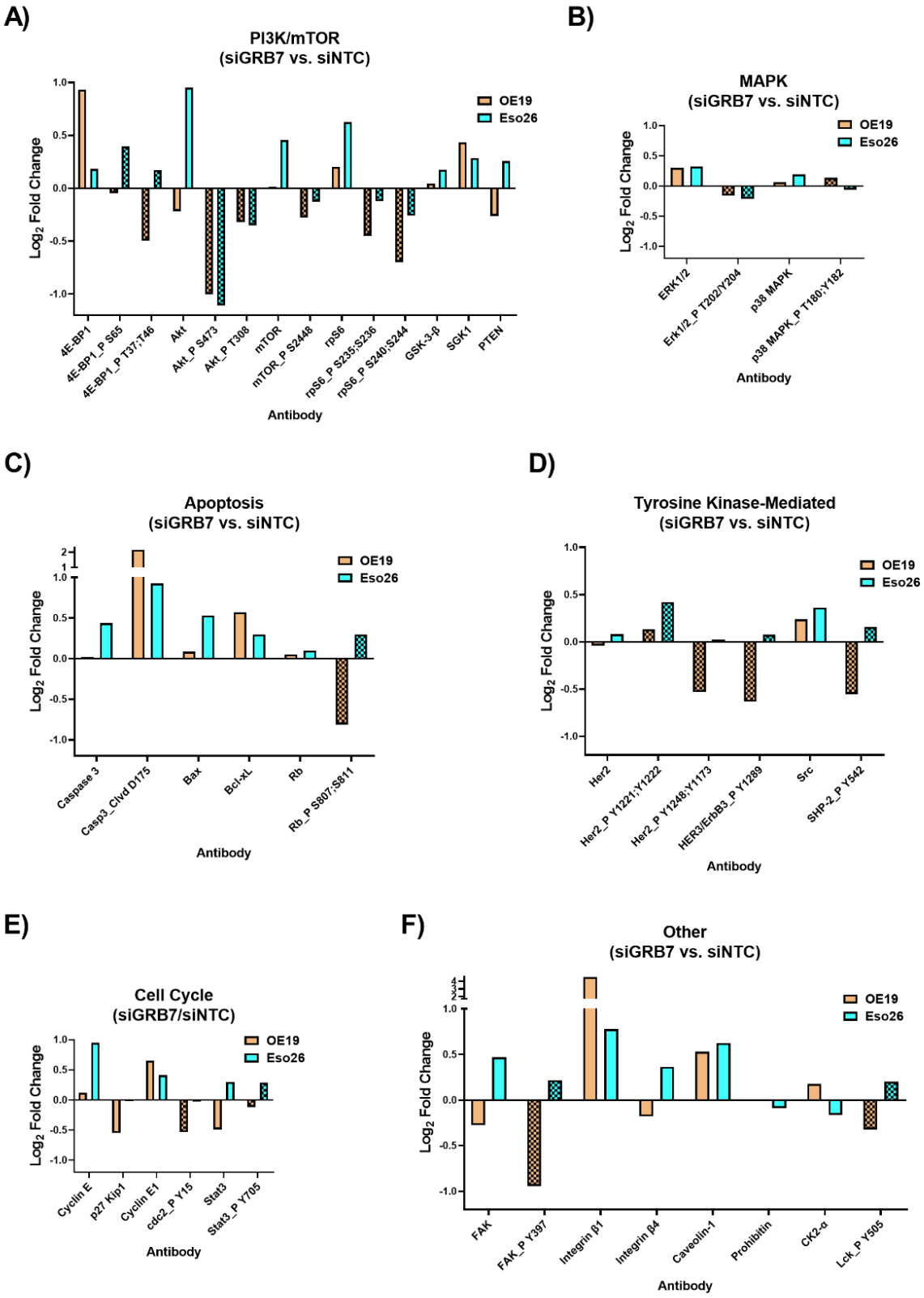

Supplementary Figure 7. GRB7 mechanism of action through signalling pathways in OAC. RPPA analyses of signalling mediators involved in (A) PI3K/mTOR; (B) MAPK; (C) apoptosis; (D) Tyrosine kinase signalling; (E) Cell Cycle and (F) Other signalling pathways in OE19 and Eso26 OAC cells upon GRB7 knockdown. Data represent Log_2 Fold Change of RFI values. Patterned and solid bars represent phosphorylated and total proteins, respectively.

MAIN TABLES:

Table 1. IHC scoring for GBR7 and HER2.

GRB7 intensity score	OAC tumours n (%)	HER2 +	HER2 –
IHC 0	28 (31.8)	2	26
IHC 1+	28 (31.8)	1	27
IHC 2+	19 (21.6)	1	18
IHC 3+	13 (14.8)	4	9
Overall	88 (100)	8	80

HER2+: either 3+ IHC staining or 2+ IHC staining and SISH positivity (6 or more HER2 gene copies and/or a HER2/chr17 ratio of >2).

Table 2. ERBB2 and GRB7 gene copy number (CN) in OAC cell lines.

Cell Line	CN ERBB2	Signal	CN GRB7	Signal
OE19	14	Gain	14	Gain
OE33	14	Gain	14	Gain
OACP4C	9	Gain	9	Gain
Eso26	8	Gain	8	Gain
OACM5.1	2	No	2	No
Eso51	2	No	2	No
SKGT4	2	No	2	No
FLO1	2	No	2	No

CN = gene copy number. Data obtained from canSAR database (cansarblack.icr.ac.uk).

SUPPLEMENTARY TABLES:

Supplementary table 1. mRNA target site for shGRB7

Name	Sequence
hGrb7.211 (sh1)	GGATCTGTCTCCACCTCATCT
hGrb7.504 (sh2)	CCCATGTAGTAAAGGTGTACA
hGrb7.1407 (sh3)	GGAGGAAGAAGACAAACCACC
hGrb7.1101 (sh4)	GTTTCTGTGTCAAGCCCAACA

Supplementary table 2. RTqPCR primer sequences

Gene	Forward (5'- 3')	Reverse (5'- 3')
GRB7	GCCTTCCGCCTCTTCAAGTA	CACTTCTCAAGGGTGGGGAG
HER2	TTGAGTCCATGCCCAATCC	GCTGTGTTCCATCCTCTGCT

Supplementary table 3. Antibodies for western blotting and immunohistochemistry

Antibody	Origin	Clone	Source	Use
Anti-GRB7	Rabbit	EPR4378	LSbio	WB and IHC
Anti-HER2	Mouse	3B5	Calbiochem	WB
Anti-β-actin	Mouse	C4	MP-Biomedical	WB
Anti- GAPDH	Mouse	6C5	Abcam	WB

WB=Western Blotting; IHC=Immunohistochemistry.

Supplementary table 4. Clinico-pathological characteristics by GRB7 status in 88 oesophageal adenocarcinomas.

		Total n=88	GRB7 +ve n=32	GRB7 –ve n=56	Odds Ratio	95% CI	p-value
Median age (range)		67 (47-95)	66 (47-94)	68 (48-95)			
Gender	Male	78	29	49	1.38	0.33-5.76	0.658
	Female	10	3	7			
HER2 Status	Positive	8	5	3	3.27	0.73-14.72	0.123
	Negative	80	27	53			
Barrett's oesophagus	Yes	44	4	4	0.467	0.10-2.14	0.327
	No	8	14	30			
	Unreported	36	14	22			
Grade differentiation	Well	3	2	1	2.31	1.03-5.16	0.041*
	Moderate	34	16	18			
	Poor	47	13	34			
	Unreported	4	1	3			

*statistically significant result

BIBLIOGRAPHY

1. Bray F, et al. Global cancer statistics 2018: GLOBOCAN estimates of incidence and mortality worldwide for 36 cancers in 185 countries. *CA Cancer J Clin.* 2018;68(6):394-424.
2. Thrift AP. The epidemic of oesophageal carcinoma: where are we now? *Cancer Epidemiol.* 2016;41:88-95.
3. Coleman HG, et al. The epidemiology of esophageal adenocarcinoma. *Gastroenterology.* 2018;154(2):390-405.
4. Pohl H, et al. Esophageal adenocarcinoma incidence: are we reaching the peak? *Cancer Epidemiol Biomarkers Prev.* 2010;19(6):1468-1470.
5. van Hagen P, et al. Recurrence pattern in patients with a pathologically complete response after neoadjuvant chemoradiotherapy and surgery for oesophageal cancer. *Br J Sur.* 2013;100(2):267-273.
6. Slamon DJ, et al. Use of chemotherapy plus a monoclonal antibody against HER2 for metastatic breast cancer that overexpresses HER2. *N Engl J Med.* 2001;344(11):783-792.
7. Piccart-Gebhart MJ, et al. Trastuzumab after adjuvant chemotherapy in HER2-positive breast cancer. *N Engl J Med.* 2005;353(16):1659-1672.
8. Blumenthal GM, et al. Current status and future perspectives on neoadjuvant therapy in lung cancer. *J Thor Onc.* 2018;13(12):1818-1831.
9. Wald O, et al. Future directions in esophageal cancer therapy. *Ann Cardiothorac Surg.* 2017;6(2):159-166.
10. Bang Y-J, et al. Trastuzumab in combination with chemotherapy versus chemotherapy alone for treatment of HER2-positive advanced gastric or gastro-oesophageal junction cancer (ToGA): a phase 3, open-label, randomised controlled trial. *The Lancet.* 2010;376(9742):687-697.
11. Paterson AL, et al. A systematic approach to therapeutic target selection in oesophago-gastric cancer. *Gut.* 2013;62(10):1415-1424.
12. Reichelt U, et al. Frequent homogeneous HER-2 amplification in primary and metastatic adenocarcinoma of the esophagus. *Mod Pathol.* 2007;20(1):120-129.
13. Ross JS, McKenna BJ. The HER-2/neu oncogene in tumors of the gastrointestinal tract. *Cancer Invest.* 2001;19(5):554-568.
14. Lote H, et al. HER2 inhibition in gastro-oesophageal cancer: A review drawing on lessons learned from breast cancer. *World J Gastrointest Oncol.* 2018;10(7):159-171.
15. Hu Y, et al. HER2 amplification, overexpression and score criteria in esophageal adenocarcinoma. *Mod Pathol.* 2011;24(7):899-907.
16. Hong J, et al. Regulation of ERBB2 receptor by t-DARPP mediates trastuzumab resistance in human esophageal adenocarcinoma. *Cancer Res.* 2012;71(14):4504-4514.
17. Han DC, et al. The Grb7 family proteins: structure, interactions with other signaling molecules and potential cellular functions. *Oncogene.* 2001;20(44):6315-6321.
18. Nadler Y, et al. Growth factor receptor-bound protein-7 (Grb7) as a prognostic marker and therapeutic target in breast cancer. *Ann Oncol.* 2009;21(3):466-473.
19. Wang Y, et al. Differential functions of growth factor receptor–bound protein 7 (GRB7) and its variant GRB7v in ovarian carcinogenesis. *Clin Cancer Res.* 2010;16(9):2529-2539.
20. Nagaraja V, et al. HER2 expression in oesophageal carcinoma and Barrett's oesophagus associated adenocarcinoma: An Australian study. *Eur J Surg Oncol.* 2016;42(1):140-148.
21. Clemons NJ, et al. Characterization of a novel tumorigenic esophageal adenocarcinoma cell line: OANC1. *Dig Dis Sci.* 2014;59(1):78-88.
22. Fellmann C, et al. An optimized microRNA backbone for effective single-copy RNAi. *Cell Rep.* 2013;5(6):1704-1713.

23. Elso C, et al. Leishmaniasis host response loci (lmr1–3) modify disease severity through a Th1/Th2-independent pathway. *Genes Immun.* 2004;5(2):93-100.
24. Baldwin T, et al. Wound healing response is a major contributor to the severity of cutaneous leishmaniasis in the ear model of infection. *Parasite Immunol.* 2007;29(10):501-513.
25. Walch A, et al. Coamplification and coexpression of GRB7 and ERBB2 is found in high grade intraepithelial neoplasia and in invasive Barrett's carcinoma. *Int J Cancer.* 2004;112(5):747-753.
26. Tanaka S, et al. A novel variant of human Grb7 is associated with invasive esophageal carcinoma. *J Clin Invest.* 1998;102(4):821-827.
27. Ma XM, Blenis J. Molecular mechanisms of mTOR-mediated translational cont*rol. Nat Rev Mol Cell Biol.* 2009;10(5):307-318.
28. Maqani N, et al. Molecular dissection of 17q12 amplicon in upper gastrointestinal adenocarcinomas. *Mol Cancer Res.* 2006;4(7):449-455.
29. Kwon MJ, et al. Genes co-amplified with ERBB2 or MET as novel potential cancer-promoting genes in gastric cancer. *Oncotarget.* 2017;8(54):92209-92226.
30. Frankell AM, et al. The landscape of selection in 551 esophageal adenocarcinomas defines genomic biomarkers for the clinic. *Nat Genet.* 2019;51(3):506-516.
31. Pero S, et al. Combination treatment with Grb7 peptide and Doxorubicin or Trastuzumab (Herceptin) results in cooperative cell growth inhibition in breast cancer cells. *Br J Cancer.* 2007;96(10):1520-1525.
32. Gunzburg MJ, et al. Unexpected involvement of staple leads to redesign of selective bicyclic peptide inhibitor of Grb7. *Sci Rep.* 2016;6:27060.
33. Watson GM, et al. Discovery, Development, and Cellular Delivery of Potent and Selective Bicyclic Peptide Inhibitors of Grb7 Cancer Target. *J Med Chem.* 2017;60(22):9349-9359.
34. Morlacchi P, et al. Targeting SH2 domains in breast cancer. *Future Med Chem.* 2014;6(17):1909-1926.

CHAPTER 6.

GENERAL DISCUSSION

6.1. Discussion

The incidence of OAC has increased drastically (600%) over the last four decades [284, 285], particularly in the regions of North America, Western Europe and Australia [10, 14]. The overall prognosis for OAC is very poor with 5 year survival rate remaining less than 20% [10, 214]. The poor prognosis is mainly due to the late presentation with over 60% of the patients have advanced metastatic disease at the time of diagnosis and deemed incurable. For patients with locally advanced disease being treated with multimodality therapy consisting of chemo- or chemoradio-therapy in combination with surgery, their 5-year survival rates remained less than 50%. Thus, we need to develop more effective therapies for these patients.

Tumour stage is the most prognostic factor, suggesting the critical importance of early detection of OAC [14]. Improvements in survival have been reported in patients on surveillance programs with detection of the disease at an early tumour stage [286]. This leads us to the conclusion that there is an essential need to understand how OAC develops in order to identify prominent molecular biomarkers of disease progression and targets for novel therapies.

It is considered that OAC develops from a condition known as Barrett's oesophagus, through intermediate stages of LGD and HGD. The annual risk of progression from Barrett's oesophagus to OAC is relatively low, ranging from 0.12 to 0.65% [39, 40]. However, this risk increases with diagnosis of patients with LGD (3.47-4.8%/year) [39, 84], and furthermore with HGD (16-25%/year) [85, 86]. Crucially, this thesis focused on understanding this essential transition from HGD towards OAC and characterization of its molecular drivers.

Regarding the genetic landscape of OAC, there are several proposed theories of Barrett's oesophagus progression towards OAC [91]. Overall, literature evidence supports a traditional pathway of Barrett's oesophagus progression towards OAC. This pathway includes gradual accumulation of losses of tumour suppressor genes during early stages of the disease, leading to instability of the genome, that is followed by genome doublings and oncogenic amplifications at the later stages, resulting in development of invasive and metastatic disease [91, 96, 119]. Therefore, it is of great

interest for current research to functionally characterise molecular drivers of this disease, in order to aid early diagnosis and develop effective therapies.

6.1.1. Summary of the biology of the SMAD4 loss in HGD and OAC

Intriguingly, it has been challenging to define molecular drivers of OAC so far. Genomic studies have reported that the majority of recurrent mutations in OAC are also present in premalignant stages of the disease development, including non-dysplastic Barrett's [206, 226]. In addition, the majority of the mutations are present at a low frequency [137], making it hard to define clear biomarkers of progression towards OAC. Importantly, mutations of *TP53* and *SMAD4* are the only reported stage specific mutations, characteristic of HGD and cancer, respectively. As such, these mutations have potential to be informative and useful as biomarkers of disease progression and targeted therapy. Considering that *SMAD4* mutations specifically happen in cancer and not at precancerous stages, the first aim of this thesis was to evaluate the effect of *SMAD4* mutation on OAC development and progression.

So far, there are no defined molecular drivers of high grade dysplastic Barrett's oesophagus progression towards OAC evident in the literature. Herein, increased tumorigenic potential of Barrett's oesophagus cells upon SMAD4 inactivation was reported. In addition, distinctive CNAs were observed among tumour cells upon SMAD4 loss, which were consistent with CNAs across OAC patients [96]. Moreover, the fraction of the genome with CNAs was significantly higher across tumour cells derived from SMAD4 knockdown and knockout tumours compared to SMAD4 wild-type cells. Based on these results from Chapter 3, SMAD4 inactivation might represent a valid predictor of Barrett's oesophagus progression towards cancer.

Given that mechanisms leading to oncogenesis following SMAD4 loss are largely unknown, this thesis further addresses some of the key questions regarding the effect of SMAD4 loss as a common mediator of TGF-β signalling on tumourigenesis. In Chapter 4, the results demonstrate that loss of SMAD4 leads to inability of the high grade dysplasia CP-B cells to up-regulate essential effectors of TGF-β tumour suppressive activity following treatment with TGF-β1 cytokine, such as cyclin dependent kinase inhibitor A1, p21. Further, this is reflected in irresponsiveness of the

cells with SMAD4 loss to TGF-β mediated cell cycle arrest. Moreover, a different TGF-β target gene expression profile of was observed in SMAD4 knockout cells compared to SMAD4 wild-type cells in response to TGF-β1. As such, SMAD4 knockout cells were unable to regulate the majority of genes during an early and late response to TGF-β1, compared to SMAD4 wild-type cells.

More strikingly, a differential gene expression profile of TGF-β signalling target genes was observed that seemed to depend highly on SMAD4 presence or absence, irrespective of TGF-β1 treatment. Thus, SMAD4 knockout cells displayed differentially expressed TGF-β signalling target genes compared to SMAD4 wild-type cells. Remarkably, SMAD4 knockout led to up-regulation of genes involved in essential processes such as EMT, immune cell function, apoptosis and regulation of origin of DNA replication. Hence, deregulation of these processes could lead to increased oncogenic features of HGD cells.

It is known that EMT represents one of the mechanisms through which epithelial cells could acquire invasive properties and subsequent metastasise [287]. EMT is characterized by the down-regulation of epithelial markers, E-cadherin and cytokeratins, such as cytokeratin 18, and up-regulation of mesenchymal markers including ACTA2 and vimentin [262, 288]. Of importance, *ACTA2* was largely up-regulated in SMAD4 knockout cells, compared to SMAD4 wild-type cells, suggestive of potential leaning towards EMT in SMAD4 knockout cells. In support of this hypothesis, the results from Chapter 3 showed that SMAD4 knockdown and knockout tumorigenic cells exhibit macro-metastatic potential to two common metastatic sites across OAC patients, including right axillary lymph node and lungs. Moreover, SMAD4 knockout leads to significant up-regulation of the *CRYAB* oncogene [289], which has been associated with potent invasion and metastasis across different cancers [290-292], including gastric [263] and colorectal [264]. Results from this part of the thesis show up-regulation of oncogenes involved in metastasis and provide deeper insights into the mechanisms of TGF-β mediated pro-tumorigenic effects upon SMAD4 loss.

Besides up-regulation of *ACTA2* and *CRYAB* genes that are involved in EMT, SMAD4 knockout cells up-regulate additional genes, such as *B2M*, *TNFSF10*, *PTK2B*, *ATF3*, *AGT*, *NFKBIA*, *EMP1* and *CDC6*. As mentioned in Chapter 4, CDC6 is involved in the

regulation of early origin of DNA replication through assembling the pre-replication complex and tight regulation of replication licencing. Initiation of replication is highly controlled process and happens only once per cell division in normal eukaryotic cells. Failure to regulate complex process such as replication might lead to replication stress and tumourigenesis. Indeed, a review of the literature over the last couple of years suggests that replication stress represents an essential hallmark of cancer cells [293-295]. Moreover, replication stress has been associated with activation of oncogenes [296, 297]. On the other hand, overexpression of CDC6 has been shown to significantly increase rereplication [298, 299], whereas low levels could potentially prevent rereplication, although this needs to be explored further. Rereplication is the aberrant phenomenon of replication more than once within the same cell cycle. Rereplication caused by overexpression of pre-replication complex assembly proteins, including CDC6 could lead to accumulation of double strand breaks (DSB) and activation of a DNA damage response [298, 300-305]. Moreover, it is unclear how frequent rereplication ultimately affects integrity of DNA, although it is thought to be through duplication of DNA fragments leading to significant genomic instability. CDC6 overexpression has been reported to be a biomarker of colorectal cancer tumorigenesis together with $p16^{INK4A}$ and MCM5 [306], but also an inducer of chromosomal instability (CIN) in combination with mutant p53 in lung cancer [307]. Notably, CP-B cells have mutant p53 (R175H) [215], therefore, it would be valuable to test effect of SMAD4 loss in null and wild-type p53 cells.

Excitingly, herein, silencing mechanism of tumour suppressor locus INK4/ARF, including genes $p14^{ARF}$, $p15^{INK4B}$ and $p16^{INK4A}$ in SMAD4 knockout cells was reported, again suggestive of important role of SMAD4 in maintaining genomic stability.

Together, overexpression of CDC6 and loss of cell cycle inhibitory control in SMAD4 knockout cells, could lead to increased rereplication and genomic instability through DSBs, which is characterized by structural chromosomal aberrations. Indeed, results from Chapter 3 show that SMAD4 knockdown and knockout initiated tumours exhibit consistent and distinctive CNAs compared to SMAD4 wild-type cells, supporting the hypothesis about high genomic instability in SMAD4 deficient cells.

6.1.2. Potential practical outcomes of research into SMAD4 loss in OAC

In addition to OAC patients with SMAD4 mutation or loss of function [256, 308, 309], there are patients with other genetic alterations in TGF-β signalling pathway that likely contribute to oncogenic potential of dysplastic Barrett's oesophagus cells [256, 310, 311]. Therefore, implementing molecular profiling for TGF-β signalling alterations into diagnostic approaches could be useful as a biomarker of tumorigenic potential in HGD.

Overall, gastrointestinal malignancies, including OAC, frequently display inactivating mutations of TGF-β signalling. Current approaches in utilizing TGF-β signalling as a therapeutic target in gastrointestinal cancers are mostly based on idea of inhibition of TGF-β immune suppressive effect [311]. Contrastingly, intrinsic alterations of TGF-β signalling leading to proliferative and tumour promoting effects in cancer cells are scarcely studied for exploitation as therapeutic approaches. A recent study has revealed that hyperactivation of TGF-β and Jun N-terminal kinase (JNK) signalling pathways in more than 80% of OAC samples [312]. Importantly, analyses of inhibiting TGF-β SMAD2/3 signalling in OAC cells had anti-tumour effects *in vitro* and *in vivo*, in SMAD4 null cell model systems [312]. Given that results in this thesis show altered TGF-β signalling response following SMAD4 loss *in vitro* via inducing potential oncogenes (Chapter 4) and further leads to increased tumourigenesis of Barrett's oesophagus cells *in vivo* (Chapter 3), it is possible that SMAD4 loss switches TGF-β signalling from tumour suppressive to tumour promoting effect in OAC. Overall, this thesis advocates developing and using TGF-β signalling as therapeutic target in OAC, upon SMAD4 loss in OAC development and progression.

6.1.3. Future directions for research into biology of SMAD4 loss

So far, there are no functionally identified molecular drivers of OAC tumorigenesis. In order to translate knowledge into effective therapies, it is essential to define functional drivers of this disease. Recent extensive genomic characterization of OAC has identified 76 putative molecular drivers [147]. Functional characterization of these drivers will deliver better treatment options for OAC patients. In this thesis, it has been shown that genetic inactivation of SMAD4 is sufficient to initiate tumorigenesis of HGD

Barrett's cells, in an *in vivo* NSG mouse model system. However, these tumours do not develop immediately after injection, suggesting further mutation events are required. Thus, the future promising aspect of this part of the project is utilizing this model for CRISPR based functional genomic approaches to identify and functionally characterize additional drivers of Barrett's oesophagus tumourigenesis in an *in vitro* and *in vivo* fashion in SMAD4 knockout cells. In this instance, genome wide functional genomic screen, such as whole genome CRISPR knockout, would be informative.

Firstly, *in vitro* analyses could include whole genome CRISPR knockout system in SMAD4 wild-type and SMAD4 knockout cells. Subsequently, the identification of genes that either aid growth of SMAD4 knockout cells should take a place, meaning that these genes represent cooperative drivers or genes which knockout leads to synthetic lethality in SMAD4 deficient cells. Further bioinformatical validation of individual genes via using publically available databases on OAC could be conducted. In addition to whole genome CRISPR knockout system in SMAD4 deficient cells *in vitro* compared to SMAD4 wild-type cells, these cells could be used to create xenograft *in vivo* mouse models in order to more closely replicate biology of OAC development. Monitoring of tumour growth, identification and functional characterisation of cooperative drivers with SMAD4 loss will create a new era of potential treatments and define putative drivers of OAC. Overall, OAC is a highly heterogeneous disease that mostly relies on more than one oncogenic pathway, meaning that targeting multiple pathways might be required [119, 147]. Based on the results from this project, an alternative therapeutic approach is to identify and target co-dependent genes and pathways within SMAD4 deficient OAC cells, which can be exploited by creating synthetic lethal interactions. Given that OAC is characterized by tumour suppressor losses, this approach is likely to be an effective therapeutic approach.

Secondly, in addition to defining genetic and molecular drivers of OAC, it would be worthwhile revealing additional genetic mechanisms contributing to the disease development. Given that following SMAD4 loss CNAs took place during the progression from HGD to invasive tumour, analyses of genes affected by these CNAs might open new horizons regarding genetic mechanisms contributing to OAC tumorigenesis. Therefore, bioinformatics analyses of the genes affected by CNAs in

the smaller genome regions upon SMAD4 loss, could be undertaken in future studies and would potentially identify additional genetic mechanisms of OAC tumorigenesis.

Thirdly, metastasis represents the major cause of cancer related deaths worldwide and the models created in this thesis could be utilized to undertake research to understand the biology of this process. Given that the majority of OAC patients present with metastatic disease at the moment of diagnosis, we need to focus on developing a deeper understanding of the molecular processes leading towards metastasis in order to effectively treat this group of patients. Generally speaking, research has confronted significant challenges to therapeutically target metastasis. This is partially due to the lack of pre-clinical model systems recapitulating metastasis in patients. Importantly, in this part of the project, re-derived cells from SMAD4 knockdown and SMAD4 knockout tumours demonstrated spontaneous macro-metastatic potential following subcutaneous injection into NSG mice (Chapter 3). Therefore, this model system represents an ideal and needed platform for uncovering molecular processes responsible for metastasis in OAC. Further, to take advantage of this model system, genome wide transcriptomic analyses of metastatic and non-metastatic cells should be performed. Transcriptomic analyses will help us to explore mechanisms and identify key driver genes of metastasis in OAC. Interestingly, initial characterisation of TGF-β1 signalling target genes has identified overexpressed genes following SMAD4 loss, that are involved in regulation of invasive and metastatic features of cancer cells, including *CRYAB* [313], *ACTA2* [262], and *EMP1* [283]. However, little is known about the effect of dysregulation of these genes in OAC metastasis. Future studies should attempt to functionally characterize the effect of high expression of these genes in driving OAC invasion and metastasis. To address this possibility, metastatic cell lines re-derived from CP-B xenograft tumours following SMAD4 knockdown and SMAD4 knockout (Chapter 3) could be used to knockdown/knockout *CRYAB*, *ACTA2* or *EMP1* gene and explore whether this could reverse metastatic potential. Given that majority of commercially available OAC cell lines are non-metastatic, overexpression of *CRYAB*, *ACTA2* or *EMP1* could be performed to explore whether these genes could initiate metastasis via functional assays *in vitro* (transwell migration assay and invasion assay) and *in vivo* xenograft cell models. Altogether, inhibition of CRYAB, ACTA2 or EMP1 may represent potential therapeutic strategy in preventing distant organ metastases.

Fourthly, an interesting finding from this part of the thesis is the overexpression of CDC6 gene in SMAD4 knockout cells and should be investigated further in the future studies. As mentioned earlier, CDC6 closely regulates homeostatic firing of DNA replication, whereas its overexpression may lead to rereplication and subsequent replication stress. In the case of replication stress, cells activate a DNA damage response aiming to resolve DNA damage or repair and restore fork progression. One of the main mediators of DNA damage response is ATR, which activates downstream machinery involved in response to DNA damage. In response to DNA damage, ATR phosphorylates histone H2AX, but also phosphorylates CHK1 that further responds to DNA damage by inducing cell cycle arrest. This complex network of DNA damage response allows the cells to recover from replication stress. Importantly, synthetic lethal approaches can be used to exploit dependence of SMAD4 knockout/CDC6 high expression cells on DNA damage response. As such, inhibiting the main mediators of DNA damage response, such as ATR and CHK1 could lead to the death of SMAD4 knockout/CDC6 high cells that exhibit replication stress. Together, replication stress is considered to be an Achilles' heel of cancer cells. In support of this idea, studies have shown that inhibition of ATR and CHK1 induces synthetic lethality in cyclin E [314], c-myc [315, 316], and HRAS [317] overexpressed cancer cells.

Fifthly, additional validation of genes regulated by SMAD4 in OAC tumourigenesis should be undertaken. In this thesis some preliminary pathway validations was performed with some initial RT PCR array results, such as ACTA2, CRYAB and CDC6. Interestingly, there was no effect of TGF-β1 ligand on the expression of these genes in CP-B cells. Hence, it is likely that other TGF-β ligands might have played role in the regulation of these genes. For instance, a previous study has shown CDC6 regulation via TGF-β3 ligand and downstream TGF-β signalling mediated SMAD4 transcriptional activity [273]. In order to further validate direct gene targets of TGF-β1 or other TGF-β ligands, chromatin immunoprecipitation experiments would be beneficial to elucidate the full range of SMAD4 target genes in OAC tumourigenesis.

Sixthly, a promising direction for this part of the project is a deeper understanding of the regulation of INK4/ARF locus through SMAD4. Recent research hinting of negative regulation of the INK4/ARF locus through CDC6 has come from using mouse fibroblasts as a model system [267]. On the other hand, literature evidence

demonstrating mechanisms of regulation of the human INK4/ARF tumour suppressor locus is lacking. Herein, down-regulation of transcript expression from the INK4/ARF tumour suppressor locus in SMAD4 knockout cells was observed. Given that SMAD4 low expressing cells have high CDC6, it is possible that the axis of SMAD4 low/CDC6 high negatively regulates the human INK4/ARF tumour suppressor locus. Future experimental investigation into SMAD4 regulation of CDC6 via Chromatin immunoprecipitation is necessary to understand the nature of this regulation, and downstream regulation of INK4/ARF genes expression.

6.1.4. Mechanism by which SMAD4 loss drives progression

Given the results from Chapter 3 that report the role of SMAD4 loss in initiation of tumourigenesis from Barrett's oesophagus cells with HGD, accompanied by significantly increased fraction of the genome with CNAs, it is clear that SMAD4 represents a key determinant of Barrett's oesophagus progression towards cancer. However, we still need to decipher the mechanisms of SMAD4 loss driven tumourigenesis. Initial *in vitro* studies into TGF-β signalling upon SMAD4 loss (Chapter 4) have revealed the inability of SMAD4 depleted cells to respond to TGF-β1 in the same way as SMAD4 wild-type cells. In addition, SMAD4 knockout cells exhibited up-regulation of potential oncogenes, such as *EMP1*, *ACTA2*, *CRYAB* and *CDC6*. Nevertheless, these results would benefit from a larger number of biological replicates for each group and additional validation of oncogenic role of genes that are specifically altered in SMAD4 knockout cells.

Although, genomic changes upon SMAD4 loss have primarily been investigated in this thesis, it is important to also consider epigenetic changes that might shape cancer cell characteristics as well. As such, one of the key epigenetic languages, DNA methylation, is largely involved in regulation of gene expression and maintaining genome stability [318]. In addition, previous studies have given insights into DNA methylation mediated gene regulation that has oncogenic potential in OAC [319-321]. Overall, it is worth noting that epigenetic changes might contribute to the tumorigenic potential following SMAD4 loss. Therefore, future research concerning potential mechanisms of SMAD4 loss driven carcinogenesis should incorporate a deeper

understanding of epigenetic alterations, in addition to genomic and transcriptomic alterations.

6.1.5. GRB7 as a promising therapeutic target in GRB7 overexpressing cancers

Another larger part of this PhD thesis was focused on deciphering the effect of GRB7 amplification and overexpression in OAC. Despite the success of using molecular targeted therapy in solid malignancies, such as anti-HER2 in breast [322], anti-BRAF in melanoma [323] or anti-c-KIT in gastrointestinal stromal tumours [324], it has been challenging to replicate this success in OAC. This is partially due to the fact that OAC is highly heterogeneous disease, with usual activation of more than one oncogenic signalling pathway through co-amplification of RTKs and mitogenic activation of downstream molecules [119]. Indeed, many of the clinical trials with inhibition of a single RTK in gastro-oesophageal cancers have been unsuccessful. Crucially, this thesis focused on targeting a signalling molecule, GRB7 that plays a role as a common mediator of signalling through numerous RTKs, but also associates with downstream effectors. Therefore, GRB7 could mediate comprehensive oncogenic signalling and targeting GRB7 could represent a novel and effective therapeutic strategy via targeting multiple axes of oncogenic signalling in cancers with GRB7 overexpression.

6.1.6. Future directions for using GRB7 as a therapeutic target in cancers

Given that GRB7 has a strong potential to be used as a therapeutic target in overexpressed OAC cancers (Chapter 5), it would seem important to pursue the possible beneficial outcome for patients when using GRB7 inhibition in combination with the current chemo-radiotherapy regimen. To test this hypothesis, *in vitro* functional assays (e.g. clonogenic survival, cell death and cell cycle) accompanied by *in vivo* experiments using a mouse model system will be needed.

One of the largest barriers that current clinical trials using molecular targeted therapy are confronting to effectively treat cancer is intrinsic resistance to the drug. As such, in this part of the project, Eso26 OAC cells with high HER2 expression were found to be insensitive to a HER2 inhibitor commonly used in the clinic, trastuzumab. Therefore, it is essential to understand molecular mechanisms of intrinsic resistance.

Future directions for this part of the project should incorporate genomic profiling of Eso26 cells and underpinning additional mutations that might render insensitivity to trastuzumab, such as *PTEN* mutations [179]. In addition, comparison of the genomic profiles of insensitive cells (Eso26) compared to sensitive cells (OE19) to trastuzumab n could aid in deciphering mechanisms of intrinsic resistance. All identified and functionally characterized mutations should be validated in OAC patients with HER2 overexpression that exhibit resistance to trastuzumab.

As mentioned earlier, most of the commercially available OAC cell lines are unable to spontaneously metastatize in *in vivo* mouse model systems with different levels of immunocompetency, apart FLO1 cells [246]. Interestingly, the extent of metastatic potential has increased following GRB7 overexpression in FLO1 cells (trans-well migration assay), means that GRB7 might enhance metastasis. To further pursue this finding, additional *in vitro* and *in vivo* model systems of metastasis are needed in order to determine how GRB7 overexpression contributes to the metastasis and whether inhibiting GRB7 has anti-metastastic effects.

6.3. Conclusions

A significant barrier in treating patients with OAC is late diagnosis. Although there have been numerous attempts to identify molecular biomarkers of OAC stage specific development, the only predictive biomarker is the presence of dysplasia. In addition, the majority of mutations present in OAC happen in non-step wise process during disease development, leaving a small room for biomarker characterization of specific stages. However, *SMAD4* mutations have been reported to be stage specific, happening only in cancer and not at earlier stages of the disease development. Therefore, it was hypothesized that SMAD4 might play a role in malignant transformation to OAC. To characterize the functional effect of *SMAD4* mutations in OAC development, dysplastic Barrett's cells were used in this theses, to develop a unique model that replicates the progression from human Barrett's to OAC. Using high grade dysplastic Barrett's cells, CP-B, which contain *TP53* mutation, but are SMAD4 wild-type, we showed that inactivation of SMAD4 by shRNA knockdown or CRISPR-mediated knockout was sufficient to promote tumourigenesis in immunocompromised NSG mice. Intriguingly, the tumours do not develop immediately, suggesting further mutation events are required for transformation. Indeed, SMAD4 loss exhibit reshaped CNA landscape in the tumours compared to the injected SMAD4 knockout cells. Furthermore, cell lines re-derived from CP-B SMAD4 knockdown and knockout xenografts acquired potent tumorigenic and metastatic capabilities. Conclusively, loss of SMAD4 is sufficient to promote tumourigenesis in a model of dysplastic Barrett's oesophagus.

In addition, *in vitro* analyses have showed that CP-B SMAD4 knockout cells lost the ability to induce cell cycle arrest in respond to TGF-β1 cytokine stimulation, in contrast to SMAD4 wild-type cells. Furthermore, SMAD4 knockout cells were unable to regulate TGF-β signalling target genes that are regulated by SMAD4 wild-type cells, meaning that SMAD4 knockout cells exhibit an altered expression profile in response to TGF-β signalling. Therefore, it is likely that cytokine dependent TGF-β signalling has a pro-tumourigenic effect in these cells, seemingly through SMAD4 independent signalling.

Thus, even though TGF-β signalling playing a tumour suppressor role, it is likely that frequent mutations within this signalling pathway switch TGF-β to being tumour promoting. As such, SMAD4 depletion results in upregulation of potential oncogenes (*ACTA2*, *CRYAB*, *CDC6*, *EMP1*), possibly leading to tumourigenesis.

Moreover, the high genomic instability, characterized by increased structural chromosomal rearrangements (CNA) within tumours upon SMAD4 loss, implicates the role of SMAD4 as a protector of genome integrity. This phenotype of cells upon SMAD4 loss could be used to target cancer cells using the concept of synthetic lethality. In this instance, increased genomic instability of cancer cells with SMAD4 loss could predispose these cells to be sensitive to the targeting of the second essential gene.

In parallel, preclinical *in vitro* and *in vivo* model systems used in this thesis have demonstrated that GRB7 overexpression has a significant oncogenic effect in OAC. Considering the redundancies in the treatment of single RTK, due to the upregulation of additional RTK within oesophageal cancer cells, it is time to think of additional approaches in targeting this tumour burden. As such, GRB7 transmits the signalling through numerous RTK, and it is likely that inhibition of GRB7 will block not just a single pathway, but rather combination. Importantly, GRB7 high expression predicts the poor outcome of OAC patients compared to the patients with GRB7 low expression, giving the strong reasoning for further developing of clinically useful GRB7 inhibitors.

BIBLIOGRAPHY

1. Bray, F., et al., *Global cancer statistics 2018: GLOBOCAN estimates of incidence and mortality worldwide for 36 cancers in 185 countries. CA: Cancer J Clin*, 2018. **68**(6): p. 394-424.
2. Lv, J., et al., *Primary small cell carcinoma of the esophagus.* Journal of Thoracic Oncology, 2008. **3**(12): p. 1460-1465.
3. Perch, S.J., et al., *Esophageal sarcomas.* Journal of Surgical Oncology, 1991. **48**(3): p. 194-198.
4. Lott, S., et al., *Gastrointestinal stromal tumors of the esophagus: evaluation of a pooled case series regarding clinicopathological features and clinical outcome.* American Journal of Cancer Research, 2015. **5**(1): p. 333-343.
5. Arnal, M.J.D., et al., *Esophageal cancer: Risk factors, screening and endoscopic treatment in Western and Eastern countries.* World Journal of Gastroenterology, 2015. **21**(26): p. 7933-7943.
6. Wheeler, J.B. and C.E. Reed, *Epidemiology of esophageal cancer.* The Surgical Clinics of North America, 2012. **92**(5): p. 1077-1087.
7. Renehan, A.G., et al., *Body-mass index and incidence of cancer: a systematic review and meta-analysis of prospective observational studies.* The Lancet, 2008. **371**(9612): p. 569-578.
8. Kubo, A. and D.A. Corley, *Body mass index and adenocarcinomas of the esophagus or gastric cardia: a systematic review and meta-analysis.* Cancer Epidemiology and Prevention Biomarkers, 2006. **15**(5): p. 872-878.
9. Oze, I., et al., *Cigarette smoking and esophageal cancer risk: an evaluation based on a systematic review of epidemiologic evidence among the Japanese population.* Japanese Journal of Clinical Oncology, 2011. **42**(1): p. 63-73.
10. Thrift, A.P., *The epidemic of oesophageal carcinoma: where are we now?* Cancer Epidemiology, 2016. **41**: p. 88-95.
11. Brown, L.M., et al., *Are racial differences in squamous cell esophageal cancer explained by alcohol and tobacco use?* Journal of the National Cancer Institute, 1994. **86**(17): p. 1340-1345.
12. Shibata, A., et al., *Trend in incidence of adenocarcinoma of the esophagus in Japan, 1993–2001.* Japanese Journal of Clinical Oncology, 2008. **38**(7): p. 464-468.
13. Cook, M., et al., *Oesophageal cancer incidence in the United States by race, sex, and histologic type, 1977–2005.* British Journal of Cancer, 2009. **101**(5): p. 855-859.
14. Coleman, H.G., et al., *The epidemiology of esophageal adenocarcinoma. Gastroenterology*, 2018. **154**(2): p. 390-405.
15. Stahl, M., et al., *Esophageal cancer: Clinical Practice Guidelines for diagnosis, treatment and follow-up.* Annals of Oncology, 2010. **21**(suppl_5): p. v46-v49.
16. Van Vliet, E., et al., *Staging investigations for oesophageal cancer: a meta-analysis.* British Journal of Cancer, 2008. **98**(3): p. 547-557.
17. Romagnuolo, J., et al., *Helical CT versus EUS with fine needle aspiration for celiac nodal assessment in patients with esophageal cancer.* Gastrointestinal Endoscopy, 2002. **55**(6): p. 648-654.
18. Flamen, P., et al., *Utility of positron emission tomography for the staging of patients with potentially operable esophageal carcinoma.* Journal of Clinical Oncology, 2000. **18**(18): p. 3202-3210.
19. Flanagan, F.L., et al., *Staging of esophageal cancer with 18F-fluorodeoxyglucose positron emission tomography.* American Journal of Roentgenology, 1997. **168**(2): p. 417-424.
20. Block, M.I., et al., *Improvement in staging of esophageal cancer with the addition of positron emission tomography.* The Annals of Thoracic Surgery, 1997. **64**(3): p. 770-777.
21. Meyers, B.F., et al., *The utility of positron emission tomography in staging of potentially operable carcinoma of the thoracic esophagus: results of the American College of Surgeons Oncology Group Z0060 trial.* The Journal of Thoracic and Cardiovascular Surgery, 2007. **133**(3): p. 738-745.

22. Kanamoto, A., et al., *Clinicopathological study of multiple superficial oesophageal carcinoma.* British Journal of Surgery, 2000. **87**(12): p. 1712-1715.
23. Tachibana, M., et al., *Clinicopathologic features of superficial esophageal cancer: results of consecutive 100 patients.* Annals of surgical Oncology, 2008. **15**(1): p. 104-116.
24. Lee, Y.T., Y.J. Tan, and C.E. Oon, *Molecular targeted therapy: Treating cancer with specificity.* European Journal of Pharmacology, 2018. **834**: p. 188-196.
25. Mayekar, M.K. and T.G. Bivona, *Current landscape of targeted therapy in lung cancer.* Clinical Pharmacology & Therapeutics, 2017. **102**(5): p. 757-764.
26. Maron, S.B. and D.V. Catenacci, *Update on gastroesophageal adenocarcinoma targeted therapies.* Hematology/Oncology Clinics of North America, 2017. **31**(3): p. 511-527.
27. Pasini, F., et al., *Targeted therapies for advanced and metastatic adenocarcinoma of the gastroesophageal junction: is there something new?* Gastric Cancer, 2017. **20**(1): p. 31-42.
28. Pectasides, E., *Genomic alterations and targeted therapy in gastric and esophageal adenocarcinoma.* Clinical Therapeutics, 2016. **38**(7): p. 1589-1599.
29. Bang, Y.-J., et al., *Trastuzumab in combination with chemotherapy versus chemotherapy alone for treatment of HER2-positive advanced gastric or gastro-oesophageal junction cancer (ToGA): a phase 3, open-label, randomised controlled trial. The Lancet*, 2010. **376**(9742): p. 687-697.
30. Ryu, M.-H., et al., *Multicenter phase II study of trastuzumab in combination with capecitabine and oxaliplatin for advanced gastric cancer.* European Journal of Cancer, 2015. **51**(4): p. 482-488.
31. Safran, H., et al., *Phase I/II study of trastuzumab, paclitaxel, cisplatin and radiation for locally advanced, HER2 overexpressing, esophageal adenocarcinoma.* International Journal of Radiation Oncology, Biology, Physics, 2007. **67**(2): p. 405-409.
32. Wilke, H., et al., *Ramucirumab plus paclitaxel versus placebo plus paclitaxel in patients with previously treated advanced gastric or gastro-oesophageal junction adenocarcinoma (RAINBOW): a double-blind, randomised phase 3 trial.* The Lancet Oncology, 2014. **15**(11): p. 1224-1235.
33. Fuchs, C.S., et al., *Ramucirumab monotherapy for previously treated advanced gastric or gastro-oesophageal junction adenocarcinoma (REGARD): an international, randomised, multicentre, placebo-controlled, phase 3 trial.* The Lancet, 2014. **383**(9911): p. 31-39.
34. Yoon, H.H., et al., *Ramucirumab combined with FOLFOX as front-line therapy for advanced esophageal, gastroesophageal junction, or gastric adenocarcinoma: a randomized, double-blind, multicenter Phase II trial.* Annals of Oncology, 2016: p. mdw423.
35. Fuchs, C.S., et al., *RAINFALL: A randomized, double-blind, placebo-controlled phase III study of cisplatin (Cis) plus capecitabine (Cape) or 5FU with or without ramucirumab (RAM) as first-line therapy in patients with metastatic gastric or gastroesophageal junction (G-GEJ) adenocarcinoma*. 2018, American Society of Clinical Oncology.
36. Kim, J., et al., *Preexisting oncogenic events impact trastuzumab sensitivity in ERBB2-amplified gastroesophageal adenocarcinoma.* The Journal of Clinical Investigation, 2014. **124**(12): p. 5145-5158.
37. Spechler, S.J., et al., *History, molecular mechanisms, and endoscopic treatment of Barrett's esophagus.* Gastroenterology, 2010. **138**(3): p. 854-869.
38. Gregson, E.M., et al., *Genetic progression of Barrett's oesophagus to oesophageal adenocarcinoma.* British Journal of Cancer, 2016. **115**(4): p. 403-410.
39. Hvid-Jensen, F., et al., *Incidence of adenocarcinoma among patients with Barrett's esophagus.* New England Journal of Medicine, 2011. **365**(15): p. 1375-1383.
40. Sikkema, M., et al., *Risk of esophageal adenocarcinoma and mortality in patients with Barrett's esophagus: a systematic review and meta-analysis.* Clinical Gastroenterology and Hepatology, 2010. **8**(3): p. 235-244.

41. Verbeek, R.E., et al., *Surveillance of Barrett's esophagus and mortality from esophageal adenocarcinoma: a population-based cohort study*. 2014, American Journal of Gastroenterology. p. 1215-1222.
42. El-Serag, H.B., et al., *Surveillance endoscopy is associated with improved outcomes of oesophageal adenocarcinoma detected in patients with Barrett's oesophagus.* Gut, 2016. **65**(8): p. 1252-1260.
43. Whiteman, D.C. and B.J. Kendall, *Barrett's oesophagus: epidemiology, diagnosis and clinical management.* Medical Journal of Australia, 2016. **205**(7): p. 317-324.
44. Que, J., et al., *Pathogenesis and Cells of Origin of Barrett's Esophagus.* Gastroenterology, 2019. **157**(2): p. 349-364.
45. Yu, W.-Y., et al., *Conversion of columnar to stratified squamous epithelium in the developing mouse oesophagus.* Developmental Biology, 2005. **284**(1): p. 157-170.
46. Kalabis, J., et al., *A subpopulation of mouse esophageal basal cells has properties of stem cells with the capacity for self-renewal and lineage specification.* The Journal of Clinical Investigation, 2008. **118**(12): p. 3860-3869.
47. Leedham, S.J., et al., *Individual crypt genetic heterogeneity and the origin of metaplastic glandular epithelium in human Barrett's oesophagus.* Gut, 2008. **57**(8): p. 1041-1048.
48. Wang, X., et al., *Residual embryonic cells as precursors of a Barrett's-like metaplasia.* Cell, 2011. **145**(7): p. 1023-1035.
49. Quante, M., et al., *Bile acid and inflammation activate gastric cardia stem cells in a mouse model of Barrett-like metaplasia.* Cancer Cell, 2012. **21**(1): p. 36-51.
50. Hu, Y., et al., *The pathogenesis of Barrett's esophagus: secondary bile acids upregulate intestinal differentiation factor CDX2 expression in esophageal cells.* Journal of Gastrointestinal Surgery, 2007. **11**(7): p. 827-834.
51. Kazumori, H., et al., *Roles of caudal-related homeobox gene Cdx1 in oesophageal epithelial cells in Barrett's epithelium development.* Gut, 2009. **58**(5): p. 620-628.
52. Pera, M., et al., *Duodenal-content reflux into the esophagus leads to expression of Cdx2 and Muc2 in areas of squamous epithelium in rats.* Journal of Gastrointestinal Surgery, 2007. **11**(7): p. 869-874.
53. Freund, J.-N., et al., *The Cdx-1 and Cdx-2 homeobox genes in the intestine.* Biochemistry and Cell Biology, 1998. **76**(6): p. 957-969.
54. Silberg, D.G., et al., *Cdx1 and cdx2 expression during intestinal development.* Gastroenterology, 2000. **119**(4): p. 961-971.
55. Suh, E., et al., *A homeodomain protein related to caudal regulates intestine-specific gene transcription.* Molecular and Cellular Biology, 1994. **14**(11): p. 7340-7351.
56. Suh, E. and P.G. Traber, *An intestine-specific homeobox gene regulates proliferation and differentiation.* Molecular and Cellular Biology, 1996. **16**(2): p. 619-625.
57. Phillips, R.W., H.F. Frierson, and C.A. Moskaluk, *Cdx2 as a marker of epithelial intestinal differentiation in the esophagus.* The American Journal of Surgical Pathology, 2003. **27**(11): p. 1442-1447.
58. Groisman, G.M., et al., *Expression of the intestinal marker Cdx2 in the columnar-lined esophagus with and without intestinal (Barrett's) metaplasia.* Modern Pathology, 2004. **17**(10): p. 1282-1288.
59. Wang, D.H., et al., *Aberrant epithelial–mesenchymal Hedgehog signaling characterizes Barrett's metaplasia.* Gastroenterology, 2010. **138**(5): p. 1810-1822.
60. van den Brink, G.R., *Hedgehog signaling in development and homeostasis of the gastrointestinal tract.* Physiological Reviews, 2007. **87**(4): p. 1343-1375.
61. Clemons, N.J., et al., *Sox9 drives columnar differentiation of esophageal squamous epithelium: a possible role in the pathogenesis of Barrett's esophagus.* American Journal of Physiology-Gastrointestinal and Liver Physiology, 2012. **303**(12): p. G1335-G1346.

62. Bhardwaj, V., et al., *Prevention of DNA damage in Barrett's esophageal cells exposed to acidic bile salts.* Carcinogenesis, 2016. **37**(12): p. 1161-1169.
63. Olyaee, M., et al., *Mucosal reactive oxygen species production in oesophagitis and Barrett's oesophagus.* Gut, 1995. **37**(2): p. 168-173.
64. Huo, X., et al., *Deoxycholic acid causes DNA damage while inducing apoptotic resistance through NF-κB activation in benign Barrett's epithelial cells.* American Journal of Physiology-Gastrointestinal and Liver Physiology, 2011. **301**(2): p. G278-G286.
65. Dvorak, K., et al., *Activation of the interleukin-6/STAT3 antiapoptotic pathway in esophageal cells by bile acids and low pH: relevance to barrett's esophagus.* Clinical Cancer Research, 2007. **13**(18): p. 5305-5313.
66. Olliver, J., et al., *DNA damage levels are raised in Barrett's oesophageal mucosa relative to the squamous epithelium of the oesophagus.* Biomarkers, 2003. **8**(6): p. 509-521.
67. Olliver, J.R., et al., *Risk factors, DNA damage, and disease progression in Barrett's esophagus.* Cancer Epidemiology and Prevention Biomarkers, 2005. **14**(3): p. 620-625.
68. von Holzen, U., et al., *Evidence for DNA damage checkpoint activation in barrett esophagus.* Translational Oncology, 2010. **3**(1): p. 33-42.
69. Burnat, G., et al., *Bile acids are multifunctional modulators of the Barrett's carcinogenesis.* Journal of Physiology and Pharmacology, 2010. **61**(2): p. 185-192.
70. Eads, C.A., et al., *Fields of aberrant CpG island hypermethylation in Barrett's esophagus and associated adenocarcinoma.* Cancer Research, 2000. **60**(18): p. 5021-5026.
71. Kaz, A.M., et al., *DNA methylation profiling in Barrett's esophagus and esophageal adenocarcinoma reveals unique methylation signatures and molecular subclasses.* Epigenetics, 2011. **6**(12): p. 1403-1412.
72. Kuester, D., et al., *Silencing of MGMT expression by promoter hypermethylation in the metaplasia–dysplasia–carcinoma sequence of Barrett's esophagus.* Cancer Letters, 2009. **275**(1): p. 117-126.
73. Esteller, M., *Cancer epigenetics: DNA methylation and chromatin alterations in human cancer*, in *New Trends in Cancer for the 21St Century*. 2003, Advances in Experimental Medicine and Biology. p. 39-49.
74. Nephew, K.P. and T.H.M. Huang, *Epigenetic gene silencing in cancer initiation and progression.* Cancer Letters, 2003. **190**(2): p. 125-133.
75. Paulson, T.G., et al., *p16 mutation spectrum in the premalignant condition Barrett's esophagus.* PloS One, 2008. **3**(11): p. e3809.
76. Contino, G., et al., *The evolving genomic landscape of Barrett's esophagus and esophageal adenocarcinoma.* Gastroenterology, 2017. **153**(3): p. 657-673.
77. Bian, Y.S., et al., *p16 inactivation by methylation of the CDKN2A promoter occurs early during neoplastic progression in Barrett's esophagus.* Gastroenterology, 2002. **122**(4): p. 1113-1121.
78. Klump, B., et al., *Hypermethylation of the CDKN2/p16 promoter during neoplastic progression in Barrett's esophagus.* Gastroenterology, 1998. **115**(6): p. 1381-1386.
79. Wong, D.J., et al., *p16INK4a lesions are common, early abnormalities that undergo clonal expansion in Barrett's metaplastic epithelium.* Cancer Research, 2001. **61**(22): p. 8284-8289.
80. Martinez, P., et al., *Dynamic clonal equilibrium and predetermined cancer risk in Barrett's oesophagus.* Nature Communications, 2016. **7**: p. 12158.
81. Martincorena, I., et al., *Somatic mutant clones colonize the human esophagus with age.* Science, 2018. **362**(6417): p. 911-917.
82. Yokoyama, A., et al., *Age-related remodelling of oesophageal epithelia by mutated cancer drivers.* Nature, 2019. **565**(7739): p. 312-317.
83. Conio, M., et al., *Long-term endoscopic surveillance of patients with Barrett's esophagus. Incidence of dysplasia and adenocarcinoma: a prospective study.* The American Journal of Gastroenterology, 2003. **98**(9): p. 1931-1939.

84. Bird–Lieberman, E.L., et al., *Population-based study reveals new risk-stratification biomarker panel for Barrett's esophagus.* Gastroenterology, 2012. **143**(4): p. 927-935.
85. Kastelein, F., et al., *Surveillance in patients with long-segment Barrett's oesophagus: a cost-effectiveness analysis.* Gut, 2015. **64**(6): p. 864-871.
86. Schnell, T.G., et al., *Long-term nonsurgical management of Barrett's esophagus with high-grade dysplasia.* Gastroenterology, 2001. **120**(7): p. 1607-1619.
87. Reid, B.J., et al., *Predictors of progression to cancer in Barrett's esophagus: baseline histology and flow cytometry identify low-and high-risk patient subsets.* The American Journal of Gastroenterology, 2000. **95**(7): p. 1669-1676.
88. Davoli, T. and T. de Lange, *The causes and consequences of polyploidy in normal development and cancer.* Annual Review of Cell and Developmental Biology, 2011. **27**: p. 585-610.
89. Galipeau, P.C., et al., *17p (p53) allelic losses, 4N (G2/tetraploid) populations, and progression to aneuploidy in Barrett's esophagus.* Proceedings of the National Academy of Sciences, 1996. **93**(14): p. 7081-7084.
90. Li, X., et al., *Temporal and spatial evolution of somatic chromosomal alterations: a case-cohort study of Barrett's esophagus.* Cancer Prevention Research, 2014. **7**(1): p. 114-127.
91. Stachler, M.D., et al., *Paired exome analysis of Barrett's esophagus and adenocarcinoma.* Nature Genetics, 2015. **47**(9): p. 1047-1055.
92. Schulmann, K., et al., *Inactivation of p16, RUNX3, and HPP1 occurs early in Barrett's-associated neoplastic progression and predicts progression risk.* Oncogene, 2005. **24**(25): p. 4138-4148.
93. Jin, Z., et al., *A multicenter, double-blinded validation study of methylation biomarkers for progression prediction in Barrett's esophagus.* Cancer research, 2009. **69**(10): p. 4112-4115.
94. Clément, G., et al., *Methylation of APC, TIMP3, and TERT: a new predictive marker to distinguish Barrett's oesophagus patients at risk for malignant transformation.* The Journal of Pathology: A Journal of the Pathological Society of Great Britain and Ireland, 2006. **208**(1): p. 100-107.
95. Tischoff, I., et al., *Methylation of SOCS-3 and SOCS-1 in the carcinogenesis of Barrett's adenocarcinoma.* Gut, 2007. **56**(8): p. 1047-1053.
96. Ross-Innes, C.S., et al., *Whole-genome sequencing provides new insights into the clonal architecture of Barrett's esophagus and esophageal adenocarcinoma.* Nature Genetics, 2015. **47**(9): p. 1038.
97. Dagogo-Jack, I. and A.T. Shaw, *Tumour heterogeneity and resistance to cancer therapies.* Nature Reviews Clinical Oncology, 2018. **15**(2): p. 81-94.
98. Andor, N., et al., *Pan-cancer analysis of the extent and consequences of intratumor heterogeneity.* Nature Medicine, 2016. **22**(1): p. 105-113.
99. Russo, M., et al., *Tumor heterogeneity and lesion-specific response to targeted therapy in colorectal cancer.* Cancer Discovery, 2016. **6**(2): p. 147-153.
100. Kwak, E.L., et al., *Molecular heterogeneity and receptor coamplification drive resistance to targeted therapy in MET-amplified esophagogastric cancer.* Cancer Discovery, 2015. **5**(12): p. 1271-1281.
101. Murugaesu, N., et al., *Tracking the genomic evolution of esophageal adenocarcinoma through neoadjuvant chemotherapy.* Cancer Discovery, 2015. **5**(8): p. 821-831.
102. Findlay, J.M., et al., *Differential clonal evolution in oesophageal cancers in response to neo-adjuvant chemotherapy.* Nature Communications, 2016. **7**: p. 11111.
103. Hao, J.-J., et al., *Spatial intratumoral heterogeneity and temporal clonal evolution in esophageal squamous cell carcinoma.* Nature Genetics, 2016. **48**(12): p. 1500-1507.
104. Pectasides, E., et al., *Genomic heterogeneity as a barrier to precision medicine in gastroesophageal adenocarcinoma.* Cancer Discovery, 2018. **8**(1): p. 37-48.
105. Hyman, E., et al., *Impact of DNA amplification on gene expression patterns in breast cancer.* Cancer Research, 2002. **62**(21): p. 6240-6245.

106. Pollack, J.R., et al., *Microarray analysis reveals a major direct role of DNA copy number alteration in the transcriptional program of human breast tumors.* Proceedings of the National Academy of Sciences, 2002. **99**(20): p. 12963-12968.
107. Phillips, J.L., et al., *The consequences of chromosomal aneuploidy on gene expression profiles in a cell line model for prostate carcinogenesis.* Cancer Research, 2001. **61**(22): p. 8143-8149.
108. Tsafrir, D., et al., *Relationship of gene expression and chromosomal abnormalities in colorectal cancer.* Cancer Research, 2006. **66**(4): p. 2129-2137.
109. Dulak, A.M., et al., *Gastrointestinal adenocarcinomas of the esophagus, stomach, and colon exhibit distinct patterns of genome instability and oncogenesis.* Cancer Research, 2012. **72**(17): p. 4383-4393.
110. Frankel, A., et al., *Genome-wide analysis of esophageal adenocarcinoma yields specific copy number aberrations that correlate with prognosis.* Genes, Chromosomes and Cancer, 2014. **53**(4): p. 324-338.
111. Bardi, G., et al., *Karyotypic characterization of colorectal adenocarcinomas.* Genes, Chromosomes and Cancer, 1995. **12**(2): p. 97-109.
112. He, Q.J., et al., *Recurrent genetic alterations in 26 colorectal carcinomas and 21 adenomas from Chinese patients.* Cancer Genetics and Cytogenetics, 2003. **144**(2): p. 112-118.
113. Molkentin, J.D., *The zinc finger-containing transcription factors GATA-4,-5, and-6 ubiquitously expressed regulators of tissue-specific gene expression.* The Journal of Biological Chemistry, 2000. **275**(50): p. 38949-38952.
114. Buffart, T.E., et al., *Gastric cancers of Western European and African patients show different patterns of genomic instability.* BMC Medical Genomics, 2011. **4**(1): p. 7.
115. Muleris, M., et al., *Predominance of normal karyotype in colorectal tumors from hereditary non-polyposis colorectal cancer patients.* Genes, Chromosomes and Cancer, 1995. **14**(3): p. 223-226.
116. Nancarrow, D.J., et al., *Genome-wide copy number analysis in esophageal adenocarcinoma using high-density single-nucleotide polymorphism arrays.* Cancer Research, 2008. **68**(11): p. 4163-4172.
117. Mermel, C.H., et al., *GISTIC2. 0 facilitates sensitive and confident localization of the targets of focal somatic copy-number alteration in human cancers.* Genome Biology, 2011. **12**(4): p. R41.
118. Kwong, D., et al., *Chromosomal aberrations in esophageal squamous cell carcinoma among Chinese: gain of 12p predicts poor prognosis after surgery.* Human Pathology, 2004. **35**(3): p. 309-316.
119. Secrier, M., et al., *Mutational signatures in esophageal adenocarcinoma define etiologically distinct subgroups with therapeutic relevance.* Nature Genetics, 2016. **48**(10): p. 1131-1141.
120. Watkins, J.A., et al., *Genomic scars as biomarkers of homologous recombination deficiency and drug response in breast and ovarian cancers.* Breast Cancer Research 2014. **16**(3): p. 211.
121. Rottenberg, S., et al., *High sensitivity of BRCA1-deficient mammary tumors to the PARP inhibitor AZD2281 alone and in combination with platinum drugs.* Proceedings of the National Academy of Sciences USA, 2008. **105**(44): p. 17079-17084.
122. Ledermann, J., et al., *Olaparib maintenance therapy in patients with platinum-sensitive relapsed serous ovarian cancer: a preplanned retrospective analysis of outcomes by BRCA status in a randomised phase 2 trial.* Lancet Oncology, 2014. **15**(8): p. 852-861.
123. Alexandrov, L.B., et al., *A mutational signature in gastric cancer suggests therapeutic strategies.* Nature Communications, 2015. **6**: p. 8683.
124. Luijten, M.N.H., et al.., *Mutational game changer: chromothripsis and its emerging relevance to cancer.* Mutation Research, 2018. **777**: p. 29-51.
125. Stephens, P.J., et al., *Massive genomic rearrangement acquired in a single catastrophic event during cancer development.* Cell, 2011. **144**(1): p. 27-40.
126. Nones, K., et al., *Genomic catastrophes frequently arise in esophageal adenocarcinoma and drive tumorigenesis.* Nature Communications, 2014. **5**: p. 5224.

127. Cheng, C., et al., *Whole-genome sequencing reveals diverse models of structural variations in esophageal squamous cell carcinoma.* American Journal of Human Genetics, 2016. **98**(2): p. 256-274.
128. Marcozzi, A., et al., *The genomic characteristics and origin of chromothripsis*, in *Chromothripsis*. 2018, Methods in Molecular Biology. p. 3-19.
129. Kloosterman, W.P., et al., *Prevalence and clinical implications of chromothripsis in cancer genomes.* Current Opinion in Oncology, 2014. **26**(1): p. 64-72.
130. Mulero-Navarro, S. and M. Esteller, *Epigenetic biomarkers for human cancer: the time is now.* Critical Reviews in Oncology/Hematology, 2008. **68**(1): p. 1-11.
131. Kailasam, A., et al., *Epigenetics in the pathogenesis of esophageal adenocarcinoma.* Clinical and Translational Science, 2015. **8**(4): p. 394-402.
132. Agarwal, A., et al., *Role of epigenetic alterations in the pathogenesis of Barrett's esophagus and esophageal adenocarcinoma.* International Journal of Clinical and Experimental Pathology, 2012. **5**(5): p. 382-396.
133. Hinoue, T., et al., *Genome-scale analysis of aberrant DNA methylation in colorectal cancer.* Genome Research, 2012. **22**(2): p. 271-282.
134. Shen, L., et al., *Integrated genetic and epigenetic analysis identifies three different subclasses of colon cancer.* Proceedings of the National Academy of Sciences, 2007. **104**(47): p. 18654-18659.
135. Imielinski, M., et al., *Mapping the hallmarks of lung adenocarcinoma with massively parallel sequencing.* Cell, 2012. **150**(6): p. 1107-1120.
136. Berger, M.F., et al., *Melanoma genome sequencing reveals frequent PREX2 mutations.* Nature, 2012. **485**(7399): p. 502-506.
137. Dulak, A.M., et al., *Exome and whole-genome sequencing of esophageal adenocarcinoma identifies recurrent driver events and mutational complexity.* Nature Genetics, 2013. **45**(5): p. 478-486.
138. Sanui, T., et al., *DOCK2 regulates Rac activation and cytoskeletal reorganization through interaction with ELMO1.* Blood, 2003. **102**(8): p. 2948-2950.
139. Hanawa-Suetsugu, K., et al., *Structural basis for mutual relief of the Rac guanine nucleotide exchange factor DOCK2 and its partner ELMO1 from their autoinhibited forms.* Proceedings of the National Academy of Sciences, 2012. **109**(9): p. 3305-3310.
140. del Pulgar, T.G., et al., *Rho GTPase expression in tumourigenesis: evidence for a significant link.* Bioessays, 2005. **27**(6): p. 602-613.
141. Sander, E.E., et al., *Matrix-dependent Tiam1/Rac signaling in epithelial cells promotes either cell–cell adhesion or cell migration and is regulated by phosphatidylinositol 3-kinase.* The Journal of Cell Biology, 1998. **143**(5): p. 1385-1398.
142. Sanz-Moreno, V., et al., *Rac activation and inactivation control plasticity of tumor cell movement.* Cell, 2008. **135**(3): p. 510-523.
143. Jarzynka, M.J., et al., *ELMO1 and Dock180, a bipartite Rac1 guanine nucleotide exchange factor, promote human glioma cell invasion.* Cancer Research, 2007. **67**(15): p. 7203-7211.
144. Schreiner, A., et al., *Junction protein shrew-1 influences cell invasion and interacts with invasion-promoting protein CD147.* Molecular Biology of the Cell, 2007. **18**(4): p. 1272-1281.
145. Network, C.G.A.R., *Integrated genomic analyses of ovarian carcinoma.* Nature, 2011. **474**(7353): p. 609-615.
146. Medina, P.P., et al., *Frequent BRG1/SMARCA4–inactivating mutations in human lung cancer cell lines.* Human Mutation, 2008. **29**(5): p. 617-622.
147. Frankell, A.M., et al., *The landscape of selection in 551 esophageal adenocarcinomas defines genomic biomarkers for the clinic.* Nature genetics, 2019. **51**(3): p. 506.
148. Tam, S.W., et al., *Differential expression and regulation of Cyclin D1 protein in normal and tumor human cells: association with Cdk4 is required for Cyclin D1 function in G1 progression.* Oncogene, 1994. **9**(9): p. 2663-2674.

149. Malumbres, M. and M. Barbacid, *Milestones in cell division: to cycle or not to cycle: a critical decision in cancer.* Nature Reviews Cancer, 2001. **1**(3): p. 222-231.
150. Fu, M., et al., *Minireview: Cyclin D1: normal and abnormal functions.* Endocrinology, 2004. **145**(12): p. 5439-5447.
151. Pagano, M., et al., *Cyclin D1-mediated inhibition of repair and replicative DNA synthesis in human fibroblasts.* Genes & Development, 1994. **8**(14): p. 1627-1639.
152. Diehl, J.A. and C.J. Sherr, *A dominant-negative cyclin D1 mutant prevents nuclear import of cyclin-dependent kinase 4 (CDK4) and its phosphorylation by CDK-activating kinase.* Molecular and Cellular Biology, 1997. **17**(12): p. 7362-7374.
153. Bani-Hani, K., et al., *Prospective study of cyclin D1 overexpression in Barrett's esophagus: association with increased risk of adenocarcinoma.* Journal of the National Cancer Institute, 2000. **92**(16): p. 1316-1321.
154. Casson, A.G., et al., *Cyclin D1 polymorphism (G870A) and risk for esophageal adenocarcinoma.* Cancer, 2005. **104**(4): p. 730-739.
155. Jiang, W., et al., *Altered expression of the cyclin D1 and retinoblastoma genes in human esophageal cancer.* Proceedings of the National Academy of Sciences, 1993. **90**(19): p. 9026-9030.
156. Boynton, R.F., et al., *Frequent loss of heterozygosity at the retinoblastoma locus in human esophageal cancers.* Cancer Research, 1991. **51**(20): p. 5766-5769.
157. Huang, Y., et al., *Altered messenger RNA and unique mutational profiles of p53 and Rb in human esophageal carcinomas.* Cancer Research, 1993. **53**(8): p. 1889-1894.
158. Singh, S.P., et al., *Loss or altered subcellular localization of p27 in Barrett's associated adenocarcinoma.* Cancer Research, 1998. **58**(8): p. 1730-1735.
159. Shinohara, M., et al., *Cell cycle-regulated factors in esophageal cancer.* Diseases of the Esophagus, 2002. **15**(2): p. 149-154.
160. Galipeau, P.C., et al., *NSAIDs modulate CDKN2A, TP53, and DNA content risk for progression to esophageal adenocarcinoma.* PLoS medicine, 2007. **4**(2): p. e67.
161. Das, M., et al., *p16 gene silencing along with p53 single-nucleotide polymorphism and risk of esophageal cancer in Northeast India.* Tumor Biology, 2017. **39**(5): p. 1010428317698384.
162. Lam, K.-O. and D.L. Kwong, *Target Therapy for Esophageal Adenocarcinoma*, in *Esophageal Adenocarcinoma*. 2018, Methods in Molecular Biology. p. 51-65.
163. Lee, K.T., et al., *Targeted Single Gene Mutation in Esophageal Adenocarcinoma*, in *Esophageal Adenocarcinoma*. 2018: Methods in Molecular Biology. p. 213-229.
164. Greally, M., et al., *Optimal management of gastroesophageal junction cancer.* Cancer, 2019. **125**(12): p. 1990-2001.
165. Ogawa, Y., et al., *Microvessel quantitation in invasive breast cancer by staining for factor VIII-related antigen.* British Journal of Cancer, 1995. **71**(6): p. 1297-1301.
166. Macchiarini, P., et al., *Relation of neovascularisation to metastasis of non-small-cell lung cancer.* The Lancet, 1992. **340**(8812): p. 145-146.
167. Weidner, N., et al., *Tumor angiogenesis correlates with metastasis in invasive prostate carcinoma.* The American Journal of Pathology, 1993. **143**(2): p. 401-409.
168. DeMeester, T.R. *Esophageal carcinoma: current controversies*. in *Seminars in surgical oncology*. 1997. Wiley Online Library.
169. Möbius, C., et al., *Vascular endothelial growth factor expression and neovascularization in Barrett's carcinoma.* World Journal of Surgery, 2004. **28**(7): p. 675-679.
170. Saad, R.S., et al., *Lymphangiogenesis in Esophageal Adenocarcinomas--Lymphatic Vessel Density as Prognostic Marker in Esophageal Adenocarcinoma.* American Journal of Clinical Pathology, 2009. **131**(1): p. 92-98.
171. Auvinen, M.I., et al., *Incipient angiogenesis in Barrett's epithelium and lymphangiogenesis in Barrett's adenocarcinoma.* Journal of Clinical Oncology, 2002. **20**(13): p. 2971-2979.

172. Salcedo, R., et al., *Vascular endothelial growth factor and basic fibroblast growth factor induce expression of CXCR4 on human endothelial cells: in vivo neovascularization induced by stromal-derived factor-1α.* The American Journal of Pathology, 1999. **154**(4): p. 1125-1135.
173. Möbius, C., et al., *The 'angiogenic switch'in the progression from Barrett's metaplasia to esophageal adenocarcinoma.* European Journal of Surgical Oncology, 2003. **29**(10): p. 890-894.
174. Xie, L.X., et al., *Lymphangiogenesis and prognostic significance of vascular endothelial growth factor C in gastro-oesophageal junction adenocarcinoma.* International Journal of Experimental Pathology, 2013. **94**(1): p. 39-46.
175. Arribas, J., et al., *p95HER2 and breast cancer.* Cancer research, 2011. **71**(5): p. 1515-1519.
176. Chandarlapaty, S., et al., *Inhibitors of HSP90 block p95-HER2 signaling in Trastuzumab-resistant tumors and suppress their growth.* Oncogene, 2010. **29**(3): p. 325-334.
177. Scaltriti, M., et al., *High HER2 expression correlates with response to the combination of lapatinib and trastuzumab.* Clinical Cancer Research, 2015. **21**(3): p. 569-576.
178. Janjigian, Y.Y., et al., *Emergence of RTK/RAS/PI3K pathway alterations in trastuzumab-refractory HER2-positive esophagogastric (EG) tumors*. 2016, American Society of Clinical Oncology.
179. Deguchi, Y., et al., *PTEN loss is associated with a poor response to trastuzumab in HER2-overexpressing gastroesophageal adenocarcinoma.* Gastric Cancer, 2017. **20**(3): p. 416-427.
180. Geddert, H., et al., *Gene amplification and protein overexpression of c-erb-b2 in Barrett carcinoma and its precursor lesions.* American Journal of Clinical Pathology, 2002. **118**(1): p. 60-66.
181. Walch, A., et al., *Evaluation of c-erbB-2 overexpression and Her-2/neu gene copy number heterogeneity in Barrett's adenocarcinoma.* Analytical Cellular Pathology, 2000. **20**(1): p. 25-32.
182. Reichelt, U., et al., *Frequent homogeneous HER-2 amplification in primary and metastatic adenocarcinoma of the esophagus.* Modern Pathology, 2007. **20**(1): p. 120.
183. Brien, T.P., et al., *HER-2/neu gene amplification by FISH predicts poor survival in Barrett's esophagus-associated adenocarcinoma.* Human pathology, 2000. **31**(1): p. 35-39.
184. Hu, Y., et al., *HER2 amplification, overexpression and score criteria in esophageal adenocarcinoma.* Modern Pathology, 2011. **24**(7): p. 899.
185. Walch, A., et al., *Coamplification and coexpression of GRB7 and ERBB2 is found in high grade intraepithelial neoplasia and in invasive Barrett's carcinoma.* International journal of cancer, 2004. **112**(5): p. 747-753.
186. Maqani, N., et al., *Molecular dissection of 17q12 amplicon in upper gastrointestinal adenocarcinomas.* Molecular cancer research, 2006. **4**(7): p. 449-455.
187. Lyons, T.G. and G.Y. Ku, *Systemic therapy for esophagogastric cancer: targeted therapies.* Chinese Clinical Oncology, 2017. **6**(5): p. 48.
188. Zhang, L., et al., *Targeted therapy in esophageal cancer.* Expert Review of Gastroenterology & Hepatology, 2016. **10**(5): p. 595-604.
189. Tabernero, J., et al., *Pertuzumab plus trastuzumab and chemotherapy for HER2-positive metastatic gastric or gastro-oesophageal junction cancer (JACOB): final analysis of a double-blind, randomised, placebo-controlled phase 3 study.* The Lancet Oncology, 2018. **19**(10): p. 1372-1384.
190. Shen, T.-L. and J.L. Guan, *Grb7 in intracellular signaling and its role in cell regulation.* Frontiers in Bioscience 9:, 2004: p. 192-200.
191. Han, D.C., et al., *The Grb7 family proteins: structure, interactions with other signaling molecules and potential cellular functions.* Oncogene, 2001. **20**(44): p. 6315.
192. Chu, P.-Y., et al., *Tyrosine phosphorylation of growth factor receptor-bound protein-7 by focal adhesion kinase in the regulation of cell migration, proliferation, and tumorigenesis.* Journal of Biological Chemistry, 2009. **284**(30): p. 20215-20226.

193. Tanaka, S., et al., *Coexpression of Grb7 with epidermal growth factor receptor or Her2/erbB2 in human advanced esophageal carcinoma.* Cancer Research, 1997. **57**(1): p. 28-31.
194. Tanaka, S., et al., *A novel variant of human Grb7 is associated with invasive esophageal carcinoma.* The Journal of clinical investigation, 1998. **102**(4): p. 821-827.
195. Tanaka, S., et al., *Grb7 signal transduction protein mediates metastatic progression of esophageal carcinoma.* Journal of Cellular Physiology, 2000. **183**(3): p. 411-415.
196. Kishi, T., et al., *Molecular Cloning of HumanGRB-7Co-amplified withCAB1and c-ERBB-2in Primary Gastric Cancer.* Biochemical and Biophysical Research Communications, 1997. **232**(1): p. 5-9.
197. Tanaka, S., et al., *Specific peptide ligand for Grb7 signal transduction protein and pancreatic cancer metastasis.* Journal of the National Cancer Institute, 2006. **98**(7): p. 491-498.
198. Wang, Y., et al., *Differential functions of growth factor receptor–bound protein 7 (GRB7) and its variant GRB7v in ovarian carcinogenesis.* Clinical Cancer Research, 2010. **16**(9): p. 2529-2539.
199. Stein, D., et al., *The SH2 domain protein GRB-7 is co-amplified, overexpressed and in a tight complex with HER2 in breast cancer.* The EMBO Journal, 1994. **13**(6): p. 1331-1340.
200. Bai, T. and S.-W. Luoh, *GRB-7 facilitates HER-2/Neu-mediated signal transduction and tumor formation.* Carcinogenesis, 2007. **29**(3): p. 473-479.
201. Kao, J. and J.R. Pollack, *RNA interference-based functional dissection of the 17q12 amplicon in breast cancer reveals contribution of coamplified genes.* Genes, Chromosomes and Cancer, 2006. **45**(8): p. 761-769.
202. Nadler, Y., et al., *Growth factor receptor-bound protein-7 (Grb7) as a prognostic marker and therapeutic target in breast cancer.* Annals of oncology, 2009. **21**(3): p. 466-473.
203. Ramsey, B., et al., *GRB7 protein over-expression and clinical outcome in breast cancer.* Breast Cancer Research and Treatment, 2011. **127**(3): p. 659-669.
204. Pero, S.C., et al., *Identification of novel non-phosphorylated ligands, which bind selectively to the SH2 domain of Grb7.* Journal of Biological Chemistry, 2002. **277**(14): p. 11918-11926.
205. Pero, S., et al., *Combination treatment with Grb7 peptide and Doxorubicin or Trastuzumab (Herceptin) results in cooperative cell growth inhibition in breast cancer cells.* British journal of cancer, 2007. **96**(10): p. 1520.
206. Weaver, J.M., et al., *Ordering of mutations in preinvasive disease stages of esophageal carcinogenesis.* Nature Genetics, 2014. **46**(8): p. 837-843.
207. Vousden, K.H. and D.P.Lane, *p53 in health and disease.* Nature Reviews. Molecular Cell Biology. , 2007. **8**(4): p. 275-283.
208. Hanel, W. and U.M. Moll, *Links between mutant p53 and genomic instability.* Journal of Cellular Biochemistry, 2012. **113**(2): p. 433-439.
209. Lambrus, B.G., et al., *p53 protects against genome instability following centriole duplication failure.* The Journal of Cell Biology, 2015. **210**(1): p. 63-77.
210. Oren, M. and V.J. Rotter, *Mutant p53 gain-of-function in cancer.* Cold Spring Harbor Perspectives in Biology, 2010. **2**(2): p. a001107.
211. Keld, R.R. and Y.S.Ang, *Targeting key signalling pathways in oesophageal adenocarcinoma: A reality for personalised medicine?* World Journal of Gastroenterology, 2011. **17**(23): p. 2781-2790.
212. Akhurst, R.J. and R. Derynck, *TGF-β signaling in cancer—a double-edged sword.* Trends in Cell Biology, 2001. **11**: p. S44-S51.
213. Massagué, J.J., *TGFβ in cancer.* Cell, 2008. **134**(2): p. 215-230.
214. Napier, K.J., et al., *Esophageal cancer: A Review of epidemiology, pathogenesis, staging workup and treatment modalities.* World Journal of Gastrointestinal Oncology, 2014. **6**(5): p. 112-120.

215. Palanca-Wessels, M.C., et al., *Genetic analysis of long-term Barrett's esophagus epithelial cultures exhibiting cytogenetic and ploidy abnormalities.* Gastroenterology, 1998. **114**(2): p. 295-304.
216. Ran, F.A., et al., *Genome engineering using the CRISPR-Cas9 system.* Nature Protocols, 2013. **8**(11): p. 2281-2308.
217. Aubrey, B.J., et al., *An inducible lentiviral guide RNA platform enables the identification of tumor-essential genes and tumor-promoting mutations in vivo.* Cell Reports, 2015. **10**(8): p. 1422-1432.
218. Martin, M., *Cutadapt removes adapter sequences from high-throughput sequencing reads.* EMBnet Journal, 2011. **17**(1): p. 10-12.
219. Li, H. and R. Durbin, *Fast and accurate short read alignment with Burrows-Wheeler transform.* Bioinformatics, 2009. **25**(14): p. 1754-60.
220. Boeva, V., et al., *Control-FREEC: a tool for assessing copy number and allelic content using next-generation sequencing data.* Bioinformatics, 2012. **28**(3): p. 423-5.
221. Scheinin, I., et al., *DNA copy number analysis of fresh and formalin-fixed specimens by shallow whole-genome sequencing with identification and exclusion of problematic regions in the genome assembly.* Genome Research, 2014. **24**(12): p. 2022-2032.
222. Livak, K.J. and T.D. Schmittgen, *Analysis of relative gene expression data using real-time quantitative PCR and the 2− ΔΔCT method.* Methods, 2001. **25**(4): p. 402-408.
223. Vrijens, K., et al., *Identification of small molecule activators of BMP signaling.* PLOS One, 2013. **8**(3) e59045.
224. Galili, T., et al., *heatmaply: an R package for creating interactive cluster heatmaps for online publishing.* Bioinformatics, 2017. **34**(9): p. 1600-1602.
225. Corley, D.A., et al., *Impact of endoscopic surveillance on mortality from Barrett's esophagus–associated esophageal adenocarcinomas.* Gastroenterology, 2013. **145**(2): p. 312-319.
226. Agrawal, N., et al., *Comparative genomic analysis of esophageal adenocarcinoma and squamous cell carcinoma.* Cancer Discovery, 2012. **2**(10): p. 899-905.
227. Bellini, M.F., et al., *Alterations of the TP53 gene in gastric and esophageal carcinogenesis.* Journal of Biomedicine and Biotechnology, 2012. **2012**: p. 891961.
228. Liu, D.S., et al., *APR-246 potently inhibits tumour growth and overcomes chemoresistance in preclinical models of oesophageal adenocarcinoma.* Gut, 2015. **64**(10): p. 1506-1516.
229. Liu, D.S., et al., *Inhibiting the system x C−/glutathione axis selectively targets cancers with mutant-p53 accumulation.* Nature Communications, 2017. **8**: p. 14844.
230. Singhi, A.D., et al., *Smad4 loss in esophageal adenocarcinoma is associated with an increased propensity for disease recurrence and poor survival.* The American Journal of Surgical Pathology, 2015. **39**(4): p. 487-495.
231. Yan, P., et al., *Reduced expression of SMAD4 is associated with poor survival in colon cancer.* Clinical Cancer Research, 2016. **22**(12): p. 3037-3047.
232. Xu, X., et al., *Haploid loss of the tumor suppressor Smad4/Dpc4 initiates gastric polyposis and cancer in mice.* Oncogene, 2000. **19**(15): p. 1868-1874.
233. Blackford, A., et al., *SMAD4 gene mutations are associated with poor prognosis in pancreatic cancer.* Clinical Cancer Research, 2009. **15**(14): p. 4674-4679.
234. Maitra, A., et al., *Loss of Dpc4 expression in colonic adenocarcinomas correlates with the presence of metastatic disease.* The American Journal of Pathology, 2000. **157**(4): p. 1105-1111.
235. Tascilar, M., et al., *The SMAD4 protein and prognosis of pancreatic ductal adenocarcinoma.* Clinical Cancer Research, 2001. **7**(12): p. 4115-4121.
236. Miyaki, M., et al., *Higher frequency of Smad4 gene mutation in human colorectal cancer with distant metastasis.* Oncogene, 1999. **18**(20): p. 3098-3103.
237. DiMaio, M.A., et al., *Immunohistochemical panel for distinguishing esophageal adenocarcinoma from squamous cell carcinoma: a combination of p63, cytokeratin 5/6,*

MUC5AC, and anterior gradient homolog 2 allows optimal subtyping. Human Pathology, 2012. **43**(11): p. 1799-1807.
238. Alberici, P., et al., *Smad4 haploinsufficiency: a matter of dosage.* Pathogenetics, 2008. **1**(1): p. 2.
239. Fidler, I.J. and M.L. Kripke, *The challenge of targeting metastasis.* Cancer and Metastasis Reviews, 2015. **34**(4): p. 635-641.
240. Smyth, E.C., et al., *Oesophageal cancer.* Nature Reviews Disease Primers, 2017. **3**: p. 17048.
241. Schweigert, M., et al., *Oesophageal cancer—an overview.* Nature Reviews Gastroenterology and Hepatology, 2013. **10**(4): p. 230-244.
242. Melsens, E., et al., *Improved xenograft efficiency of esophageal adenocarcinoma cell lines through in vivo selection.* Oncology Reports, 2017. **38**(1): p. 71-81.
243. Raggi, M., et al., *Successful evaluation of a new animal model using mice for esophageal adenocarcinoma.* Langenbeck's Archives of Surgery, 2010. **395**(4): p. 347-350.
244. Zaidi, A.H., et al., *MicroRNA signature characterizes primary tumors that metastasize in an esophageal adenocarcinoma rat model.* PloS One, 2015. **10**(3): p. e0122375.
245. Luketich, J.D., et al., *Evaluation of distant metastases in esophageal cancer: 100 consecutive positron emission tomography scans.* The Annals of Thoracic Surgery, 1999. **68**(4): p. 1133-1136.
246. Liu, D.S., et al., *Novel metastatic models of esophageal adenocarcinoma derived from FLO-1 cells highlight the importance of E-cadherin in cancer metastasis.* Oncotarget, 2016. **7**(50): p. 83342-83358.
247. Khatib, Z.A., et al., *Coamplification of the CDK4 gene with MDM2 and GLI in human sarcomas.* Cancer Research, 1993. **53**(22): p. 5535-5541.
248. Oliner, J.D., et al., *The role of MDM2 amplification and overexpression in tumorigenesis.* Cold Spring Harbor Perspectives in Medicine, 2016. **6**(6): p. a026336.
249. Michalk, M., et al., *MDM2 gene amplification in esophageal carcinoma.* Oncology Reports, 2016. **35**(4): p. 2223-2227.
250. Hamilton, E. and J.R. Infante, *Targeting CDK4/6 in patients with cancer.* Cancer Treatment Reviews, 2016. **45**: p. 129-138.
251. Kim, Y.J., et al., *Co-expression of MDM2 and CDK4 in transformed human mesenchymal stem cells causes high-grade sarcoma with a dedifferentiated liposarcoma-like morphology.* Laboratory Investigation, 2019. **99**(9): p. 1309-1320.
252. Pasello, G., et al., *DNA copy number alterations correlate with survival of esophageal adenocarcinoma patients.* Modern Pathology, 2009. **22**(1): p. 58-65.
253. Patel, S.A. and S. Vanharanta, *Epigenetic determinants of metastasis.* Molecular oncology, 2017. **11**(1): p. 79-96.
254. Lagna, G., et al., *Partnership between DPC4 and SMAD proteins in TGF-β signalling pathways.* Nature, 1996. **383**(6603): p. 832-836.
255. Seoane, J., et al., *Integration of Smad and forkhead pathways in the control of neuroepithelial and glioblastoma cell proliferation.* Cell, 2004. **117**(2): p. 211-223.
256. Onwuegbusi, B.A., et al., *Impaired transforming growth factor β signalling in Barrett's carcinogenesis due to frequent SMAD4 inactivation.* Gut, 2006. **55**(6): p. 764-774.
257. Onwuegbusi, B.A., et al., *Selective loss of TGFβ Smad-dependent signalling prevents cell cycle arrest and promotes invasion in oesophageal adenocarcinoma cell lines.* PLoS One, 2007. **2**(1): p. e177.
258. Bierie, B. and H.L. Moses, *Tumour microenvironment: TGFβ: the molecular Jekyll and Hyde of cancer.* Nature Reviews Cancer, 2006. **6**(7): p. 506-520.
259. Pickup, M., et al., *The roles of TGFβ in the tumour microenvironment.* Nature Reviews Cancer, 2013. **13**(11): p. 788-799.
260. Levy, L. and C.S. Hill, *Smad4 dependency defines two classes of transforming growth factor β (TGF-β) target genes and distinguishes TGF-β-induced epithelial-mesenchymal transition from*

its antiproliferative and migratory responses. Molecular and Cellular Biology, 2005. **25**(18): p. 8108-8125.
261. Jazag, A., et al., *Smad4 silencing in pancreatic cancer cell lines using stable RNA interference and gene expression profiles induced by transforming growth factor-β.* Oncogene, 2005. **24**(4): p. 662-671.
262. Rees, J.R., et al., *In vivo and in vitro evidence for transforming growth factor-β1-mediated epithelial to mesenchymal transition in esophageal adenocarcinoma.* Cancer Research, 2006. **66**(19): p. 9583-9590.
263. Chen, D., et al., *Alpha B-crystallin promotes the invasion and metastasis of gastric cancer via NF-κB-induced epithelial-mesenchymal transition.* Journal of Cellular and Molecular Medicine, 2018. **22**(6): p. 3215-3222.
264. Shi, C., et al., *Alpha B-crystallin promotes the invasion and metastasis of colorectal cancer via epithelial-mesenchymal transition.* Biochemical and Biophysical Research Communications, 2017. **489**(4): p. 369-374.
265. Chen, S., et al., *Cdc6 contributes to cisplatin-resistance by activation of ATR-Chk1 pathway in bladder cancer cells.* Oncotarget, 2016. **7**(26): p. 40362-40376.
266. Borlado, L.R. and J. Méndez, *CDC6: from DNA replication to cell cycle checkpoints and oncogenesis.* Carcinogenesis, 2007. **29**(2): p. 237-243.
267. Gamell, C., et al., *Reduced abundance of the E3 ubiquitin ligase E6AP contributes to decreased expression of the INK4/ARF locus in non–small cell lung cancer.* Science Signaling, 2017. **10**(461): p. eaaf8223.
268. Warner, B.J., et al., *Myc downregulation by transforming growth factor β required for activation of the p15Ink4b G1 arrest pathway.* Molecular and cellular biology, 1999. **19**(9): p. 5913-5922.
269. Claassen, G.F. and S.R. Hann, *A role for transcriptional repression of p21CIP1 by c-Myc in overcoming transforming growth factor β-induced cell-cycle arrest.* Proceedings of the National Academy of Sciences, 2000. **97**(17): p. 9498-9503.
270. Li, Q., et al., *RUNX1 promotes tumour metastasis by activating the Wnt/β-catenin signalling pathway and EMT in colorectal cancer.* Journal of Experimental and Clinical Cancer Research: CR., 2019. **38**(1): p. 334.
271. Sangpairoj, K., et al., *RUNX1 regulates migration, invasion, and angiogenesis via p38 MAPK pathway in human glioblastoma.* Cellular and Molecular Neurobiology, 2017. **37**(7): p. 1243-1255.
272. Browne, G., et al., *Runx1 is associated with breast cancer progression in MMTV-PyMT transgenic mice and its depletion in vitro inhibits migration and invasion.* Journal of Cellular Physiology, 2015. **230**(10): p. 2522-2532.
273. Koinuma, D., et al., *Promoter-wide analysis of Smad4 binding sites in human epithelial cells.* Cancer Science, 2009. **100**(11): p. 2133-2142.
274. Petrova, R. and A.L. Joyner, *Roles for Hedgehog signaling in adult organ homeostasis and repair.* Development, 2014. **141**(18): p. 3445-3457.
275. di Magliano, M.P. and M. Hebrok, *Hedgehog signalling in cancer formation and maintenance.* Nature Reviews Cancer, 2003. **3**(12): p. 903-911.
276. Katoh, Y. and M. Katoh, *Hedgehog signaling pathway and gastrointestinal stem cell signaling network.* International Journal of Molecular Medicine, 2006. **18**(6): p. 1019-1023.
277. Wang, D., et al., *Hedgehog Pathway as a Potential Intervention Target in Esophageal Cancer.* Cancers, 2019. **11**(6): p. 821.
278. Lau, E., et al., *The functional role of Cdc6 in S–G2/M in mammalian cells.* EMBO Reports, 2006. **7**(4): p. 425-430.
279. Mahadevappa, R., et al., *The prognostic significance of Cdc6 and Cdt1 in breast cancer.* Scientific Reports, 2017. **7**(1): p. 985.

280. Kennedy, B.A., et al., *ChIP-seq defined genome-wide map of TGFβ/SMAD4 targets: implications with clinical outcome of ovarian cancer.* PLoS One, 2011. **6**(7): p. e22606.
281. Kim, W.Y. and N.E. Sharpless, *The regulation of INK4/ARF in cancer and aging.* Cell, 2006. **127**(2): p. 265-275.
282. Petropoulos, M., et al., *Replication Licensing Aberrations, Replication Stress, and Genomic Instability.* Trends in Biochemical Sciences, 2019. **44**(9).
283. Amin, M.K.B.A., et al., *Epithelial membrane protein 1 promotes tumor metastasis by enhancing cell migration via copine-III and Rac1.* Oncogene, 2018. **37**(40): p. 5416-5434.
284. Pohl, H. and H.G. Welch, *The role of overdiagnosis and reclassification in the marked increase of esophageal adenocarcinoma incidence.* Journal of the National Cancer Institute, 2005. **97**(2): p. 142-146.
285. Lepage, C., et al., *Continuing rapid increase in esophageal adenocarcinoma in England and Wales.* The American Journal of Gastroenterology, 2008. **103**(11): p. 2694.
286. Grant, K.S., et al., *Effect of Barrett's esophagus surveillance on esophageal preservation, tumor stage, and survival with esophageal adenocarcinoma.* The Journal of Thoracic and Cardiovascular Surgery, 2013. **146**(1): p. 31-37.
287. Thiery, J.P., *Epithelial–mesenchymal transitions in tumour progression.* Nature Reviews Cancer, 2002. **2**(6): p. 442-454.
288. Thiery, J.P., *Epithelial–mesenchymal transitions in development and pathologies.* Current Opinion in Cell Biology, 2003. **15**(6): p. 740-746.
289. Moyano, J.V., et al., *αB-crystallin is a novel oncoprotein that predicts poor clinical outcome in breast cancer.* The Journal of Clinical Investigation, 2006. **116**(1): p. 261-270.
290. Malin, D., et al., *αB-crystallin: a novel regulator of breast cancer metastasis to the brain.* Clinical Cancer Research, 2014. **20**(1): p. 56-67.
291. van de Schootbrugge, C., et al., *αB-crystallin stimulates VEGF secretion and tumor cell migration and correlates with enhanced distant metastasis in head and neck squamous cell carcinoma.* BMC Cancer, 2013. **13**(1): p. 128.
292. Voduc, K.D., et al., *αB-crystallin expression in breast cancer is associated with brain metastasis.* NPJ Breast Cancer, 2015. **1**: p. 15014.
293. Zeman, M.K. and K.A. Cimprich, *Causes and consequences of replication stress.* Nature Cell Biology, 2014. **16**(1): p. 2.
294. Macheret, M. and T.D. Halazonetis, *DNA replication stress as a hallmark of cancer.* Annual Review of Pathology: Mechanisms of Disease, 2015. **10**: p. 425-448.
295. Gaillard, H., et al, *Replication stress and cancer.* Nature Reviews Cancer, 2015. **15**(5): p. 276-289.
296. Kotsantis, P., et al., *Mechanisms of oncogene-induced replication stress: jigsaw falling into place.* Cancer Discovery, 2018. **8**(5): p. 537-555.
297. Hills, S.A. and J.F. Diffley, *DNA replication and oncogene-induced replicative stress.* Current Biology, 2014. **24**(10): p. R435-R444.
298. Vaziri, C., et al., *A p53-dependent checkpoint pathway prevents rereplication.* Molecular Cell, 2003. **11**(4): p. 997-1008.
299. Kim, J., et al., *C. elegans CUL-4 prevents rereplication by promoting the nuclear export of CDC-6 via a CKI-1-dependent pathway.* Current Biology, 2007. **17**(11): p. 966-972.
300. Mihaylov, I.S., et al., *Control of DNA replication and chromosome ploidy by geminin and cyclin A.* Molecular and Cellular Biology, 2002. **22**(6): p. 1868-1880.
301. Melixetian, M., et al., *Loss of Geminin induces rereplication in the presence of functional p53.* Journal of Cell Biology, 2004. **165**(4): p. 473-482.
302. Jin, J., et al., *A family of diverse Cul4-Ddb1-interacting proteins includes Cdt2, which is required for S phase destruction of the replication factor Cdt1.* Molecular Cell, 2006. **23**(5): p. 709-721.
303. Li, A. and J.J. Blow, *Cdt1 downregulation by proteolysis and geminin inhibition prevents DNA re-replication in Xenopus.* The EMBO Journal, 2005. **24**(2): p. 395-404.

304. Zhu, W., et al., *Rereplication by depletion of geminin is seen regardless of p53 status and activates a G2/M checkpoint.* Molecular and Cellular Biology, 2004. **24**(16): p. 7140-7150.
305. Davidson, I.F., et al., *Deregulated replication licensing causes DNA fragmentation consistent with head-to-tail fork collision.* Molecular Cell, 2006. **24**(3): p. 433-443.
306. Murphy, N., et al., *p16INK4A, CDC6, and MCM5: predictive biomarkers in cervical preinvasive neoplasia and cervical cancer.* Journal of Clinical Pathology, 2005. **58**(5): p. 525-534.
307. Karakaidos, P., et al., *Overexpression of the replication licensing regulators hCdt1 and hCdc6 characterizes a subset of non-small-cell lung carcinomas: synergistic effect with mutant p53 on tumor growth and chromosomal instability—evidence of E2F-1 transcriptional control over hCdt1.* The American Journal of Pathology, 2004. **165**(4): p. 1351-1365.
308. Barrett, M.T., et al., *Allelic loss and mutational analysis of the DPC4 gene in esophageal adenocarcinoma.* Cancer Research, 1996. **56**(19): p. 4351-4353.
309. Wu, T.-T., et al., *Genetic alterations in Barrett esophagus and adenocarcinomas of the esophagus and esophagogastric junction region.* The American Journal of Pathology, 1998. **153**(1): p. 287-294.
310. von Rahden, B.H., et al., *Overexpression of TGF-β1 in esophageal (Barrett's) adenocarcinoma is associated with advanced stage of disease and poor prognosis.* Molecular Carcinogenesis, 2006. **45**(10): p. 786-794.
311. Gotovac, J.R., et al., *TGF-beta signaling and its targeted therapy in gastrointestinal cancers.* Discovery Medicine, 2018. **26**(142): p. 103-112.
312. Blum, A.E., et al., *Systems Biology Analyses Show Hyperactivation of Transforming Growth Factor-β and JNK Signaling Pathways in Esophageal Cancer.* Gastroenterology, 2019. **156**(6): p. 1761-1774.
313. Zhang, J., et al., *Progression of the role of CRYAB in signaling pathways and cancers.* OncoTargets and therapy, 2019. **12**: p. 4129-4139.
314. Toledo, L.I., et al., *A cell-based screen identifies ATR inhibitors with synthetic lethal properties for cancer-associated mutations.* Nature structural & molecular biology, 2011. **18**(6): p. 721-727.
315. Schoppy, D.W., et al., *Oncogenic stress sensitizes murine cancers to hypomorphic suppression of ATR.* The Journal of Clinical Investigation, 2012. **122**(1): p. 241-252.
316. Murga, M., et al., *Exploiting oncogene-induced replicative stress for the selective killing of Myc-driven tumors.* Nature Structural and Molecular Biology, 2011. **18**(12): p. 1331-1335.
317. Gilad, O., et al., *Combining ATR suppression with oncogenic Ras synergistically increases genomic instability, causing synthetic lethality or tumorigenesis in a dosage-dependent manner.* Cancer research, 2010. **70**(23): p. 9693-9702.
318. Robertson, K.D., *DNA methylation and chromatin–unraveling the tangled web.* Oncogene, 2002. **21**(35): p. 5361-5379.
319. Peng, D., et al., *Glutathione peroxidase 7 has potential tumour suppressor functions that are silenced by location-specific methylation in oesophageal adenocarcinoma.* Gut, 2014. **63**(4): p. 540-551.
320. Jammula, S., et al., *Identification of Subtypes of Barrett's Esophagus and Esophageal Adenocarcinoma Based on DNA Methylation Profiles and Integration of Transcriptome and Genome Data.* Gastroenterology, 2020. pii: S0016-5085(20)30156-6. doi: 10.1053/j.gastro.2020.01.044. [Epub ahead of print].
321. Lin, D.-C., et al., *Identification of distinct mutational patterns and new driver genes in oesophageal squamous cell carcinomas and adenocarcinomas.* Gut, 2018. **67**(10): p. 1769-1779.
322. Higgins, M.J. and J. Baselga, *Targeted therapies for breast cancer.* The Journal of Clinical Investigation, 2011. **121**(10): p. 3797-3803.
323. Gray-Schopfer, V., et al., *Melanoma biology and new targeted therapy.* Nature, 2007. **445**(7130): p. 851-857.

324. Druker, B.J., *Imatinib as a paradigm of targeted therapies.* Advances in Cancer Research, 2004. **91**(1): p. 1-30.